MACROPHAGE METABOLIC REPROGRAMMING IN CHRONIC DISEASES

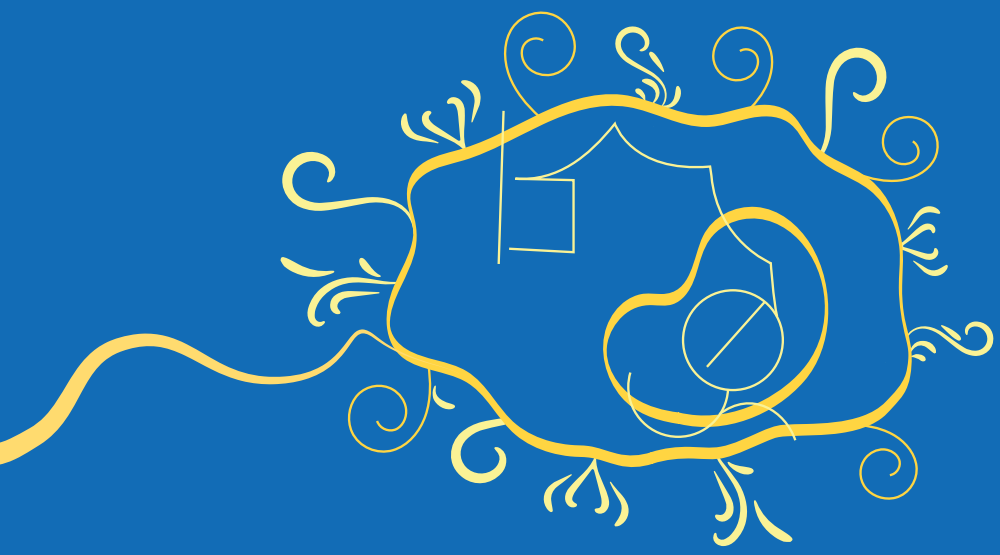

SARA RUSSO

Macrophage metabolic reprogramming in chronic diseases

Sara Russo

The research described in this thesis was carried out in the Department of Analytical Biochemistry and Molecular Pharmacology (Groningen Research Institute of Pharmacy, University of Groningen, The Netherlands) according to the requirements of the Graduate School of Science and Engineering, Faculty of Science and Engineering, University of Groningen, The Netherlands.

The studies presented in this thesis were conducted in the context of the PROMINENT project of the Groningen University Institute for Drug Exploration (GUIDE). This project has received funding from the European Union's Horizon 2020 research and innovation program under the Marie Skłodowska-Curie grant agreement No 754425.

Printing of this thesis was financially supported by the University Library and the Graduate School of Science and Engineering, Faculty of Science and Engineering, University of Groningen, The Netherlands.

Cover design:	Ridderprint | www.ridderprint.nl
Lay-out:	Ridderprint | www.ridderprint.nl
Print:	Ridderprint | www.ridderprint.nl

© Copyright 2024: Sara Russo, The Netherlands

All rights reserved. No part of this publication may be reproduced, stored in a retrieval system, or transmitted in any form or by any means, electronic, mechanical, by photocopying, recording, or otherwise, without the prior written permission of the author.

university of groningen

Macrophage metabolic reprogramming in chronic diseases

PhD thesis

to obtain the degree of PhD at the
University of Groningen
on the authority of the
Rector Magnificus Prof. J.M.A. Scherpen
and in accordance with
the decision by the College of Deans.

This thesis will be defended in public on

Tuesday 26 March 2024 at 14:30 hours

by

Sara Russo
born on 7 August 1992
in Pisa, Italy

Supervisors

Prof. R.P.H. Bischoff

Prof. B.N. Melgert

Assessment Committee

Prof. M. Schmidt

Prof. G. Hopfgartner

Prof. F.J. Dekker

TABLE OF CONTENTS

Chapter 1	General Introduction	7
Chapter 2	Meta-inflammation and metabolic reprogramming of macrophages in diabetes and obesity: the importance of metabolites	23
Chapter 3	Effects of lysine deacetylase inhibitor treatment on LPS responses of alveolar-like macrophages	59
Chapter 4	Collagen Type I Alters the Proteomic Signature of Macrophages in a Collagen Morphology-Dependent Manner	103
Chapter 5	General Discussion	139
Appendix	English summary	158
	Nederlandse Samenvatting	160
	Italian summary (Riassunto in Italiano)	162
	Acknowledgements	164
	Curriculum Vitae	169

1

CHAPTER 1

General Introduction

CHRONIC DISEASES

Chronic obstructive pulmonary disease (COPD), cardiovascular disease, and diabetes are the most common chronic diseases worldwide.

COPD is a progressive and debilitating respiratory condition characterized by persistent lung airflow limitation (1). It encompasses a group of chronic lung disorders, primarily chronic bronchitis, and emphysema (2). COPD gradually worsens over time, leading to significant respiratory symptoms, reduced lung function, and impaired quality of life. It is a global health concern, affecting millions of people worldwide and imposing a substantial burden on individuals, healthcare systems, and society as a whole. Understanding the causes, symptoms, diagnosis, and management of COPD is crucial in order to improve patient outcomes and alleviate the impact of this chronic respiratory condition.

Diabetes mellitus is a chronic condition characterized by high blood sugar levels resulting from insulin deficiency or resistance. It can be classified into Type 1 diabetes, caused by a lack of insulin production, and Type 2 diabetes (T2DM), caused by insulin resistance. Globally, there are approximately 415 million diagnosed cases of diabetes (of which 87–91% have T2DM in high-income countries), a number expected to rise to 642 million by 2040 (3). Diabetes is a significant cause of morbidity and mortality, with complications including diabetic nephropathy, peripheral neuropathy, and cardiovascular diseases. Despite advancements in treatment and decreasing complication rates (4), the prevalence of newly diagnosed cases continues to rise (5).

INFLAMMATION

COPD is characterized by chronic inflammation that affects various tissues involved in respiratory function, including the lungs and airways. This persistent inflammation is marked by increased levels of pro-inflammatory cytokines and other immune mediators. In COPD, chronic inflammation is primarily triggered by long-term exposure to irritants, such as cigarette smoke or environmental pollutants. The inflammatory response in the lungs leads to structural changes, airway remodeling, and narrowing of the air passages, resulting in airflow limitation and respiratory symptoms. Pro-inflammatory cytokines, including tumor necrosis factor (TNF)-α, interleukin (IL)-6, IL-1β, and others, contribute to the perpetuation of the inflammatory process and tissue damage in COPD. This chronic inflammation not only worsens respiratory symptoms but also contributes to the development of comorbidities, such as cardiovascular disease. Understanding the role of chronic inflammation in COPD is crucial for the development of targeted therapies aimed

at reducing inflammation, slowing disease progression, and improving the quality of life for individuals living with this chronic respiratory condition.

T2DM is characterized by chronic low-grade inflammation in various tissues involved in energy regulation, including fat, liver, and pancreatic islets (6). This inflammation is marked by increased levels of pro-inflammatory cytokines and non-esterified free fatty acids (FFA), which contribute to insulin resistance and beta-cell dysfunction. In T2DM, pro-inflammatory cytokines such as TNF-α, IL-6, IL-1β, and IL-1α are produced in higher quantities, contributing to obesity-related inflammation and impairing insulin signaling (7). These cytokines also contribute to the development of microvascular complications associated with diabetes, including retinopathy, polyneuropathy, and nephropathy (8). The inflammatory effects of obesity were defined for the first time in 1993 when it was shown that adipose tissue from obese individuals expressed elevated levels of TNF-α, a pro-inflammatory cytokine, primarily secreted by macrophages (9).

MACROPHAGES

Macrophages are cells of the innate immune system derived from hematopoietic stem cells (HSCs) of the bone marrow or from erythro-myeloid progenitors (EMPs) of the fetal yolk sac (10). HSCs differentiate in myeloid (MPs) and lymphoid (LPs) committed precursors. MPs will then differentiate into monocytes, macrophages, and dendritic cell precursors (MDP). Two monocyte subsets (resident, lymphocyte antigen 6c negative, $Ly6C^{-/low}$, and inflammatory $Ly6C^{+/high}$) are released in the circulation, and, in case of infection, $Ly6C^{+}$ can migrate into local inflammatory sites and differentiate into inflammatory macrophages (11,12).

Macrophage polarization

Macrophages, a type of immune cell, can be polarized into different groups based on their response to the microenvironment. The three main groups are M1 (classically activated) macrophages, M2 (alternatively activated) macrophages, and M2-like (regulatory) macrophages (13). The classification is determined by specific molecular markers, chemokine receptors, and cytokine production (14). M1 macrophages are activated by inflammatory stimuli and produce pro-inflammatory cytokines, promoting a Th1 immune response (15,16). They express markers like MHC II, CD68, CD80, and CD86 (17). M2 macrophages are associated with tissue remodeling and are activated by interleukins 4 and 13 (18–20). They express CD206 and transglutaminase 2, and have limited antigen-presenting capabilities. M2-like macrophages are induced by anti-inflammatory stimuli and secrete high levels of

IL-10, exhibiting potent anti-inflammatory effects. These macrophages are also characterized by TGFβ production (21).

Adipose tissue macrophages

Obesity is associated with the development of type 2 diabetes (T2DM), and the immune system in adipose tissue plays a role in this process. Adipose tissue consists of white adipose tissue (WAT) and brown adipose tissue (BAT) (22). In obesity, WAT shows increased levels of pro-inflammatory cytokines, primarily secreted by macrophages (9). Adipose tissue macrophages (ATMs) significantly impact adipose tissue homeostasis. In lean individuals, ATMs resemble M2 macrophages, promoting insulin sensitivity through the production of anti-inflammatory cytokines (23). However, in obesity, excessive growth of WAT leads to lipid accumulation, cellular stress, and hypoxia (24,25), triggering the release of free fatty acids, pro-inflammatory cytokines, and reactive oxygen species (ROS) (26,27), resulting in impaired insulin sensitivity (28). Monocytes are recruited to adipose tissue in obesity, differentiating into M1-like macrophages that secrete inflammatory factors (29,30). Interestingly, macrophages in obesity display unique characteristics and do not align with the classical activation phenotype (31). They accumulate lipids, express fatty acid transporters such as CD36, and exhibit markers associated with metabolic activation (31,32). These changes in macrophage activation contribute to obesity-related meta-inflammation, characterized by elevated pro-inflammatory cytokines and insulin resistance. The dysregulation of the adipose tissue immune system and the accumulation of inflammatory macrophages play crucial roles in the development and progression of metabolic disorders.

Lung macrophages

The phenotype and transcriptional signature of alveolar macrophages (AMs), which are macrophages specific to the lung tissue, are shaped by the surrounding lung microenvironment (33). They reside within the alveolar niche, which is composed of type I and type II alveolar epithelial cells, capillary endothelial cells, and alveolar interstitial fibroblasts. This niche provides a cytokine-rich environment that supports the survival and function of AMs (34).

In terms of abundance, the lung contains a significant number of AMs. For instance, the upper lobe of the human lung alone houses approximately 1.5×10^9 AMs. The majority of these macrophages are located in the diffusing area of the lung, where they are in close proximity to the gas-exchange region, while a smaller population is found in the conducting small airways (35). Traditionally, AMs were thought to be

a relatively homogeneous population of cells. However, recent advances in single-cell sequencing have revealed the heterogeneity of AMs in healthy individuals. Studies have identified at least four superclusters of AMs with distinct subclusters, characterized by different gene expression profiles (36).

One of the key factors contributing to the heterogeneity of AMs is the highly regulated production of specific combinations of chemokines, metallothioneins, interferon (IFN)-inducible genes, cholesterol-biosynthesis-related genes, and insulin-like growth factor 1 (IGF1) by different subsets of AMs. These subsets exhibit unique functional properties and may play specialized roles in immune responses and tissue homeostasis.

Moreover, the observed heterogeneity of AMs is not limited to healthy individuals but extends to various lung diseases. Studies investigating diseases such as cystic fibrosis, COPD, and COVID-19 have consistently demonstrated the presence of these superclusters and subclusters across different individuals and disease conditions. This suggests that the heterogeneity of AMs is a universal feature and may have implications for understanding the pathogenesis and progression of lung diseases (37).

In conclusion, lung macrophages, specifically alveolar macrophages, exhibit unique characteristics and heterogeneity in the lung microenvironment. They are highly abundant in the lung and display distinct gene expression profiles and functional properties. Understanding the heterogeneity of AMs has the potential to shed light on their diverse roles in lung health and disease.

METABOLIC REPROGRAMMING OF MACROPHAGES

Macrophages, as sentinel cells, need to respond rapidly to alterations in their microenvironment. They modify their metabolic pathways to ensure proper activation and function. One of the initial differences observed in macrophage metabolism during polarization is the alteration of amino acid metabolism. Classically activated macrophages convert arginine to nitric oxide (NO) and citrulline, while alternatively activated macrophages convert arginine to proline and polyamines (38). Furthermore, macrophages can reprogram their energy generation methods. Nonpolarized or alternatively activated macrophages use fatty acid beta-oxidation and mitochondrial oxidative phosphorylation (OXPHOS) to produce ATP (39). In contrast, pro-inflammatory stimuli induce a metabolic shift in macrophages towards aerobic glycolysis, similar to the Warburg effect observed in tumor cells (40). This metabolic reprogramming results in lactate secretion and the accumulation of citrate and succinate (41).

The metabolic reprogramming of macrophages has several consequences. First, there is a breakpoint in the tricarboxylic acid (TCA) cycle after citrate due to lower expression of isocitrate dehydrogenase, leading to citrate accumulation. Citrate can be transported to the cytosol (42) and converted into acetyl-CoA (43), which can be used for fatty acid synthesis or lysine acetylation of proteins. Second, there is a breakpoint after succinate caused by the inhibition of succinate dehydrogenase by itaconate, resulting in succinate accumulation. Succinate accumulation leads to the stabilization of the transcription factor HIF-1α (44), promoting the switch to glycolysis and inducing the expression of glycolytic enzymes. This metabolic shift also activates the pentose phosphate pathway, generating NADPH for ROS production (45). Additionally, HIF-1α promotes the expression of lactate dehydrogenase (46), which converts pyruvate to lactate, and pyruvate dehydrogenase kinase 1, inhibiting mitochondrial function further (47).

In summary, macrophages undergo metabolic reprogramming to adapt to different activation states. The shift towards glycolysis and altered metabolism of amino acids and fatty acids provide the necessary energy and biosynthetic precursors for macrophage activation and function during inflammatory responses (48).

ANALYSIS OF METABOLITES

Flow cytometry is commonly used to characterize macrophage phenotypes but does not provide information on cellular metabolism (49). Recent efforts have utilized flow cytometry with antibodies against metabolic enzymes to investigate single-cell metabolism, although quantitative insight into metabolite production and enzyme activity is still lacking (50). Other techniques such as extracellular flux analysis, colorimetric/fluorometric enzyme activity assays, and mass spectrometry (MS)-based metabolomics and flux analysis are used to measure the metabolic status of cells. Extracellular flux analyzers provide a functional readout of glycolytic or mitochondrial activity but do not directly measure individual metabolites (51). MS, coupled with gas or liquid chromatography, allows for detecting and quantifying a wide range of metabolites (52–54). Stable isotope labeling combined with MS can be used to study metabolic flux and pathway analysis (55). Targeted and untargeted MS methods can provide quantitative information on known metabolites as well as reveal new metabolites (56). Combining multiple analytical approaches, including metabolomics, lipidomics, fluxomics, transcriptomics, and proteomics, can help gain a comprehensive understanding of the mechanisms involved in macrophage metabolic reprogramming. This integrated approach has the potential to discover mechanistic links between inflammation and metabolic disturbances in chronic diseases.

IMMUNOMETABOLISM AND LYSINE ACETYLATION

The concept of immunometabolism involves the interaction between immune and metabolic processes (57). Recent research suggests that chronic inflammation is connected to changes in energy metabolism through lysine acetylation, a post-translational modification of proteins. Lysine acetylation alters the behavior of acetylated proteins, affecting their interactions with other molecules, catalytic activity, subcellular localization, and stability (58). Lysine acetyltransferases (KATs) and lysine deacetylases (KDACs) regulate the precise stoichiometry of site-specific lysine acetylation (59). KDACs are classified into four groups, while KATs are divided into three. Lysine acetylation can also occur non-enzymatically, especially in alkaline environments like the mitochondrial matrix (58). Fluctuations in acetyl-CoA concentration, which vary in different cellular compartments, can influence the catalytic activity and selectivity of KATs (60). Reversible protein acetylation plays a role in gene expression, affecting histones, transcription factors, and enzymes involved in cellular energy metabolism (61). Changes in glycolysis, the tricarboxylic acid cycle (TCA), and fatty acid oxidation impact cellular acetyl-CoA levels, establishing a connection between energy metabolism, protein acetylation, and gene expression.

Histone acetylation

Chromatin is a complex of DNA and proteins called histones. The nucleosome is the fundamental subunit of chromatin, which is formed of an octamer of histones, an H3/H4 tetramer, and two H2A/H2B dimers, around which 146 bp of DNA is wrapped (62). The conformation of the chromatin changes to allow gene transcription due to changes in the histone acetylation stoichiometry and dynamics (63)

Histone acetylation is a key component in the regulation of gene expression: during activation of gene transcription, chromatin conformation changes from tightly compacted to relaxed, allowing DNA binding proteins to interact with the DNA. The interaction of positively-charged epsilon amino groups in histones belonging to lysine residues with the negatively charged phosphate groups of DNA will decrease due to the removal of the positive charges on the histones upon acetylation.

The fact that acetylation is a key component in the regulation of gene expression and that elevated levels of histone deacetylation are evident in several chronic human diseases has motivated the study of KDACs in relation to the often observed aberrant gene expression.

The KDAC family consists of different classes of enzymes involved in the regulation of protein acetylation. Class I KDACs, including KDAC1, 2, 3, and 8, are primarily

located in the nucleus due to the absence of a nuclear export signal sequence. KDAC3, however, has a nuclear export signal and can be found in both the cytoplasmic and nuclear compartments. Class I KDACs are widely distributed in various tissues (64). Class II KDACs, divided into IIA (KDAC4, 5, 7, 9) and IIB (KDAC6, 10), can shuttle between the nucleus and cytoplasm in response to cellular signals (65). Sirtuins, the third group of KDACs, rely on NAD hydrolysis for their deacetylase activity and are located in different subcellular compartments. For example, SIRT1, SIRT6, and SIRT7 are found in the nucleus, SIRT2 is primarily cytosolic, and SIRT3–5 are located in mitochondria. Recent research has highlighted the role of sirtuins in connecting deacetylation with cellular metabolism, as deacetylation is responsive to metabolic cues (66). Additionally, KDAC11, the sole member of its class, shares similarities with both Class I and II KDACs. KDAC11 is involved in regulating the protein stability of DNA replication factor CDT1 (67) and negatively regulates the expression of interleukin 10, leading to an inflammatory response when overexpressed (68).

KDAC inhibitors

Lysine deacetylases (KDACs) are regulated by protein-protein interactions, post-translational modifications, and subcellular localization. Dysregulation of KDACs is associated with various human diseases, leading to the development of KDAC inhibitors (KDACi) as therapeutic agents. Clinical trials have resulted in the approval of vorinostat and romidepsin for the treatment of cutaneous T-cell lymphoma (69). Classical KDACi act on Class I, II, and Class IV HDACs by binding to the zinc ion in the catalytic pocket. They inhibit deacetylation by preventing the binding of the natural substrate. On the other hand, romidepsin inhibits KDAC enzymatic activity by interacting with the zinc ion through its reduced disulfide bond (70). However, these inhibitors are not highly specific and can cause side effects. Newer KDACi, such as MS-275 (entinostat), based on a benzamide group as a Zn2+ binder, offer improved specificity. Class III KDACs, which are NAD+-dependent, can be inhibited by compounds like nicotinamide and derivatives of NAD (71).

SCOPE OF THIS THESIS

The work described in this thesis aimed to improve our understanding of the different phenotypes and functional properties of macrophages in chronic inflammation, specifically in the different tissue niches. Particular attention was paid to the role of metabolism in macrophage characterization.

In **Chapter 2,** macrophages' role in the development of obesity and diabetes mellitus type II was reviewed. Insight into the different subsets associated with these diseases and how their metabolism changes depending on their microenvironment was provided. This chapter also describes different available possibilities for measuring cellular metabolites.

In **Chapter 3**, we investigated whether the shown anti-inflammatory effects of KDACis in the COPD context apply also in our cell model of primary murine alveolar-like macrophages after lipopolysaccharide (LPS)-induced activation. We hypothesized that these anti-inflammatory effects may be associated with metabolic changes in macrophages. To validate this hypothesis, an unbiased and a targeted proteomic approach to investigate metabolic enzymes as well as LC- and GC-MS to quantify metabolites in combination with the measurement of functional parameters was used. While minimal metabolic changes were observed, KDAC inhibition reduced the production of inflammatory mediators. Interestingly, it specifically enhanced the expression of proteins involved in ubiquitination. The findings highlight the potential of KDAC inhibitors as anti-inflammatory drugs for diseases like COPD.

In **Chapter 4**, primary murine alveolar-like macrophages to examine the impact of collagen morphology on macrophage marker expression, behaviour, and shape were used. Proteomic analysis revealed increased expression of glycolysis-related proteins, although this did not result in higher glycolytic activity, potentially due to reduced enzyme activity. Overall, our findings indicate that macrophages can detect collagen morphologies and adjust the expression and activity of metabolism-related proteins. This suggests a significant interplay between macrophages and their microenvironment, which could be crucial in the progression of tissue repair to fibrosis in the lungs.

Finally, in **Chapter 5**, the conclusions of this thesis are summarized and future implications are examined. The research presented in this thesis establishes a foundation for gaining a deeper understanding of macrophages and their intricate relationship with metabolism, as well as the implications of these metabolic changes in chronic diseases. These findings open up possibilities for therapeutic interventions targeting chronic inflammation.

REFERENCES

1. Adeloye D, Song P, Zhu Y, Campbell H, Sheikh A, Rudan I. Global, regional, and national prevalence of, and risk factors for, chronic obstructive pulmonary disease (COPD) in 2019: a systematic review and modelling analysis. *Lancet Respir Med* (2022) 10:447–458. doi: 10.1016/S2213-2600(21)00511-7

2. Vogelmeier CF, Criner GJ, Martinez FJ, Anzueto A, Barnes PJ, Bourbeau J, Celli BR, Chen R, Decramer M, Fabbri LM, et al. Global strategy for the diagnosis, management, and prevention of chronic obstructive lung disease 2017 report. *Am J Respir Crit Care Med* (2017) 195:557–582. doi: 10.1164/RCCM.201701-0218PP

3. Ogurtsova K, da Rocha Fernandes JD, Huang Y, Linnenkamp U, Guariguata L, Cho NH, Cavan D, Shaw JE, Makaroff LE. IDF Diabetes Atlas: Global estimates for the prevalence of diabetes for 2015 and 2040. *Diabetes Res Clin Pract* (2017) 128:40–50. doi: 10.1016/j.diabres.2017.03.024

4. Madan S. Changes in Diabetes-Related Complications in the United States. *New England Journal of Medicine* (2014) 371:284–287. doi: 10.1056/NEJMc1406009

5. Association AD. Diagnosis and classification of diabetes mellitus. *Diabetes Care* (2009) 32:S62–S67. doi: 10.2337/dc09-S062

6. Wellen KE, Hotamisligil GS. Inflammation, stress, and diabetes. *Journal of Clinical Investigation* (2005) 115:1111–1119. doi: 10.1172/jci25102

7. Vachharajani V, Granger DN. Adipose tissue: A motor for the inflammation associated with obesity. *IUBMB Life* (2009) 61:424–430. doi: 10.1002/iub.169

8. Satoh J, Yagihashi S, Toyota T. The Possible Role of Tumor Necrosis Factor-α in Diabetic Polyneuropathy. *Exp Diabesity Res* (2003) 4:65. doi: 10.1155/EDR.2003.65

9. Hotamisligil GS, Shargill NS, Spiegelman BM. Adipose expression of tumor necrosis factor-α: Direct role in obesity-linked insulin resistance. *Science (1979)* (1993) 259:87–91. doi: 10.1126/science.7678183

10. Ginhoux F, Jung S. Monocytes and macrophages: Developmental pathways and tissue homeostasis. *Nat Rev Immunol* (2014) 14:392–404. doi: 10.1038/nri3671

11. Geissmann F, Jung S, Littman DR. Blood monocytes consist of two principal subsets with distinct migratory properties. *Immunity* (2003) 19:71–82. doi: 10.1016/S1074-7613(03)00174-2

12. Varol C, Mildner A, Jung S. Macrophages: Development and Tissue Specialization. *Annu Rev Immunol* (2015) 33:643–675. doi: 10.1146/annurev-immunol-032414-112220

13. Patel PS, Buras ED, Balasubramanyam A. The role of the immune system in obesity and insulin resistance. *J Obes* (2013) 2013: doi: 10.1155/2013/616193

14. Geissmann F, Manz MG, Jung S, Sieweke MH, Merad M, Ley K. Development of Monocytes, Macrophages, and Dendritic Cells. http://science.sciencemag.org/

15. Italiani P, Boraschi D. From Monocytes to M1/M2 Macrophages: Phenotypical vs. Functional Differentiation. *Front Immunol* (2014) 5: doi: 10.3389/fimmu.2014.00514

16. Murray PJ. Macrophage Polarization. *The Annual Review of Physiology is online at* (2017) 79:541–66. doi: 10.1146/annurev-physiol-022516-034339

17. Martinez FO, Helming L, Gordon S. Alternative Activation of Macrophages: An Immunologic Functional Perspective. *Annu Rev Immunol* (2009) 27:451–483. doi: 10.1146/annurev.immunol.021908.132532

18. Reyes JL, Terrazas LI. The divergent roles of alternatively activated macrophages in helminthic infections. *Parasite Immunol* (2007) 29:609–619. doi: 10.1111/j.1365-3024.2007.00973.x

19. Luca C, Edana C, Guido P. Macrophage Polarization in Health and Disease. *Hindawi* (2011) 11: doi: 10.1100/2011/213962

20. Satoh T, Takeuchi O, Vandenbon A, Yasuda K, Tanaka Y, Kumagai Y, Miyake T, Matsushita K, Okazaki T, Saitoh T, et al. The Jmjd3-Irf4 axis regulates M2 macrophage polarization and host responses against helminth infection. *Nature Immunology 2010 11:10* (2010) 11:936–944. doi: 10.1038/ni.1920

21. Mantovani A, Sica A, Sozzani S, Allavena P, Vecchi A, Locati M. The chemokine system in diverse forms of macrophage activation and polarization. *Trends Immunol* (2004) 25:677–686. doi: 10.1016/J.IT.2004.09.015

22. Saely CH, Geiger K, Drexel H. Brown versus White Adipose Tissue: A Mini-Review. *Gerontology* (2012) 58:15–23. doi: 10.1159/000321319

23. Bays HE, González-Campoy JM, Bray GA, Kitabchi AE, Bergman DA, Schorr AB, Rodbard HW, Henry RR. Pathogenic potential of adipose tissue and metabolic consequences of adipocyte hypertrophy and increased visceral adiposity. *Expert Rev Cardiovasc Ther* (2008) 6:343–368. doi: 10.1586/14779072.6.3.343

24. O'rourke RW, White AE, Metcalf MD, Olivas AS, Mitra P, Larison WG, Cheang EC, Varlamov O, Corless CL, Roberts CT, et al. Hypoxia-induced inflammatory cytokine secretion in human adipose tissue stromovascular cells. *Diabetologia* (2011) 54:1480–1490. doi: 10.1007/s00125-011-2103-y

25. Engin A. "Adipose tissue hypoxia in obesity and its impact on preadipocytes and macrophages: Hypoxia hypothesis.," *Advances in Experimental Medicine and Biology*. Springer New York LLC (2017). p. 305–326 doi: 10.1007/978-3-319-48382-5_13

26. Monteiro R, Azevedo I. Chronic Inflammation in Obesity and the Metabolic Syndrome. *Mediators Inflamm* (2010) 2010:1–10. doi: 10.1155/2010/289645

27. Cucak H, Grunnet LG, Rosendahl A. Accumulation of M1-like macrophages in type 2 diabetic islets is followed by a systemic shift in macrophage polarization. *J Leukoc Biol* (2014) 95:149–60. doi: 10.1189/jlb.0213075

28. Tilg H, Moschen AR. Inflammatory Mechanisms in the Regulation of Insulin Resistance. *Molecular Medicine* (2008) 14:222–231. doi: 10.2119/2007-00119.Tilg

29. Dalmas E, Clément K, Guerre-Millo M. Defining macrophage phenotype and function in adipose tissue. *Trends Immunol* (2011) 32:307–314. doi: 10.1016/j.it.2011.04.008

30. Donath MY, Dalmas É, Sauter NS, Böni-Schnetzler M. Inflammation in obesity and diabetes: Islet dysfunction and therapeutic opportunity. *Cell Metab* (2013) 17:860–872. doi: 10.1016/j.cmet.2013.05.001

31. Kratz M, Coats BR, Hisert KB, Hagman D, Mutskov V, Peris E, Schoenfelt KQ, Kuzma JN, Larson I, Billing PS, et al. Metabolic dysfunction drives a mechanistically distinct proinflammatory phenotype in adipose tissue macrophages. *Cell Metab* (2014) 20:614–625. doi: 10.1016/j.cmet.2014.08.010

32. Castoldi A, de Souza CN, Saraiva Câmara NO, Moraes-Vieira PM. The macrophage switch in obesity development. *Front Immunol* (2016) 6: doi: 10.3389/fimmu.2015.00637

33. Gautiar EL, Shay T, Miller J, Greter M, Jakubzick C, Ivanov S, Helft J, Chow A, Elpek KG, Gordonov S, et al. Gene expression profiles and transcriptional regulatory pathways underlying mouse tissue macrophage identity and diversity. *Nat Immunol* (2012) 13:1118. doi: 10.1038/NI.2419

34. Westphalen K, Gusarova GA, Islam MN, Subramanian M, Cohen TS, Prince AS, Bhattacharya J. Sessile alveolar macrophages communicate with alveolar epithelium to modulate immunity. *Nature* (2014) 506:503–506. doi: 10.1038/nature12902

35. Hume PS, Gibbings SL, Jakubzick C V., Tuder RM, Curran-Everett D, Henson PM, Smith BJ, Janssen WJ. Localization of Macrophages in the Human Lung via Design-based Stereology. *Am J Respir Crit Care Med* (2020) 201:1209–1217. doi: 10.1164/rccm.201911-2105OC

36. Mould KJ, Moore CM, McManus SA, McCubbrey AL, McClendon JD, Griesmer CL, Henson PM, Janssen WJ. Airspace Macrophages and Monocytes Exist in Transcriptionally Distinct Subsets in Healthy Adults. *Am J Respir Crit Care Med* (2021) 203:946–956. doi: 10.1164/rccm.202005-1989OC

37. Li X, Kolling FW, Aridgides D, Mellinger D, Ashare A, Jakubzick C V. ScRNA-seq expression of IFI27 and APOC2 identifies four alveolar macrophage superclusters in healthy BALF. *Life Sci Alliance* (2022) 5:e202201458. doi: 10.26508/lsa.202201458

38. Modolell M, Corraliza IM, Link F, Soler G, Eichmann K. Reciprocal regulation of the nitric oxide synthase/arginase balance in mouse bone marrow□derived macrophages by TH 1 and TH 2 cytokines. *Eur J Immunol* (1995) 25:1101–1104. doi: 10.1002/eji.1830250436

39. Huang SC-C, Everts B, Ivanova Y, O'Sullivan D, Nascimento M, Smith AM, Beatty W, Love-Gregory L, Lam WY, O'Neill CM, et al. Cell-intrinsic lysosomal lipolysis is essential for alternative activation of macrophages. *Nature Immunology 2014 15:9* (2014) 15:846–855. doi: 10.1038/ni.2956

40. Newsholme P, Curi R, Gordon S, Newsholme EA. Metabolism of glucose, glutamine, long-chain fatty acids and ketone bodies by murine macrophages. *Biochemical Journal* (1986) 239:121–125. doi: 10.1042/bj2390121

41. Ryan DG, O'neill LAJ. Krebs Cycle Reborn in Macrophage Immunometabolism. *Annual Review of Immunology* (2020) 38:289–313. doi: 10.1146/annurev-immunol-081619

42. Infantino V, Convertini P, Cucci L, Panaro MA, di Noia MA, Calvello R, Palmieri F, Iacobazzi V. The mitochondrial citrate carrier: A new player in inflammation. *Biochemical Journal* (2011) 438:433–436. doi: 10.1042/BJ20111275

43. Lauterbach MA, Hanke JE, Serefidou M, Mangan MSJ, Kolbe C-C, Hess T, Rothe M, Kaiser R, Hoss F, Gehlen J, et al. Toll-like Receptor Signaling Rewires Macrophage Metabolism and Promotes Histone Acetylation via ATP-Citrate Lyase. *Immunity* (2019) 51:997-1011.e7. doi: 10.1016/J.IMMUNI.2019.11.009

44. Tannahill GM, Curtis AM, Adamik J, Palsson-Mcdermott EM, McGettrick AF, Goel G, Frezza C, Bernard NJ, Kelly B, Foley NH, et al. Succinate is an inflammatory signal that induces IL-1β through HIF-1α. *Nature* (2013) 496:238–242. doi: 10.1038/nature11986

45. O'Neill LAJ, Kishton RJ, Rathmell J. A guide to immunometabolism for immunologists. *Nat Rev Immunol* (2016) 16:553–565. doi: 10.1038/nri.2016.70

46. Kelly B, O'Neill LAJ. Metabolic reprogramming in macrophages and dendritic cells in innate immunity. *Cell Res* (2015) 25:771–784. doi: 10.1038/cr.2015.68

47. Papandreou I, Cairns RA, Fontana L, Lim AL, Denko NC. HIF-1 mediates adaptation to hypoxia by actively downregulating mitochondrial oxygen consumption. *Cell Metab* (2006) 3:187–197. doi: 10.1016/j.cmet.2006.01.012

48. Caslin HL, Bhanot M, Bolus WR, Hasty AH. Adipose tissue macrophages: Unique polarization and bioenergetics in obesity. *Immunol Rev* (2020) 295:101–113. doi: 10.1111/imr.12853

49. Nicola NA, Burgess AW, Staber FG, Johnson GR, Metcalf D, Battye FL. Differential expression of lectin receptors during hemopoietic differntiation: Enrichment for granulocyte□macrophage progenitor cells. *J Cell Physiol* (1980) 103:217–237. doi: 10.1002/jcp.1041030207

50. Ahl PJ, Hopkins RA, Xiang WW, Au B, Kaliaperumal N, Fairhurst AM, Connolly JE. Met-Flow, a strategy for single-cell metabolic analysis highlights dynamic changes in immune subpopulations. *Commun Biol* (2020) 3:1–15. doi: 10.1038/s42003-020-1027-9

51. van den Bossche J, Baardman J, de Winther MPJ. Metabolic characterization of polarized M1 and M2 bone marrow-derived macrophages using real-time extracellular flux analysis. *Journal of Visualized Experiments* (2015) 2015:53424. doi: 10.3791/53424

52. Pinu FR, Beale DJ, Paten AM, Kouremenos K, Swarup S, Schirra HJ, Wishart D. Systems biology and multi-omics integration: Viewpoints from the metabolomics research community. *Metabolites* (2019) 9:76. doi: 10.3390/metabo9040076

53. Patti GJ, Yanes O, Siuzdak G. Innovation: Metabolomics: the apogee of the omics trilogy. *Nat Rev Mol Cell Biol* (2012) 13:263–269. doi: 10.1038/nrm3314

54. Kuehnbaum NL, Britz-Mckibbin P. New advances in separation science for metabolomics: Resolving chemical diversity in a post-genomic era. *Chem Rev* (2013) 113:2437–2468. doi: 10.1021/cr300484s

55. Yuan J, Bennett BD, Rabinowitz JD. Kinetic flux profiling for quantitation of cellular metabolic fluxes. *Nat Protoc* (2008) 3:1328–1340. doi: 10.1038/nprot.2008.131

56. Puchalska P, Huang X, Martin SE, Han X, Patti GJ, Crawford PA. Isotope Tracing Untargeted Metabolomics Reveals Macrophage Polarization-State-Specific Metabolic Coordination across Intracellular Compartments. *iScience* (2018) 9:298–313. doi: 10.1016/j.isci.2018.10.029

57. Mathis D, Shoelson SE. Immunometabolism: an emerging frontier. *Nature Reviews Immunology* (2011) 11:81–83. doi: 10.1038/nri2922

58. Choudhary C, Weinert BT, Nishida Y, Verdin E, Mann M. The growing landscape of lysine acetylation links metabolism and cell signalling. *Nat Rev Mol Cell Biol* (2014) 15:536–550. doi: 10.1038/nrm3841

59. Kim G-W, Gocevski G, Wu C-J, Yang X-J. Dietary, Metabolic, and Potentially Environmental Modulation of the Lysine Acetylation Machinery. *Int J Cell Biol* (2010) 2010:1–14. doi: 10.1155/2010/632739

60. Henry RA, Kuo Y-M, Bhattacharjee V, Yen TJ, Andrews AJ. Changing the Selectivity of p300 by Acetyl-CoA Modulation of Histone Acetylation. *ACS Chem Biol* (2015) 10:146–156. doi: 10.1021/cb500726b

61. Zhao S, Xu W, Jiang W, Yu W, Lin Y, Zhang T, Yao J, Zhou L, Zeng Y, Li H, et al. Regulation of cellular metabolism by protein lysine acetylation. *Science (1979)* (2010) 327:1000–1004. doi: 10.1126/science.1179689

62. Strahl BD, Allis CD. The language of covalent histone modifications. *Nature* (2000) 403:41–45. doi: 10.1038/47412

63. RUIJTER AJM de, GENNIP AH van, CARON HN, KEMP S, KUILENBURG ABP van. Histone deacetylases (HDACs): characterization of the classical HDAC family. *Biochemical Journal* (2003) 370:737–749. doi: 10.1042/bj20021321

64. Yang X-J, Seto E. The Rpd3/Hda1 family of lysine deacetylases: from bacteria and yeast to mice and men. *Nat Rev Mol Cell Biol* (2008) 9:206–218. doi: 10.1038/nrm2346

65. Morris MJ, Monteggia LM. Unique functional roles for class I and class II histone deacetylases in central nervous system development and function. *International Journal of Developmental Neuroscience* (2013) 31:370–381. doi: 10.1016/j.ijdevneu.2013.02.005

66. Vaquero A, Sternglanz R, Reinberg D. NAD+-dependent deacetylation of H4 lysine 16 by class III HDACs. *Oncogene* (2007) 26:5505–5520. doi: 10.1038/sj.onc.1210617

67. Glozak MA, Seto E. Acetylation/Deacetylation Modulates the Stability of DNA Replication Licensing Factor Cdt1. *Journal of Biological Chemistry* (2009) 284:11446–11453. doi: 10.1074/jbc.M809394200

68. Villagra A, Cheng F, Wang H-W, Suarez I, Glozak M, Maurin M, Nguyen D, Wright KL, Atadja PW, Bhalla K, et al. The histone deacetylase HDAC11 regulates the expression of interleukin 10 and immune tolerance. *Nat Immunol* (2009) 10:92–100. doi: 10.1038/ni.1673

69. Khan O, La Thangue NB. HDAC inhibitors in cancer biology: emerging mechanisms and clinical applications. *Immunol Cell Biol* (2012) 90:85–94. doi: 10.1038/icb.2011.100

70. Valdez BC, Brammer JE, Li Y, Murray D, Liu Y, Hosing C, Nieto Y, Champlin RE, Andersson BS. Romidepsin targets multiple survival signaling pathways in malignant T cells. *Blood Cancer J* (2015) 5:e357–e357. doi: 10.1038/bcj.2015.83

71. Porcu M, Chiarugi A. The emerging therapeutic potential of sirtuin-interacting drugs: from cell death to lifespan extension. *Trends Pharmacol Sci* (2005) 26:94–103. doi: 10.1016/j.tips.2004.12.009

2

Chapter 2

Meta-inflammation and metabolic reprogramming of macrophages in diabetes and obesity: the importance of metabolites

Sara Russo [1], Marcel Kwiatkowski [2], Natalia Govorukhina [1], Rainer Bischoff [1†], Barbro N. Melgert [3,4†*]

Frontiers in Immunology 2021; 12: 746151.
Published online 2021 Nov 5. doi: 10.3389/fimmu.2021.746151

ABSTRACT

Diabetes mellitus type II and obesity are two important causes of death in modern society. They are characterized by low-grade chronic inflammation and metabolic dysfunction (meta-inflammation), which is observed in all tissues involved in energy homeostasis. A substantial body of evidence has established an important role for macrophages in these tissues during the development of diabetes mellitus type II and obesity. Macrophages can activate into specialized subsets by cues from their microenvironment to handle a variety of tasks. Many different subsets have been described and in diabetes/obesity literature two main classifications are widely used that are also defined by differential metabolic reprogramming taking place to fuel their main functions. Classically activated, pro-inflammatory macrophages (often referred to as M1) favor glycolysis, produce lactate instead of metabolizing pyruvate to acetyl-CoA, and have a tricarboxylic acid cycle that is interrupted at two points. Alternatively activated macrophages (often referred to as M2) mainly use beta-oxidation of fatty acids and oxidative phosphorylation to create energy-rich molecules such as ATP and are involved in tissue repair and downregulation of inflammation. Since diabetes type II and obesity are characterized by metabolic alterations at the organism level, these alterations may also induce changes in macrophage metabolism resulting in unique macrophage activation patterns in diabetes and obesity. This review describes the interactions between metabolic reprogramming of macrophages and conditions of metabolic dysfunction like diabetes and obesity. We also focus on different possibilities of measuring a range of metabolites intra-and extracellularly in a precise and comprehensive manner to better identify the subsets of polarized macrophages that are unique to diabetes and obesity. Advantages and disadvantages of the currently most widely used metabolite analysis approaches are highlighted. We further describe how their combined use may serve to provide a comprehensive overview of the metabolic changes that take place intracellularly during macrophage activation in conditions like diabetes and obesity.

Keywords: M1, M2, Metabolic syndrome, DMTII, alternatively activated, classically activated, Metabolite analysis, MS.

INTRODUCTION

Diabetes mellitus type II (DMTII) is one of the main causes of death in modern society according to the World Health Organization (1). It correlates with long-term complications that include nephropathy, peripheral neuropathy, and cardiovascular disease. The International Diabetes Federation has estimated that globally the diagnosis of DMTII has been made in 415 million people and anticipates growth to up to 642 million by the year 2040 (2).

Several factors can contribute to a higher risk of developing DMTII, but it has been proven that overweight or obesity are the most important ones (3). DMTII is often linked to obesity and both are associated with metabolic syndrome, which encompasses conditions such as high blood pressure, excess body fat around the waist, high blood sugar, high serum cholesterol or triglyceride levels, and low high-density lipoprotein (HDL) cholesterol. Metabolic syndrome is characterized by low-grade chronic inflammation (meta-inflammation) (4) in all tissues involved in energy homeostasis, including adipose tissue, pancreatic islets, and liver (5). Studies have shown that the metabolic consequences of adipose tissue dysfunction increase mortality in patients with DMTII, emphasizing the importance of meta-inflammation in the context of DMTII (6)

Macrophages are part of the innate immune system and are present in all tissues of our body, including adipose tissues (7). They play a crucial role in the first line of defense against microorganisms and other external or internal threats to homeostasis by initiating essential inflammatory responses (8). These inflammatory responses are facilitated by changes in macrophage cellular metabolism, with a focus on glycolysis that is induced in cells producing inflammatory mediators. The inflammatory response is counter-balanced by stimulation of tissue repair and anti-inflammatory mechanisms once the threat has been overcome. At the same time, the cellular metabolism changes from glycolysis to oxidative phosphorylation to aid in tissue repair. Continuous exposure to pro-inflammatory stimuli, however, can shift the balance of inflammation and repair in favor of chronic inflammation and tissue damage. Excessive activation of macrophage inflammatory responses is seen in many diseases characterized by the continuous presence of pro-inflammatory stimuli, including DMTII, and explains in part the meta-inflammation found in this condition.

Many studies have described how macrophages become activated by inflammatory stimuli (9,10) and there is increasing consensus that a particular macrophage activation state is associated with DMTII. Characterization of the different macrophage activation states is complicated, but in recent years has been aided by the development and use of novel techniques like multiparametric flow cytometry,

single-cell RNA sequencing, and real-time extracellular flux analysis. Especially the latter has the potential to improve our understanding of how macrophages can switch between different types of responses. In DMTII and obesity, the changes in macrophage cellular metabolism coincide with profound changes in metabolism on a tissue and organism level, that probably interact and give rise to a specific DMTII-associated macrophage activation state (11). This review aims to summarize what is currently known about macrophage activation in DMTII-related meta-inflammation, how changes in intracellular metabolism are influenced by the changed presence in extracellular nutrients and metabolites, and how fluctuations in key metabolic intermediates could also play a role in cellular processes like gene expression. This overview emphasizes that profiling metabolites can help to characterize macrophages and their responses and to understand how changes in their intracellular metabolites affect DMTII progression. Therefore, we finish with a comparison between different approaches to metabolite analysis to provide an overview of the currently available methods and their pros and cons, highlighting metabolomics studies that have made use of these methods and have been central to characterizing macrophages.

INSULIN RESISTANCE AND INFLAMMATION

One of the key characteristics of DMTII is the altered insulin response. In healthy individuals, with a body mass index (BMI) in the normal range, pancreatic β cells produce insulin in response to circulating glucose levels. This will bind and activate insulin receptors on the cell membrane of different cell types, including macrophages, to lower blood glucose levels by enhancing its uptake by these cells. The binding of insulin to its receptor drives a cascade of events ultimately leading to uptake of glucose and further downstream effects (**Figure 1**). First glucose transporters, GLUT4 in most cell types and GLUT1 in macrophages, will either translocate from vesicles in the cytoplasm to the cell surface or their expression is upregulated, both increasing glucose influx into cells up to 10 times (12). Mammalian target of rapamycin (mTOR) will then be activated and protein synthesis will be induced. Furthermore, glycogen synthase kinase-3β (GSK3B) is inhibited allowing the activation of glycogen synthesis. When GSK3B is activated, it phosphorylates and inactivates glycogen synthase, decreasing glycogen synthesis, therefore GSK3B inhibition by Akt results in higher glycogen production. A change in gene transcription will also be initiated: expression of genes that favor either the synthesis of glycogen from glucose in the liver and muscles or of triglycerides from free fatty acids (FFA) in adipocytes will be induced and expression of genes that favor glycolysis will be transiently inhibited (13).

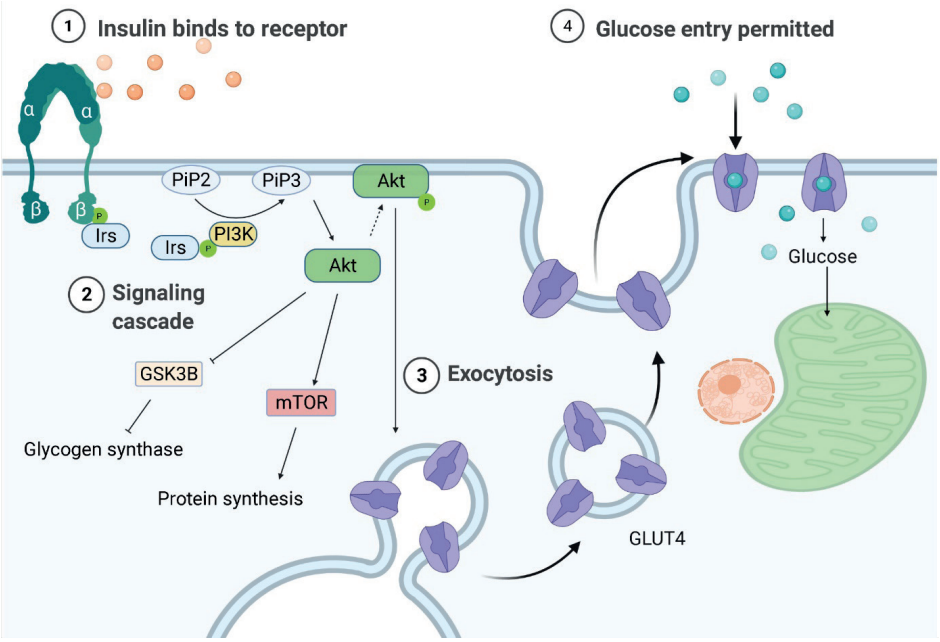

Figure 1: Regulation of glucose entrance through insulin signaling. Insulin receptors are tyrosine kinases consisting of two extracellular α-subunits and two transcellular β-subunits. In healthy individuals, insulin will bind the α subunit of the insulin receptor, causing a conformational change that leads to phosphorylation of tyrosine residues in its β subunit. The proteins insulin receptor substrates 1 or 2 (Irs-1/-2) will then bind to the tyrosine-phosphorylated region of insulin receptors and be themselves phosphorylated. Phosphoinositide-3-kinase (PI3K) will bind to the phosphorylated IRS-1 or -2 and be activated, producing 3-phosphorylated polyphosphoinositides (PiP3) from phosphatidylinositol 4,5-bisphosphate (PiP2). PiP3 will recruit the serine/threonine kinase Akt (also known as protein kinase B) from the cytosol to the plasma membrane, where it will be phosphorylated and activated, leading to glycogen synthase kinase-3β (GSK3B) inhibition and therefore to higher glycogen synthesis. AKT is also responsible for the translocation of the glucose transporter (GLUT) to the plasma membrane, allowing glucose entry.

DMTII is caused by the development of insulin resistance, meaning the inability of cells to respond to insulin due to a transmission blockage of the insulin receptor, mainly in muscle and liver cells. Pancreatic β-cells will at first try to compensate for the higher levels of glucose by increasing insulin production. This will eventually lead to lower glucose availability in combination with lower tissue insulin sensitivity resulting in loss of β-cell function. This will result in lower insulin secretion, which will consequently lead to a higher concentration of glucose in blood (14).

Insulin resistance can be caused by many different factors, with obesity being the most important one (14). Elevated levels of circulating free fatty acids are one of the reasons for the development of insulin resistance in obese patients. These

high levels of fatty acids are caused by increased basal lipolysis in adipose tissues and this elevated concentration has been proposed to serve as a stimulus for the entry and accumulation of macrophages in adipose tissue by increasing the local production and release of pro-inflammatory cytokines and chemokines (15). High concentrations of saturated free fatty acids will also induce pro-inflammatory effects through activation of Toll-like receptors (16). A consequence of this activation is the induction of the Jun N-terminal kinase and inhibitor of κB kinase (JNK/IKK-κB) pathways, which is then followed by an inflammatory cascade. Both JNK and IKK are believed to promote insulin resistance because they phosphorylate serine/threonine residues on insulin receptor substrate (IRS) proteins. By phosphorylating these residues, their phosphorylation by insulin receptors is blocked, which prevents the activation of insulin receptors by insulin. The result is inhibition of insulin-driven signal transduction and downstream effects thus inhibiting glucose entry into the cell and its accumulation in the blood.

MACROPHAGES AND INFLAMMATION IN OBESITY AND DMTII

The inflammation related to obesity was first described in 1993 when Hotamisligil *et al.* showed that adipose tissue from obese rats expressed more tumor necrosis factor-α (TNF-α) (17) than adipose tissue from lean animals. Weisberg and colleagues further showed that TNF-α was not secreted by adipocytes but by macrophages and that the number of macrophages increased in adipose tissue during weight gain (10). Macrophages develop either from self-renewing fetal progenitors that can populate tissues before birth and maintain their numbers after birth or from circulating monocytes recruited to tissues after birth (18). Studies have shown a higher number of macrophages in white adipose tissue of obese subjects compared to people of normal BMI, going from 10% of total cells to more than 50% (19). The origin of these macrophages, either through local proliferation or monocyte recruitment, remains to be established in detail. A recent study in mice found that local proliferation of adipose tissue-resident macrophages at least contributes to macrophage accumulation during obesity too (20).

Studies have shown that during obesity, triglyceride accumulation causes stress on adipocytes due to an increase in cell size and subsequent hypoxia (21). Capillary network development cannot keep up with fat mass expansion, resulting in adipocytes that are too far away from the vasculature to be efficiently supplied with oxygen (22). This leads to higher expression of hypoxia-inducible factor, adipocyte activation, and production and subsequent release of free fatty acids and pro-inflammatory mediators such as interleukin-1β (IL-1β), IL-6, macrophage migration inhibitory factor (MIF), monocyte chemoattractant protein 1 (MCP-1, also

known as CCL2), as well as reactive oxygen species (ROS). Further studies showed that ROS, together with the increased adipocytes size, will induce endoplasmic reticulum stress, leading to a pro-inflammatory and insulin-resistant phenotype in adipocytes (23). The pro-inflammatory mediators were found to induce recruitment of circulating monocytes and accumulation of adipose tissue macrophages (24).

Macrophages can respond in many different ways to stimuli from their microenvironment. In the past, this was described as macrophage activation, but since the discovery of the many different types of responses of macrophages, this is also called macrophage polarization (25). Polarized macrophages were broadly classified into two main groups, i.e. classically activated (or M1) macrophages and alternatively activated (or M2) macrophages, similar to the T helper 1/T helper 2 (Th1/Th2) dichotomy of helper T lymphocytes (26). However, it is now recognized that this view is too simplistic and that polarization states are better described as a continuous spectrum of responses (27).

Macrophage responses are currently mostly described by a combination of expression of extracellular and intracellular markers, including production of specific cytokines. The most widely studied and longest known activation response, i.e. classical activation, is induced by pro-inflammatory stimuli generated by infections with micro-organisms (25). These classically activated macrophages (often still called M1 macrophages) possess high antigen-presenting capacity and high potency to produce pro-inflammatory cytokines such as tumor necrosis factor-α (TNF-α), interleukin-12 (IL-12), IL-1β, and IL-23, as well as toxic mediators, such as ROS and nitric oxide (NO) (28). This type of response induces and supports Th1 responses (29). Phenotypically, classically activated macrophages express high levels of major histocompatibility complex class II (MHC II) proteins, and co-stimulatory molecules CD80 and CD86 in humans (7,30), as shown in **Figure 2**.

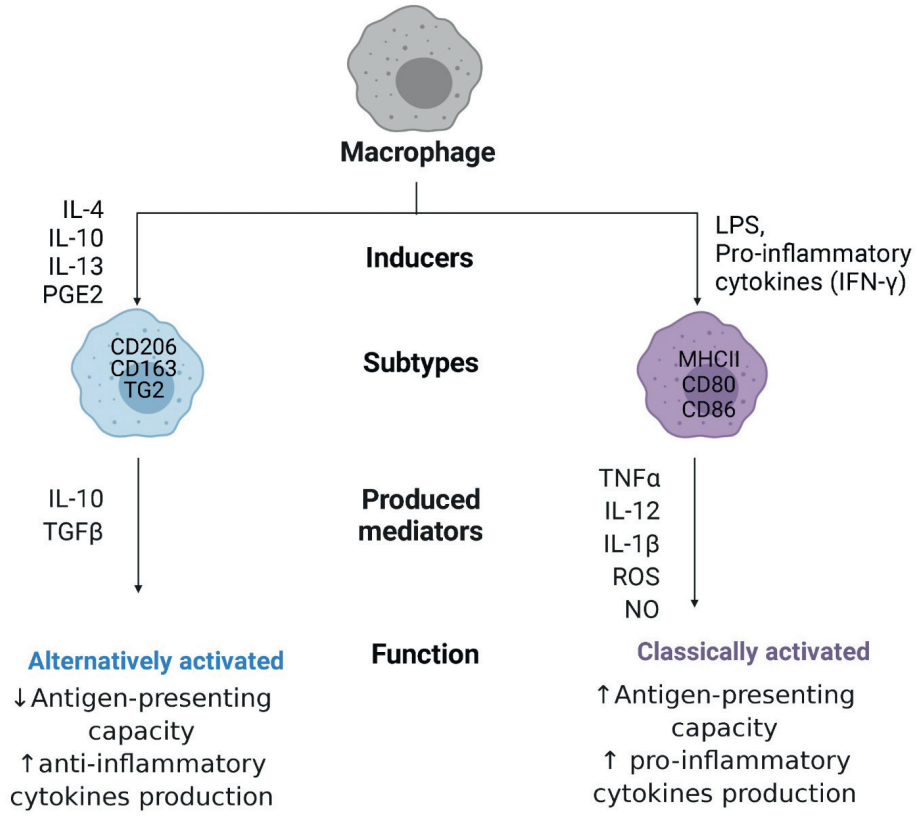

Figure 2: Macrophage polarization. Macrophages can polarize to classically activated macrophages, when stimulated with pro-inflammatory cytokines like interferon-γ (IFN-γ) or with bacterial products (LPS, lipopolysaccharides), or alternatively activated macrophages, when stimulated with interleukins 4,10, 13 (IL-4/10/13), or prostaglandin E2 (PGE2). Classically activated macrophages express major histocompatibility complex class II (MHC II) proteins and co-stimulatory molecules CD80 and CD86, while alternatively activated macrophages are characterized by high expression of mannose receptors CD206, high-affinity scavenger receptors CD163, and transglutaminase 2 (TG2). These cells produce, respectively, pro-inflammatory cytokines like tumor necrosis factor-α (TNF-α), IL-12, IL-1β, and IL-23 together with reactive oxygen species (ROS) and nitric oxide (NO) or anti-inflammatory cytokines like transforming growth factor β (TGFβ), and IL-10, with opposite capacity in presenting antigens.

When it became clear that macrophages could also become activated in ways not resembling the classical way, studies have been trying to delineate these different types of activation states. Many different types of stimuli induce slightly different alternatives to classical activation that are mostly involved in stimulating tissue repair and downregulating inflammation. These stimuli include IL-4 and IL-13, glucocorticosteroids, prostaglandin E2 (PGE2), immune complexes, transforming growth factor β (TGFβ), and IL-10 (31). These alternatively activated macrophages

are associated with physiological and pathological tissue remodeling (e.g. fibrosis) and can have anti-inflammatory effects by secreting high levels of IL-10 and TGFβ. Depending on the stimulus, these macrophages (often still called M2 macrophages) are characterized by high expression of mannose receptors (CD206), high-affinity scavenger receptors (CD163), and transglutaminase 2 in humans (32) and they have poor antigen-presenting capabilities (33) These M2 macrophages have been further divided into subgroups, such as wound-healing and regulatory macrophages (34), or into M2a, M2b, M2c, and M2d subtypes (35), which rendered the nomenclature in the field more complex and has been advised against (25). The advent of new techniques like single-cell transcriptomics (36), proteomics (37), and metabolomics are helping to understand the enormous diversity in macrophages present in tissues and will hopefully lead to better classifications, although this point has not been reached yet. For the purpose of this review, the M1 and M2 nomenclature will only be used when citing studies that use these names.

Adipose tissue macrophages are resident macrophages contributing to adipose tissue homeostasis. *In vivo*, adipose tissue macrophages from healthy mice express high levels of CD206, whereas adipose tissue macrophages from obese mice express low levels of CD206 (38) and high levels of integrin CD11c (39). These CD11c-expressing macrophages are associated with insulin resistance (40) and are situated in crown-like structures, surrounding necrotic adipocytes with the goal to remove them through exophagy. This will lead to free fatty acid and lipid internalization by macrophages and foam cells formation (41). Interestingly, it has been shown that murine bone marrow-derived macrophages can upregulate the expression of CD11c when differentiated in co-culture with normal adipocytes, underpinning the importance of the microenvironment in which macrophages grow (36). In adipose tissue, different kinds of immune cells may contribute to this change in macrophage polarization, including neutrophils through the protease elastase (42), T lymphocytes through interferon-γ (43), natural killer cells through TNFα and MCP1 (44), and B cells through IgG antibodies (45).

As discussed above it is clear obesity changes macrophage activation status. Even though levels of pro-inflammatory cytokines produced by macrophages in obesity are higher compared to non-obese individuals, contributing to the onset of obesity related meta-inflammation, their activation status does not coincide with a classically activated status of macrophages (37). To identify which markers characterize these macrophages, monocyte-derived macrophages were cultured in media conditioned by adipose tissue of obese mice or humans to mimic the presence of the metabolic syndrome and it was shown that these macrophages accumulate lipids and have high expression of fatty acid transporters like CD36 but do not

express the markers associated with classical activation (37,46). The presence of the CD36 marker was confirmed in adipose tissue macrophages from obese subjects and was not seen in macrophages of lean individuals. This macrophage subset is defined as metabolically activated and specific markers for this type of macrophages are suggested to be macrophage scavenger receptor 1 (Msr1), ATP-binding cassette A1 (ABCA1), and the adipose differentiation-related protein (Perilipin-2, PLIN2), in addition to CD11c and CD36 (37,46).

MACROPHAGE METABOLIC REPROGRAMMING

Since macrophages are key sentinel cells in charge of detecting alterations in their microenvironment, they need to be able to respond rapidly. To do so, they also need flexible metabolic pathways and must be able to reprogram their metabolism for proper activation and function. In fact, when macrophages polarize to a different phenotype, they also modify how they process their energy substrates, such as glucose or fatty acids. One of the first differences shown in macrophage metabolism related to polarization differences was seen in amino acid metabolism, in which classically activated macrophages were found to convert arginine to NO and citrulline by inducible NO synthase (iNOS) activity, while alternatively activated macrophages convert arginine in proline and polyamines through arginase-1 (47). Following this initial observation, our knowledge has expanded and it is now known that macrophages can also reprogram the way they generate ATP for energy. Nonpolarized or alternatively activated macrophages are involved in processes that are less time-pressured and use beta-oxidation of fatty acids and mitochondrial oxidative phosphorylation (OXPHOS) to produce ATP. This is achieved by lipolysis of triglycerides (48), generating fatty acids that will be oxidized by beta-oxidation, and obtaining acetyl-CoA plus NADH and $FADH_2$. The first will enter the tricarboxylic acid (TCA) cycle, while the latter are used to produce ATP by OXPHOS. In addition, these macrophages can produce pyruvate from glycolysis, convert this to acetyl-CoA, which is then used by the TCA cycle to give electrons in the form of NADH and $FADH_2$ to the OXPHOS complexes (**Figure 3A**). In response to pro-inflammatory stimuli, macrophages reprogram their metabolism to create energy and biosynthetic precursors rapidly in order to fight fast-growing microbes. This phenomenon is similar to the Warburg effect observed in tumor cells (49) and favors aerobic glycolysis over OXPHOS. While this is an inefficient way of generating ATP as compared to the TCA cycle (2 ATPs compared to 36 per glucose molecule), it can be quickly induced which is beneficial when trying to fight microbes that quickly replicate (50). As a result of this metabolic reprogramming, the excess carbon from glycolysis in classically activated macrophages is secreted as lactate instead of being used to produce acetyl-CoA from pyruvate, and the TCA cycle is broken at two

points, after citrate, and after succinate, resulting in the accumulation of these two metabolites. The TCA cycle in macrophages has been elegantly reviewed in detail by Ryan and O'Neill (51). A short summary of the most important consequences of metabolic reprogramming is given below.

The first consequence of metabolic reprogramming is a breakpoint of the TCA cycle after citrate, due to lower expression of isocitrate dehydrogenase (**Figure 3B**). This enzyme is responsible for the conversion of isocitrate to α-ketoglutarate and when expressed at lower levels results in more citrate in cells. The accumulated citrate can be transported into the cytosol by mitochondrial citrate carrier family 25 member 1 (SLC25a1) in exchange for malate (52). This carrier is highly expressed in macrophages stimulated by inflammatory signals leading to citrate accumulation in the cytosol (53). Once in the cytosol, citrate can be converted by ATP citrate lyase into acetyl-CoA and oxaloacetate and used for the synthesis of fatty acids, cell membranes and prostaglandins (54), or it can be transported into the nucleus and converted into acetyl-CoA by citrate lyase (55). As the enzyme ATP citrate lyase is upregulated in classically activated macrophages (56) this could lead to higher levels of cellular acetyl-CoA. Acetyl-CoA can then be used for lysine acetylation of proteins, such as histones, by acetyltransferases, therefore having an impact on gene expression (as explained in later paragraphs), or for *de novo* lipogenesis.

The second consequence of metabolic reprogramming is a breakpoint after succinate due to the inhibition of succinate dehydrogenase by competitive inhibitor itaconate, which will result in succinate accumulation (**Figure 3C**). Itaconate is produced by cis-aconitate decarboxylase, also called immune-responsive gene 1, and is present in higher quantities in classically activated macrophages, in which it also induces lactate dehydrogenase, contributing to the buildup of lactate (57). In addition, the above-mentioned accumulation of citrate can contribute to succinate accumulation because citrate can be converted to cis-aconitate in mitochondria and can then be further converted to itaconate by cis-aconitate decarboxylase. The levels of succinate are also increasing as a consequence of increasing levels of glutamine anaplerosis. This means that glutamine is converted via α-ketoglutarate into succinate through glutaminolysis or through an upregulated γ-aminobutyric acid (GABA) shunt. This shunt is a TCA cycle bypass which uses glutamine as a substrate to produce succinate, passing through glutamate, GABA, and succinic semialdehyde (58). Incidentally, succinate dehydrogenase is also the second complex of the mitochondrial respiratory chain, which is a series of enzyme complexes that transfer electrons inside the mitochondrial matrix in exchange for protons, that are then pumped out. Succinate dehydrogenase generates ubiquinol from ubiquinone using the electrons obtained from succinate oxidation. Ubiquinol is

then reoxidized by complex III, which also reduces cytochrome c, that in its turn will reduce complex IV. This complex then reduces molecular oxygen to water. The transfer of electrons that takes place in the respiratory chain provides the potential energy necessary to generate the proton-motive force required for ATP synthesis (59). Therefore, inhibition of succinate dehydrogenase by itaconate could also lead to decreased mitochondrial respiration in macrophages, providing a link between these two pathways, and leading to higher ROS production due to reverse electron transport to complex one, rather than complex III, that will receive the electrons from ubiquinol and generate NADH from NAD^+ (60).

Higher levels of succinate also lead to stabilization of transcription factor hypoxia-inducible factor 1-alpha (HIF-1α) because succinate inhibits prolyl hydroxylase domain proteins, which normally hydroxylate HIF-1α leading to its ubiquitination and proteasomal degradation (61). The stabilization of HIF-1α will lead to its binding to hypoxia response elements on target genes and induce their expression. HIF-1α regulates expression of genes associated with angiogenesis, proliferation, inflammation, and cellular metabolism. HIF-1α in fact promotes the switch to glycolysis by inducing expression of glycolytic enzymes like hexokinase 2, glucose-6-phosphate isomerase, and pyruvate kinase M2. These are involved in the first, second, and tenth reactions of glycolysis respectively, to ensure these cells can continue to produce ATP when oxygen is limited. Glycolysis will also supply metabolic intermediates, like glucose-6-phosphate, to the pentose phosphate pathway to produce NADPH (62). This can then be used by the enzyme NADPH oxidase to produce ROS. Members of the oxidative phase of the pentose phosphate pathway (from the entrance of glycolytic glucose-6-phosphate to the production of ribulose-5-phosphate) are all upregulated in classically activated macrophages (63), while members of the nonoxidative phase are downregulated due to downregulation of sedoheptulose kinase, which converts sedoheptulose in sedoheptulose-7-phosphate (64).

HIF-1α also promotes expression of lactate dehydrogenase, which metabolizes pyruvate to lactate (65) and expression of pyruvate dehydrogenase kinase 1. The latter inhibits pyruvate dehydrogenase, therefore inhibiting the conversion of pyruvate in acetyl-CoA, repressing mitochondrial function even more (66).

In summary, highly active glycolysis combined with increased glucose uptake results in improved availability of glycolytic intermediates, meeting one of the requirements of an inflammatory response, such as an increased demand for energy (67).

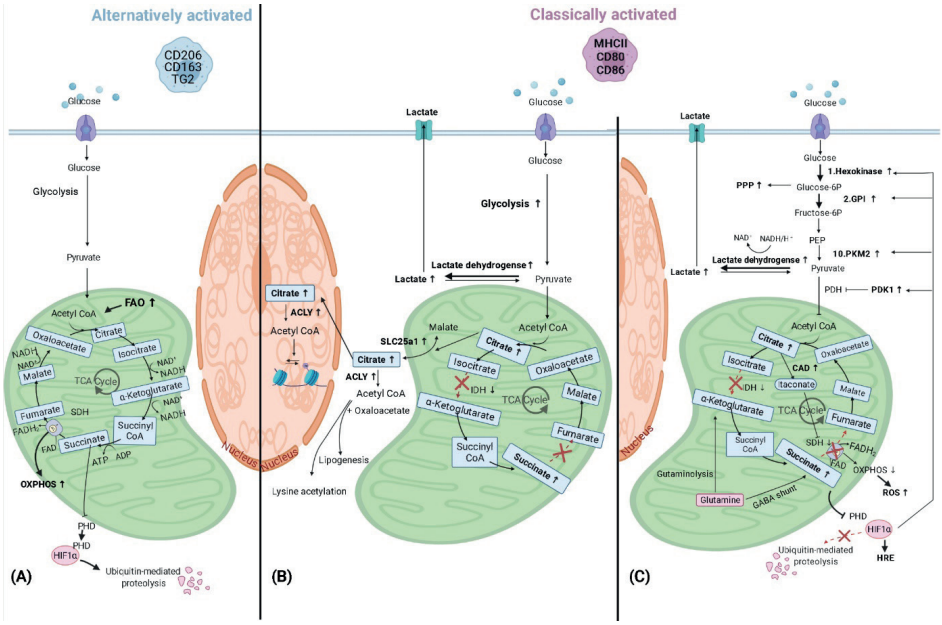

Figure 3: Macrophage metabolic reprograming. (A) Alternatively activated macrophages have an induced fatty acid oxidation (FAO) and produce pyruvate from glycolysis and this is converted in acetyl-CoA, which is then used by the tricarboxylic acid (TCA) cycle to give electrons in the form of NADH and $FADH_2$ to the mitochondrial oxidative phosphorylation (OXPHOS) complexes to produce ATP. **(B)** When macrophages polarize to classically activated macrophages, metabolic reprogramming takes place and lactate is produced instead of pyruvate, and the TCA cycle is broken at two points, after citrate, and after succinate, resulting in the accumulation of these three metabolites. Citrate accumulates due to lower expression of isocitrate dehydrogenase (IDH) and can either be transported to the cytosol through solute carrier family 25 member 1 (SLC25a1), where it can be converted in acetyl-CoA by ATP citrate lyase (ACLY), or to the nucleus where the same conversion can take place. Acetyl-CoA can then be used for lysine acetylation or for lipogenesis. **(C)** Other changes in classically activated macrophages include succinate dehydrogenase (SDH) inhibition by itaconate, which is produced by upregulated cis-aconitate decarboxylase (CAD), and this results in succinate accumulation. Succinate levels can also increase as a consequence of augmented levels of glutamine anaplerosis, either through an upregulated GABA (γ-aminobutyric acid) shunt or through glutaminolysis. SDH is also part of the mitochondrial respiratory chain and its inhibition will lead to decreased mitochondrial respiration and increased ROS (reactive oxygen species) production. Succinate inhibits prolyl hydroxylase domain (PHD) proteins, resulting in less hydroxylation of hypoxia-inducible factor 1-alpha (HIF-1a), which circumvents its degradation and allows its binding to hypoxia response elements (HRE) on target genes (61). HIF-1α also promotes the switch to glycolysis by inducing glycolytic enzymes like hexokinase 2 (1^{st} reaction of glycolysis), pyruvate kinase M2 (PKM2, 10^{th} reaction), and glucose-6-phosphate isomerase (GPI, 2^{nd} reaction). The enzyme product of the latter is used in the oxidative phase of the pentose phosphate pathway (PPP), which is also upregulated in classically activated macrophages. HIF-1α also upregulates the enzymes lactate dehydrogenase and pyruvate dehydrogenase kinase 1 (PDK1) leading to higher lactate production and lower acetyl-CoA synthesis, respectively.
Abbreviations: PEP (Phosphoenolpyruvate), PDH (Pyruvate dehydrogenase).

Metabolic reprogramming of macrophages in DMTII and obesity

The exact mechanism of how macrophages reprogram their metabolism after activation in DMTII and obesity is still unknown. As discussed in the previous paragraph, macrophages undergo metabolic reprogramming when classically activated, but also availability of energy sources influences their metabolism, implying that abundant availability of energy sources (for instance during hyperglycemia or obesity) can also impact their metabolism. Since it has been shown that the phenotype of metabolically activated macrophages differs from classically activated macrophages (36,37), this may indicate that their metabolism could differ as well.

This situation is particularly relevant in DMTII and insulin resistance for adipose tissue macrophages. Similar to classically activated macrophages, metabolically activated macrophages have higher glycolytic rates and produce more lactate (**Figure 4**) compared to adipose tissue macrophages from lean subjects (11). The glucose transporter GLUT1 is overexpressed in metabolically activated adipose tissue macrophages of obese mice and rats (68) and overexpression of this transport was shown to drive more glycolysis and pentose phosphate pathway metabolism in these cells, in addition to higher ROS production (68). Moreover, a higher level of glucose present in the environment can affect macrophage activation state, inducing a phenotypic switch to $CD11c^{+}$ macrophages (69). It has been shown that CD11c+ macrophages have enriched expression of genes encoding glucose metabolism, fatty acid metabolism, and lysosomal proteins (40) emphasizing a central role for these genes in adipose tissue macrophages.

Lipid metabolism also seems to differ between metabolically and classically activated macrophages. As mentioned before, macrophages in crown-like structures in fat tissue internalize the free fatty acids and lipids released from dead adipocytes, thereby becoming foam cells (41). Xu *et al.* demonstrated that obesity induces lysosomal biogenesis and lipid metabolism pathways in adipose tissue macrophages due to the higher accumulation of lipids in these cells, events that do not take place in classically activated macrophages (36). Adipose tissue macrophages from obese subjects also metabolize lipids differently and a detailed description has been compiled by Dahik *et al.* (70). A combination of studies has shown that adipose tissue macrophages from obese subjects can synthesize lipids from free fatty acids, store them in lipid droplets, catabolize them through the lysosomal pathway or produce inflammatory lipid mediators called eicosanoids (70,71). In contrast, adipose tissue macrophages from lean subjects take up free fatty acids and subject them to oxidation (72) The higher levels of free fatty acids, coupled with higher levels of other inflammatory mediators like TNFα, IL6, and IL-1β will lead to the development of insulin resistance which can develop in obesity.

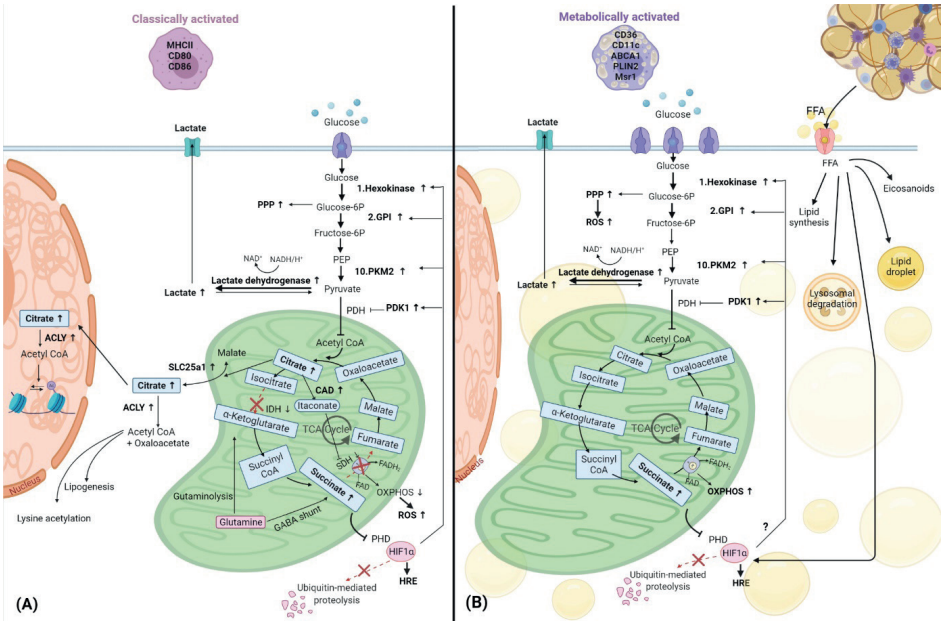

Figure 4: Comparison of metabolic reprogramming of classically and metabolically activated macrophages. **(A)** Classically activated macrophages and their metabolism. **(B)** Metabolically activated macrophages and their metabolism. Adipose tissue macrophages in obesity internalize free fatty acids (FFA) and lipids from the dying adipocytes, becoming foam cells. These FFA can be used to synthesize new lipids, can be stored in lipid droplets, can be catabolized through the lysosomal pathway or be used to produce inflammatory lipid mediators called eicosanoids. Glucose is the main source of energy also in metabolically activated macrophages, where the glucose transporter is overexpressed, and it is catabolized by glycolysis, which is upregulated, providing substrates for the pentose phosphate pathway (PPP), also upregulated. Also the metabolic pathway OXPHOS (oxidative phosphorylation) is upregulated in these cells, underlying their high energy demand. Succinate production is increased in these cells. This metabolite inhibits prolyl hydroxylase domain (PHD) proteins, resulting in less hydroxylation of hypoxia-inducible factor 1-alpha (HIF-1α), which circumvents its degradation, allowing its binding to hypoxia response elements (HRE) on target genes (61). HIF-1α is also promoted by FFA and we hypothesize it might promote the switch to glycolysis by inducing glycolytic enzymes as it happens in classically activated macrophages.

Abbreviations: TCA (tricarboxylic acid) cycle, SLC25a1 (solute carrier family 25 member 1), ACLY (ATP citrate lyase), IDH (isocitrate dehydrogenase), SDH (succinate dehydrogenase), CAD (cis-aconitate decarboxylase), GABA (γ-aminobutyric acid), PHD (prolyl hydroxylase domain), ROS (reactive oxygen species), PKM2 (pyruvate kinase M2), GPI (glucose-6-phosphate isomerase), PEP (Phosphoenolpyruvate), PDH (Pyruvate dehydrogenase), PDK1 (pyruvate dehydrogenase kinase 1), FAO (fatty acid oxidation).

In accordance with their activated status, metabolically activated macrophages were also shown to contain a higher number of mitochondria and have higher mitochondrial activity compared to adipose tissue macrophages from lean subjects (40,73) and this was associated with higher OXPHOS activity (73,74).In addition, expression of insulin-like growth factor 1 receptors (IGF1R) was shown to be suppressed in adipose tissue macrophages from obese subjects (75), altering the insulin receptor pathway leading to lower phosphorylation of IRS1-2, lower PI3K activation, and decreased Akt serine phosphorylation. Lower Akt phosphorylation translates into lower mTOR activity and activation of glycolysis (46).

Another major characteristic of adipose tissue in obesity is the hypoxia present and therefore HIF-1α may be overexpressed in adipose tissue macrophages due to oxidative stress, due to a higher content of the metabolite succinate (73,76), due to the higher levels of free fatty acids (73), or a combination thereof. Therefore, one could speculate that the glycolytic enzymes that are induced by HIF-1α in classically activated macrophages are also induced in metabolic syndrome, but more studies on this topic are needed.

In summary, the metabolic changes found in metabolically activated macrophages resemble the ones that occur when macrophages polarize toward a pro-inflammatory phenotype but rely mostly on high levels of free fatty acids present in the microenvironment and differ in the induction of oxidative phosphorylation.

METABOLIC CHANGES, LYSINE ACETYLATION AND GENE EXPRESSION

In recent years it has also become apparent how variations in metabolite levels due to the onset of disease are connected to epigenetic modifications, which lead to changes in gene expression (77).

As mentioned above when discussing the interruptions in the TCA cycle, levels of acetyl-CoA may change due to changes in macrophage metabolism. Acetyl-CoA is generated in the mitochondrial matrix from pyruvate by the pyruvate dehydrogenase complex as part of glycolysis, by β-oxidation of fatty acids, or by the catabolism of branched-chain amino acids. Mitochondrial acetyl-CoA enters the tricarboxylic acid cycle and is converted to citrate (78). It can then be transported out of the mitochondria and reconverted to acetyl-CoA, thus contributing to cytoplasmic protein acetylation. It can also be transported into the nucleus as citrate and reconverted to acetyl-CoA by ATP citrate lyase to serve as a substrate for lysine acetyl transferases.

In addition to being a metabolic intermediate, acetyl-CoA is also a substrate used by lysine acetyl transferases to reversibly transfer an acetyl group to the ε-amino group of lysine residues in target proteins. Therefore, altered levels of acetyl-CoA resulting from macrophage metabolic reprogramming will result in different levels of lysine acetylation (79). Acetylation neutralizes the positive charge on lysine, altering the way the acetylated protein interacts with surrounding proteins and other molecules, most notably histones (80). This highlights an interesting and yet still not widely studied consequence of changes in macrophage metabolism: the effect this can have on protein acetylation and consequently on gene expression.

Reversible protein acetylation regulates a number of important cellular processes including gene expression via acetylation of histones. In fact, acetylation is one of the most frequent reversible posttranslational modifications histone proteins are subjected to. Other posttranslational modifications include methylation, phosphorylation, and ubiquitylation, which all regulate gene expression by influencing the folding of chromatin. Chromatin is a complex of DNA wrapped around an octamer of histone proteins, one H3/H4 tetramer, and two H2A/H2B dimers, forming nucleosomes (81). During activation of gene transcription, the chromatin conformation changes from tightly packed to relaxed allowing DNA-binding proteins to interact with the DNA. Histone acetylation favors gene transcription because interactions of positively-charged amino groups in histones (belonging to lysine residues) with negatively charged phosphate groups in DNA will decrease due to the removal of positive charges on histones upon acetylation. Interestingly, protein acetylation also regulates the activity of enzymes involved in cellular energy metabolism such as hexokinase, pyruvate kinase isozymes M2, and pyruvate dehydrogenase (79).

Protein acetylation in obesity and DMTII, immunomodulatory epigenetics as new therapies

Due to the changes of intracellular acetyl-CoA concentrations in obesity and DMTII, an effect on protein acetylation and therefore posttranslational protein modifications (i.e. epigenetic modifications) seems probable. Indeed, a link between epigenetic changes and DMTII-related meta- inflammation has been reported in a variety of studies, suggesting that metabolic changes induced by obesity/DMTII can lead to epigenetic changes, which then result in transcription of pro-inflammatory genes (82,83).

In particular, changes in the levels of lysine deacetylases (KDACs), enzymes responsible for the deacetylation of lysine residues in proteins, have been reported

in obese mice and patients (84,85). KDACs can be classified into four groups (86): Class I comprises KDAC1, 2, 3, and 8; Class II is divided into two sub-groups, IIA (KDAC4, 5, 7, 9) and IIB (KDAC6 and 10); Class III includes the sirtuins, which differ from the other KDACs because they depend on NAD for their deacetylase activity instead of being zinc-dependent like the others; Class IV encompasses KDAC11.

Bricambert *et al.* have described how lower activity of KDACs, KDAC5 and 6 in particular, in white adipose tissue of obese mice and patients correlated with higher levels of pro-inflammatory adipokines (hormones and cytokines secreted by adipocytes) and with impaired glucose uptake (84). However, other studies have shown that sirtuins are probably more important in regulating metabolism (85,87). SIRT1 appears to be most closely linked to the metabolic syndrome and is primarily affected by changes in nutrient conditions like caloric restriction (88) or overnutrition. Cao *et al.* showed that SIRT1 is intimately connected to insulin resistance by regulating insulin signaling and therefore metabolism of glucose and lipids (89). Yeung *et al.* reported that SIRT1 inhibited inflammatory responses by deacetylating the p65 subunit of transcription factor Nuclear Factor kappa b (NFkB) (88). NFkb regulates a number of processes involved in inflammation, including induction of the expression of pro-inflammatory genes in many cells (91). A negative correlation between SIRT1 gene expression levels and BMI values of patients (92) was previously shown and this was also associated with more pro-inflammatory gene expression contributing to insulin resistance. Similarly, SIRT1 levels were also inversely proportional to infiltration of adipose tissue macrophages in human subcutaneous fat (93). This finding was confirmed in vitro by studies showing that SIRT1 inhibits recruitment of macrophages by co-culturing them with SIRT1-deficient adipocytes and showing that the absence of SIRT1 induced their recruitment and a pro-inflammatory phenotype (94). In addition, lower mRNA levels of SIRT1were detected in macrophages of mice fed a high-fat diet that developed obesity (94).

These findings on KDACs suggest that combining KDAC activators with anti-diabetic drugs could be a more efficient way to treat metabolic syndrome. A wide array of KDAC activators is already available and more specific ones are being developed. Examples of KDAC activators that have been used in the context of metabolic syndrome show beneficial effects by inhibiting expression of pro-inflammatory cytokines in adipocytes and higher insulin sensitivity and glucose uptake after treatment (83). Importantly, a SIRT1 activator (SRT2104) has entered clinical trials for treatment of DMTII (95). Encouraging findings in mice on a high-fat diet preceded this clinical trial, showing for example that SIRT1 over-

expressing mice had fewer macrophages in adipose tissue (94). Moreover, treatment of RAW264.7 macrophages and primary intraperitoneal macrophages with SIRT1 activators inhibited inflammatory responses to LPS (96). The same treatment in Zucker fatty rats induced a shift from pro- to anti-inflammatory behavior in adipose tissue macrophages, in addition to improved glucose tolerance (96).

In addition to activating KDACs, deacetylase inhibitors have also been used in the context of chronic inflammatory diseases, like chronic obstructive pulmonary disease (97,98), rheumatoid arthritis (99), and cancer (100) with positive outcomes. This suggests that inhibiting certain deacetylases associated with chronic inflammation in diabetes and obesity may also have therapeutic potential. Inhibitors of Class I KDACs, particularly KDAC3 (101) have been used in vitro and in vivo in the context of diabetes and obesity (102–104). None of them have reached the stage of clinical trials yet, even though promising results have been achieved in glycemic control and reduction of obesity, highlighting their potential as therapeutic treatment for metabolic disorders.

The above paragraphs have highlighted that macrophages, inflammation and metabolic changes are intimately connected in DMTII and obesity. However how metabolic pathways in macrophages are changed is still unclear and many knowledge gaps remain. To be able to address the lack of knowledge on which metabolic pathways are affected by reprogramming, different techniques must be used and the results integrated. In the following paragraph, the most common ones will be described along with advantages and disadvantages and suggestions which would be most appropriate to use when.

ANALYTICAL METHODS TO CHARACTERIZE MACROPHAGE METABOLIC REPROGRAMMING

The most widely used method to characterize macrophage polarization and the corresponding phenotypes is flow cytometry (105). This technique determines properties of single cells by assessing the presence of proteins on the surface of cells or intracellularly with fluorescently-labeled antibodies using laser-induced excitation of the fluorescent labels. However, this approach does not provide information on cellular metabolism. Recent work has tried to fill this gap by using flow cytometry to investigate single-cell metabolism using antibodies against key metabolic enzymes (106). Although this work is a major step forwards, it still does not provide quantitative insight into metabolite production and enzyme activity, which is why other analytical methods are needed to gain a better mechanistic understanding of macrophage metabolic reprogramming.

Different techniques are used to measure the metabolic status of cells, including extracellular flux analysis, colorimetric/fluorometric enzyme activity assays, and mass spectrometry (MS) based metabolomics and flux analysis (12). These techniques provide complementary information about the metabolic state of cells. We aim to clarify some of their advantages and disadvantages and provide an overview of when to use which method as well as how to combine them.

Functional assays

Widely used assays in the field of immunology are extracellular flux analyzers that give a functional readout of glycolytic or mitochondrial metabolic activity by measuring changes in energy metabolism in culture medium of cells (107). Mitochondrial function and respiratory capacity are assessed by measuring the oxygen consumption rate, which correlates with ATP-linked respiration, maximal and basal respiration, and proton leakage. It is a functional, real-time assay that does not measure the level of individual metabolites, but indirectly measures OXPHOS activity. Glycolytic activity can be assessed by using a glycolytic stress assay that forces the cells to use glycolysis by initial glucose starvation followed by glucose administration and ATP synthase inhibition. The extracellular pH is monitored to calculate the acidification rate. When glucose is converted to pyruvate and subsequently lactate during anaerobic glycolysis, H^+ ions will be produced, shifting the pH of the medium.

These assays have the advantage of being performed in living cells, but they are indirect indicators of changes in metabolic pathways or mitochondrial function, which play a pivotal role in macrophage activation and function as outlined above (108). However, individual metabolite levels or activity of individual enzymes are not quantified emphasizing the need for complementary analytical approaches to understand how metabolic pathways change during macrophage polarization.

Enzymatic assays

Key metabolites to follow with respect to the different macrophage phenotypes are listed in **Table 1** and are part of glycolysis and the TCA cycle. The consumption rate of glucose, as the major source of energy for classically activated macrophages, gives an indication of the overall energy requirement. The conversion of glucose to pyruvate by the action of glycolytic enzymes is an indicator of the role of glycolysis and therefore it is of interest to measure some of its intermediates like glucose-6-phosphate, fructose-6-phosphate or phosphoenolpyruvate. Since classically activated macrophages shift pyruvate conversion from acetyl-CoA production to

lactate production, it is critical to quantify lactate. In addition, since the TCA cycle is interrupted at two points, due to a reduced activity of isocitrate and succinate dehydrogenases, leading to accumulation of succinate and citrate, these two metabolites should be measured to assess the contribution of the TCA cycle to the overall conversion of glucose to ATP. Another reason for quantifying citrate is that it can be converted to acetyl-CoA, which serves as substrate for lysine acetyltransferases and is thus linked to protein acetylation and the regulation of gene expression (see paragraph "Lysine acetylation links metabolism and gene expression" for further details). Itaconate is another interesting metabolite to measure, since it plays a role in connecting the two breakpoints of the TCA cycle.

To quantify lactate, an enzymatic assay can be used for in vitro studies (12). This assay is based on generating a luminescent signal that is proportional to the lactate concentration in the cell culture medium. Other enzymatic assays with colorimetric or fluorimetric readouts are available for most, but not for all of the metabolites of interest mentioned above (109,110). Moreover, these assays do not measure metabolite concentrations directly, but make use of enzymatic reactions that oxidize them, generating a product that reacts with a probe, producing a colorimetric or fluorimetric readout. Techniques that allow quantifying a wider range of metabolites simultaneously are therefore of increasing relevance to gain a more comprehensive view of metabolic changes in cells.

Table 1. Metabolite analysis in macrophages metabolic reprogramming. Rows represent key metabolites or metabolic processes that can be measured in order to differentiate macrophage phenotypes. Columns present examples of references that use the different analytical techniques either alone or in combination.

	Extracellular flux analyzers	Enzymatic essays	Mass spectrometry
Glycolytic activity	(55,107,124–127)		(55,128)
OXPHOS activity	(55,107,125–127,129)		(55,128)
Glucose		(109,110,126)	(55,109,110,128)
Pyruvate		(130)	(55,125)
Glucose-6-phosphate			(55,125)
Phosphoenolpyruvate			(55)
Lactate		(12,127,131)	(55,125,129,132)
Succinate		(109,110)	(55,125,128,132–134)
Citrate		(127)	(55,128,132–134)
Acetyl-CoA			(133)
Itaconate			(55,128,132,133)

Mass spectrometric assays

The main analytical platform that is used to detect and quantify a wider range of metabolites is MS (111–113). Different kinds of separation methods can be coupled to MS to increase the depth of analysis as well as to cover a wider range of compounds. Gas chromatography (GC) and liquid chromatography (LC) are most widely used (114). LC is better suited to measure polar and charged molecules, whereas GC is preferred when investigating short-chain fatty acids, esters, hydrocarbons, and volatile and thermally stable molecules.

Most metabolite measurements are done at a fixed time point, while it is of interest to rather assess turnover rates, as this will provide a more dynamic picture of the contribution of a given metabolic pathway in, for example, central carbon metabolism. Such measurements can be done using stable-isotope-labeled metabolic substrates (see paragraph "Mass spectrometric metabolic flux analysis").

Metabolite analyses by MS can be performed in a targeted or untargeted manner. With targeted MS methods it is possible to have accurate and precise quantitative information on known metabolites, such as those that are involved in metabolic reprogramming of macrophages. While many metabolites, that play a key role in macrophage metabolic reprogramming, are known, recent work shows that new metabolites are still being discovered using untargeted MS (115). One example is the discovery of the role of uridine diphosphate N-acetylglucosamine in macrophage polarization (116).Once such a metabolite has been discovered, it may be further investigated in greater detail with a targeted MS approach.

Mass Spectrometric metabolic flux analysis

Knowing the concentration and/or abundance of the metabolites at a given moment in time can help to understand which metabolite levels are altered at the moment of metabolite extraction. However, to understand the dynamics of metabolic reprogramming, it is also relevant to know which metabolic pathways are up- or down-regulated, which can be deduced from measuring production and consumption rates of metabolites by following the incorporation of stable isotopes into metabolites over time. This is accomplished by using stable isotope labelled metabolic tracer molecules to study the flux of stable isotopes through different pathways for a set of key metabolites (117). An untargeted LC-MS metabolomics flux analysis approach with stable isotope labeling of metabolites was used to get more insight into substrate use in different macrophage phenotypes after stimulation with LPS or IL4 (118). A change in phenotype due to a certain stimulation was first confirmed by flow cytometry and then different metabolic pathways were

followed by adding isotopically labelled substrates. This study confirmed that LPS-stimulated macrophages use citrate to synthesize itaconate and transport it to the cytosol to produce lipids. The study established further that IL4-stimulated macrophages rely on oxidative metabolism as their main energy source (see **Figure 3**). Furthermore, the study showed that some metabolites, like itaconate, are only synthesized in mitochondria, while others were produced by both cytosolic and mitochondrial enzymes, depending on the polarization status of macrophages. The integration of different levels of biological information has been used by Jha *et al.* in a pipeline named "concordant metabolomics integration with transcription" (CoMBI-T) that integrates MS metabolomics data with RNA-seq results in order to characterize macrophage polarization (116). Polarization was first confirmed by flow cytometry and then metabolic profiles were acquired using non-targeted MS-analysis. Altered metabolic pathways were further studied by metabolite flux analysis using ^{13}C labeled glucose and ^{13}C- and ^{15}N-labeled glutamine combined with a targeted LC-MS approach (selective reaction monitoring (SRM)). Using this pipeline they showed that glutamine is a major source of nitrogen in alternatively activated macrophages and that these cells have an augmented metabolism of amino sugars and nucleotide sugars like uridine diphosphate N-acetylglucosamine. This metabolite is known to link signaling and metabolism through glycosylation of proteins that are localized at the cell-surface, for example, various growth factor receptors (119). By using this combined approach a new metabolite was found, which plays a major role in alternatively activated macrophages (116). The authors also investigated breakpoints in the TCA cycle using metabolic flux analysis experiments and found that the aspartate-argininosuccinate shunt, a series of reactions that connect the TCA cycle and the urea cycle (120), plays a role in pro-inflammatory macrophages.

To summarize, a number of analytical approaches can be used to study metabolic reprogramming in macrophages. Flow cytometry analysis allows to define the different phenotypes of macrophages on which subsequent comparative analyses are based. Extracellular flux analysis provides functional insight into macrophage metabolic reprogramming at the level of metabolic pathways that are altered but does not quantify individual metabolites. Enzymatic assays with luminescent, colorimetric or fluorimetric readouts quantify a number of key metabolites. These assays are relatively easy to perform and data analysis does not require specific expertise as is the case for MS analysis. MS in combination with GC or LC allows to cover a wider range of metabolites both known and unknown. It thus allows to follow known key metabolites as well as to potentially gain insights into new metabolites or metabolite patterns. MS analysis can be extended to comprise metabolic flux analysis in order to follow how metabolites are consumed and produced in cell

systems and how this varies in the context of changing conditions, for example during the development of DMTII. It is thus of particular interest to combine multiple analytical approaches to gain a comprehensive overview of mechanisms related to macrophage metabolic reprograming. Moreover, even though there is considerable knowledge about metabolic reprogramming during macrophage polarization in cell culture under defined conditions, there is still a large knowledge gap when it comes to diseases like DMTII. Here metabolic changes are key disease features, which most probably will also reflect in changes in the metabolism of macrophages and their polarization. That is why metabolomics in combination with lipidomics, fluxomics, transcriptomics, and proteomics has the potential to lead to the discovery of further mechanistic links between inflammation and metabolic disturbances (121).

FUTURE PERSPECTIVES

A new branch of immunology, called immunometabolism, has been developing rapidly in the past ten years (**Figure 5**). It is defined as the interplay between immunological and metabolic processes and has solid foundations in macrophage biology research, which is illustrated by the fact that 29% of the 2027 publications since 1975 also had the key word 'macrophages'.

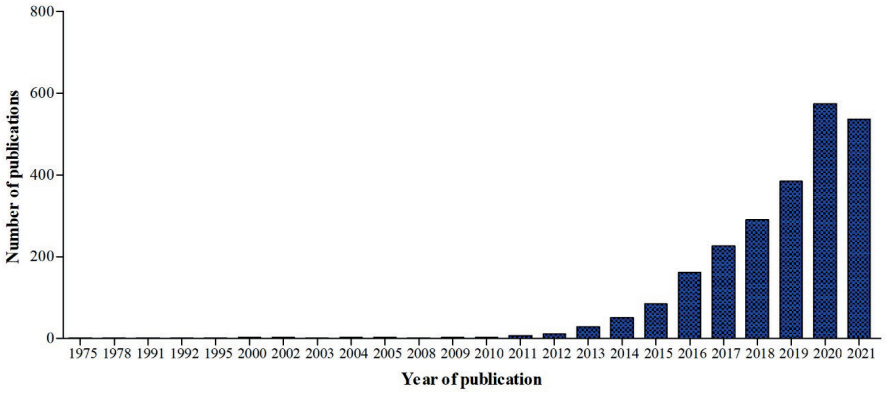

Figure 5: Graphic representation of the number of publications in Pubmed.gov using the keyword 'Immunometabolism' from 1975 until 2021.

We now have clear evidence that macrophages can change metabolic pathways to respond to challenges they encounter. Macrophage polarization and function are highly dependent on fast changes in intracellular metabolism, which explains why macrophages can be extremely versatile in function. While this field is moving forward fast, our understanding of interactions between metabolic changes at the organism level such as found in DMTII/obesity and intracellular metabolic changes in macrophages still lags behind. Macrophages in adipose tissue from individuals with DMTII or obesity clearly show a different but pro-inflammatory phenotype from those of lean individuals or individuals without DMTII. However, those pro-inflammatory phenotypes appear to be unique to DMTII and obesity and are not found when macrophages are M1-polarized in acute inflammation (37), suggesting that metabolic changes at the organism level influence macrophage activation and metabolism. How they interact exactly remains an open question that could potentially be answered by improved analysis of macrophage cellular metabolism. To do this in complex conditions like DMTII and obesity, an approach from different angles is needed and integration of results from different analytical platforms is the way forward. This could help to better understand the mechanism underlying macrophages polarization in DMTII-related chronic inflammation and, even more importantly, how this affects disease progression.

A better understanding of interaction between different metabolic pathways could also result in the development of new treatment options. Diabetes treatment now focuses on weight loss, rebalancing insulin resistance, and lowering blood glucose levels by using mostly gluconeogenesis inhibitors like metformin or hypoglycemic drugs that stimulate β-cells to release insulin (122). While weight loss should always remain the number one priority, redirecting adipose tissue macrophage metabolic programs, and thereby polarization, could be another interesting approach since pro-inflammatory macrophages contribute to onset of insulin resistance (123) and overall to DMTII-related meta-inflammation. Inhibiting chronic inflammation, would not only improve the comorbidities, like diabetic retinopathy, polyneuropathy, or nephropathy but also one of the main causes of diabetes onset.

Another aspect that should be further investigated and could develop into a promising therapeutic approach is the link between metabolism and inflammation via epigenetic regulation of gene expression. Recent studies indicate that chronic inflammation is linked to changes in energy metabolism via lysine acetylation of both histones and non-histone proteins (77). Therefore, deacetylase inhibitors or activators may be additional approaches to inhibit macrophage-induced meta-inflammation by rebalancing the expression of pro- and anti-inflammatory mediators.

CONFLICT OF INTEREST

The authors declare that the research was conducted in the absence of any commercial or financial relationships that could be construed as a potential conflict of interest.

AUTHORS CONTRIBUTION

SR, MK, NG, RB, and BM conceived and designed the set-up of the manuscript. SR drafted the manuscript and prepared figures. SR, MK, NG, RB, and BM edited and revised the manuscript and all approved the final version.

FUNDING

This project has received funding from the European Union's Horizon 2020 research and innovation program under the Marie Skłodowska-Curie grant agreement No 754425.

ACKNOWLEDGMENTS

The Figures 1,2,3,4,5 were created with BioRender.com.

REFERENCES

1. Diabetes. https://www.who.int/news-room/fact-sheets/detail/diabetes [Accessed May 4, 2021]
2. Ogurtsova K, da Rocha Fernandes JD, Huang Y, Linnenkamp U, Guariguata L, Cho NH, Cavan D, Shaw JE, Makaroff LE. IDF Diabetes Atlas: Global estimates for the prevalence of diabetes for 2015 and 2040. *Diabetes Res Clin Pract* (2017) 128:40–50. doi: 10.1016/j.diabres.2017.03.024
3. Okamura T, Hashimoto Y, Hamaguchi M, Obora A, Kojima T, Fukui M. Ectopic fat obesity presents the greatest risk for incident type 2 diabetes: a population-based longitudinal study. *Int J Obes* (2019) 43:139–148. doi: 10.1038/s41366-018-0076-3
4. Hotamisligil GS. Inflammation, metaflammation and immunometabolic disorders. *Nature* (2017) 542:177–185. doi: 10.1038/nature21363
5. Wellen KE, Hotamisligil GS. Inflammation, stress, and diabetes. *Journal of Clinical Investigation* (2005) 115:1111–1119. doi: 10.1172/jci25102
6. Franssens BT, Westerink J, van der Graaf Y, Nathoe HM, Visseren FLJ. Metabolic consequences of adipose tissue dysfunction and not adiposity per se increase the risk of cardiovascular events and mortality in patients with type 2 diabetes. *Int J Cardiol* (2016)72–77. doi: 10.1016/j.ijcard.2016.07.081
7. Murray PJ, Wynn TA. Protective and pathogenic functions of macrophage subsets. *Nat Rev Immunol* (2011) 11:723–737. doi: 10.1038/nri3073
8. Galli G, Saleh M. Immunometabolism of Macrophages in Bacterial Infections. *Front Cell Infect Microbiol* (2021) 0:903. doi: 10.3389/FCIMB.2020.607650
9. Robbe P, Draijer C, Borg TR, Luinge M, Timens W, Wouters IM, Melgert BN, Hylkema MN. Distinct macrophage phenotypes in allergic and nonallergic lung inflammation. *Am J Physiol Lung Cell Mol Physiol* (2015) 308:L358–L467. doi: 10.1152/ajplung.00341.2014
10. Weisberg SP, McCann D, Desai M, Rosenbaum M, Leibel RL, Ferrante AW. Obesity is associated with macrophage accumulation in adipose tissue. *Journal of Clinical Investigation* (2003) 112:1796–1808. doi: 10.1172/jci19246
11. Boutens L, Hooiveld GJ, Dhingra S, Cramer RA, Netea MG, Stienstra R. Unique metabolic activation of adipose tissue macrophages in obesity promotes inflammatory responses. *Diabetologia 2018 61:4* (2018) 61:942–953. doi: 10.1007/S00125-017-4526-6
12. Freemerman AJ, Johnson AR, Sacks GN, Milner JJ, Kirk EL, Troester MA, Macintyre AN, Goraksha-Hicks P, Rathmell JC, Makowski L. Metabolic reprogramming of macrophages: Glucose transporter 1 (GLUT1)-mediated glucose metabolism drives a proinflammatory phenotype. *Journal of Biological Chemistry* (2014) 289:7884–7896. doi: 10.1074/jbc.M113.522037
13. IJsbrand M. Kramer. "Signaling through the Insulin Receptor: Phosphoinositide 3-Kinases and AKT- ClinicalKey.," *Signal Transduction*. (2016). p. 849–886 https://www-clinicalkey-com.proxy-ub.rug.nl/#!/content/book/3-s2.0-B9780123948038000164 [Accessed April 17, 2020]
14. Cersosimo E, Triplitt C, Mandarino LJ, DeFronzo RA. Pathogenesis of Type 2 Diabetes Mellitus. (2015) http://www.ncbi.nlm.nih.gov/books/NBK279115/ [Accessed October 20, 2020]
15. Han CY, Kargi AY, Omer M, Chan CK, Wabitsch M, O'Brien KD, Wight TN, Chait A. Differential effect of saturated and unsaturated free fatty acids on the generation of monocyte adhesion and chemotactic factors by adipocytes: Dissociation of adipocyte hypertrophy from inflammation. *Diabetes* (2010) 59:386–396. doi: 10.2337/db09-0925

16. Nguyen MTA, Favelyukis S, Nguyen AK, Reichart D, Scott PA, Jenn A, Liu-Bryan R, Glass CK, Neels JG, Olefsky JM. A subpopulation of macrophages infiltrates hypertrophic adipose tissue and is activated by free fatty acids via toll-like receptors 2 and 4 and JNK-dependent pathways. *Journal of Biological Chemistry* (2007) 282:35279–35292. doi: 10.1074/jbc.M706762200

17. Hotamisligil GS, Shargill NS, Spiegelman BM. Adipose expression of tumor necrosis factor-α: Direct role in obesity-linked insulin resistance. *Science (1979)* (1993) 259:87–91. doi: 10.1126/science.7678183

18. Varol C, Mildner A, Jung S. Macrophages: Development and Tissue Specialization. *Annu Rev Immunol* (2015) 33:643–675. doi: 10.1146/annurev-immunol-032414-112220

19. O'rourke RW, White AE, Metcalf MD, Olivas AS, Mitra P, Larison WG, Cheang EC, Varlamov O, Corless CL, Roberts CT, et al. Hypoxia-induced inflammatory cytokine secretion in human adipose tissue stromovascular cells. *Diabetologia* (2011) 54:1480–1490. doi: 10.1007/s00125-011-2103-y

20. Zheng C, Yang Q, Cao J, Xie N, Liu K, Shou P, Qian F, Wang Y, Shi Y. Local proliferation initiates macrophage accumulation in adipose tissue during obesity. *Cell Death Dis* (2016) 7:e2167. doi: 10.1038/cddis.2016.54

21. McLaughlin T, Craig C, Liu L-F, Perelman D, Allister C, Spielman D, Cushman SW. Adipose Cell Size and Regional Fat Deposition as Predictors of Metabolic Response to Overfeeding in Insulin-Resistant and Insulin-Sensitive Humans. *Diabetes* (2016) 65:1245–1254. doi: 10.2337/DB15-1213

22. Lempesis IG, Meijel RLJ van, Manolopoulos KN, Goossens GH. Oxygenation of adipose tissue: A human perspective. *Acta Physiol (Oxf)* (2020) 228: doi: 10.1111/APHA.13298

23. Vachharajani V, Granger DN. Adipose tissue: A motor for the inflammation associated with obesity. *IUBMB Life* (2009) 61:424–430. doi: 10.1002/iub.169

24. Jiao P, Chen Q, Shah S, Du J, Tao B, Tzameli I, Yan W, Xu H. Obesity-Related Upregulation of Monocyte Chemotactic Factors in Adipocytes : Involvement of Nuclear Factor-κB and c-Jun NH2-Terminal Kinase Pathways. *Diabetes* (2009) 58:104. doi: 10.2337/DB07-1344

25. Murray PJ. Macrophage Polarization. *The Annual Review of Physiology is online at* (2017) 79:541–66. doi: 10.1146/annurev-physiol-022516-034339

26. Mills CD, Kincaid K, Alt JM, Heilman MJ, Hill AM. M-1/M-2 Macrophages and the Th1/Th2 Paradigm. *The Journal of Immunology* (2000) 164:6166–6173. doi: 10.4049/jimmunol.164.12.6166

27. Murray PJ, Allen JE, Biswas SK, Fisher EA, Gilroy DW, Goerdt S, Gordon S, Hamilton JA, Ivashkiv LB, Lawrence T, et al. Macrophage Activation and Polarization: Nomenclature and Experimental Guidelines. *Immunity* (2014) 41:14–20. doi: 10.1016/j.immuni.2014.06.008

28. Mantovani A, Sica A, Sozzani S, Allavena P, Vecchi A, Locati M. The chemokine system in diverse forms of macrophage activation and polarization. *Trends Immunol* (2004) 25:677–686. doi: 10.1016/J.IT.2004.09.015

29. Mills CD, Kincaid K, Alt JM, Heilman MJ, Hill AM. M-1/M-2 Macrophages and the Th1/Th2 Paradigm. *The Journal of Immunology* (2000) 164:6166–6173. doi: 10.4049/JIMMUNOL.164.12.6166

30. Kang S, Kumanogoh A. The spectrum of macrophage activation by immunometabolism. *Int Immunol* (2020) 32:467–473. doi: 10.1093/intimm/dxaa017

31. Martinez FO, Helming L, Gordon S. Alternative Activation of Macrophages: An Immunologic Functional Perspective. *Annu Rev Immunol* (2009) 27:451–483. doi: 10.1146/annurev.immunol.021908.132532

32. Martinez FO, Helming L, Milde R, Varin A, Melgert BN, Draijer C, Thomas B, Fabbri M, Crawshaw A, Ho LP, et al. Genetic programs expressed in resting and IL-4 alternatively activated mouse and human macrophages: similarities and differences. *Blood* (2013) 121:e57–e69. doi: 10.1182/BLOOD-2012-06-436212

33. Arnold CE, Gordon P, Barker RN, Wilson HM. The activation status of human macrophages presenting antigen determines the efficiency of Th17 responses. *Immunobiology* (2015) 220:10–19. doi: 10.1016/J.IMBIO.2014.09.022

34. Boorsma CE, Draijer C;, Melgert BN. Macrophage Heterogeneity in Respiratory Diseases. *Mediators Inflamm* (2013) 2013: doi: 10.1155/2013/769214

35. Ryszer T. Understanding the Mysterious M2 Macrophage through Activation Markers and Effector Mechanisms. (2015) doi: 10.1155/2015/816460

36. Xu X, Grijalva A, Skowronski A, van Eijk M, Serlie MJ, Ferrante AW. Obesity Activates a Program of Lysosomal-Dependent Lipid Metabolism in Adipose Tissue Macrophages Independently of Classic Activation. doi: 10.1016/j.cmet.2013.11.001

37. Kratz M, Coats BR, Hisert KB, Hagman D, Mutskov V, Peris E, Schoenfelt KQ, Kuzma JN, Larson I, Billing PS, et al. Metabolic dysfunction drives a mechanistically distinct proinflammatory phenotype in adipose tissue macrophages. *Cell Metab* (2014) 20:614–625. doi: 10.1016/j.cmet.2014.08.010

38. Zeyda M, Gollinger K, Kriehuber E, Kiefer FW, Neuhofer A, Stulnig TM. Newly identified adipose tissue macrophage populations in obesity with distinct chemokine and chemokine receptor expression. *International Journal of Obesity 2010 34:12* (2010) 34:1684–1694. doi: 10.1038/ijo.2010.103

39. Lumeng CN, Bodzin JL, Saltiel AR. Obesity induces a phenotypic switch in adipose tissue macrophage polarization. *Journal of Clinical Investigation* (2007) 117:175–184. doi: 10.1172/JCI29881

40. Wentworth JM, Naselli G, Brown WA, Doyle L, Phipson B, Smyth GK, Wabitsch M, O'Brien PE, Harrison LC. Pro-Inflammatory CD11c+CD206+ Adipose Tissue Macrophages Are Associated With Insulin Resistance in Human Obesity. *Diabetes* (2010) 59:1648–1656. doi: 10.2337/DB09-0287

41. Haka AS, Barbosa-Lorenzi VC, Lee HJ, Falcone DJ, Hudis CA, Dannenberg AJ, Maxfield FR. Exocytosis of macrophage lysosomes leads to digestion of apoptotic adipocytes and foam cell formation [S]. *J Lipid Res* (2016) 57:980–992. doi: 10.1194/JLR.M064089

42. Talukdar S, Oh DY, Bandyopadhyay G, Li D, Xu J, McNelis J, Lu M, Li P, Yan Q, Zhu Y, et al. Neutrophils mediate insulin resistance in mice fed a high-fat diet through secreted elastase. *Nat Med* (2012) 18:1407–1412. doi: 10.1038/NM.2885

43. Rocha VZ, Folco EJ, Sukhova G, Shimizu K, Gotsman I, Vernon AH, Libby P. Interferon-γ, a Th1 cytokine, regulates fat inflammation: A role for adaptive immunity in obesity. *Circ Res* (2008) 103:467–476. doi: 10.1161/CIRCRESAHA.108.177105

44. Lee B-C, Kim M-S, Pae M, Yamamoto Y, Eberlé D, Shimada T, Kamei N, Park H-S, Sasorith S, Woo JR, et al. Adipose Natural Killer Cells Regulate Adipose Tissue Macrophages to Promote Insulin Resistance in Obesity. *Cell Metab* (2016) 23:685–698. doi: 10.1016/J.CMET.2016.03.002

45. Winer DA, Winer S, Shen L, Wadia PP, Yantha J, Paltser G, Tsui H, Wu P, Davidson MG, Alonso MN, et al. B cells promote insulin resistance through modulation of T cells and production of pathogenic IgG antibodies. *Nat Med* (2011) 17:610–617. doi: 10.1038/nm.2353

46. Castoldi A, de Souza CN, Saraiva Câmara NO, Moraes-Vieira PM. The macrophage switch in obesity development. *Front Immunol* (2016) 6: doi: 10.3389/fimmu.2015.00637

47. Modolell M, Corraliza IM, Link F, Soler G, Eichmann K. Reciprocal regulation of the nitric oxide synthase/arginase balance in mouse bone marrow□derived macrophages by TH 1 and TH 2 cytokines. *Eur J Immunol* (1995) 25:1101–1104. doi: 10.1002/eji.1830250436

48. Huang SC-C, Everts B, Ivanova Y, O'Sullivan D, Nascimento M, Smith AM, Beatty W, Love-Gregory L, Lam WY, O'Neill CM, et al. Cell-intrinsic lysosomal lipolysis is essential for alternative activation of macrophages. *Nature Immunology 2014 15:9* (2014) 15:846–855. doi: 10.1038/ni.2956

49. Newsholme P, Curi R, Gordon S, Newsholme EA. Metabolism of glucose, glutamine, long-chain fatty acids and ketone bodies by murine macrophages. *Biochemical Journal* (1986) 239:121–125. doi: 10.1042/bj2390121

50. Palsson-McDermott EM, O'Neill LAJ. The Warburg effect then and now: From cancer to inflammatory diseases. *BioEssays* (2013) 35:965–973. doi: 10.1002/bies.201300084

51. Ryan DG, O'neill LAJ. Krebs Cycle Reborn in Macrophage Immunometabolism. *Annual Review of Immunology* (2020) 38:289–313. doi: 10.1146/annurev-immunol-081619

52. Infantino V, Convertini P, Cucci L, Panaro MA, di Noia MA, Calvello R, Palmieri F, Iacobazzi V. The mitochondrial citrate carrier: A new player in inflammation. *Biochemical Journal* (2011) 438:433–436. doi: 10.1042/BJ20111275

53. Infantino V, Iacobazzi V, Menga A, Avantaggiati ML, Palmieri F. A key role of the mitochondrial citrate carrier (SLC25A1) in TNFα- and IFNγ-triggered inflammation. *Biochim Biophys Acta Gene Regul Mech* (2014) 1839:1217–1225. doi: 10.1016/j.bbagrm.2014.07.013

54. Williams NC, O'Neill LAJ. A role for the krebs cycle intermediate citrate in metabolic reprogramming in innate immunity and inflammation. *Front Immunol* (2018) 9:1. doi: 10.3389/fimmu.2018.00141

55. Lauterbach MA, Hanke JE, Serefidou M, Mangan MSJ, Kolbe C-C, Hess T, Rothe M, Kaiser R, Hoss F, Gehlen J, et al. Toll-like Receptor Signaling Rewires Macrophage Metabolism and Promotes Histone Acetylation via ATP-Citrate Lyase. *Immunity* (2019) 51:997-1011.e7. doi: 10.1016/J.IMMUNI.2019.11.009

56. Infantino V, Iacobazzi V, Palmieri F, Menga A. ATP-citrate lyase is essential for macrophage inflammatory response. *Biochem Biophys Res Commun* (2013) 440:105–111. doi: 10.1016/j.bbrc.2013.09.037

57. Lampropoulou V, Sergushichev A, Bambouskova M, Nair S, Vincent EE, Loginicheva E, Cervantes-Barragan L, Ma X, Huang SC-C, Griss T, et al. Itaconate Links Inhibition of Succinate Dehydrogenase with Macrophage Metabolic Remodeling and Regulation of Inflammation. *Cell Metab* (2016) 24:158–166. doi: 10.1016/J.CMET.2016.06.004

58. Ren W, Xia Y, Chen S, Wu G, Bazer FW, Zhou B, Tan B, Zhu G, Deng J, Yin Y. Glutamine Metabolism in Macrophages: A Novel Target for Obesity/Type 2 Diabetes. *Advances in Nutrition* (2019) 10:221–230. doi: 10.1093/advances/nmy084

59. Rich PR, Maréchal A. The mitochondrial respiratory chain. *Essays Biochem* (2010) 47:1–23. doi: 10.1042/BSE0470001

60. Scialò F, Fernández-Ayala DJ, Sanz A. Role of mitochondrial reverse electron transport in ROS signaling: Potential roles in health and disease. *Front Physiol* (2017) 8:428. doi: 10.3389/fphys.2017.00428

61. Tannahill GM, Curtis AM, Adamik J, Palsson-Mcdermott EM, McGettrick AF, Goel G, Frezza C, Bernard NJ, Kelly B, Foley NH, et al. Succinate is an inflammatory signal that induces IL-1β through HIF-1α. *Nature* (2013) 496:238–242. doi: 10.1038/nature11986

62. O'Neill LAJ, Kishton RJ, Rathmell J. A guide to immunometabolism for immunologists. *Nat Rev Immunol* (2016) 16:553–565. doi: 10.1038/nri.2016.70

63. Nagy C, Haschemi A. Time and Demand are Two Critical Dimensions of Immunometabolism: The Process of Macrophage Activation and the Pentose Phosphate Pathway. *Front Immunol* (2015) 6: doi: 10.3389/FIMMU.2015.00164

64. Haschemi A, Kosma P, Gille L, Evans CR, Burant CF, Starkl P, Knapp B, Haas R, Schmid JA, Jandl C, et al. The sedoheptulose kinase CARKL directs macrophage polarization through control of glucose metabolism. *Cell Metab* (2012) 15:813–826. doi: 10.1016/j.cmet.2012.04.023

65. Kelly B, O'Neill LAJ. Metabolic reprogramming in macrophages and dendritic cells in innate immunity. *Cell Res* (2015) 25:771–784. doi: 10.1038/cr.2015.68

66. Papandreou I, Cairns RA, Fontana L, Lim AL, Denko NC. HIF-1 mediates adaptation to hypoxia by actively downregulating mitochondrial oxygen consumption. *Cell Metab* (2006) 3:187–197. doi: 10.1016/j.cmet.2006.01.012

67. Caslin HL, Bhanot M, Bolus WR, Hasty AH. Adipose tissue macrophages: Unique polarization and bioenergetics in obesity. *Immunol Rev* (2020) 295:101–113. doi: 10.1111/imr.12853

68. Freemerman AJ, Johnson AR, Sacks GN, Milner JJ, Kirk EL, Troester MA, Macintyre AN, Goraksha-Hicks P, Rathmell JC, Makowski L. Metabolic Reprogramming of Macrophages. *Journal of Biological Chemistry* (2014) 289:7884–7896. doi: 10.1074/jbc.M113.522037

69. Torres-Castro I, Arroyo-Camarena ÚD, Martínez-Reyes CP, Gómez-Arauz AY, Dueñas-Andrade Y, Hernández-Ruiz J, Béjar YL, Zaga-Clavellina V, Morales-Montor J, Terrazas LI, et al. Human monocytes and macrophages undergo M1-type inflammatory polarization in response to high levels of glucose. *Immunol Lett* (2016) 176:81–89. doi: 10.1016/J.IMLET.2016.06.001

70. Dahik VD, Frisdal E, Goff W le. Rewiring of Lipid Metabolism in Adipose Tissue Macrophages in Obesity: Impact on Insulin Resistance and Type 2 Diabetes. *Int J Mol Sci* (2020) 21:1–30. doi: 10.3390/IJMS21155505

71. Norris PC, Reichart D, Dumlao DS, Glass CK, Dennis EA. Specificity of eicosanoid production depends on the TLR-4-stimulated macrophage phenotype. *J Leukoc Biol* (2011) 90:563. doi: 10.1189/JLB.0311153

72. Remmerie A, Scott CL. Macrophages and lipid metabolism. *Cell Immunol* (2018) 330:27–42. doi: 10.1016/j.cellimm.2018.01.020

73. Sharma M, Boytard L, Hadi T, Koelwyn G, Simon R, Ouimet M, Seifert L, Spiro W, Yan B, Hutchison S, et al. Enhanced glycolysis and HIF-1α activation in adipose tissue macrophages sustains local and systemic interleukin-1β production in obesity. *Sci Rep* (2020) 10: doi: 10.1038/S41598-020-62272-9

74. Boutens L, Hooiveld GJ, Dhingra S, Cramer RA, Netea MG, Stienstra R. Unique metabolic activation of adipose tissue macrophages in obesity promotes inflammatory responses. *Diabetologia 2018 61:4* (2018) 61:942–953. doi: 10.1007/S00125-017-4526-6

75. Tsatsanis Neofotistou-Themeli C, Eliopoulos AG, Al-Qahtani K, Aznaourova M, Ahmed Konstantina Lyroni E, Vergadi E, Lagoudaki E, Ieronymaki E, Theodorakis EM. Insulin Resistance in Macrophages Alters Their Metabolism and Promotes an M2-Like Phenotype. *The Journal of immunology* (2019) doi: 10.4049/jimmunol.1800065

76. Poblete JMS, Ballinger MN, Bao S, Alghothani M, Jr. JBN, Eubank TD, Christman JW, Magalang UJ. Macrophage HIF-1α mediates obesity-related adipose tissue dysfunction via interleukin-1 receptor-associated kinase M. *https://doi.org/101152/ajpendo001742019* (2020) 318:E689–E700. doi: 10.1152/AJPENDO.00174.2019

77. Drazic A, Myklebust LM, Ree R, Arnesen T. The world of protein acetylation. *Biochim Biophys Acta Proteins Proteom* (2016) 1864:1372–1401. doi: 10.1016/j.bbapap.2016.06.007

78. Choudhary C, Weinert BT, Nishida Y, Verdin E, Mann M. The growing landscape of lysine acetylation links metabolism and cell signalling. *Nat Rev Mol Cell Biol* (2014) 15:536–550. doi: 10.1038/nrm3841

79. Wellen KE, Hatzivassiliou G, Sachdeva UM, Bui T v., Cross JR, Thompson CB. ATP-citrate lyase links cellular metabolism to histone acetylation. *Science (1979)* (2009) 324:1076–1080. doi: 10.1126/science.1164097

80. Zhao S, Xu W, Jiang W, Yu W, Lin Y, Zhang T, Yao J, Zhou L, Zeng Y, Li H, et al. Regulation of cellular metabolism by protein lysine acetylation. *Science (1979)* (2010) 327:1000–1004. doi: 10.1126/science.1179689

81. de Ruijter AJM, van Gennip AH, Caron HN, Kemp S, van Kuilenburg A! BP. Histone deacetylases (HDACs) : characterization of the classical HDAC family. (2003). 737–749 p.

82. Raghuraman S, Donkin I, Versteyhe S, Barrès R, Simar D. The Emerging Role of Epigenetics in Inflammation and Immunometabolism. *Trends in Endocrinology and Metabolism* (2016) 27:782–795. doi: 10.1016/j.tem.2016.06.008

83. Akbari M, Hassan-Zadeh V. The inflammatory effect of epigenetic factors and modifications in type 2 diabetes. *Inflammopharmacology* (2019) doi: 10.1007/s10787-019-00663-9

84. Bricambert J, Favre D, Brajkovic S, Bonnefond A, Boutry R, Salvi R, Plaisance V, Chikri M, Chinetti-Gbaguidi G, Staels B, et al. Impaired histone deacetylases 5 and 6 expression mimics the effects of obesity and hypoxia on adipocyte function. *Mol Metab* (2016) 5:1200–1207. doi: 10.1016/j.molmet.2016.09.011

85. Zhou S, Tang X, Chen H-Z. Sirtuins and Insulin Resistance. *Frontiers in Endocrinology | www.frontiersin.org* (2018) 9:748. doi: 10.3389/fendo.2018.00748

86. Vana Dyke MW. Lysine deacetylase (KDAC) regulatory pathways: An alternative approach to selective modulation. *ChemMedChem* (2014) 9:511–522. doi: 10.1002/cmdc.201300444

87. Wang C-H, Wei Y-H. Roles of Mitochondrial Sirtuins in Mitochondrial Function, Redox Homeostasis, Insulin Resistance and Type 2 Diabetes. *Int J Mol Sci* (2020) 21:5266. doi: 10.3390/ijms21155266

88. Rodgers JT, Lerin C, Haas W, Gygi SP, Spiegelman BM, Puigserver P. Nutrient control of glucose homeostasis through a complex of PGC-1α and SIRT1. *Nature* (2005) 434:113–118. doi: 10.1038/nature03354

89. Cao Y, Jiang X, Ma H, Wang Y, Xue P, Liu Y. SIRT1 and insulin resistance. *J Diabetes Complications* (2016) 30:178–183. doi: 10.1016/j.jdiacomp.2015.08.022

90. Yeung F, Hoberg JE, Ramsey CS, Keller MD, Jones DR, Frye RA, Mayo MW. Modulation of NF-κB-dependent transcription and cell survival by the SIRT1 deacetylase. *EMBO J* (2004) 23:2369–2380. doi: 10.1038/sj.emboj.7600244

91. Liu T, Zhang L, Joo D, Sun SC. NF-κB signaling in inflammation. *Signal Transduct Target Ther* (2017) 2:1–9. doi: 10.1038/sigtrans.2017.23

92. Martínez-Jiménez V, Cortez-Espinosa N, Rodríguez-Varela E, Vega-Cárdenas M, Briones-Espinoza M, Ruíz-Rodríguez VM, López-López N, Briseño-Medina A, Turiján-Espinoza E, Portales-Pérez DP. Altered levels of sirtuin genes (SIRT1, SIRT2, SIRT3 and SIRT6) and their target genes in adipose tissue from individual with obesity. *Diabetes and Metabolic Syndrome: Clinical Research and Reviews* (2019) 13:582–589. doi: 10.1016/j.dsx.2018.11.011

93. Hui X, Zhang M, Gu P, Li K, Gao Y, Wu D, Wang Y, Xu A. Adipocyte SIRT 1 controls systemic insulin sensitivity by modulating macrophages in adipose tissue . *EMBO Rep* (2017) 18:645–657. doi: 10.15252/embr.201643184

94. Gillum MP, Kotas ME, Erion DM, Kursawe R, Chatterjee P, Nead KT, Muise ES, Hsiao JJ, Frederick DW, Yonemitsu S, et al. SirT1 regulates adipose tissue inflammation. *Diabetes* (2011) 60:3235–3245. doi: 10.2337/db11-0616

95. Dai H, Sinclair DA, Ellis JL, Steegborn C. Sirtuin activators and inhibitors: Promises, achievements, and challenges. *Pharmacol Ther* (2018) 188:140–154. doi: 10.1016/j.pharmthera.2018.03.004

96. Yoshizaki T, Schenk S, Imamura T, Babendure JL, Sonoda N, Bae EJ, Oh DY, Lu M, Milne JC, Westphal C, et al. SIRT1 inhibits inflammatory pathways in macrophages and modulates insulin sensitivity. *Am J Physiol Endocrinol Metab* (2010) 298: doi: 10.1152/ajpendo.00417.2009

97. Leus NGJ, van der Wouden PE, van den Bosch T, Hooghiemstra WTR, Ourailidou ME, Kistemaker LEM, Bischoff R, Gosens R, Haisma HJ, Dekker FJ. HDAC 3-selective inhibitor RGFP966 demonstrates anti-inflammatory properties in RAW 264.7 macrophages and mouse precision-cut lung slices by attenuating NF-κB p65 transcriptional activity. *Biochem Pharmacol* (2016) 108:58–74. doi: 10.1016/j.bcp.2016.03.010

98. Leus NGJ, van den Bosch T, van der Wouden PE, Krist K, Ourailidou ME, Eleftheriadis N, Kistemaker LEM, Bos S, Gjaltema RAF, Mekonnen SA, et al. HDAC1-3 inhibitor MS-275 enhances IL10 expression in RAW264.7 macrophages and reduces cigarette smoke-induced airway inflammation in mice. *Sci Rep* (2017) 7:1–18. doi: 10.1038/srep45047

99. Oh BR, Suh D hyeon, Bae D, Ha N, Choi Y il, Yoo HJ, Park JK, Lee EY, Lee EB, Song YW. Therapeutic effect of a novel histone deacetylase 6 inhibitor, CKD-L, on collagen-induced arthritis in vivo and regulatory T cells in rheumatoid arthritis in vitro. *Arthritis Res Ther* (2017) 19: doi: 10.1186/s13075-017-1357-2

100. Eckschlager T, Plch J, Stiborova M, Hrabeta J. Histone deacetylase inhibitors as anticancer drugs. *Int J Mol Sci* (2017) 18: doi: 10.3390/ijms18071414

101. Meier BC, Wagner BK. Inhibition of HDAC3 as a strategy for developing novel diabetes therapeutics. *Epigenomics* (2014) 6:209–214. doi: 10.2217/epi.14.11

102. Galmozzi A, Mitro N, Ferrari A, Gers E, Gilardi F, Godio C, Cermenati G, Gualerzi A, Donetti E, Rotili D, et al. Inhibition of class i histone deacetylases unveils a mitochondrial signature and enhances oxidative metabolism in skeletal muscle and adipose tissue. *Diabetes* (2013) 62:732–742. doi: 10.2337/db12-0548

103. Ferrari A, Fiorino E, Longo R, Barilla S, Mitro N, Cermenati G, Giudici M, Caruso D, Mai A, Guerrini U, et al. Attenuation of diet-induced obesity and induction of white fat browning with a chemical inhibitor of histone deacetylases. *Int J Obes* (2017) 41:289–298. doi: 10.1038/ijo.2016.191

104. Bele S, Girada SB, Ray A, Gupta A, Oruganti S, Babu PP, Rayalla RSR, Kalivendi SV, Ibrahim A, Puri V, et al. Ms-275, a class 1 histone deacetylase inhibitor augments glucagon-like peptide-1 receptor agonism to improve glycemic control and reduce obesity in diet-induced obese mice. *Elife* (2020) 9:1–33. doi: 10.7554/ELIFE.52212

105. Nicola NA, Burgess AW, Staber FG, Johnson GR, Metcalf D, Battye FL. Differential expression of lectin receptors during hemopoietic differntiation: Enrichment for granulocyte□macrophage progenitor cells. *J Cell Physiol* (1980) 103:217–237. doi: 10.1002/jcp.1041030207

106. Ahl PJ, Hopkins RA, Xiang WW, Au B, Kaliaperumal N, Fairhurst AM, Connolly JE. Met-Flow, a strategy for single-cell metabolic analysis highlights dynamic changes in immune subpopulations. *Commun Biol* (2020) 3:1–15. doi: 10.1038/s42003-020-1027-9

107. van den Bossche J, Baardman J, de Winther MPJ. Metabolic characterization of polarized M1 and M2 bone marrow-derived macrophages using real-time extracellular flux analysis. *Journal of Visualized Experiments* (2015) 2015:53424. doi: 10.3791/53424

108. Jones AE, Divakaruni AS. Macrophage activation as an archetype of mitochondrial repurposing. *Mol Aspects Med* (2020) 71:100838. doi: 10.1016/j.mam.2019.100838

109. Ma J, Wei K, Liu J, Tang K, Zhang H, Zhu L, Chen J, Li F, Xu P, Chen J, et al. Glycogen metabolism regulates macrophage-mediated acute inflammatory responses. *Nat Commun* (2020) 11:1–16. doi: 10.1038/s41467-020-15636-8

110. Jones AJY, Hirst J. A spectrophotometric coupled enzyme assay to measure the activity of succinate dehydrogenase. *Anal Biochem* (2013) 442:19–23. doi: 10.1016/j.ab.2013.07.018

111. Pinu FR, Beale DJ, Paten AM, Kouremenos K, Swarup S, Schirra HJ, Wishart D. Systems biology and multi-omics integration: Viewpoints from the metabolomics research community. *Metabolites* (2019) 9:76. doi: 10.3390/metabo9040076

112. Patti GJ, Yanes O, Siuzdak G. Innovation: Metabolomics: the apogee of the omics trilogy. *Nat Rev Mol Cell Biol* (2012) 13:263–269. doi: 10.1038/nrm3314

113. Kuehnbaum NL, Britz-Mckibbin P. New advances in separation science for metabolomics: Resolving chemical diversity in a post-genomic era. *Chem Rev* (2013) 113:2437–2468. doi: 10.1021/cr300484s

114. Büscher JM, Czernik D, Ewald JC, Sauer U, Zamboni N. Cross-platform comparison of methods for quantitative metabolomics of primary metabolism. *Anal Chem* (2009) 81:2135–2143. doi: 10.1021/ac8022857

115. Puchalska P, Huang X, Martin SE, Han X, Patti GJ, Crawford PA. Isotope Tracing Untargeted Metabolomics Reveals Macrophage Polarization-State-Specific Metabolic Coordination across Intracellular Compartments. *iScience* (2018) 9:298–313. doi: 10.1016/j.isci.2018.10.029

116. Jha AK, Huang SCC, Sergushichev A, Lampropoulou V, Ivanova Y, Loginicheva E, Chmielewski K, Stewart KM, Ashall J, Everts B, et al. Network integration of parallel metabolic and transcriptional data reveals metabolic modules that regulate macrophage polarization. *Immunity* (2015) 42:419–430. doi: 10.1016/j.immuni.2015.02.005

117. Yuan J, Bennett BD, Rabinowitz JD. Kinetic flux profiling for quantitation of cellular metabolic fluxes. *Nat Protoc* (2008) 3:1328–1340. doi: 10.1038/nprot.2008.131

118. Puchalska P, Huang X, Martin SE, Han X, Patti GJ, Crawford PA. Isotope Tracing Untargeted Metabolomics Reveals Macrophage Polarization-State-Specific Metabolic Coordination across Intracellular Compartments. *iScience* (2018) 9:298–313. doi: 10.1016/j.isci.2018.10.029

119. Wellen KE, Thompson CB. A two-way street: Reciprocal regulation of metabolism and signalling. *Nat Rev Mol Cell Biol* (2012) 13:270–276. doi: 10.1038/nrm3305

120. Pesi R, Balestri F, Ipata PL. Metabolic interaction between urea cycle and citric acid cycle shunt: A guided approach. *Biochemistry and Molecular Biology Education* (2018) 46:182–185. doi: 10.1002/bmb.21099

121. Guijas C, Montenegro-Burke JR, Warth B, Spilker ME, Siuzdak G. Metabolomics activity screening for identifying metabolites that modulate phenotype. *Nat Biotechnol* (2018) 36:316–320. doi: 10.1038/nbt.4101

122. Vijan S. In the clinic. Type 2 diabetes. *Ann Intern Med* (2015) 162:ITC1–ITC16. doi: 10.7326/AITC201503030

123. Osborn O, Olefsky JM. The cellular and signaling networks linking the immune system and metabolism in disease. *Nat Med* (2012) 18:363–374. doi: 10.1038/nm.2627

124. Eshghjoo S, Kim DM, Jayaraman A, Sun Y, Alaniz RC. A Comprehensive High-Efficiency Protocol for Isolation, Culture, Polarization, and Glycolytic Characterization of Bone Marrow-Derived Macrophages. *J Vis Exp* (2021) 2021:1–16. doi: 10.3791/61959

125. Palsson-McDermott EM, Curtis AM, Goel G, Lauterbach MAR, Sheedy FJ, Gleeson LE, van den Bosch MWM, Quinn SR, Domingo-Fernandez R, Johnston DGW, et al. Pyruvate Kinase M2 Regulates Hif-1α Activity and IL-1β Induction and Is a Critical Determinant of the Warburg Effect in LPS-Activated Macrophages. *Cell Metab* (2015) 21:65–80. doi: 10.1016/J.CMET.2014.12.005

126. Na YR, Jung D, Song J, Park J-W, Hong JJ, Seok SH. Pyruvate dehydrogenase kinase is a negative regulator of interleukin-10 production in macrophages. *J Mol Cell Biol* (2020) 12:543–555. doi: 10.1093/JMCB/MJZ113

127. Bailey JD, Diotallevi M, Nicol T, McNeill E, Shaw A, Chuaiphichai S, Hale A, Starr A, Nandi M, Stylianou E, et al. Nitric Oxide Modulates Metabolic Remodeling in Inflammatory Macrophages through TCA Cycle Regulation and Itaconate Accumulation. *Cell Rep* (2019) 28:218-230.e7. doi: 10.1016/J.CELREP.2019.06.018

128. A A, C M, AM G, DH K. Metabolic characterisation of THP-1 macrophage polarisation using LC-MS-based metabolite profiling. *Metabolomics* (2020) 16: doi: 10.1007/S11306-020-01656-4

129. Semba H, Takeda N, Isagawa T, Sugiura Y, Honda K, Wake M, Miyazawa H, Yamaguchi Y, Miura M, Jenkins DMR, et al. HIF-1α-PDK1 axis-induced active glycolysis plays an essential role in macrophage migratory capacity. *Nat Commun* (2016) 7: doi: 10.1038/NCOMMS11635

130. Triboulet S, Aude-Garcia C, Armand L, Gerdil A, Diemer H, Proamer F, Collin-Faure V, Habert A, Strub J-M, Hanau D, et al. Analysis of cellular responses of macrophages to zinc ions and zinc oxide nanoparticles: a combined targeted and proteomic approach. *Nanoscale* (2014) 6:6102–6114. doi: 10.1039/C4NR00319E

131. D Z, Z T, H H, G Z, C C, Y W, W L, S K, S L, M P-N, et al. Metabolic regulation of gene expression by histone lactylation. *Nature* (2019) 574:575–580. doi: 10.1038/S41586-019-1678-1

132. Meiser J, Krämer L, Sapcariu SC, Battello N, Ghelfi J, D'Herouel AF, Skupin A, Hiller K. Pro-inflammatory Macrophages Sustain Pyruvate Oxidation through Pyruvate Dehydrogenase for the Synthesis of Itaconate and to Enable Cytokine Expression. *Journal of Biological Chemistry* (2016) 291:3932–3946. doi: 10.1074/JBC.M115.676817

133. Cordes T, Metallo CM. Itaconate Alters Succinate and Coenzyme A Metabolism via Inhibition of Mitochondrial Complex II and Methylmalonyl-CoA Mutase. *Metabolites 2021, Vol 11, Page 117* (2021) 11:117. doi: 10.3390/METABO11020117

134. Ko CW, Counihan D, Wu J, Hatzoglou M, Puchowicz MA, Croniger CM. Macrophages with a deletion of the phosphoenolpyruvate carboxykinase 1 (Pck1) gene have a more proinflammatory phenotype. *Journal of Biological Chemistry* (2018) 293:3399–3409. doi: 10.1074/JBC.M117.819136/ATTACHMENT/2E807966-9995-4072-B691-0317F2F6EDA5/MMC1.PDF

CHAPTER 3

Effects of lysine deacetylase inhibitor treatment on LPS responses of alveolar-like macrophages

Sara Russo[1], Marcel Kwiatkowski[2], Justina C. Wolters[3], Albert Gerding, Jos Hermans[1], Natalia Govorukhina[1], Rainer Bischoff [†], Barbro N. Melgert[4,5 †*]

Journal of Leukocyte Biology 2023 :qiad121.
Published online 2023 Oct 9. Doi: 10.1093/jleuko/qiad121

TOC SUMMARY

This study explores how inhibiting lysine deacetylases (KDAC) affects macrophages, which play a key role in the immune system. KDAC inhibition resulted in reduced production of inflammatory mediators in lipopolysaccharide-treated macrophages, however, only minor changes in macrophage metabolism were observed. KDAC inhibition specifically enhanced the expression of proteins involved in ubiquitination, which may be a driver of the anti-inflammatory effects of KDAC inhibitors. A multi-omics approach provides novel insights into how macrophages interact with cues from their environment.

ABSTRACT

Macrophages are key immune cells that can adapt their metabolic phenotype in response to different stimuli. Lysine deacetylases (KDAC) are important enzymes regulating inflammatory gene expression and KDAC inhibitors have been shown to exert anti-inflammatory effects in models of chronic obstructive pulmonary disease (COPD). We hypothesized that these anti-inflammatory effects may be associated with metabolic changes in macrophages. To validate this hypothesis, we used an unbiased and a targeted proteomic approach to investigate metabolic enzymes as well as LC- and GC-MS to quantify metabolites in combination with the measurement of functional parameters in primary murine alveolar-like macrophages after lipopolysaccharide (LPS)-induced activation in the presence or absence of KDAC inhibition. We found that KDAC inhibition resulted in reduced production of inflammatory mediators such as TNF-α and IL-1β. However, only minor changes in macrophage metabolism were observed, as only one of the KDAC inhibitors slightly increased mitochondrial respiration while no changes in metabolite levels were seen. However, KDAC inhibition specifically enhanced expression of proteins involved in ubiquitination, which may be a driver of the anti-inflammatory effects of KDAC inhibitors. Our data illustrate that a multi-omics approach provides novel insights into how macrophages interact with cues from their environment. More detailed studies investigating ubiquitination as a potential driver of KDAC inhibition will help developing novel anti-inflammatory drugs for difficult to treat diseases such as COPD.

Keywords: Lung, proteasome, immunometabolism, metabolome analysis, proteome analysis, multi-omics.

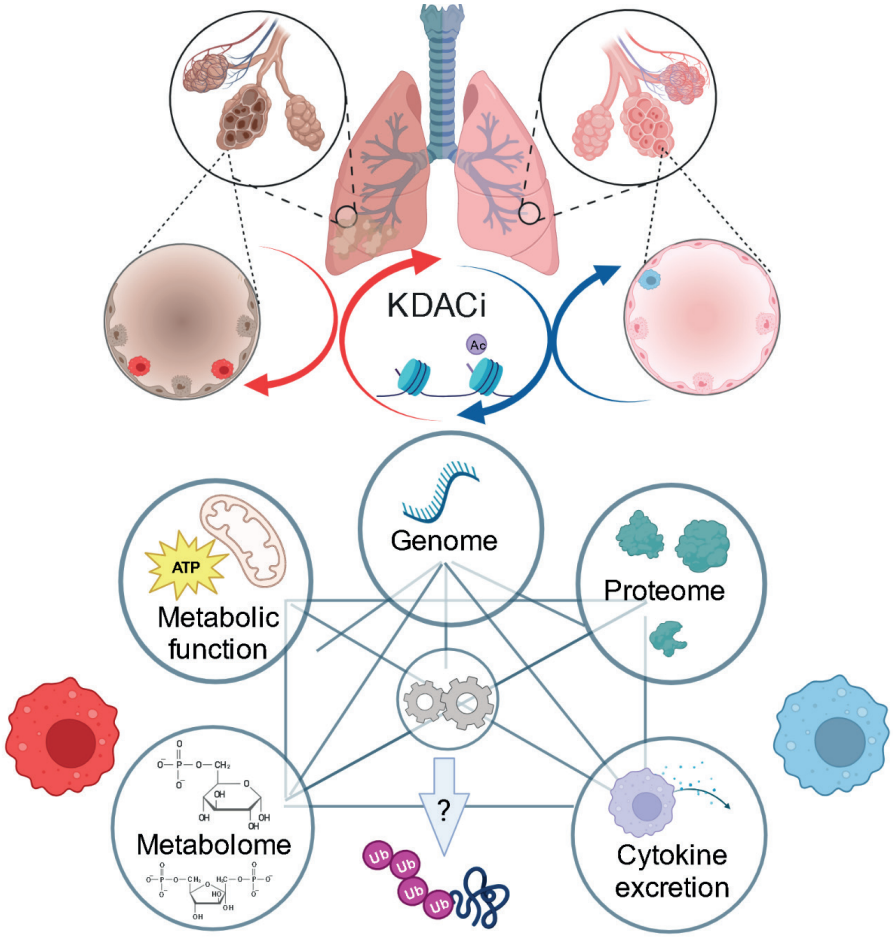
KDACi
Ac
Genome
ATP
Metabolic function
Proteome
Metabolome
?
Ub
Ub
Ub
Ub
Cytokine excretion

INTRODUCTION

Alveolar macrophages are self-renewing tissue-resident macrophages that derive from fetal liver progenitors without contribution from circulating monocytes under steady-state conditions (1). They are part of the first line of defense in the lungs and need to respond to dangers without impairing lung function. Depending on which environmental factors alveolar macrophages are exposed to, even in healthy individuals, these cells can change their phenotype swiftly to deal with a threat as efficiently as possible (2). Alveolar macrophages, therefore, play a dual role in the lung: initiating lung inflammation to neutralize threats and resolving inflammation to prevent lung function loss (3,4). These two seemingly opposite functions appear to be regulated by changes in metabolism, called metabolic reprogramming. Many studies have shown that induction of macrophage glycolysis favors inflammation while induction of macrophage oxidative phosphorylation favors tissue repair (5). However, Woods and colleagues recently showed that alveolar macrophages do not rely on glycolysis as their main source of energy during inflammatory responses, challenging this view for tissue-resident macrophages in the lung (6).

Most chronic respiratory diseases are characterized by an imbalance between pro and anti-inflammatory responses (7), with alveolar macrophages showing phenotypical and functional changes (8). Chronic obstructive pulmonary disease (COPD) is one of these diseases affecting more than 300 million patients worldwide (9). COPD is characterized by chronic inflammation which leads to small airway inflammation and obstruction (chronic bronchitis) together with parenchymal destruction (emphysema) (10). Alveolar macrophages are important contributors to chronic inflammation through the secretion of a number of pro-inflammatory cytokines like tumor necrosis factor (TNF)-α, and interleukin (IL)-1 β (7). Moreover, previous work has shown an increase in pro-inflammatory macrophages in bronchoalveolar lavage fluid and sputum of patients with COPD compared to healthy individuals (11,12). Furthermore, resolution of inflammation and initiation of tissue repair through the production of IL-10 and transforming growth factor (TGF)-β (7) seems to be deficient in lung tissue of patients with COPD (13). To overcome this deficit, patients are often treated with corticosteroids, which can induce an anti-inflammatory phenotype in macrophages (14–16). However, corticosteroids are not effective in many COPD patients as some patients develop resistance and others have a nonresponsive phenotype (17–19). Therefore, there is a pressing need to find alternative therapeutics that can be used to treat COPD patients and to rebalance macrophage-driven inflammation with macrophage-driven tissue repair. An interesting approach was recently postulated by Leus et al., showing that inhibitors of lysine deacetylases (KDACs also known as histone deacetylases or HDACs) have anti-inflammatory effects. They found that KDAC inhibitors reduced

lung inflammation in smoke-exposed mice and inflammatory mediator production in lipopolysaccharide (LPS)-exposed lung slices (20,21).

KDACs are executors of epigenetic mechanisms by removing acetyl groups from the ϵ-amino group of lysine residues in target proteins, thereby altering the way these proteins interact with other proteins/nucleic acids (22) or altering their activity (23). Acetyl-CoA, an important metabolic intermediate, is the substrate of lysine acetyltransferases (KATs) that acetylate proteins. Therefore, altered levels of acetyl-CoA during metabolic reprogramming of macrophages may alter the level of lysine acetylation (23), which may subsequently affect gene expression.

The focus of this study was to investigate whether lysine deacetylase inhibitors inhibit activation of primary macrophages by changing metabolic processes in these cells. To this end, we used self-propagating murine alveolar-like macrophages derived from fetal liver monocytes, a well-established model for alveolar macrophages (24–26). To investigate the relationship between anti-inflammatory effects of KDAC inhibition and metabolic processes in alveolar-like macrophages, we studied metabolites, metabolic enzymes, and amino acids by targeted liquid chromatography–mass spectrometry (LC-MS_, gas chromatography–mass spectrometry (GC-MS), and high-performance liquid chromatography (HPLC) with fluorescence detection, as well as cellular responses by extracellular flux analysis.

MATERIALS AND METHODS

Cell culture

Self-propagating murine alveolar-like macrophages (a kind gift from dr. G.Fejer, Plymouth University, UK (27)) isolated from fetal livers were cultured in plastic tissue culture flasks (Costar Europe) at 37^{0}C with 5% CO_2/95% air in RPMI 1640 medium containing GlutaMAX™ (Gibco® ; Thermo Fisher Scientific, Inc., Waltham, MA, USA) supplemented with 10% (vol/vol) heat-inactivated fetal bovine serum, 100 U/mL penicillin and 100 µg/mL streptomycin (Gibco®), and 20 ng/mL murine granulocyte-macrophage colony-stimulating factor (PeproTech; Thermo Fisher Scientific, Inc., Waltham, MA, USA). Once a week, cells were detached with 1mM EDTA (Merck, Darmstadt, Germany) and reseeded at a density of 1,5 x 10^6 cells/mL. Cell culture medium was replaced after 4 days. For experiments, macrophages were used between passage 3 and 15.

KDAC inhibitor and LPS treatments

Alveolar-like macrophages were seeded at a cell density of 300,000 cells/well in 12-wells plates with 1 mL medium/well, prior to incubation with the KDAC inhibitors. After culturing for 72 hours, they were either treated with 10 ng/mL lipopolysaccharide (LPS, Escherichia coli, serotype 0111:B4, Sigma-Aldrich; Merck, Darmstadt, Germany) for the last 4 hours of the experiment, with KDAC inhibitors for the last 20 hours, or with the combination of the two. KDAC inhibitors were dissolved in dimethyl sulfoxide (DMSO). MS275 (also known as Entinostat, Axon Medchem, Reston, Virginia, United States) and RGFP966 (Selleckchem, Houston, Texas, United States) were used at a concentration of 1μM. Treated cells were subsequently used for different analyses as depicted in **Figure 1** and described below.

Cytokine analysis by enzyme-linked immune-sorbent assay (ELISA)

Cell culture medium was collected, centrifuged, and supernatants were analyzed for TNF-a and IL-10 by ELISA (both from R&D Systems, Minneapolis, MN, respectively DY410-05 and DY417-05), according to the manufacturer's instructions.

Gene expression analysis by reverse transcription quantitative polymerase chain reaction (RT-qPCR)

Messenger RNA was isolated from cells using Maxwell® LEV Simply RNA Cells/Tissue kit (Promega, Madison, Wisconsin, US). A NanoDrop® ND-1000 Spectrophotometer (Thermo Scientific) was used to measure total mRNA concentration in samples. cDNA synthesis from mRNA was performed using a Moloney Murine Leukemia Virus Reverse Transcriptase (M-MLV RT) kit (Promega, Madison, Wisconsin, USA) in a Mastercycler® Gradient (Eppendorf, Hamburg, Germany) programmed for 10 minutes at 20°C, 30 minutes at 42°C, 12 minutes at 20°C, 5 minutes at 99°C, and 5 minutes at 20°C. Transforming growth factor beta (TGFβ; F: AGGGCTACCATGCCAACTTC, R: GTTGGACAACTGCTCCACCT), Suppressor Of Cytokine Signaling 3 (SOCS3; F: CCTTTGACAAGCGGACTCTC, R: GCCAGCATAAAAACCCTTCA) genes were quantified using quantitative real-time PCR (RT qPCR) from the synthesized cDNA, using SensiMixTM SYBR® Green (Bioline, London, UK) in a 7900HT Real-Time PCR sequence detection system (Applied Biosystems, Waltham, Massachussets, US). PCR analysis consisted of 45 cycles of 10 min at 95°C, 15 seconds at 95°C, and 25 seconds at 60°C (repeated for 40 times) followed by a dissociation stage of 95°C for 15 seconds, 60°C for 15 seconds, and 95°C for 15 seconds. Output data were analyzed using SDS 2.4 software (Applied Biosystems) and ΔCt values were calculated after β-actin normalization. Two to the power of -ΔCt ($2^{-\Delta Ct}$) was used as a final value for plotting and group comparisons.

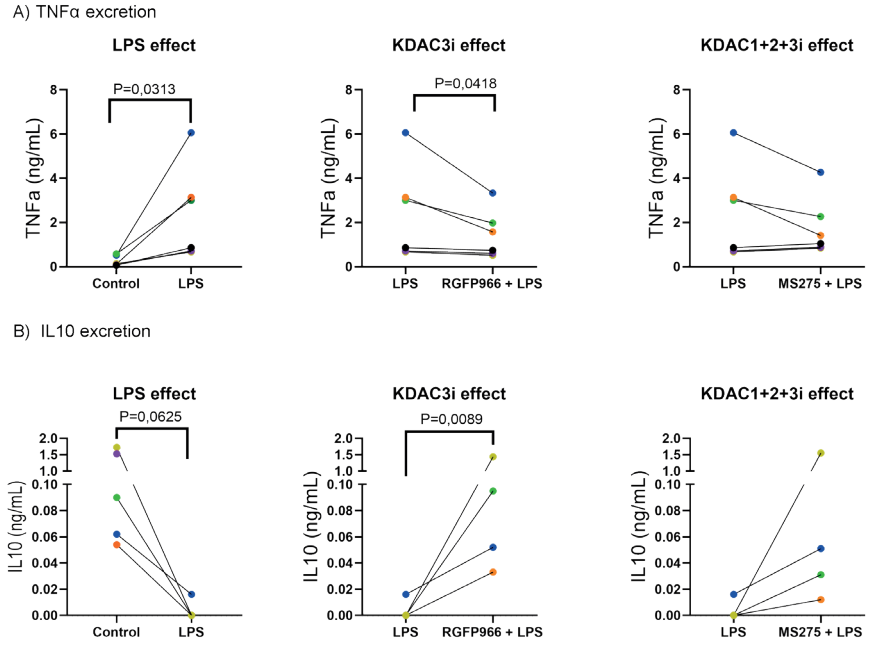

Figure 1: Representation of the workflow used to obtain different samples from alveolar-like macrophages. Depicted in red and represented by a pentagon are the steps necessary to measure cytokine secretion, in purple and represented by a triangle the steps necessary to measure gene expression, in green and represented by a circle the steps necessary to measure metabolite levels, in blue and represented by a square the steps necessary to measure protein expression, and in orange and represented by a star the steps necessary to perform extracellular flux analysis. Figure created with Biorender.com.

Functional metabolic assays

Macrophage glycolytic rates were measured using a Seahorse XFe96 Extracellular Flux Analyzer (Agilent, Santa Clara, USA). Macrophages were seeded at a density of 3.7 x 10^3/well in Seahorse XF96 cell culture microplates for 72 hours. Cells were then treated with KDAC inhibitors for 20 hours (MS275, RGFP966) and LPS was added for the last 4 hours of the experiment (KDAC inhibitor+LPS) or not (control). Cells were then equilibrated for 1 hour in the absence of CO_2 at 37 °C with XF base media, which does not contain glucose but was complemented with glutamine (2 mM). The manufacturer's Seahorse XF glycolysis stress test protocol was used to assess glycolytic rate. After equilibration, sequential injections of glucose (20 mM), oligomycin (1µM), and 2-deoxy-D-glucose (50 mM) were performed. Glycolytic function is represented as glycolysis, glycolytic capacity, and glycolytic reserve. Glycolysis was calculated as the difference between the maximal rate before oligomycin addition and the last rate measurement before glucose addition.

Glycolytic capacity was calculated as the difference between the maximal rate after oligomycin addition and the last rate measurement before glucose addition. The glycolytic reserve was calculated as the difference between glycolytic capacity and glycolysis. The measurements were normalized to the protein content in each well using a BCA assay.

The same cell seeding density and treatments were used to measure mitochondrial respiration, measured as oxygen consumption rate (OCR). Cells were equilibrated for 1 hour in the absence of CO_2 at 37 °C with XF base media, which was supplemented with glucose (20 mM), glutamine (2 mM), and pyruvate. The Seahorse XF cell mito stress test protocol was used to assess glycolytic rate. After equilibration, sequential injections of oligomycin (1µM), carbonyl cyanide-p- trifluoromethoxyphenyl-hydrazon (FCCP) (4µM), and rotenone/antimycin (1µM each) were performed. Mitochondrial respiration is represented as basal respiration, maximal respiration, spare respiratory capacity, spare capacity, ATP production, and proton leakage. Basal respiration is calculated as the difference between the last rate measurement before oligomycin addition and the minimum rate measurement after rotenone/antimycin addition (which is defined as nonmitochondrial oxygen consumption). Maximal respiration is calculated as the difference between the maximum rate measurement after FCCP injection and the non-mitochondrial respiration. Spare respiratory capacity is calculated as the difference between maximal respiration and basal respiration. ATP production is calculated as the difference between the last rate measurement before oligomycin injection and the minimum rate measurement after oligomycin injection. The measurements were normalized to protein content in each well using a BCA assay following the manufacturer's instructions (Pierce™ Microplate BCA Protein Assay Kit, Thermo Fisher Scientific).

Tricarboxylic acid (TCA) cycle metabolites measurement by GC-MS

Metabolite extraction and measurement methods were described by Bakker *et al.* (28). In short, cells were washed three times with ice-cold PBS and then quenched with methanol while being placed on ice. Ultrapure water was then added (with the addition of internal standards for quantification) and cells were removed from the flasks. Cell extracts were transferred into tubes containing chloroform. Methanol and chloroform were stored at -20°C until the moment of use. Methanol/chloroform-containing cell extracts were first shaken for 30 minutes at 4°C and then centrifuged for 10 minutes at 16100 g at 4°C. The upper aqueous phase was then transferred to a new tube and evaporated under nitrogen. The lower non-polar fraction was also transferred to a new tube and the solvent was evaporated under nitrogen. The interphase was washed with methanol and centrifuged for 10 minutes at 16000 g

at 4°C. The supernatant was removed and a small volume of fresh methanol was added to the pellet and samples were stored at -80°C for further protein analysis (see the paragraph "Targeted proteomics of metabolic enzymes by QconCATs").

The dried metabolites present in the upper aqueous phase were dissolved in 2% methoxyamine HCL in pyridine and incubated for 90 minutes at 37°C. The samples were then silylated for 1 hour at 55°C by adding N-tert-butyldimethysilyl-N-methyltrifluoroacetamide with 1% tert-butyldimethylchlorosilane. The derivates were transferred to a GC/MS vial with a micro-insert and analyzed by GC/MS. GC/MS measurements were carried out on a 7890A GC (Agilent) coupled to a 5975C Quadrupole MS (Agilent), equipped with a CTC Analytics PAL autosampler (CTC Analytics AG, Switzerland). Quantification of the amino acids and TCA cycle metabolites was performed based on 6-point internal standard corrected calibration curves in water, treated like the cell samples to follow the complete extraction method.

Amino acid quantification by HPLC

Amino acids were extracted by washing cells three times with ice-cold PBS and then quenched with methanol while being placed on ice. Millipore water was then added and the cells were scraped off the plastic. The cell extract was transferred to an Eppendorf tube containing chloroform. Methanol and chloroform were stored at -20°C until use. Cells were first shaken for 20 minutes at 1400 rpm, at 4°C, and then centrifuged for 5 minutes at of 16100 g at 4°C. The upper aqueous phase was then transferred to a new tube and dried overnight. Sample preparation and amino acid measurements were performed as described by Hernandez-Valdes *et al.* (29). Briefly, samples were first resuspended in water-acetonitrile (1:4), aliquoted, dried again, and then resuspended in water containing three internal standards (citrulline, norvaline and sarcosine). Standard amino acids and samples were derivatized automatically in an HPLC autosampler with o-phtalaldehyde and 9-fluorenylmethyloxycarbonyl reagent solutions. HPLC amino acid analysis was performed on an Agilent 1100 HPLC binary system (Agilent, Santa Clara, USA) equipped with an 1100 Fluorescence detector (FLD) and a Zorbax Eclipse C18 column (Ø3 × L250 mm, 3 µm particle size, Agilent, Santa Clara, USA) at 40°C. A 10mM $Na_2HPO_4/Na_2B_4O_7$ pH 8.2 buffer was used as solvent A and a mixture of 45:45:10 acetonitrile/methanol/water as solvent B at a flow-rate of 0.5 ml/min and a gradient from 2-57% B from 0.5-20 min after the injection followed by respectively a 4 min 100% cleaning and 9 min 2% B reconditioning period. The fluorescence detector was set to λEx = 340 nm, λEm = 450 nm for all 2-O-phthaldialdehyde (OPA) derivatives and λEx = 266, λEm = 305 nm for the 9-fluorenylmethyl chloroformate (FMOC)

derivatives at 18 min, eluting at the end of the chromatogram. Quantification of amino acids was performed based on 5-point internal standard corrected calibration curves in water ranging from 2-250 µM (r^2>0.99).

Targeted proteomics of metabolic enzymes in the interphase by quantification concatemers (QconCATs)

For proteome analysis, interphases obtained during metabolite extractions as described in the section "TCA cycle metabolites measurement by GC-MS" were used. Samples stored at -80°C were dried and resuspended in 8M Urea, 100 mM ammonium bicarbonate to be further diluted with 100 mM AmBiCa to 2M urea. Samples were then sonicated (Vibra-Cell, Sonics, Newton, United States) for 3×10 seconds, 30% without pulse. Protein concentrations were determined with a microplate BCA protein assay following the manufacturer's instructions (Pierce™ Microplate BCA Protein Assay Kit, Thermo Fisher Scientific). For in-solution digestion, 10 µg of sample was diluted in 2M Urea, 100 mM ammonium bicarbonate (AmBiCa) to a final volume of 300 µL. Proteins were reduced in 10mM dithiothreitol for 30 minutes at 37°C, alkylated with 55 mM iodoacetamide, and incubated in the dark at room temperature for 60 minutes. To further dilute the urea concentration, 300 µL of 100 mM AmBiCa was added. Samples were then digested with 100 ng of trypsin (sequencing grade modified trypsin V5111, Promega) at 37 °C for 16 hours and the trypsin was deactivated with formic acid before cleanup using C18 SPE columns (Gracepure TM SPE C18-Aq, 50 mg/1mL). Targeted proteome analyses were performed by injecting 1 µg total protein starting material plus 2 ng high abundant proteins or 0.1 ng low abundant proteins of predigested QconCAT standards (quantification concatemers; designed to target a set of proteins details about the assay development and applications for quantification have been described elsewhere previously) (30,31).

Untargeted proteomics of the interphase

For proteome analysis, the same digested samples from the interphases obtained during metabolite extractions as described in the section "TCA cycle metabolites measurement by GC-MS" and processed as described in the section "Targeted proteomics of metabolic enzymes by QconCATs" were analyzed. Untargeted proteome analyses were performed by injecting 1 µg total protein starting material on a quadrupole orbitrap mass spectrometer equipped with a nano-electrospray ion source (Orbitrap Exploris 480, Thermo Scientific). Chromatographic separation of the peptides was performed by liquid chromatography (LC) on an Evosep system (Evosep One, Evosep) using a nano-LC column (EV1137 Performance column 15 cm

x 150 µm, 1.5 µm, Evosep; buffer A: 0.1% v/v formic acid, dissolved in milliQ-H_2O, buffer B: 0.1% v/v formic acid, dissolved in acetonitrile). Peptides were separated using the 30SPD workflow (Evosep). The mass spectrometer was operated in positive ion mode and data-independent acquisition mode (DIA) using isolation windows of 16 m/z with a precursor mass range of 400-1000, switching the high-field

asymmetric waveform ion mobility spectrometry (FAIMS) between CV-45V and -60V with three scheduled MS1 scans during each screening of the precursor mass range. LC-MS raw data were processed with Spectronaut (version 16.0.220606) (Biognosys) using the standard settings of the directDIA workflow except that quantification was performed on MS1, with a mouse Swissprot database (17021 protein entries, downloaded in December 2019). For the quantification, local normalization was applied and the Q-value filtering was set to the classic setting without imputing.

Statistical analysis

Analyses were performed using GraphPad Prism 8.0 (GraphPad Software, La Jolla, USA). Due to the limited sample size in our experiments, nonparametric testing was used to compare groups. For nonparametric testing between two groups a Mann-Whitney U test was used for unpaired or a Wilcoxon test for paired data. For comparison of multiple groups, a Kruskall Wallis or Friedman test was used for nonpaired or paired nonparametric data, respectively, with Dunn's correction for multiple testing. Proteomics data were normalized using Local Normalization based on the Local Regression Normalization described by Callister *et al.* (32) and Log2 transformed. Groups were subsequently compared using a paired one-way ANOVA with Holm-Sidak's correction for multiple testing. When comparing lists of proteins fold changes and p-values adjusted for multiple testing (q values) were generated. Differentially expressed protein were subsequently selected having q-values <0.05.

Data Availability

The untargeted mass spectrometry proteomics data have been deposited to the ProteomeXchange Consortium via the PRIDE partner repository (33) with the dataset identifier PXD040933. The targeted mass spectrometry proteomics data have been deposited on the PASSEL server with the data identifier PASS04816. Data access is available upon request.

RESULTS

KDAC inhibition inhibits alveolar macrophage activation upon LPS stimulation

Previous work from Leus *et al.* showed that class I KDACs (KDAC 1, 2, 3 and 8), and in particular KDAC3, play a key role in pro-inflammatory gene expression in monocyte-derived RAW 264.7 macrophages and precision-cut lung slices (20,21). To study their influence on the pro- and anti-inflammatory responses in alveolar-like macrophages, we used MS275 (KDAC1,2, and 3 inhibitor) and RGFP966 (KDAC3 inhibitor) (34) in combination with LPS exposure.

We first investigated the effects of these treatments on the excretion of the cytokines TNF-α and IL-10 in the culture supernatant. LPS treatment resulted in a significantly more excretion of the pro-inflammatory cytokine TNFα compared to vehicle-treated controls, which was inhibited by pretreatment with KDAC3 inhibitor RGFP966 but not by pretreatment with KDAC1,2 and 3 inhibitor MS275 (**Figure 2A**). Similar findings were found for IL-6 (supplementary data, **Supplementary Figure 1**). Conversely, LPS treatment resulted in lower excretion of the anti-inflammatory cytokine IL-10 compared to vehicle-treated control (**Figure 2B**). Again, only KDAC3 inhibitor RGFP966 inhibited this effect of LPS significantly, while MS275 had a minor effect that was not statistically significant. This was specific for the combination of LPS and RGFP966 as treatment of unstimulated macrophages with either KDAC inhibitor alone did not induce IL-10 excretion (supplementary data **Supplementary Figure 1**)

We subsequently investigated the effect of KDAC inhibition on the expression of additional anti-inflammatory factors, (i.e. SOCS3 and TGFβ) (35–37) by qPCR to confirm an anti-inflammatory phenotypic shift in alveolar-like macrophages after treatment with KDAC inhibitors upon LPS treatment. SOCS3 is an important negative regulator of innate immune responses and is induced together with pro-inflammatory cytokines during LPS stimulation in macrophages to control inflammation and eventually induce resolution (38–40). LPS treatment indeed induced the expression of SOCS3 in alveolar-like macrophages and this induction was enhanced when macrophages were pretreated with KDAC1/2/3 inhibitor MS275, but not with KDAC3 inhibitor RGFP966 (**Figure 3A**). TGFβ, produced in an autocrine manner by adult alveolar macrophages, plays a critical role in alveolar macrophage development (41) and is also an important anti-inflammatory cytokine (42). While treatment with LPS did not induce TGFβ expression (**Figure 3B**), pretreatment with KDAC1/2/3 inhibitor MS275, but not with KDAC3 inhibitor RGFP966, resulted in significantly higher TGFβ expression compared to LPS treatment alone, further supporting an anti-inflammatory effect of MS275.

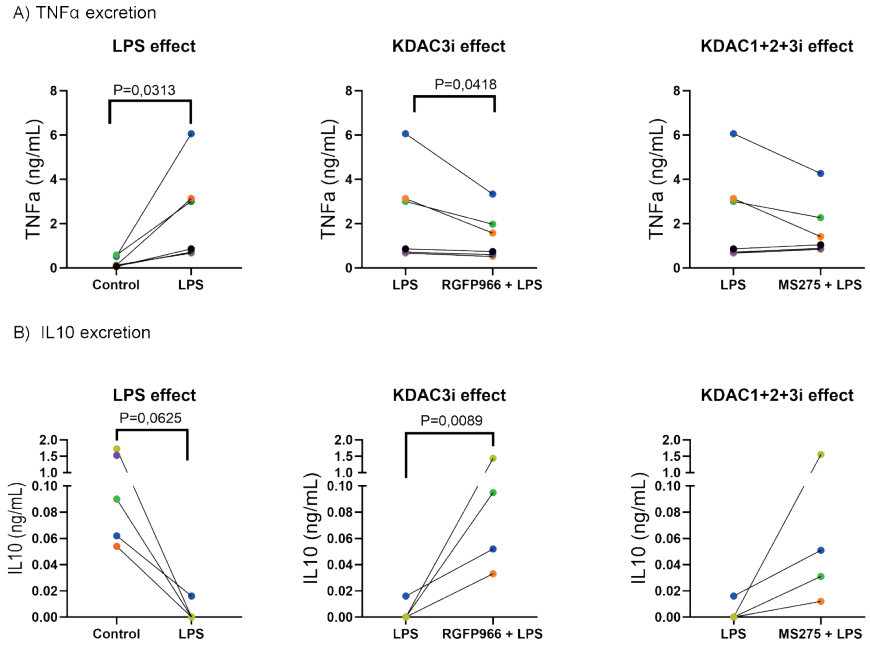

Figure 2: Effects of LPS and/or KDAC inhibitors MS275 or RGFP966 on TNF-α and IL-10 excretion in culture supernatant of alveolar-like macrophages. Alveolar-like macrophages were incubated with 1 ug/ml KDAC1/2/3 inhibitor MS275 (KDAC1+2+3i), KDAC3 inhibitor RGFP966 (KDAC3i), or vehicle for 16 h and then stimulated with 10 ng/ml LPS or vehicle for 4 h. (A) Effects on TNFα excretion. Colored dots indicate the different independent replicates. (B) Effects on IL-10 excretion. Colored dots indicate the different independent replicates. A Wilcoxon test was used to compare control versus LPS stimulation. Groups stimulated with or without KDAC inhibitors were compared using a Friedman test with a Dunn's correction for multiple testing (n=5). P<0.05 was considered significant.

Taken together, these results confirm previous observations in monocyte-derived macrophages (20,21) and show that in alveolar-like macrophages, KDAC3 inhibition blocks pro-inflammatory responses and stimulates anti-inflammatory ones, while the effects of KDAC1/3 inhibition are mixed.

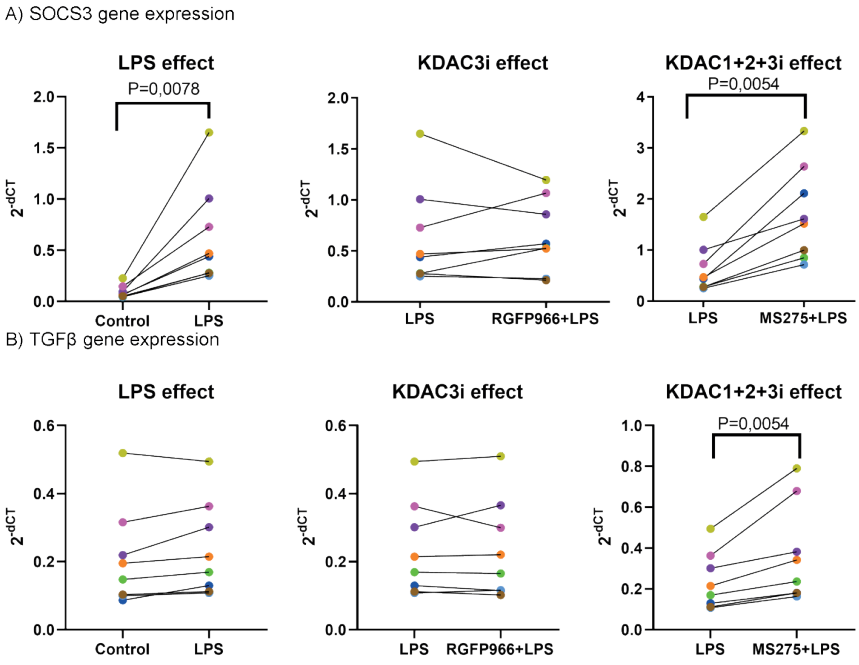

Figure 3: Effects of LPS and/or KDAC inhibitors MS275 or RGFP966 on SOCS3 and TGFβ mRNA expression in alveolar-like macrophages. Alveolar-like macrophages were incubated with 1 ug/ml (1 μM) KDAC1/2/3 inhibitor MS275 (KDAC1+2+3i), KDAC3 inhibitor RGFP966 (KDAC3i), or vehicle for 16 h and then stimulated with 10 ng/ml LPS or vehicle for 4 h. (A) Effects on SOCS3 mRNA expression. Colored dots indicate the different independent replicates. (B) Effects on TGFβ mRNA expression. A Wilcoxon test was used to compare control versus LPS stimulation. Colored dots indicate the different independent replicates. Groups stimulated with or without KDAC inhibitors were compared using a Friedman test with a Dunn's correction for multiple testing (n=5). P<0.05 was considered significant.

KDAC inhibition and metabolic reprogramming

To understand the molecular mechanisms behind the anti-inflammatory effects of KDAC inhibitors we performed an untargeted proteome analysis on proteins isolated from macrophages (see **Figure 1**). We identified more than 4000 proteins and determined differentially expressed proteins between control and different treatment conditions.

We identified 318 significantly upregulated and 85 downregulated proteins in cells treated with MS275+LPS compared to LPS (supplementary data, Supplementary Table 1). The proteins were considered upregulated if their fold change was higher than 1.5 and downregulated if the fold change was lower than 0.7 in combination with q-values lower than 0.05. The resulting list of proteins was used for pathway

enrichment analysis and protein interaction network building (**Figure 4A**) (43). The most significant cluster identified after MS275+LPS treatment compared to LPS treatment alone was "Protein processing in endoplasmic reticulum" which also encompasses "Modification-dependent macromolecule catabolic process" and "cellular macromolecule catabolic process". This cluster mainly comprised proteins that take part in the ubiquitination of other proteins. The second most significant cluster found was "Biosynthesis of amino acids", which also includes "alpha-amino acid biosynthetic process" and "2-oxocarboxylic acid metabolism" pathways. These pathways comprise the mechanisms necessary to synthesize amino acids, including glycolysis, the TCA cycle, and the pentose phosphate pathway. Other relevant clusters were the "fructose 6-metabolic process" and the "tricarboxylic acid (TCA) cycle and respiratory electron transport". These pathways collectively include the major metabolic pathways that are involved in macrophage polarization and that provide energy to cells.

We only found 7 up- and 13 downregulated proteins in cells treated with RGFP966+LPS compared to LPS (reported in the supplementary data, Supplementary Table 2). Pathway enrichment analysis and protein interaction network building (**Figure 4B**) once again showed that the most significant cluster "Ub-specific processing proteases", was related to the ubiquitination and deubiquitination of proteins. The cluster "RNA polymerase II transcription regulator complex" was the second most significantly enriched pathway. This cluster encompasses proteins that regulate transcription by RNA polymerase II, a process that is regulated by a number of mechanisms, including alterations of chromatin structure (44), and therefore it is not surprising that inhibition of lysine deacetylation leads to changes in proteins belonging to this pathway.

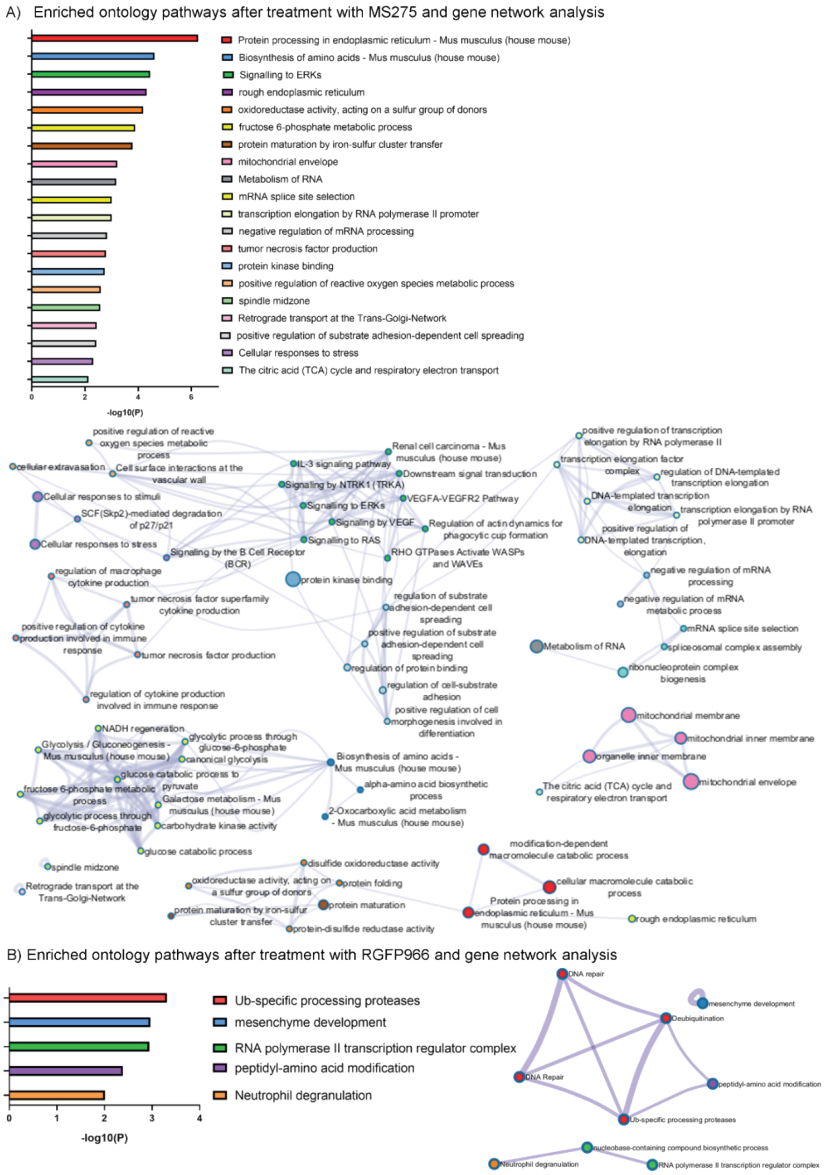

Figure 4: Functional enrichment and interactome analyses of proteins upregulated or downregulated by LPS treatment in combination with KDAC inhibitors. Alveolar-like macrophages were incubated with 1 ug/ml KDAC1/2/3 inhibitor MS275 or KDAC3 inhibitor RGFP966, or vehicle for 16 h and then stimulated with 10 ng/ml LPS or vehicle for 4 h. (A) Enriched ontology pathways and gene network analysis of 83 >1.5-fold upregulated and 85 < 0.7-fold downregulated proteins in MS275+LPS compared to LPS treatment alone. (B) Enriched ontology pathways and gene network analysis of 7 >1.5-fold upregulated and 13 < 0.7-fold downregulated proteins in RGFP966+LPS compared to LPS treatment alone. A matched one-way ANOVA test was used to compare groups with a Bonferroni's correction for multiple testing. (n=6). The website Metascape was used to perform the functional enrichment and interactome analyses (43).

Class I KDAC inhibitors do not affect the levels of metabolic enzymes

Our untargeted proteomic analysis identified different metabolic pathways as processes that may be affected by treatment with KDAC1/2/3 inhibitors. This is interesting because metabolic reprogramming has been shown to be important in determining pro-and anti-inflammatory responses in different types of macrophages (45,46). We, therefore, investigated the metabolism of alveolar-like macrophages after KDAC inhibition in more detail.

We first measured protein levels of enzymes that are part of the major metabolic pathways depicted in **Figure 5**. To obtain absolute values for these proteins, we used a targeted proteomic approach that used internal standards of concatenated signature peptides encoded by QconCAT proteins (47). None of the 59 proteins that we quantified (see Supplementary Table 3 and **Supplementary Figure 3**, supplementary material) was expressed at significantly different levels in any of our comparisons. These results suggest that even though a first exploratory proteome analysis suggested that alveolar-like macrophages may have changes in metabolism induced by LPS and/or KDAC inhibition, they did not seem to change their primary metabolism in response to these treatments.

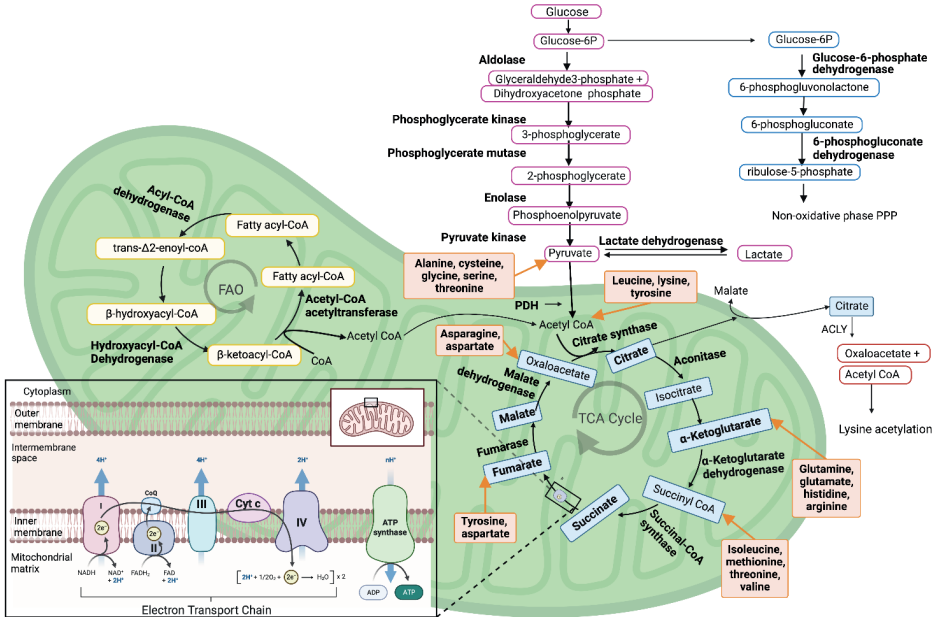

Figure 5: Proteins and metabolites measured in the context of macrophage metabolism. Macrophages can rely on different metabolic pathways depending on their activation state. Here the glycolytic, pentose phosphate, fatty acid oxidation, tricarboxylic acid, and electron transport chain pathways are depicted. Metabolites and proteins that were measured in this study are indicated in bold. Figure created with Biorender.com.

KDAC inhibition has only a minor effect on the metabolism of alveolar-like macrophages

Since protein levels alone may not suffice to determine whether metabolic activity has changed upon LPS stimulation with or without KDAC inhibition, we assessed cellular metabolic rates using extracellular flux analysis. We first measured glycolytic function showing that LPS does not induce a glycolytic shift in alveolar-like macrophages, in accordance with results in primary alveolar macrophages by Woods et al (6) (**Figure 6A-B**). In addition, prior treatment with either KDAC3 or KDAC1/2/3 inhibitors did not affect glycolytic function, suggesting that the shift from pro- to anti-inflammatory behavior in these macrophages was not accompanied by a change in glycolytic activity (**Figure 6**).

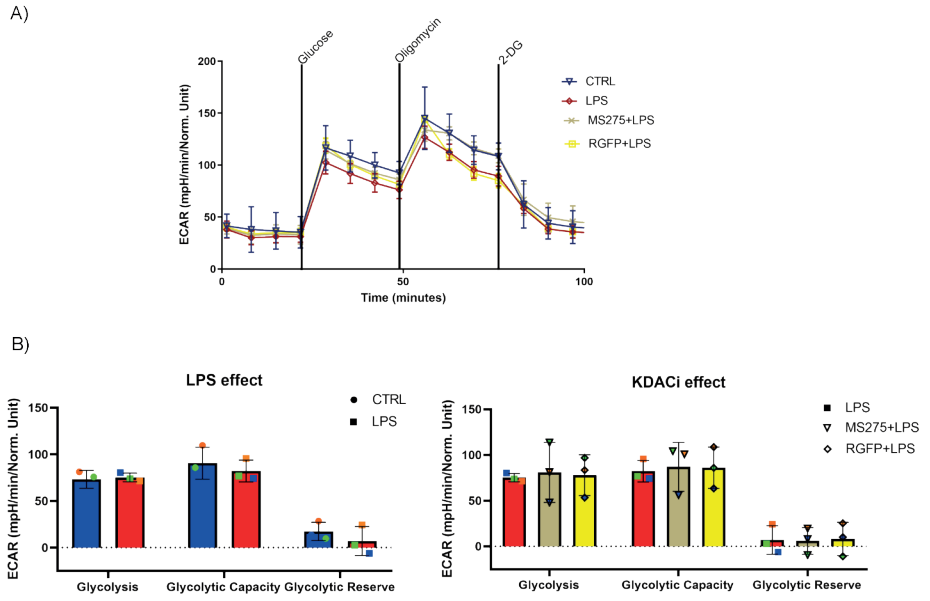

Figure 6: Effects of LPS and/or KDAC inhibitors MS275 or RGFP966 on glycolytic function of alveolar-like macrophages. Alveolar-like macrophages were incubated with 1 ug/ml KDAC1/2/3 inhibitor MS275, KDAC3 inhibitor RGFP966, or vehicle for 16 h and then stimulated with 10 ng/ml LPS or vehicle for 4 h. Extracellular acidification rates (ECAR) were measured with a glycolysis stress test using a Seahorse XF96 and normalized to protein concentration in each well using a BCA assay. **(A)** Macrophages were treated sequentially with glucose, oligomycin (ATP synthase inhibitor), and 2-DG (2-deoxyglucose, a glucose analogue). **(B)** Bars quantify glycolytic function. Data represent three biological replicates which are the average of 6 technical replicates per biological replicate. Colored dots indicate the different independent replicates. Glycolysis parameters were compared among treatments using a Wilcoxon test for CTRL vs LPS and Friedman test with a Dunn's correction for multiple testing for LPS vs KDAC inhibitor+LPS. $P<0.05$ was considered significant.

We next assessed mitochondrial respiration in alveolar-like macrophages to investigate whether LPS-induced production of inflammatory mediators was fueled by oxidative phosphorylation and if so, whether this was affected by KDAC inhibitors. Treatment with only LPS did not change any of the mitochondrial respiration parameters compared to untreated controls (**Figure 7**). However, pretreatment with KDAC3 inhibitor RGFP966 resulted in a slightly higher spare capacity compared to treatment with LPS alone. Pretreatment with KDAC1/2/3 inhibitor MS275 did not affect mitochondrial respiration and neither did treatment with the KDAC inhibitors in absence of LPS (**Supplementary Figure 2**).

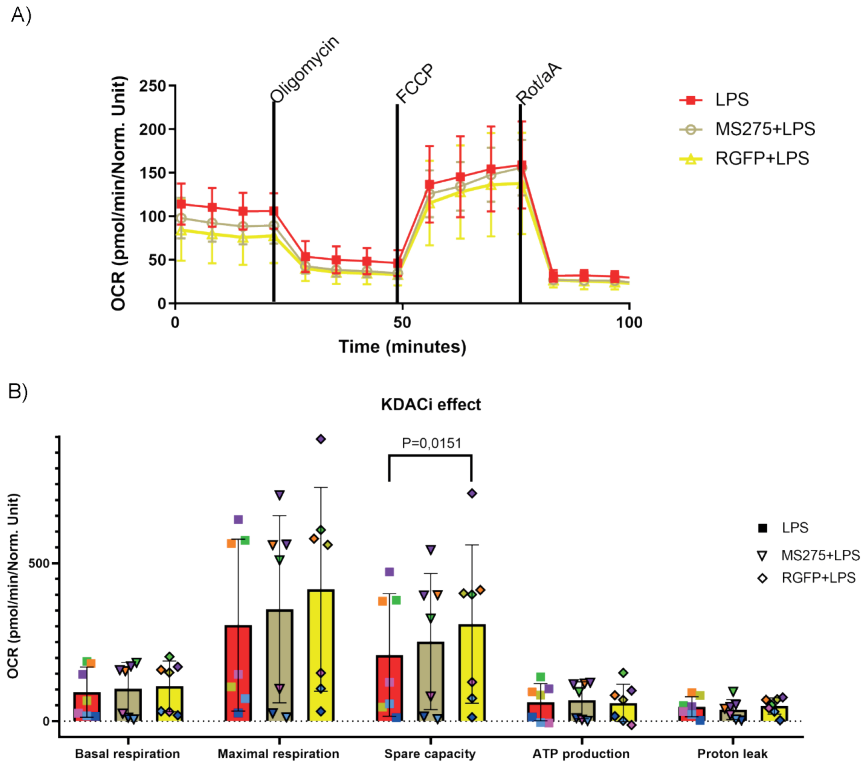

Figure 7: Effects of LPS and/or KDAC inhibitors MS275 or RGFP966 on mitochondrial respiration in alveolar-like macrophages. Alveolar-like macrophages were incubated with 1 ug/ml KDAC1/2/3 inhibitor MS275, KDAC3 inhibitor RGFP966, or vehicle for 16 h and then stimulated with 10 ng/ml LPS or vehicle for 4 h. Oxygen consumption rates (OCR) were measured with a mitochondrial stress test using Seahorse XF96 and normalized to protein concentration in each well using a BCA assay. **(A)** Macrophages were treated sequentially with oligomycin (ATP synthase inhibitor), FCCP (carbonyl cyanide-p- trifluoromethoxyphenyl-hydrazon), and rotenone. **(B)** Bars quantify mitochondrial respiration of macrophages treated with either LPS and/or KDAC inhibitors. Data represent seven biological replicates which is the average of 6 technical replicates per biological replicate. Colored dots indicate the different independent replicates. Mitochondrial parameters were compared among treatments using a Friedman with a Dunn's correction for multiple testing for LPS vs KDACi+LPS. P<0.05 was considered significant.

KDAC inhibition does not affect the levels of metabolites in alveolar-like macrophages

Pro-inflammatory activation of many types of macrophages is not only characterized by a shift from oxidative phosphorylation to glycolysis, but also by interruptions in the TCA cycle (48). Breaks after the generation of citrate and after succinate (**Figure 5**) result in the accumulation of these two metabolites (48). To investigate these responses in alveolar-like macrophages in the context of LPS stimulation and KDAC inhibition, we investigated levels of the main metabolites of the TCA cycle and of the amino acids that are substrates of the TCA cycle.

Stimulation of alveolar-like macrophages with LPS resulted in significantly more succinate but no changes in citrate compared to untreated controls (**Figure 8A**). However, we found significantly higher levels of α-ketoglutarate and malate after LPS stimulation, key TCA cycle metabolites that support immune responses (49,50). Pretreatment with either KDAC inhibitor prior to LPS stimulation did not change the levels of any of the measured metabolites or amino acids compared to LPS stimulation alone (**Figure 8**). Bar plots of individual metabolite levels can be found in **Supplementary Figure 4** and **Supplementary Figure 5**.

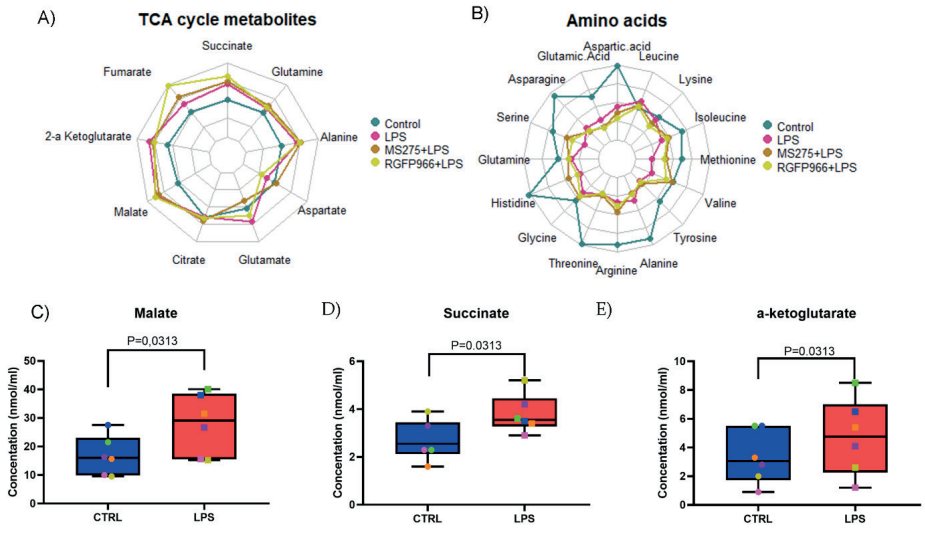

Figure 8: Effects of LPS and/or KDAC inhibitors MS275 or RGFP966 on TCA cycle metabolite and amino acid levels in alveolar-like macrophages. Alveolar-like macrophages were incubated with 1 ug/ml KDAC1/2/3 inhibitor MS275, KDAC3 inhibitor RGFP966, or vehicle for 16 h and then stimulated with 10 ng/ml LPS or vehicle for 4 h. Metabolite concentration levels were measured **(A)** with GC-MS or **(B)** with HPLC. Data are represented as a radar plot (as % of control, n=6). Levels of three metabolites were significantly higher in LPS-treated macrophages compared to control, respectively **(C)** malate, **(D)** succinate, and **(E)** α-ketoglutarate. Colored dots indicate the different independent replicates.

DISCUSSION

Our main aim was to investigate if anti-inflammatory effects of lysine deacetylase inhibitors in alveolar-like macrophages were associated with metabolic changes in these cells to elucidate their mechanism of action. We focused on macrophage metabolism as metabolic adaptations are functionally important in many types of macrophages and lysine acetylation is closely associated with cell metabolism. To our knowledge, this is the first study to investigate the effects of lysine deacetylase inhibitors in this context using a multi-omics approach. Our finding that alveolar-like macrophage metabolism is mostly unchanged after a pro-inflammatory stimulus like LPS was rather unexpected. It suggests that, even though metabolic reprogramming is crucial in many other types of macrophages to respond to pro- and anti-inflammatory stimuli, alveolar-like macrophages do not seem to rely on this mechanism. This is in agreement with data reported by Woods et al. (6). Based on our proteomics results, we hypothesize that other post-translational modifications, such as ubiquitination, may be potential drivers of the anti-inflammatory effects of KDAC inhibitors. Our data illustrate that a multi-omics approach is necessary to discover how a complex cell model interacts with its environment. More detailed studies investigating ubiquitination as a potential driver of KDAC inhibition may help developing novel anti-inflammatory drugs for difficult to treat diseases such as COPD.

Leus et al (20,21) previously showed that KDAC inhibitors MS275 and RGFP966 attenuated smoke- and LPS-induced inflammation in lung tissue. Our results confirm that these inhibitors exert similar anti-inflammatory effects in alveolar-like macrophages and they suggest further that KDAC3 inhibition by RGFP966 results in a more pronounced inhibitory effect than inhibiting KDAC1, 2, and 3 by MS275 in LPS-stimulated macrophages. This latter inhibitor only induced significantly higher expression of SOCS3 mRNA, suggesting a time lag compared to RGFP966, that already resulted in differential expression at the cytokine secretion level. This may be related to the lower specificity of MS275, a fact that is corroborated by our finding that MS275 treatment induced more changes to the proteome than RGFP966. In fact, in a cell-free system MS275 inhibited KDAC1, 2, and 3 (IC_{50} 0.228, 0.364, and 0.744 μM, respectively), while RGFP966 only selectively inhibited KDAC3 (IC_{50} 2.686 μM) (51), and similar values were obtained in RAW264.7 macrophages (52).

Our proteomics results in conjunction with subsequent pathway analyses suggest that MS275 and RGFP966 mediate their anti-inflammatory effects by increasing protein ubiquitination and that this may be a potential driver of the anti-inflammatory effects of KDAC inhibitors. Protein ubiquitination is a post-translational modification process that plays a crucial role in maintaining cellular

homeostasis (53) and it has been shown that alterations in this process can lead to changes in macrophage function, especially in generation of reactive oxygen species (54). It has been reported that the activity of the TNFα signaling pathway is controlled by ubiquitination and that inhibiting protein ubiquitination leads to increased inflammatory activity in macrophages (54–56). Since ubiquitination and acetylation are mutually exclusive post-translational modifications, meaning that they share the same modification site, i.e. the epsilon amino group of lysine (57,58), it is conceivable that changing protein acetylation patterns results in a modified ubiquitination pattern. The balance between protein acetylation and protein ubiquitination plays an important role in regulating protein stability, since an acetylated lysine residue cannot be ubiquitinated, therefore enhancing protein stability. For acetylated lysine residues to be ubiquitinated, they need to be deacetylated by KDAC and this process is blocked by treatment with the inhibitors. This could be one of the reasons why many more proteins (403 versus 20) were differentially expressed in macrophages pre-treated with MS275 compared to those pre-treated with RGFP966, since MS275 has a broader activity spectrum than RGFP966.

While pathway enrichment provided insights into possible biological mechanisms, specific proteins that were strongly upregulated after MS275 and LPS treatment may give further insights into particular responses. The top 3 most upregulated proteins in alveolar-like macrophages pre-treated with MS275 compared to LPS-only treatment, were INCA1 (Inhibitor Of CDK, Cyclin A1 Interacting Protein 1), JAM-A (junctional adhesion molecule A), and MMP12 (macrophage metalloelastase 12). The function of INCA1 is still relatively unknown, but it has been reported to inhibit the activity of cyclin-dependent kinases and cell proliferation (59). However, no clear connection to the lung (60) has been described. JAM-A was shown to have an important role in inflammatory processes, since it is a transmembrane domain protein that is necessary for diapedesis at inflammatory sites (61). A recent publication by Kiss *et al.* demonstrated that JAM-A expression increased in tumors during monocyte-to-macrophage differentiation (62) indicating that it may play a role in macrophage-mediated inflammation. Furthermore, JAM-A was shown to play a key role in maintaining lung epithelial barrier function (63), making this protein a potential candidate for further investigations in the context of macrophage-epithelial communication. MMP12 is an endopeptidase that plays a crucial role in smoke-induced inflammation in COPD by contributing to alveolar tissue destruction and subsequent emphysema development (64). Its higher expression after KDAC inhibitor treatment is therefore somewhat puzzling. However, MMP12 has been reported to have a dual role by being associated with both pro-inflammatory (65,66) and anti-inflammatory (65,66) effects, reflecting the

plasticity of alveolar macrophages. In our case, we found more MMP12 in cells that have higher expression of anti-inflammatory genes. This could be one of the first steps leading to an attenuation of inflammatory responses through downregulation of recruitment of polymorphonuclear leukocytes *in vivo* (67).

The only significantly differentially expressed proteins affected by both KDAC inhibitor treatments were Lims1 (LIM and senescent cell antigen-like-containing domain protein 1) and Ltv1 (low temperature viability protein 1), which were downregulated in both cases. Lims 1, also known as Pinch1, is a focal adhesion protein important in cellular processes like cell shape modulation, motility, and survival (68). Ltv1 is an assembly factor, that together with ribosomal proteins helps correct ribosome assembly (69). No direct correlation was found between Lims1 or Ltv1 expression and macrophage activity, indicating two possible proteins of interest to investigate further in alveolar macrophages.

The aim of our studies was to investigate whether anti-inflammatory effects of KDAC inhibitors could be driven by metabolic changes in macrophages. Many studies have shown that when macrophages polarize to an anti-inflammatory or alternatively activated phenotype they rely on oxidative phosphorylation and on the beta-oxidation of fatty acids to produce ATP, while they rely on glycolysis when they polarize to a pro-inflammatory or classically activated phenotype. This dualistic view is now recognized as being overly simplistic (46,70), since it has recently been shown that tissue-resident alveolar macrophages do not rely on glycolysis to respond to pro-inflammatory stimuli (6). Using a multi-omics approach allowed us to confirm this recent finding in our model system and to study whether effects of KDAC inhibitors depend on metabolic changes in alveolar-like macrophages from many different angles. While we did not see any functional metabolic changes using extracellular flux analysis, treatment with LPS resulted in higher levels of three key intracellular metabolites of the TCA cycle. This finding is in line with pro-inflammatory metabolic reprogramming with a broken TCA cycle, represented by higher levels of succinate, and is also coupled with higher concentrations of malate and α-ketoglutarate. These two latter metabolites correlated to inflammation in macrophages by supporting the production of cytokines and other immune effector molecules in previous studies (49,50), suggesting that the changes in metabolism in alveolar macrophages may be too subtle to pick up with extracellular flux analysis. Mitochondrial respiration at the spare respiratory capacity level was slightly higher when cells were treated with KDAC inhibitor RGFP966. This deacetylase inhibitor clearly inhibited release of proinflammatory cytokines in LPS-treated macrophages and therefore the small but significant induction of mitochondrial respiration fits with this metabolic reprogramming (71,72). One limitation of our study was the

use of self-propagating cells, which was necessary to obtain a sufficient protein yield for proteomics analysis and metabolite production. However, it should be noted that our model does not accurately replicate the in vivo environment as it only represents a single immune cell population and lacks the complex matrix in which the cells reside. Nonetheless, this model holds potential for investigating the influence of lysine deacetylation on diseases regulated by macrophages and exploring therapeutic interventions.

In conclusion, we found that inhibition of protein deacetylation and notably of KDAC3 attenuates activation of LPS-stimulated alveolar-like macrophages but has surprisingly little effect on macrophage metabolism. Other inhibitory mechanisms, such as a reduced level of protein ubiquitination, may open new avenues for the treatment of diseases characterized by chronic inflammation, like COPD, that do not respond well to corticosteroids.

CONFLICT OF INTEREST

The authors declare that the research was conducted in the absence of any commercial or financial relationships that could be construed as a potential conflict of interest.

AUTHORS CONTRIBUTION

SR, MK, NG, RB, and BM conceived and designed the set-up of the manuscript. SR drafted the manuscript and prepared figures. SR, RB, and BM edited and revised the manuscript. SR, JC, AG, and JH performed experiments and all approved the final version.

ACKNOWLEDGMENTS AND FUNDING

The Noordelijke CARA stichting is gratefully acknowledged for funding part of the work described (project number 134426).

This project has received funding from the European Union's Horizon 2020 research and innovation program under the Marie Skłodowska-Curie grant agreement No 754425.

REFERENCES

1. Mould KJ, Barthel L, Mohning MP, Thomas SM, McCubbrey AL, Danhorn T, Leach SM, Fingerlin TE, O'Connor BP, Reisz JA, et al. Cell Origin Dictates Programming of Resident versus Recruited Macrophages during Acute Lung Injury. *Am J Respir Cell Mol Biol* (2017) 57:294–306. doi: 10.1165/rcmb.2017-0061OC
2. Li X, Kolling FW, Aridgides D, Mellinger D, Ashare A, Jakubzick C v, Jakubzick C. ScRNA-seq Expression of IFI27 and APOC2 Identifies Four Alveolar Macrophage Superclusters in Healthy BALF. *bioRxiv* (2022)2022.01.30.478325. doi: 10.1101/2022.01.30.478325
3. Branchett WJ, Cook J, Oliver RA, Bruno N, Walker SA, Stölting H, Mack M, O'Garra A, Saglani S, Lloyd CM. Airway macrophage-intrinsic TGF-β1 regulates pulmonary immunity during early-life allergen exposure. *Journal of Allergy and Clinical Immunology* (2021) 147:1892–1906. doi: 10.1016/J.JACI.2021.01.026
4. Mould KJ, Jackson ND, Janssen WJ. Single cell RNA sequencing identifies unique inflammatory airspace macrophage subsets. *JCI Insight* (2019) 4:126556. doi: 10.1172/jci.insight.126556
5. Viola A, Munari F, Sánchez-Rodríguez R, Scolaro T, Castegna A. The metabolic signature of macrophage responses. *Front Immunol* (2019) 10:1462. doi: 10.3389/fimmu.2019.01462
6. Woods PS, Kimmig LM, Meliton AY, Sun KA, Tian Y, O'Leary EM, Gökalp GA, Hamanaka RB, Mutlu GM. Tissue-resident alveolar macrophages do not rely on glycolysis for LPS-induced inflammation. *Am J Respir Cell Mol Biol* (2020) 62:243–255. doi: 10.1165/RCMB.2019-0244OC
7. Boorsma CE, Draijer C, Melgert BN. Macrophage Heterogeneity in Respiratory Diseases. *Mediators Inflamm* (2013) 2013:1–19. doi: 10.1155/2013/769214
8. Aegerter H, Lambrecht BN, Jakubzick C v. Biology of lung macrophages in health and disease. *Immunity* (2022) 55:1564–1580. doi: 10.1016/j.immuni.2022.08.010
9. Adeloye D, Song P, Zhu Y, Campbell H, Sheikh A, Rudan I. Global, regional, and national prevalence of, and risk factors for, chronic obstructive pulmonary disease (COPD) in 2019: a systematic review and modelling analysis. *Lancet Respir Med* (2022) 10:447–458. doi: 10.1016/S2213-2600(21)00511-7
10. Vogelmeier CF, Criner GJ, Martinez FJ, Anzueto A, Barnes PJ, Bourbeau J, Celli BR, Chen R, Decramer M, Fabbri LM, et al. Global strategy for the diagnosis, management, and prevention of chronic obstructive lung disease 2017 report. *Am J Respir Crit Care Med* (2017) 195:557–582. doi: 10.1164/RCCM.201701-0218PP
11. Pesci A, Balbi B, Majori M, Cacciani G, Bertacco S, Alciato P, Donner C. Inflammatory cells and mediators in bronchial lavage of patients with chronic obstructive pulmonary disease. *European Respiratory Journal* (1998) 12:380–386. doi: 10.1183/09031936.98.12020380.
12. Keatings VM, Collins PD, Scott DM, Barnes PJ. Differences in interleukin-8 and tumor necrosis factor-alpha in induced sputum from patients with chronic obstructive pulmonary disease or asthma. *Am J Respir Crit Care Med* (2012) 153:530–534. doi: 10.1164/AJRCCM.153.2.8564092
13. Branchett WJ, Lloyd CM. Regulatory cytokine function in the respiratory tract. *Mucosal Immunol* (2019) 12:589–600. doi: 10.1038/s41385-019-0158-0
14. Ehrchen JM, Roth J, Barczyk-Kahlert K. More than suppression: Glucocorticoid action on monocytes and macrophages. *Front Immunol* (2019) 10: doi: 10.3389/fimmu.2019.02028
15. Barczyk K, Ehrchen J, Tenbrock K, Ahlmann M, Kneidl J, Viemann D, Roth J. Glucocorticoids promote survival of anti-inflammatory macrophages via stimulation of adenosine receptor A3. *Blood* (2010) 116:446–455. doi: 10.1182/BLOOD-2009-10-247106

16. Ehrchen J, Steinmüller L, Barczyk K, Tenbrock K, Nacken W, Eisenacher M, Nordhues U, Sorg C, Sunderkötter C, Roth J. Glucocorticoids induce differentiation of a specifically activated, anti-inflammatory subtype of human monocytes. *Blood* (2007) 109:1265–1274. doi: 10.1182/BLOOD-2006-02-001115

17. Barnes PJ. Corticosteroid resistance in patients with asthma and chronic obstructive pulmonary disease. *Journal of Allergy and Clinical Immunology* (2013) 131:636–645. doi: 10.1016/J.JACI.2012.12.1564

18. Barnes PJ. Mechanisms and resistance in glucocorticoid control of inflammation. *J Steroid Biochem Mol Biol* (2010) 120:76–85. doi: 10.1016/J.JSBMB.2010.02.018

19. Snoeck-Stroband JB, Lapperre TS, Sterk PJ, Hiemstra PS, Thiadens HA, Boezen HM, ten Hacken NHT, Kerstjens HAM, Postma DS, Timens W, et al. Prediction of Long-Term Benefits of Inhaled Steroids by Phenotypic Markers in Moderate-to-Severe COPD: A Randomized Controlled Trial. *PLoS One* (2015) 10:e0143793. doi: 10.1371/JOURNAL.PONE.0143793

20. Leus NGJ, Van Der Wouden PE, Van Den Bosch T, Hooghiemstra WTR, Ourailidou ME, Kistemaker LEM, Bischoff R, Gosens R, Haisma HJ, Dekker FJ. HDAC 3-selective inhibitor RGFP966 demonstrates anti-inflammatory properties in RAW 264.7 macrophages and mouse precision-cut lung slices by attenuating NF-κB p65 transcriptional activity. *Biochem Pharmacol* (2016) 108:58–74. doi: 10.1016/J.BCP.2016.03.010

21. Leus NGJ, Van Den Bosch T, Van Der Wouden PE, Krist K, Ourailidou ME, Eleftheriadis N, Kistemaker LEM, Bos S, Gjaltema RAF, Mekonnen SA, et al. HDAC1-3 inhibitor MS-275 enhances IL10 expression in RAW264.7 macrophages and reduces cigarette smoke-induced airway inflammation in mice. *Sci Rep* (2017) 7:1–18. doi: 10.1038/srep45047

22. Zhao S, Xu W, Jiang W, Yu W, Lin Y, Zhang T, Yao J, Zhou L, Zeng Y, Li H, et al. Regulation of cellular metabolism by protein lysine acetylation. *Science (1979)* (2010) 327:1000–1004. doi: 10.1126/science.1179689

23. Wellen KE, Hatzivassiliou G, Sachdeva UM, Bui T v., Cross JR, Thompson CB. ATP-citrate lyase links cellular metabolism to histone acetylation. *Science (1979)* (2009) 324:1076–1080. doi: 10.1126/science.1164097

24. Fejer G, Wegner MD, Györy I, Cohen I, Engelhard P, Voronov E, Manke T, Ruzsics Z, Dölken L, Da Costa OP, et al. Nontransformed, GM-CSF-dependent macrophage lines are a unique model to study tissue macrophage functions. *Proc Natl Acad Sci U S A* (2013) 110: doi: 10.1073/PNAS.1302877110

25. Boorsma CE, Anienke Van Der Veen T, Putri KSS, de Almeida A, Draijer C, Mauad T, Fejer G, Brandsma CA, van den Berge M, Bossé Y, et al. A Potent Tartrate Resistant Acid Phosphatase Inhibitor to Study the Function of TRAP in Alveolar Macrophages. *Scientific Reports 2017 7:1* (2017) 7:1–14. doi: 10.1038/s41598-017-12623-w

26. Thomas ST, Wierenga KA, Pestka JJ, Olive AJ. Fetal Liver–Derived Alveolar-like Macrophages: A Self-Replicating Ex Vivo Model of Alveolar Macrophages for Functional Genetic Studies. *Immunohorizons* (2022) 6:156–169. doi: 10.4049/IMMUNOHORIZONS.2200011

27. Bakker BM, Evers B, Gerding A, Boer T, Rebecca Heiner-Fokkema M, Jalving M, Wahl SA, Reijngoud DJ. Simultaneous quantification of the concentration and carbon isotopologue distribution of polar metabolites in a single analysis by gas chromatography and mass spectrometry. *Anal Chem* (2021) 93:8248–8256. doi: doi: 10.1021/acs.analchem.1c01040

28. Hernandez-Valdes JA, aan de Stegge M, Hermans J, Teunis J, van Tatenhove-Pel RJ, Teusink B, Bachmann H, Kuipers OP. Enhancement of amino acid production and secretion by Lactococcus lactis using a droplet-based biosensing and selection system. *Metab Eng Commun* (2020) 11: doi: 10.1016/J.MEC.2020.E00133

29. Wolters JC, Ciapaite J, Van Eunen K, Niezen-Koning KE, Matton A, Porte RJ, Horvatovich P, Bakker BM, Bischoff R, Permentier HP. Translational Targeted Proteomics Profiling of Mitochondrial Energy Metabolic Pathways in Mouse and Human Samples. *J Proteome Res* (2016) 15:3204–3213. doi: 10.1021/acs.jproteome.6b00419

30. Vieira-Lara MA, Dommerholt MB, Zhang W, Blankestijn M, Wolters JC, Abegaz F, Gerding A, van der Veen YT, Thomas R, van Os RP, et al. Age-related susceptibility to insulin resistance arises from a combination of CPT1B decline and lipid overload. *BMC Biol* (2021) 19: doi: 10.1186/S12915-021-01082-5

31. Callister SJ, Barry RC, Adkins JN, Johnson ET, Qian W, Webb-Robertson B-JM, Smith RD, Lipton MS. Normalization Approaches for Removing Systematic Biases Associated with Mass Spectrometry and Label-Free Proteomics. *J Proteome Res* (2006) 5:277–286. doi: 10.1021/pr050300l

32. Perez-Riverol Y, Bai J, Bandla C, García-Seisdedos D, Hewapathirana S, Kamatchinathan S, Kundu DJ, Prakash A, Frericks-Zipper A, Eisenacher M, et al. The PRIDE database resources in 2022: a hub for mass spectrometry-based proteomics evidences. *Nucleic Acids Res* (2022) 50:D543–D552. doi: 10.1093/nar/gkab1038

33. Cao F, Zwinderman MRH, van Merkerk R, Ettema PE, Quax WJ, Dekker FJ. Inhibitory selectivity among class I HDACs has a major impact on inflammatory gene expression in macrophages. *Eur J Med Chem* (2019) 177:457–466. doi: 10.1016/J.EJMECH.2019.05.038

34. Sanjabi S, Zenewicz LA, Kamanaka M, Flavell RA. Anti- and Pro-inflammatory Roles of TGF-β, IL-10, and IL-22 In Immunity and Autoimmunity. *Curr Opin Pharmacol* (2009) 9:447. doi: 10.1016/J.COPH.2009.04.008

35. Murray PJ. Understanding and exploiting the endogenous interleukin-10/STAT3-mediated anti-inflammatory response. *Curr Opin Pharmacol* (2006) 6:379–386. doi: 10.1016/J.COPH.2006.01.010

36. Saperstein S, Chen L, Oakes D, Pryhuber G, Finkelstein J. IL-1β Augments TNF-α–Mediated Inflammatory Responses from Lung Epithelial Cells. *Journal of Interferon & Cytokine Research* (2009) 29:273. doi: 10.1089/JIR.2008.0076

37. Lee Y-J, Han J-Y, Byun J, Park H-J, Park E-M, Chong YH, Cho M-S, Kang JL. Inhibiting Mer receptor tyrosine kinase suppresses STAT1, SOCS1/3, and NF-κB activation and enhances inflammatory responses in lipopolysaccharide-induced acute lung injury. *J Leukoc Biol* (2012) 91:921–932. doi: 10.1189/jlb.0611289

38. Qin H, Roberts KL, Niyongere SA, Cong Y, Elson CO, Benveniste EN. Molecular Mechanism of Lipopolysaccharide-Induced SOCS-3 Gene Expression in Macrophages and Microglia. *The Journal of Immunology* (2007) 179:5966–5976. doi: 10.4049/jimmunol.179.9.5966

39. Bode JG, Ehlting C, Häussinger D. The macrophage response towards LPS and its control through the p38MAPK–STAT3 axis. *Cell Signal* (2012) 24:1185–1194. doi: 10.1016/j.cellsig.2012.01.018

40. Yu X, Buttgereit A, Lelios I, Utz SG, Cansever D, Becher B, Greter M. The Cytokine TGF-β Promotes the Development and Homeostasis of Alveolar Macrophages. *Immunity* (2017) 47:903-912.e4. doi: 10.1016/j.immuni.2017.10.007

41. Batlle E, Massagué J. Transforming Growth Factor-β Signaling in Immunity and Cancer. *Immunity* (2019) 50:924–940. doi: 10.1016/j.immuni.2019.03.024

42. Zhou Y, Zhou B, Pache L, Chang M, Khodabakhshi AH, Tanaseichuk O, Benner C, Chanda SK. Metascape provides a biologist-oriented resource for the analysis of systems-level datasets. *Nat Commun* (2019) 10:1523. doi: 10.1038/s41467-019-09234-6

43. Hirano R, Ehara H, Kujirai T, Uejima T, Takizawa Y, Sekine S, Kurumizaka H. Structural basis of RNA polymerase II transcription on the chromatosome containing linker histone H1. *Nat Commun* (2022) 13:7287. doi: 10.1038/s41467-022-35003-z

44. Palsson-McDermott EM, O'Neill LAJ. The Warburg effect then and now: From cancer to inflammatory diseases. *BioEssays* (2013) 35:965–973. doi: 10.1002/bies.201300084

45. Russo S, Kwiatkowski M, Govorukhina N, Bischoff R, Melgert BN. Meta-Inflammation and Metabolic Reprogramming of Macrophages in Diabetes and Obesity: The Importance of Metabolites. *Front Immunol* (2021) 12:4656. doi: 10.3389/FIMMU.2021.746151

46. Pratt JM, Simpson DM, Doherty MK, Rivers J, Gaskell SJ, Beynon RJ. Multiplexed absolute quantification for proteomics using concatenated signature peptides encoded by QconCAT genes. *Nat Protoc* (2006) 1:1029–1043. doi: 10.1038/NPROT.2006.129

47. Ryan DG, O'neill LAJ. Krebs Cycle Reborn in Macrophage Immunometabolism. *Annual Review of Immunology* (2020) 38:289–313. doi: 10.1146/annurev-immunol-081619

48. O'Neill LAJ, Pearce EJ. Immunometabolism governs dendritic cell and macrophage function. *J Exp Med* (2016) 213:15–23. doi: 10.1084/jem.20151570

49. Liu S, Yang J, Wu Z. The Regulatory Role of α-Ketoglutarate Metabolism in Macrophages. *Mediators Inflamm* (2021) 2021:1–7. doi: 10.1155/2021/5577577

50. Ryu Y, Kee HJ, Sun S, Seok YM, Choi SY, Kim GR, Kee SJ, Pflieger M, Kurz T, Kim HS, et al. Class I histone deacetylase inhibitor MS-275 attenuates vasoconstriction and inflammation in angiotensin II-induced hypertension. *PLoS One* (2019) 14: doi: 10.1371/JOURNAL.PONE.0213186

51. D'Urzo A, Boichenko AP, van den Bosch T, Hermans J, Dekker F, Andrisano V, Bischoff R. Site-specific quantification of lysine acetylation in the N-terminal tail of histone H4 using a double-labelling, targeted UHPLC MS/MS approach. *Anal Bioanal Chem* (2016) 408:3547–3553. doi: 10.1007/S00216-016-9431-1

52. Park C-W, Ryu K-Y. Cellular ubiquitin pool dynamics and homeostasis. *BMB Rep* (2014) 47:475–482. doi: 10.5483/BMBRep.2014.47.9.128

53. Charbonneau M-E, Passalacqua KD, Hagen SE, Showalter HD, Wobus CE, O'Riordan MXD. Perturbation of ubiquitin homeostasis promotes macrophage oxidative defenses. *Sci Rep* (2019) 9:10245. doi: 10.1038/s41598-019-46526-9

54. West AP, Brodsky IE, Rahner C, Woo DK, Erdjument-Bromage H, Tempst P, Walsh MC, Choi Y, Shadel GS, Ghosh S. TLR signalling augments macrophage bactericidal activity through mitochondrial ROS. *Nature* (2011) 472:476–480. doi: 10.1038/nature09973

55. Cockram PE, Kist M, Prakash S, Chen S-H, Wertz IE, Vucic D. Ubiquitination in the regulation of inflammatory cell death and cancer. *Cell Death Differ* (2021) 28:591–605. doi: 10.1038/s41418-020-00708-5

56. Liu Z, Wang Y, Gao T, Pan Z, Cheng H, Yang Q, Cheng Z, Guo A, Ren J, Xue Y. CPLM: a database of protein lysine modifications. *Nucleic Acids Res* (2014) 42:D531–D536. doi: 10.1093/NAR/GKT1093

57. Caron C, Boyault C, Khochbin S. Regulatory cross-talk between lysine acetylation and ubiquitination: role in the control of protein stability. *BioEssays* (2005) 27:408–415. doi: 10.1002/bies.20210

58. Bäumer N, Tickenbrock L, Tschanter P, Lohmeyer L, Diederichs S, Bäumer S, Skryabin B v., Zhang F, Agrawal-Singh S, Köhler G, et al. Inhibitor of Cyclin-dependent Kinase (CDK) Interacting with Cyclin A1 (INCA1) Regulates Proliferation and Is Repressed by Oncogenic Signaling. *Journal of Biological Chemistry* (2011) 286:28210–28222. doi: 10.1074/JBC.M110.203471

59. Diederichs S, Bäumer N, Ji P, Metzelder SK, Idos GE, Cauvet T, Wang W, Möller M, Pierschalski S, Gromoll J, et al. Identification of Interaction Partners and Substrates of the Cyclin A1-CDK2 Complex. *Journal of Biological Chemistry* (2004) 279:33727–33741. doi: 10.1074/JBC.M401708200

60. Bonilha CS, Benson RA, Brewer JM, Garside P. Targeting Opposing Immunological Roles of the Junctional Adhesion Molecule-A in Autoimmunity and Cancer. *Front Immunol* (2020) 11: doi: 10.3389/fimmu.2020.602094

61. Kiss M, Lebegge E, Murgaski A, van Damme H, Kancheva D, Brughmans J, Scheyltjens I, Talebi A, Awad RM, Elkrim Y, et al. Junctional adhesion molecule-A is dispensable for myeloid cell recruitment and diversification in the tumor microenvironment. *Front Immunol* (2022) 13: doi: 10.3389/fimmu.2022.1003975

62. Mitchell LA, Ward C, Kwon M, Mitchell PO, Quintero DA, Nusrat A, Parkos CA, Koval M. Junctional Adhesion Molecule A Promotes Epithelial Tight Junction Assembly to Augment Lung Barrier Function. *Am J Pathol* (2015) 185:372–386. doi: 10.1016/j.ajpath.2014.10.010

63. Lagente V, le Quement C, Boichot E. Macrophage metalloelastase (MMP-12) as a target for inflammatory respiratory diseases. *Expert Opin Ther Targets* (2009) 13:287–295. doi: 10.1517/14728220902751632

64. Zhou Y, Xu M, Gong W, Kang X, Guo R, Wen J, Zhou D, Wang M, Shi D, Jing Q. Circulating MMP-12 as Potential Biomarker in Evaluating Disease Severity and Efficacy of Sublingual Immunotherapy in Allergic Rhinitis. *Mediators Inflamm* (2022) 2022:1–10. doi: 10.1155/2022/3378035

65. Chiba Y, Yu Y, Sakai H, Misawa M. Increase in the Expression of Matrix Metalloproteinase-12 in the Airways of Rats with Allergic Bronchial Asthma. *Biol Pharm Bull* (2007) 30:318–323. doi: 10.1248/bpb.30.318

66. Dean RA, Cox JH, Bellac CL, Doucet A, Starr AE, Overall CM. Macrophage-specific metalloelastase (MMP-12) truncates and inactivates ELR+ CXC chemokines and generates CCL2, -7, -8, and -13 antagonists: potential role of the macrophage in terminating polymorphonuclear leukocyte influx. *Blood* (2008) 112:3455–3464. doi: 10.1182/blood-2007-12-129080

67. Fukuda T, Chen K, Shi X, Wu C. PINCH-1 Is an Obligate Partner of Integrin-linked Kinase (ILK) Functioning in Cell Shape Modulation, Motility, and Survival. *Journal of Biological Chemistry* (2003) 278:51324–51333. doi: 10.1074/jbc.M309122200

68. Collins JC, Ghalei H, Doherty JR, Huang H, Culver RN, Karbstein K. Ribosome biogenesis factor Ltv1 chaperones the assembly of the small subunit head. *Journal of Cell Biology* (2018) 217:4141–4154. doi: 10.1083/jcb.201804163

69. Murray PJ, Allen JE, Biswas SK, Fisher EA, Gilroy DW, Goerdt S, Gordon S, Hamilton JA, Ivashkiv LB, Lawrence T, et al. Macrophage Activation and Polarization: Nomenclature and Experimental Guidelines. *Immunity* (2014) 41:14–20. doi: 10.1016/j.immuni.2014.06.008

70. Khaing P, Summer R. Maxed out on glycolysis: Alveolar macrophages rely on oxidative phosphorylation for cytokine production. *Am J Respir Cell Mol Biol* (2020) 62:139–140. doi: 10.1165/rcmb.2019-0329ED

71. Andrews JT, Voth DE, Huang SCC, Huang L. Breathe In, Breathe Out: Metabolic Regulation of Lung Macrophages in Host Defense Against Bacterial Infection. *Front Cell Infect Microbiol* (2022) 12: doi: 10.3389/FCIMB.2022.934460

SUPPLEMENTARY MATERIAL

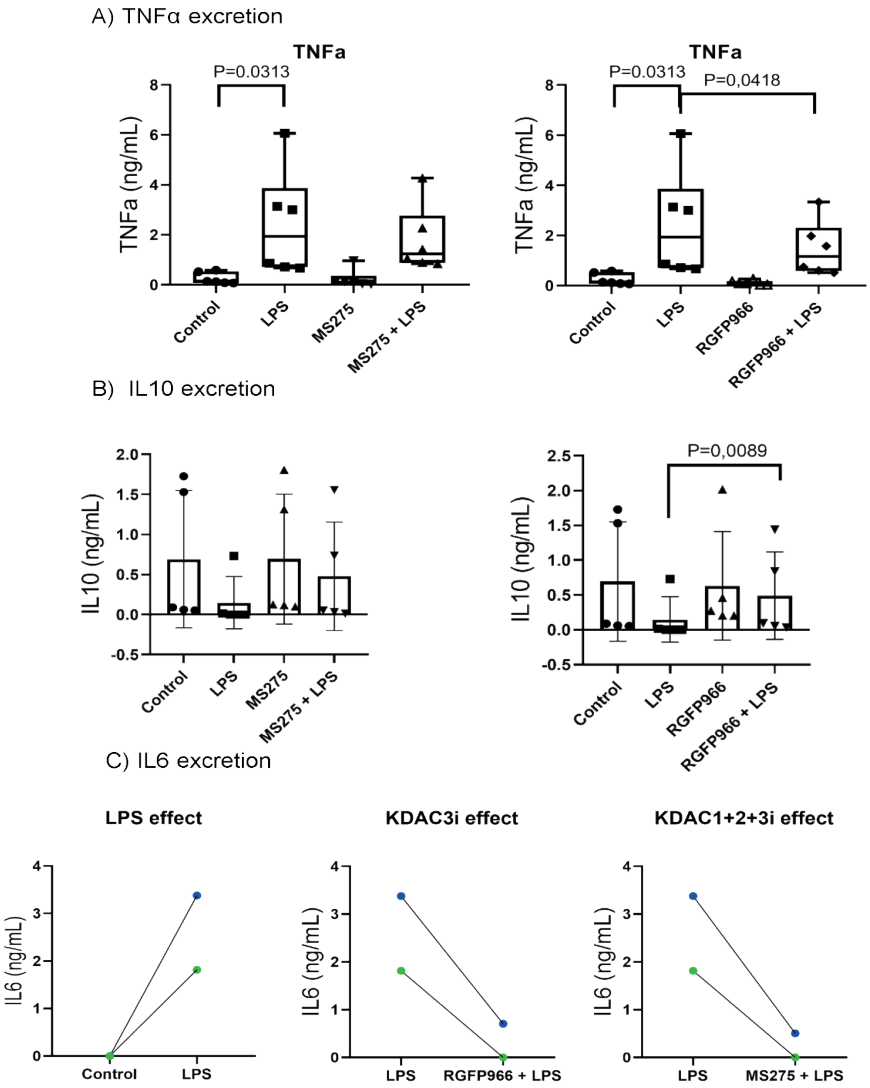

Supplementary Figure 1: **Effects of KDAC inhibitors MS275 or RGFP966 on TNF-α, IL-10, and IL-6 excretion in culture supernatant of alveolar-like macrophages stimulated with lipopolysaccharide (LPS) for 4 hours.** **(A)** Effect of KDAC inhibition and LPS stimulation on IL-10 cytokine excretion levels. **(B)** Effect of KDACi inhibition and LPS stimulation on TNF-α cytokine excretion levels. **(C)** Effect of KDACi inhibition and LPS stimulation on IL-6 cytokine excretion levels. A Wilcoxon test was used to compare control versus LPS stimulation. Groups stimulated with or without KDAC inhibitors were compared using a Friedman test with a Dunn's correction for multiple testing (n=5). P<0.05 was considered significant. In panel (C) no statistical analysis was performed as only 2 biological replicates were compared.

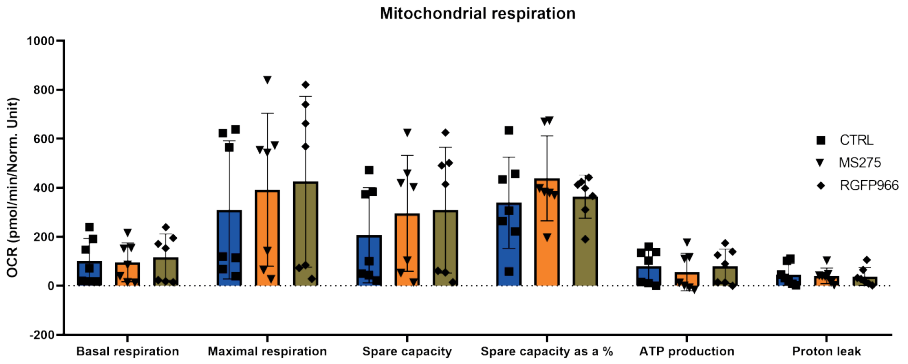

Supplementary Figure 2: **Effect of KDAC inhibitor pre-treatment on mitochondrial respiration in alveolar-like macrophages.** Bars quantify mitochondrial respiration of macrophages when treated with KDAC inhibitors. Data represent seven biological replicates (n=6 separate wells per condition). Mitochondrial parameters were compared among treatments and significance was calculated by Friedman test with a Dunn's correction for multiple testing for CTRL vs KDAC inhibition. All error bars are shown as mean ± SD.

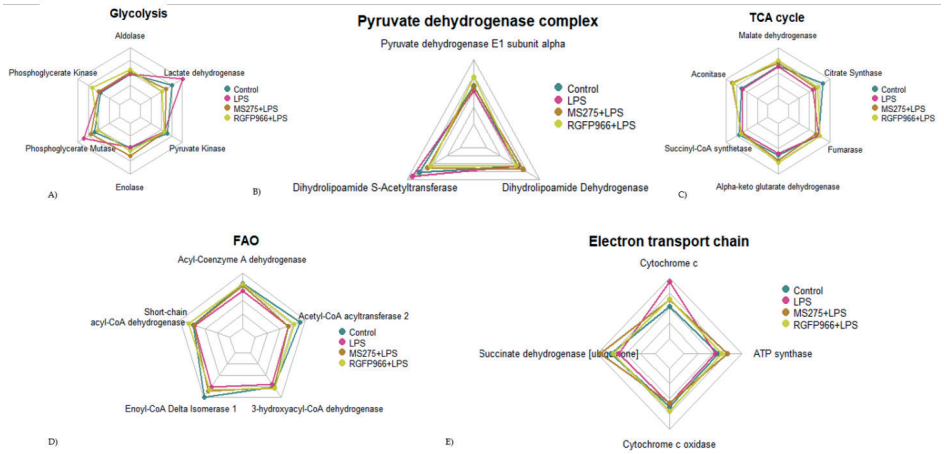

Supplementary Figure 3: **Protein expression of metabolic enzymes in alveolar-like macrophages after KDAC inhibitor treatment in combination or not with LPS.** Cells were incubated with KDAC inhibitors (MS275/RGFP966) with or without LPS (LPS, control) for 16 h. After 16 h cells were stimulated with LPS (10 ng/mL). Protein expression levels were measured with a targeted approach, using concatenated peptides as internal standards for protein quantification. Data are represented as radar plots (as percentage of control, n=6). **(A)** Proteins belonging to the glycolytic pathway, **(B)** proteins belonging to the connection between glycolysis and the TCA cycle as part of the pyruvate dehydrogenase complex, **(C)** proteins belonging to the TCA cycle, **(D)** proteins belonging to the fatty acid oxidation processes (FAO), and **(E)** proteins belonging to the electron transport chain (see Figure 5 for details).

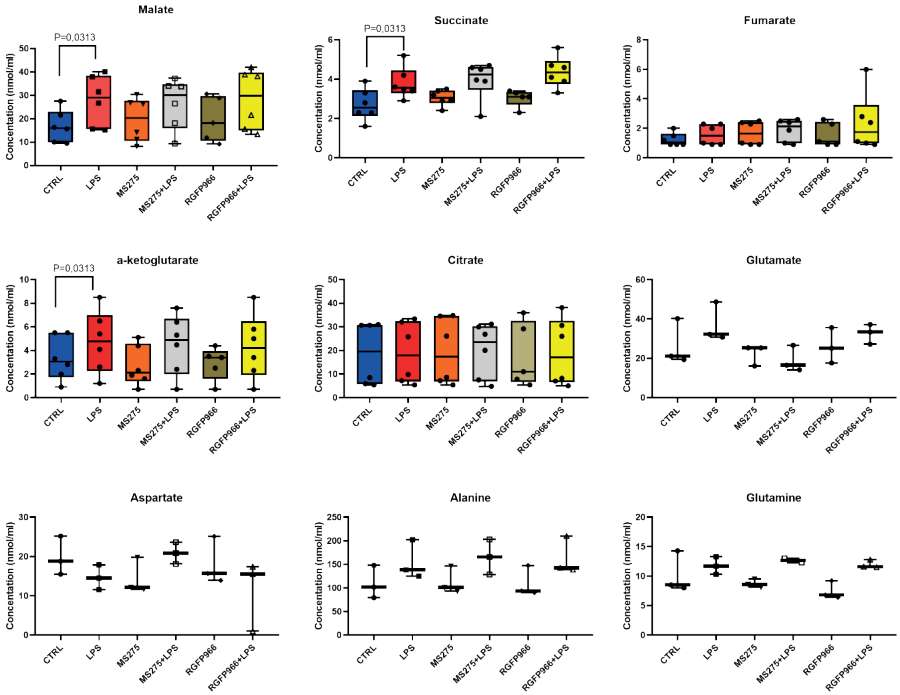

Supplementary Figure 4: **Levels of TCA cycle metabolites in alveolar-like macrophages after KDAC inhibitor treatment in the presence of absence of LPS.** A Wilcoxon test was used to compare control versus LPS stimulation. Groups stimulated with or without KDAC inhibitors were compared using a Friedman test with a Dunn's correction for multiple testing (n=6 for malate, succinate, fumarate, α-ketoglutarate, citrate; n=3 for glutamate, aspartate, alanine, glutamine). P<0.05 was considered significant.

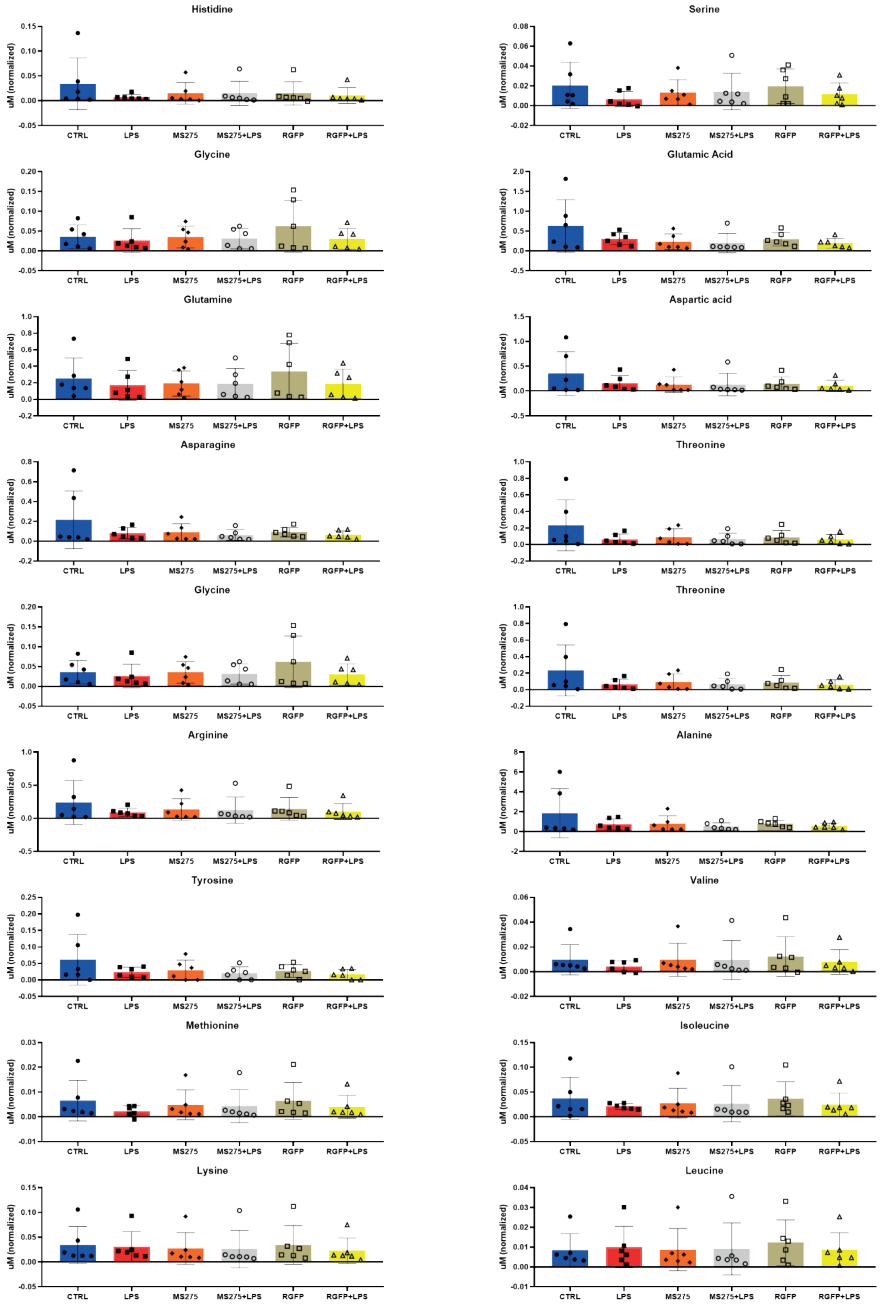

Supplementary Figure 5: Levels of amino acids in alveolar-like macrophages after KDAC inhibitor treatment in the presence or absence of LPS. A Wilcoxon test was used to compare control versus LPS stimulation. Groups stimulated with or without KDAC inhibitors were compared using a Friedman test with a Dunn's correction for multiple testing (n=6). P<0.05 was considered significant.

Supplementary Table 1: Protein expression in alveolar-like macrophages after KDAC inhibitor treatment in combination with LPS or not. Cells were incubated with and without KDAC inhibitor MS275 (MS275+LPS, LPS) for 16 h. After 16 h cells were stimulated with LPS (10 ng/mL). Protein expression levels were measured with an untargeted approach.

Protein	Corrected p value	Fold change MS275+LPS vs LPS	Median LPS (Log_2 Intensity)	Median MS275+LPS (Log_2 Intensity)
Protein INCA1	0.038	15.78	15.74	19.22
Junctional adhesion molecule A	0.022	4.91	13.53	15.84
Macrophage metalloelastase	0.038	4.69	13.8	16.59
Glutamine synthetase	0.007	3.88	16.03	17.18
Hyccin	0.03	3.73	12.52	14.83
Plasminogen activator inhibitor 1	0.028	3.56	14.08	16.73
39S ribosomal protein L37, mitochondrial	0.031	3.43	13.69	15.54
Cytoskeleton-associated protein 4	0.001	3.31	14.39	16.36
Platelet glycoprotein 4	0.006	3	14.69	16.57
Conserved oligomeric Golgi complex subunit 4	0.029	2.99	12.82	14.46
2-(3-amino-3-carboxypropyl) histidine synthase subunit 2	0.018	2.97	12.13	13.42
Cyclin-dependent kinase inhibitor 1	0.014	2.88	14.54	16.12
G protein-coupled receptor kinase 6	0.023	2.81	13.42	15.29
Fibronectin type III domain-containing protein 3B	0.029	2.58	12.65	14.2
5-aminolevulinate synthase, nonspecific, mitochondrial	0.026	2.58	13.16	15.73
Transmembrane protein 245	0.03	2.56	14.16	15.21
Microtubule-associated protein RP/EB family member 3	0.014	2.49	14.86	16.15
CDGSH iron-sulfur domain-containing protein 3, mitochondrial	0.048	2.41	14.19	15.49
ER membrane protein complex subunit 1	0.033	2.39	16.05	17.04
Uncharacterized protein KIAA0513	0.037	2.19	13	14.64
Vacuolar protein sorting-associated protein 16 homolog	0.036	2.18	15.27	15.92
Bcl-2-like protein 11	0.04	2.17	14.13	14.82
Aldehyde dehydrogenase, dimeric NADP-preferring	0.024	2.17	16.48	17.78
Microtubule-associated protein RP/EB family member 2	0.01	2.1	14.64	15.93
Stimulator of interferon genes protein	0.047	2.07	14.75	15.5
Store-operated calcium entry-associated regulatory factor	0.046	2.01	16.02	17.13
ADP-ribosylation factor-like protein 8B	0.038	1.95	17.41	18.82

Protein	Corrected p value	Fold change MS275+LPS vs LPS	Median LPS (Log_2 Intensity)	Median MS275+LPS (Log_2 Intensity)
Carbonic anhydrase 4	0.004	1.91	20.64	21.79
ATP-dependent zinc metalloprotease YME1L1	0.005	1.9	15.28	16.39
Misshapen-like kinase 1	0.012	1.89	17.26	18.31
Protein transport protein Sec61 subunit beta	0.032	1.86	17.04	17.86
Nuclear pore membrane glycoprotein 210	0.007	1.84	15.87	16.83
Melanoma inhibitory activity protein 2	0.039	1.82	12.9	13.87
Myeloid leukemia factor 2	0.031	1.82	16.12	16.8
Dehydrogenase/reductase SDR family member 1	0.04	1.82	17.15	18.07
Conserved oligomeric Golgi complex subunit 2	0.034	1.81	12.94	13.88
Adhesion G protein-coupled receptor L2	0.032	1.8	14.59	15.37
Disintegrin and metalloproteinase domain-containing protein 10	0.012	1.79	14.56	15.27
Ras-related protein Rab-8B	0.03	1.78	15.76	16.35
Ubiquitin-conjugating enzyme E2 J1	0.021	1.78	15.31	16.04
NADH dehydrogenase [ubiquinone] 1 beta subcomplex subunit 5, mitochondrial	0.047	1.76	16.01	17.34
Serine/threonine-protein kinase Nek4	0.045	1.76	12.04	13.42
Vesicle-associated membrane protein 4	0.000525	1.75	14.77	15.68
MAP kinase-activated protein kinase 2	0.001	1.75	16.54	17.14
Tyrosine-protein kinase ABL2	0.037	1.75	14.07	14.5
Sentrin-specific protease 3	0.019	1.75	13.51	14.74
Unconventional myosin-Ie	0.046	1.74	16.12	17.37
Kinesin-like protein KIF1B	0.017	1.74	15.4	16.35
Complex I assembly factor ACAD9, mitochondrial	0.021	1.74	15.81	16.52
Mitochondrial proton/calcium exchanger protein	0.001	1.73	16.55	17.29
Prenylcysteine oxidase	0.008	1.72	16.19	17.38
Brain-specific angiogenesis inhibitor 1-associated protein 2	0.049	1.71	13.87	14.78
Nardilysin	0.02	1.7	14.56	15.33
Dolichyl-diphosphooligosaccharide--protein glycosyltransferase subunit 1	0.037	1.68	18.81	19.42
Proteolipid protein 2	0.049	1.68	18.17	18.51
Long-chain-fatty-acid--CoA ligase 4	0.048	1.66	15.23	15.86

Protein	Corrected p value	Fold change MS275+LPS vs LPS	Median LPS (Log_2 Intensity)	Median MS275+LPS (Log_2 Intensity)
Citrate synthase, mitochondrial	0.002	1.64	18.9	19.5
Unconventional myosin-VI	0.017	1.63	15.59	16.15
Ubiquitin carboxyl-terminal hydrolase MINDY-2	0.024	1.63	14.6	15.32
Vesicle transport through interaction with t-SNAREs homolog 1B	0.041	1.61	15.26	15.8
Cytoplasmic FMR1-interacting protein 2	0.007	1.61	12.66	13.34
Selenocysteine-specific elongation factor	0.024	1.61	16.11	16.41
ATP-dependent 6-phosphofructokinase, platelet type	0.015	1.6	17.84	18.48
Supervillin	0.038	1.59	15.36	16.26
Branched-chain-amino-acid aminotransferase, mitochondrial	0.032	1.58	16.69	17.51
Pyruvate carboxylase, mitochondrial	0.01	1.58	18.92	19.53
Terminal uridylyltransferase 7	0.019	1.58	16.05	16.54
Sulfide:quinone oxidoreductase, mitochondrial	0.042	1.58	15.55	16.47
E3 ubiquitin-protein ligase ZNF598	0.033	1.57	14.59	15.21
N-alpha-acetyltransferase 25, NatB auxiliary subunit	0.023	1.56	14.56	15.3
Septin-10	0.005	1.56	14.91	15.48
39S ribosomal protein L53, mitochondrial	0.017	1.56	15.98	16.62
Lamina-associated polypeptide 2, isoforms beta/delta/epsilon/ gamma	0.035	1.55	17.54	18.43
Integrin beta-2	0.014	1.54	19.08	19.58
RNA polymerase II elongation factor ELL	0.002	1.53	15.64	16.35
ATP-dependent 6-phosphofructokinase, liver type	0.045	1.53	16.91	17.36
GTPase KRas	0.02	1.53	15.46	15.77
Adipocyte plasma membrane-associated protein	0.024	1.53	15.66	16.12
Hexokinase-1	0.02	1.52	17.01	17.76
Protein unc-45 homolog A	0.002	1.52	16.93	17.68
ERO1-like protein alpha	0.05	1.51	18.63	19.28
Cytochrome b-c1 complex subunit 8	0.026	1.51	17.32	17.77
Geranylgeranyl transferase type-2 subunit alpha	0.039	1.51	13.71	14.51
MAPK-interacting and spindle-stabilizing protein-like	0.009	0.3	18.38	16.93

Protein	Corrected p value	Fold change MS275+LPS vs LPS	Median LPS (Log_2 Intensity)	Median MS275+LPS (Log_2 Intensity)
Transcription elongation factor 1 homolog	0.034	0.4	14.72	13.06
Probable RNA-binding protein EIF1AD	0.019	0.4	14.04	13.22
Sorting nexin-15	0.028	0.4	15.2	14.22
LIM and senescent cell antigen-like-containing domain protein 1	0.05	0.4	16.22	15.16
Eukaryotic translation initiation factor 3 subunit J-A;Eukaryotic translation initiation factor 3 subunit J-B	0.044	0.41	19.92	18.11
Desumoylating isopeptidase 1	0.047	0.42	17.66	16.62
Keratin, type I cytoskeletal 42	0.007	0.44	16.71	15.74
Protein SSXT	0.04	0.47	17.1	16.15
1,2-dihydroxy-3-keto-5-methylthiopentene dioxygenase	0.006	0.47	16.26	14.94
S-phase kinase-associated protein 1	0.031	0.47	17.94	16.76
Protein LTV1 homolog	0.004	0.49	16.97	15.87
Mediator of RNA polymerase II transcription subunit 4	0.049	0.49	14.5	13.4
Protein Spindly	0.041	0.5	15.82	14.94
Uncharacterized protein C7orf50 homolog	0.047	0.5	15.29	14.76
Coagulation factor X	0.00022	0.51	15.73	14.66
G-protein-signaling modulator 3	0.033	0.51	16.23	15.32
Centrosomal protein of 55 kDa	0.016	0.51	16.06	14.67
Intraflagellar transport protein 22 homolog	0.045	0.52	15.64	14.32
Filamin A-interacting protein 1-like	0.007	0.53	13.75	13.05
Protein LZIC	0.019	0.53	17.39	16.68
Sperm-associated antigen 7	0.006	0.54	15.89	14.99
UV excision repair protein RAD23 homolog B	0.009	0.55	19.02	18.25
Tyrosine-protein phosphatase non-receptor type 18	0.021	0.55	17.52	16.57
Zinc finger CCCH domain-containing protein 14	0.038	0.55	15.97	14.63
Probable cytosolic iron-sulfur protein assembly protein CIAO1	0.026	0.55	16.51	15.76
SAP30-binding protein	0.011	0.56	16.71	15.55
ETS-related transcription factor Elf-1	0.038	0.56	15.65	14.22
Coiled-coil domain-containing protein 50	0.01	0.56	16.16	15.61
U3 small nucleolar RNA-associated protein 15 homolog	0.045	0.56	15.92	15.13
Bromodomain-containing protein 7	0.021	0.57	15.11	14.53

Protein	Corrected p value	Fold change MS275+LPS vs LPS	Median LPS (Log_2 Intensity)	Median MS275+LPS (Log_2 Intensity)
Transducin-like enhancer protein 3	0.02	0.57	13.2	12.11
Protein dpy-30 homolog	0.000852	0.57	16.15	15.36
Lactoylglutathione lyase	0.049	0.57	14.97	14.36
Copper chaperone for superoxide dismutase	0.046	0.57	17.21	16.17
E3 ubiquitin-protein ligase RNF149	0.028	0.58	12.92	11.96
Pre-mRNA-splicing factor ISY1 homolog	0.041	0.58	16.88	15.81
Adapter molecule crk	0.013	0.59	17.64	16.45
Protein N-terminal asparagine amidohydrolase	0.011	0.59	14.3	13.05
PSME3-interacting protein	0.006	0.59	15.78	15.17
Interferon regulatory factor 2-binding protein 2	0.008	0.6	17.59	16.98
Prefoldin subunit 2	0.037	0.6	18.72	18
Growth factor receptor-bound protein 2	0.024	0.61	19.26	18.55
Protein canopy homolog 4	0.012	0.61	17.36	16.55
Protein PBDC1	0.041	0.61	18.79	18.17
EF-hand domain-containing protein D2	0.025	0.61	18.69	18.11
Zinc finger protein ubi-d4	0.002	0.62	16.89	16.22
Astrocytic phosphoprotein PEA-15	0.012	0.62	15.92	15.57
SAM and SH3 domain-containing protein 3	0.016	0.62	17.06	16.09
Nucleoplasmin-3	0.000666	0.62	17.3	16.52
Disabled homolog 2	0.043	0.63	20.87	20.32
SH3 domain-binding glutamic acid-rich-like protein 2	0.037	0.63	17.24	15.98
Protein canopy homolog 2	0.046	0.63	17.39	16.93
Desmoplakin	0.03	0.64	16.71	15.69
Proteasome activator complex subunit 3	0.032	0.64	17.99	17.21
Enhancer of rudimentary homolog	0.013	0.64	19.03	18.64
Growth arrest-specific protein 7	0.019	0.64	14.84	14.21
Coiled-coil domain-containing protein 25	0.034	0.64	16.51	16.13
CGG triplet repeat-binding protein 1	0.003	0.64	16.66	15.94
Interferon regulatory factor 2-binding protein 1	0.032	0.64	13.58	12.86
StAR-related lipid transfer protein 4	0.039	0.64	14.4	13.32
Translation machinery-associated protein 16	0.004	0.64	15.28	14.56
NSFL1 cofactor p47	0.045	0.64	18.54	18.14

Protein	Corrected p value	Fold change MS275+LPS vs LPS	Median LPS (Log_2 Intensity)	Median MS275+LPS (Log_2 Intensity)
MAP7 domain-containing protein 1	0.007	0.65	17.08	16.26
Nuclear autoantigenic sperm protein	0.006	0.65	19.17	18.38
Ribonuclease H2 subunit C	0.022	0.65	14.76	14.02
Glutaredoxin-3	0.000369	0.65	17.05	16.41
Mitochondrial import inner membrane translocase subunit Tim10 B	0.038	0.65	16.43	15.67
MKI67 FHA domain-interacting nucleolar phosphoprotein	0.018	0.66	17.21	16.33
Tetratricopeptide repeat protein 1	0.036	0.66	18.09	17.6
Pre-mRNA-splicing factor SYF2	0.038	0.66	15.15	14.66
DnaJ homolog subfamily B member 1	0.009	0.66	17.13	16.47
Eukaryotic translation initiation factor 4H	0.022	0.66	19.72	19.11
Epididymis-specific alpha-mannosidase	0.004	0.67	15.36	14.96
Transcription elongation factor SPT5	0.039	0.67	17.76	17.27
Cellular nucleic acid-binding protein	0.048	0.67	18.7	17.91
Thioredoxin domain-containing protein 5	0.014	0.67	16.94	16.44
Zinc finger protein 593	0.043	0.67	16.88	16.27
DNA-directed RNA polymerases I and III subunit RPAC1	0.015	0.68	18.98	18.22
Serine/arginine-rich splicing factor 6	0.047	0.68	20.1	19.72
Poly(U)-binding-splicing factor PUF60	0.009	0.68	19	18.44
Protein FAM76B	0.038	0.68	14.62	14.11
Mitochondrial import inner membrane translocase subunit Tim8 A	0.043	0.68	20.38	19.62
Cleavage stimulation factor subunit 2	0.044	0.69	19.82	19.17
Aminoacylase-1	0.017	0.69	16.22	15.81

Supplementary Table 2: Protein expression in alveolar-like macrophages after KDAC inhibitor treatment in combination with LPS or not. Cells were incubated with and without KDAC inhibitor RGFP966 (RGFP966+LPS, LPS) for 16 h. After 16 h cells were stimulated with LPS (10 ng/mL). Protein expression levels were measured with an untargeted approach.

Protein	Corrected p value	Fold change RGFP+LPS vs LPS	Median LPS (Log_2 Intensity)	Median RGFP+LPS (Log_2 Intensity)
Pre-mRNA-splicing factor 38A	0.041	2.49	13.97	16.6
Protein spire homolog 1	0.011	2.19	11.44	12.13
Class E basic helix-loop-helix protein 41	0.017	2.01	12.17	13.08
CUGBP Elav-like family member 1	0.028	1.94	12.41	13.31
Prolactin-7C1	0.01	1.7	12.33	13.54
Ubiquitin carboxyl-terminal hydrolase 10	0.015	1.59	14.8	15.39
NAD-dependent malic enzyme, mitochondrial	0.036	1.57	15.63	16.51
Transcription initiation factor TFIID subunit 10	0.029	0.48	16.21	14.92
Protein disulfide isomerase Creld2	0.021	0.53	16.92	16.13
Volume-regulated anion channel subunit LRRC8C	0.018	0.55	15.66	15.22
Protein Dr1	0.036	0.55	15.86	15.29
LIM and senescent cell antigen-like-containing domain protein 1	0.017	0.6	16.22	15.5
U6 snRNA-associated Sm-like protein LSm6	0.05	0.61	16.03	15.41
WASH complex subunit 3	0.034	0.62	15.84	15.28
Mediator of RNA polymerase II transcription subunit 10	0.047	0.63	15	14.26
Acylphosphatase-1	0.02	0.64	16.93	16.32
Charged multivesicular body protein 3	0.031	0.66	16.68	15.98
Protein LTV1 homolog	0.012	0.67	16.97	16.35
Guanylate-binding protein 1	0.017	0.68	13.13	12.57
Calmodulin-1;Calmodulin-2;Calmodulin-3	0.006	0.68	17.65	17.01

Supplementary Table 3: Protein expression of metabolic enzymes in alveolar-like macrophages after KDAC inhibitor treatment in combination with LPS or not. Cells were incubated with KDAC inhibitors (MS275/RGFP966) with and without LPS (LPS, control) for 16 h. After 16 h cells were stimulated with LPS (10 ng/mL). Protein expression levels were measured with a targeted approach, using concatenated peptides as internal standards for protein quantification. Data reported as the percentage of control.

Proteins	CTRL (%CTRL)	LPS (%CTRL)	MS275+ LPS (%CTRL)	RGFP966+ LPS (%CTRL)	p-value CTRL vs LPS	Corrected p-value MS275+ LPS vs LPS	Corrected p-value RGFP966+ LPS vs LPS
Aldolase	95.19	94.63	101.90	112.43	>0,999	>0,999	0,742
Phosphoglycerate Kinase	91.82	97.54	101.17	131.23	>0,999	0,527	0,527
Phosphoglycerate Mutase	121.66	171.53	136.66	104.34	0,844	0,742	>0,999
Enolase	96.65	95.48	129.77	108.68	0,844	>0,999	0,742
Pyruvate Kinase	129.11	113.63	115.39	114.46	0,844	>0,999	>0,999
Lactate dehydrogenase	151.49	202.41	123.19	102.28	0,688	0,147	0,088
Pyruvate dehydrogenase E1 subunit alpha	99.05	87.96	96.93	123.47	0,438	0,773	0,773
Dihydrolipoamide S-Acetyltransferase	132.41	153.35	105.81	95.92	0,844	0,773	0,167
Dihydrolipoamide Dehydrogenase	97.94	95.85	115.87	93.82	0,688	>0,999	0,773
Malate dehydrogenase	95.94	93.70	104.36	112.62	0,688	0,773	>0,999
Aconitase	94.08	91.12	129.31	123.77	0,438	0,773	>0,999
Succinyl-CoA synthetase	104.35	93.08	93.92	96.52	0,688	>0,999	0,773
Alpha-keto glutarate dehydrogenase	95.77	89.38	109.49	117.86	0,844	0,087	0,298
Fumarase	109.35	108.58	99.26	113.23	0,563	>0,999	>0,999
Citrate Synthase	124.72	87.77	98.52	104.11	0,500	>0,999	>0,999
acyl-Coenzyme A dehydrogenase	105.68	88.28	100.49	104.14	0,313	>0,999	>0,999
short-chain acyl-CoA dehydrogenase	96.07	92.95	93.98	107.08	0,844	>0,999	>0,999
Enoyl-CoA Delta Isomerase 1	128.55	98.64	111.86	106.98	0,563	>0,999	>0,999
3-hydroxyacyl-CoA dehydrogenase	99.96	91.03	100.99	103.41	0,438	0,496	>0,999
Acetyl-CoA acyltransferase 2	116.47	86.80	85.65	101.49	0,500	>0,999	>0,999
ATP synthase	95.14	87.23	121.80	104.92	0,563	0,298	>0,999
Cytochrome c oxidase	101.80	93.18	90.47	113.76	0,688	>0,999	>0,999
Cytochrome c	84.59	148.67	101.14	103.92	0,156	0,167	0,167
Electron-transfer-flavoprotein	124.28	133.36	104.00	104.15	0,844	0,773	0,773
Glucose-6-phosphate dehydrogenase	99.21	83.65	109.86	101.85	0,438	0,087	0,298
Glutathione reductase	90.36	92.56	95.40	107.42	0,563	0,496	0,298
Pyruvate carboxylase	109.64	112.12	126.14	101.54	>0,999	>0,999	0,773
Phosphoenolpyruvate Carboxykinase 2	101.10	109.87	154.27	130.70	0,844	0,773	0,773
Phosphogluconate dehydrogenase	123.30	105.77	109.17	96.53	0,563	>0,999	0,773

Proteins	CTRL (%CTRL)	LPS (%CTRL)	MS275+ LPS (%CTRL)	RGFP966+ LPS (%CTRL)	p-value CTRL vs LPS	Corrected p-value MS275+ LPS vs LPS	Corrected p-value RGFP966+ LPS vs LPS
Peroxiredoxin 6	123.05	122.64	192.77	128.34	0,844	>0,999	>0,999
Succinate dehydrogenase [ubiquinone]	122.31	100.32	151.73	115.61	0,563	0,298	>0,999
Superoxide dismutase 2	121.96	96.55	115.44	112.88	0,313	0,496	>0,999
UDP-Glucose Pyrophosphorylase 2	97.25	92.60	121.44	104.00	0,688	0,773	0,773
Very long-chain acyl-CoA dehydrogenase	97.82	101.10	107.48	95.56	>0,999	>0,999	>0,999
ATP Citrate Lyase	116.79	138.50	107.97	103.41	0,563	0,298	0,496
2,4-Dienoyl-CoA Reductase 1	112.03	103.07	166.51	155.27	0,438	0,773	0,773
Enoyl-CoA Hydratase	136.28	85.76	96.54	107.75	0,313	>0,999	0,298
Electron Transfer Flavoprotein Dehydrogenase	113.78	107.48	86.60	110.61	0,844	>0,999	>0,999
Glycosylphosphatidylinositol	111.27	95.98	115.89	99.29	0,750	0,829	0,615
Glutathione Peroxidase 4	121.15	96.62	96.72	88.64	0,563	0,625	>0,999
Hydroxyacyl-CoA Dehydrogenase	93.15	90.66	133.22	75.52	0,500	0,829	0,829
Hydroxyacyl-CoA Dehydrogenase Trifunctional Multienzyme Complex Subunit Alpha	108.28	93.54	92.65	116.56	0,563	>0,999	0,497
Hydroxyacyl-CoA Dehydrogenase Trifunctional Multienzyme Complex Subunit Beta	113.16	103.12	115.04	103.80	0,563	0,773	0,773
Hexokinase 1	105.92	120.26	87.72	105.64	>0,999	>0,999	>0,999
Hexokinase 2	159.59	122.77	146.52	105.82	0,438	>0,999	>0,999
Lactate Dehydrogenase B	96.82	91.97	96.78	145.49	>0,999	>0,999	0,298
NADH:Ubiquinone Oxidoreductase Core Subunit S1	129.64	80.19	97.10	93.88	0,500	0,828	>0,999
Phosphoenolpyruvate Carboxykinase 1	109.58	85.08	100.82	107.00	0,750	0,441	0,441
Phosphoinositide-dependent kinase-1	103.86	98.15	111.24	106.87	0,438	>0,999	0,496
Pyruvate Dehydrogenase Kinase 3	123.51	92.71	88.41	95.17	0,500	>0,999	>0,999
Phosphofructokinase	131.34	112.18	110.32	78.32	0,844	>0,999	0,773
Phosphoglucomutase 2	112.16	98.88	198.58	116.76	0,688	0,298	0,087
Solute Carrier Family 25 Member 1	91.66	117.11	144.88	127.98	0,844	0,773	0,773
solute carrier family 25 member 10	100.19	105.25	164.85	90.73	>0,999	>0,999	>0,999
solute carrier family 25 member 22	113.16	103.96	179.42	112.78	0,844	0,298	>0,999

Proteins	CTRL (%CTRL)	LPS (%CTRL)	MS275+ LPS (%CTRL)	RGFP966+ LPS (%CTRL)	p-value CTRL vs LPS	Corrected p-value MS275+ LPS vs LPS	Corrected p-value RGFP966+ LPS vs LPS
solute carrier family 25 member 5	87.37	86.65	109.02	98.94	>0,999	0,298	>0,999
Succinate-CoA Ligase ADP-Forming	104.42	92.48	100.28	97.57	0,438	>0,999	>0,999
Succinate-CoA ligase [GDP-forming]	150.73	78.80	105.99	99.36	0,500	>0,999	>0,999
Ubiquinol-Cytochrome C Reductase Core Protein 2	137.83	76.94	97.91	100.49	0,500	0,828	>0,999

4

Chapter 4

Collagen Type I Alters the Proteomic Signature of Macrophages in a Collagen Morphology-Dependent Manner

Gwenda F. Vasse[1,2,3,4,#,*], Sara Russo[5,#], Andrei Barcaru[6], Asmaa A.A. Oun[3,7], Amalia M. Dolga[3], Patrick van Rijn[1,2], Marcel Kwiatkowski[8], Natalia Govorukhina[5], Rainer Bischoff[5], Barbro N. Melgert[3,4]

Scientific Reports 2023; 13: 5670.
Published online 2023 Apr 6. doi: 10.1038/s41598-023-32715-0

ABSTRACT

Idiopathic pulmonary fibrosis is a progressive lung disease that causes scarring and loss of lung function. Macrophages play a key role in fibrosis, but their responses to altered morphological and mechanical properties of the extracellular matrix in fibrosis is relatively unexplored. Our previous work showed functional changes in murine fetal liver-derived alveolar macrophages on fibrous or globular collagen morphologies. In this study, we applied differential proteomics to further investigate molecular mechanisms underlying the observed functional changes. Macrophages cultured on uncoated, fibrous, or globular collagen-coated plastic were analyzed by liquid chromatography-mass spectrometry. The presence of collagen affected expression of 77 proteins, while 142 were differentially expressed between macrophages grown on fibrous or globular collagen. Biological process and pathway enrichment analysis revealed that culturing on any type of collagen induced higher expression of enzymes involved in glycolysis. However, this did not lead to a higher rate of glycolysis, probably because of a concomitant decrease in activity of these enzymes. Our data suggest that macrophages sense collagen morphologies and can respond with changes in expression and activity of metabolism-related proteins. These findings suggest intimate interactions between macrophages and their surroundings that may be important in repair or fibrosis of lung tissue.

Keywords: Macrophage polarization, Topography, Fibrosis, Metabolism, Extracellular matrix.

INTRODUCTION

Fibrosis is defined as excessive accumulation of extracellular matrix (ECM), which eventually impairs the function of an affected organ. Idiopathic pulmonary fibrosis (IPF) is a chronic and progressive lung disease with a short life expectancy of 2-3 years after diagnosis. Treatment options are limited, as only two drugs have been approved that slow down disease progression: nintedanib and pirfenidone [1].

The characteristic excessive deposition of ECM proteins in fibrosis, mostly by myofibroblasts, changes the biochemical composition of a tissue. However, it is becoming clear that ECM can also be structurally different because of aberrant post-translational modifications [2]. For example, fibrils of collagen type I, the most abundant ECM protein in fibrosis, are structurally different in lung tissue from patients with IPF compared to control lung tissue [3]. All changes in biochemical composition and post-translational modifications also affect the biophysical properties of fibrotic tissue, such as tissue stiffness and topography [4-6]. The resulting biochemically and biophysically altered ECM can be sensed by resident cells and subsequently change their behavior, resulting in constant two-way interactions [7].

Macrophages are important regulators of ECM homeostasis, as they can stimulate both the production and degradation of ECM proteins [8]. Their ability to prevent or resolve fibrosis in combination with the aberrant macrophage polarization observed in fibrosis, makes studying their possible role in the pathogenesis of fibrosis crucial. Although the effect of fibrosis-related soluble factors (such as cytokines) on macrophage polarization and function has been studied extensively [9,10], their ability to respond to fibrosis-related morphological changes in the ECM is relatively unexplored [10].

Previously, we have shown that changes in the morphology of collagen type I, either globular or fibrous, can affect the shape, marker expression and behavior of murine fetal liver-derived alveolar macrophages [11]. Higher expression of the mannose receptor (CD206), known to be upregulated on alveolar macrophages in IPF, was found when alveolar macrophages were cultured on globular collagen. Fibrous collagen led to higher expression of Ym1, a murine marker of pro-healing macrophages. Moreover, macrophage shape changed distinctly in response to fibrous and globular collagen, with a more amoeboid appearance on fibrous collagen and a more mesenchymal appearance with many filopodia on globular collagen. In parallel with these alterations in macrophage shape, transmigration was higher when macrophages were cultured on fibrous collagen compared to the uncoated condition [11]. However, the exact mechanisms behind these characteristic responses are still elusive. In this study, we applied differential proteomics and

metabolic analysis to further elucidate macrophage responses to distinct collagen type I morphologies and to unravel possible molecular mechanisms by which the altered ECM in fibrosis affects macrophage function.

MATERIALS AND METHODS

Substrate preparation

Sterile cell culture plates were coated with 75 µl/cm^2 rat-tail collagen type I (Ibidi, Martinsried, Germany) at a concentration of 2.8 mg/mL at pH 3 (globular structured collagen layers) or pH 7 (fibrous collagen layers), as described before [11]. The desired pH was achieved by diluting the collagen type I stock in either 17.5 mM NaOH or 17.5 mM CH_3COOH. Collagen layers were incubated at 37 °C for one hour, subsequently washed twice with sterile water and allowed to dry overnight at 37 °C.

Cell culture

Alveolar macrophages derived from fetal monocytes according to the protocol of Fejer et al. [12] (a kind gift by Dr. G. Fejer) were cultured in RPMI (Gibco Laboratories, Grand Island, USA) supplemented with 10% heat-inactivated FCS (Biowest, Nuaillè, France), 10 µg/mL gentamycin (Gibco Laboratories) and 20 ng/mL murine GM-CSF (Peprotech, Rocky Hill, USA). Once a week, macrophages were detached with 1 mM EDTA (Merck, Darmstadt, Germany) and reseeded at a density of 1×10^5 cells/mL. The cells were incubated at 37 °C and 5% CO_2, and cell culture medium was refreshed after 4 days. Macrophages between passage number 6 and 12 were seeded at a density of 5.7×10^4 cells/cm^2 for proteomic analysis or at a density of 35×10^4 cells/cm^2 for extracellular flux analysis.

Sample preparation for proteomic analysis

Macrophages were cultured on collagen-coated or non-coated surfaces for 72 hours before harvesting for proteomic analysis. Cell culture medium was collected and centrifuged to collect detached macrophages. The cell pellet was subsequently washed in PBS. Adherent macrophages were washed five times in PBS, followed by cell lysis with SDC lysis buffer: 1% w/v sodium deoxycholate (Sigma-Aldrich, Zwijndrecht, the Netherlands) and 1 mM EDTA in 0.1 M triethylammonium bicarbonate (TEAB) buffer (Thermo Fisher Scientific, Landsmeer, the Netherlands). The lysate of the adherent macrophages was then added to the pellet of detached macrophages and mixed. Subsequently, the total lysate was denatured at 98 °C for 5 minutes and sonicated with a tip sonicator (Vibra-Cell, Sonics, Newton, United States) for 3×10 seconds, 50% without pulse. Protein concentrations were

determined with a microplate BCA protein assay following the manufacturer's instructions (Pierce™ Microplate BCA Protein Assay Kit, Thermo Fisher Scientific). For tryptic in-solution digestion, 50 µg of the samples was diluted in 0.1 M TEAB (pH 8.3) to a final volume of 100 µL. For reduction, the samples were incubated with 10 mM dithiothreitol (DTT, dissolved in 0.1 M TEAB, pH 8.3) on a shaker (600 rpm) at 57 °C for 10 minutes. Afterwards, the samples were alkylated with 20 mM iodacetamide (0.1 M TEAB, pH 8.3) and incubated in the dark at room temperature for 30 minutes. Subsequently, free iodoacetamide was quenched by adding 10 mM of DTT (0.1 M TEAB, pH 8.3). For tryptic digestion, the samples were incubated in 1 µL trypsin solution (0.5 µg/µL sequencing grade modified trypsin, dissolved in trypsin resuspension buffer (Promega, Walldorf, Germany) at 37 °C for 16 hours. Afterwards, the samples were acidified by adding formic acid to a final concentration of 1% and centrifuged at 16,000 g at room temperature for 5 minutes. The supernatants were then transferred to a new reaction vial and evaporated to dryness.

Liquid chromatography (LC)-mass spectrometry (MS)/MS analysis in data-dependent acquisition mode

For data independent analysis (DIA), a macrophage-specific protein/peptide library of the alveolar macrophages was generated using data dependent acquisition (DDA) mode. For this purpose, 100 µg of a dried tryptic digest of an alveolar macrophage reference sample was separated by high pH reversed-phase chromatography using a Dionex Ultimate 3000 ultra-performance liquid chromatography (UPLC) system equipped with a fraction collector. Peptides were separated with a C18 column (ACQUITY UPLC BEH C18 Column, 130 Å, 1.7 µm, 1 mm × 150 mm, Waters, Manchester, UK, buffer A: 5% acetonitrile (ACN), dissolved in HPLC-$H_2$0, pH 9.5 adjusted with NH_4OH; buffer B: 95% ACN, dissolved in HPLC-$H_2$0, pH 9.5 adjusted with NH_4OH) using a gradient from 1-50% buffer B in 60 minutes and a flow-rate of 100 µL/min. 30 fractions were collected with a volume of 200 µL. The fractions were pooled into 13 fractions and evaporated to dryness.

For LC-MS/MS analysis in data-dependent acquisition mode, the samples were dissolved in 20 µL of 0.1% formic acid and 1 µL was injected into a nano-ultra pressure liquid chromatography system (Dionex UltiMate 3000 RSLCnano pro flow, Thermo Fisher Scientific, Bremen, Germany) coupled via electrospray-ionization source to a tribrid orbitrap mass spectrometer (Orbitrap Fusion Lumos, Thermo Fisher Scientific, San Jose, CA, USA). The samples were loaded (15 µL/min) on a trapping column (nanoE MZ Sym C18, 5 µm, 180 µm × 20 mm, Waters, Eschborn, Germany, buffer A: 0.1% formic acid in HPLC-H_2O; buffer B: 80% acetonitrile, 0.1%

formic acid in HPLC-H_2O) with 5% buffer B. After sample loading, the trapping column was washed with 5% buffer B for 2 minutes (15 µL/min) and the peptides were eluted (250 nL/min) onto the separation column (nanoE MZ PST CSH C18, 130 Å, 1.7 µm, 75 µm × 250 mm, Waters) and separated with a gradient of 5–37.5% B in 90 minutes. The spray was generated from a steel emitter (Thermo Fisher Scientific, Dreieich, Germany) at a capillary voltage of 1900 V. Full scan spectra were acquired over a m/z range from 400-1000 with a resolution of 60k (at m/z 200) using a normalized automatic gain control target of 100% and a maximum injection time of 50 ms. Fragment spectra were acquired in data-dependent acquisition mode with a normalized high energy collision-induced dissociation energy of 28%, an orbitrap resolution of 30k (at m/z 200), a normalized automatic gain control target of 100%, a maximum injection time of 100 ms and an intensity threshold for the precursor of 5e4. Fragment spectra were acquired in top-speed mode, with a full scan spectrum recorded every 3 seconds, and an exclusion time of 60 seconds.

Peptide and protein identification were performed with the Proteome Discoverer software suite (Thermo Fisher Scientific, version 2.4) using the Sequest search algorithm and PercolatorHT for false discovery rate calculation. The LC-MS/MS data were searched against the SwissProt mouse database (17.023 protein entries, UP000000589) and a contaminant database (235 entries) using the following parameters: precursor mass tolerance: 10 ppm, fragment mass tolerance: 0.02 Da, carbamidomethylation of cysteines was considered as a static modification, and the following modifications were considered as variable modifications: methionine oxidation, deamidation of glutamine and asparagine, Gln→pyro-Glu as N-terminal peptide modification, and an acetyl-loss, methionine-loss+Acetylation and a methionine-loss as N-terminal protein modification. Peptides and proteins were identified with a false discovery rate-cut-off of 0.01.

LC-data independent acquisition (DIA)-MS analysis and data analysis

For DIA analysis, 1 µg of tryptic peptides was injected into a nano-ultra pressure liquid chromatography system and separated using the same parameters and conditions as described above (LC-MS/MS analysis in data-dependent acquisition mode). MS analysis was performed in DIA mode. Full scan spectra were acquired from 400-1000 with a resolution of 60k (at m/z 200) using a normalized automatic gain control target of 100% and a maximum injection time of 50 ms. DIA fragment spectra were acquired with isolation windows of 10 m/z covering a m/z-range from 400-1000, a normalized high energy collision-induced dissociation energy of 28%, an orbitrap resolution of 30k (at m/z 200), a normalized automatic gain control target of 100% and a maximum injection time of 54 ms. Fragment spectra were

recorded over a m/z-range from 350-1500. One full spectrum was followed by a DIA scan from m/z 400-700, followed by a full spectrum and a DIA scan from m/z 700-1000.

For protein identification and quantification, a library was created with Skyline (MacCoss Lab, University of Washington, USA, version 19.1.0.193) based on the DDA data. The Proteome Discoverer results were imported in Skyline and the peptide library was generated using the following parameters: transition settings: precursor charges: 2, 3, 4, 5; fragment ion charges: 1, 2; ion types: p (precursor), b, y; ion match tolerance: 0.02 Da; minimum number of product ions: 4; m/z-range: 350-2000; the DIA acquisition method file was uploaded to determine the DIA isolation scheme; RT tolerance: 5 minutes. The generated library consisted of 6.310 proteins with at least one unique peptide for each protein and 74.654 unique peptides, covering 37% of the theoretical mouse proteome. The LC-DIA-MS files were imported and filtered with a dotp-threshold of 0.85 (best match). Only proteins with at least one unique peptide were kept. The Skyline results were exported for further data analysis in R and Python. This included missing values imputations, median normalization and log2 transformation of the protein intensities. For feature selection, partial least squares discriminant analysis and statistical analysis were performed.

Extracellular flux analysis

The glycolytic rate was measured using an XFe96 Extracellular Flux Analyzer (Agilent Technologies, Santa Clara, California). Alveolar macrophages were seeded into Seahorse XF96 cell culture microplates that were coated with either fibrous or globular collagen or left uncoated (control) and incubated for 72 hours. To measure extracellular acidification and oxygen consumption rates, cells were equilibrated for 1 hour in the absence of CO_2 at 37 °C in XF base media (Agilent Technologies, Santa Clara, California). The manufacturer's protocol for the XF Glycolysis Stress Test was used to assess the glycolytic rate (Agilent Technologies). After equilibration, macrophages were stimulated with sequential injections of glucose (20 mM), oligomycin (1 μM), and 2-deoxy-D-glucose (50 mM). Glycolytic function is represented as glycolysis, glycolytic capacity and glycolytic reserve. Glycolysis was calculated as the difference between the maximal rate before oligomycin addition and the last rate measurement before glucose addition. Glycolytic capacity was calculated as the difference between the maximal rate after oligomycin addition and the last rate measurement before glucose addition. The glycolytic reserve was calculated as the difference between glycolytic capacity and glycolysis. Measurements were normalized to the protein amount in each well using a microplate BCA protein assay.

Glycolytic enzyme kinetics

Glycolytic enzyme-catalyzed reactions were measured by means of photometric assays. Alveolar macrophages were seeded on plates coated with either fibrous or globular collagen, or left uncoated (control) and incubated for 72 hours. Adherent cells were then detached with 1mM EDTA, centrifuged, and washed twice with ice-cold PBS. Cells were then resuspended in PBS containing protease inhibitors (Sigma-Aldrich, cOmplete™ Protease Inhibitor Cocktail) and stored at -80 °C. On the day of analysis, Triton X-100 (Sigma-Aldrich) was added to a final concentration of 0.1% and the suspension was centrifuged at 21000 g for 10 min at 4 °C. The cell-free supernatant was collected and used for the analysis. The enzyme activity, expressed in µmol/min/mg protein was determined from the difference in the slope of NAD(P)H absorbance (340 nm) before and after the addition of a substrate. The activities, unless stated otherwise, were measured in buffers with 5 mM KCl, 1 M Tris-HCl, 0.15 M NaCl, 5 mM $CaCl_2$, and 0.1 M $MgSO_4$, pH 7.4, 37 °C. The contents of the reaction mixtures were as follows: the phosphofructokinase (PFK) reaction mixture contained 0.1 M ATP, 15 mM NADH, 620 U/mL glycerol-3-phosphate dehydrogenase (G3PDH), 330 U/mL aldolase, 1800 U/mL triosephosphate isomerase (TPI), and 0.1 M fructose-6-phosphate. The phosphoglycerate kinase mixture contained 0.1 M ATP, 15 mM NADH, 800 U/mL glyceraldehyde-3P-dehydrogenase (GAPDH), and 0.125 M 3-phosphoglyceric acid. The aldolase mixture contained 15 mM NADH, 620 U/mL G3PDH, 1800 U/mL TPI, and 0.02 M of fructose-1,6-bisphosphate (F-1,6-BP). The pyruvate kinase mixture contained 0.1 M ADP, 0.02 M of F-1,6-BP, 15 mM NADH, 9300 U/mL lactate dehydrogenase, and 0.02 M phosphoenolpyruvate.

Statistical analysis

Differentially expressed proteins by cells growing on collagen were investigated by comparing macrophages grown on plastic with macrophages grown on any type of collagen (globular + fibrous) using an unpaired two-sided two-sample Wilcoxon test with a Benjamini-Hochberg correction for multiple testing. To uncover differentially expressed proteins induced by a specific type of collagen, we compared macrophages grown on globular collagen with macrophages grown on fibrous collagen using a paired two-sided two-sample Wilcoxon test with a Benjamini-Hochberg correction for multiple testing. A corrected p-value <0.05 was considered significant. No proteins were found to be significantly differentially expressed when using this correction. For pathway analyses we therefore used the uncorrected p-values and included all proteins that had an uncorrected p-value <0.025 (collagen versus control) or <0.05 (fibrous versus globular) and a fold change <0.875 or >1.25. Analyses were performed using R (version 4.2.0 (2022-04-22)—"Vigorous Calisthenics").

Pathway analysis: Enrichment of biological processes and pathways was analyzed by performing GO enrichment analysis with the annotation data sets 'Panther GO-Slim Biological Process' and 'Panther Pathways', using a Fisher's Exact test to determine the p-value with a Benjamini-Hochberg correction to compensate for the false discovery rate. Results with a corrected p-value <0.05 were considered to be significant.

All other statistics: Experimental groups for other parameters were compared using GraphPad Prism 8.0 (GraphPad Software, La Jolla, USA). Control macrophages cultured on plastic were compared to macrophages cultured on any type of collagen using a Mann-Whitney U test, while the effect of collagen morphology was investigated by comparing macrophages grown on fibrous or globular collagen using a Wilcoxon matched-pairs signed-rank test. A p-value <0.05 was considered significant.

RESULTS

Proteome analysis

To investigate the effect of collagen morphology on the proteome signature of macrophages, fetal liver-derived alveolar macrophages were cultured on tissue culture plastic coated with either fibrous or globular collagen, or left uncoated (control) for 72 hours. The reason for using this model instead of primary alveolar macrophages was to eliminate any potential interference of transplantation effects that primary alveolar macrophages may experience in cell culture [12]. Primary alveolar macrophages that are removed from their lung-specific environment, which includes exposure to air and cyclic stretch, may experience changes that could affect their responses to collagen sensing. Cell lysates were analyzed by LC-MS in DIA mode. After data processing using our fetal liver-derived alveolar macrophage-specific protein library, 2.870 unique proteins were reproducibly quantified in the three distinct conditions. Partial least squares discriminant analysis indicated that all conditions could be separated based on their proteomic profile (**Figure 1a**) after data normalization (**Supplementary Figure 1**).

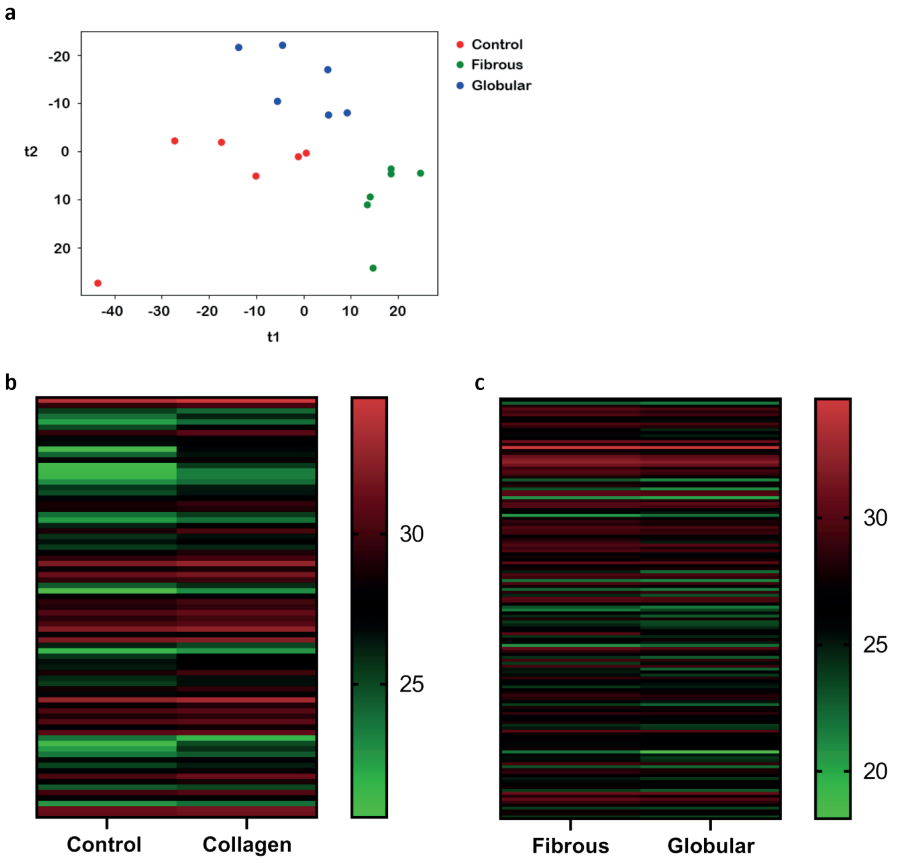

Figure 1: Effect of culturing conditions on the protein expression profile of macrophages. Alveolar macrophages were cultured on uncoated, globular collagen-coated or fibrous collagen-coated tissue culture plastic (n=6). **a.** Partial least squares-discriminant analysis plot of alveolar macrophages in the different conditions showing that the 3 conditions cluster separately. **b.** Heatmap of 77 proteins that were differentially expressed ($p<0.025$) between uncoated and collagen type I-coated conditions (fibrous and globular pooled). **c.** Heatmap of 142 proteins that were differentially expressed ($p<0.05$) between macrophages cultured on fibrous or globular collagen. Expressed as Log2 of the median values and statistically tested with an unpaired (b) or a paired (c) Wilcoxon test.

We first investigated the effects of culturing macrophages on collagen versus uncoated plastic. Culturing macrophages on collagen type I-coated tissue culture plastic resulted in differential expression of 77 proteins compared to macrophages on uncoated plastic (**Figure 1b** and **Supplementary Table 1**). 69 of these proteins were more than 1.25-fold upregulated, whereas only three proteins were more than 1.25 fold downregulated (fold change >0.875) (**Supplementary Table 1**). To assess

collagen morphology-specific effects, we also compared protein expression levels of macrophages cultured on fibrous or globular collagen. 142 proteins were found to be differentially expressed (**Figure 1c** and **Supplementary Table 2**) and 101 of these proteins were more than 1.25-fold upregulated in macrophages cultured on fibrous collagen, whereas only 19 proteins were downregulated (**Supplementary table 2**).

Culturing macrophages on collagen results in higher expression of proteins involved in glycolysis

Out of the 77 differentially expressed proteins between macrophages cultured on collagen type I and uncoated controls, 30 proteins showed a more than two-fold higher expression in collagen-coated conditions (**Table 1**). Three proteins even increased more than ten-fold: pigment epithelium-derived factor (Serpfin1), protein FAM118B (Fam118B), and guanylate-binding protein 4 (GBP4). Only the proteins caspase-9 (Casp9), Rac GTPase-activating protein 1 (Racgap1), and SOSS complex subunit B1 (Nabp2) were expressed at lower levels in macrophages cultured on collagen-coated samples (**Table 1**).

Analysis of the biological processes in which the proteins that are upregulated by culturing on collagen type I are involved (**Supplementary Table 1**), indicated an effect on macrophage metabolism (**Figure 2a**). Pathway analysis revealed enrichment of the glycolysis pathway under collagen-coated conditions (**Figure 2b**). The presence of either fibrous or globular collagen induced a more than two-fold higher expression of liver type ATP-dependent 6-phosphofructokinase (Pfkl), a key enzyme in glycolysis. Additionally, the expression levels of two other members of the glycolysis pathway, fructose-biphosphate aldolase C (Aldoc) and phosphoglycerate kinase-1 (Pgk1) were higher in the presence of collagen type I (**Figure 2c**). An overview of the main enzymes involved in the glycolysis pathway can be found in **Figure 3a**.

Table 1: Effect of collagen type I on macrophage protein expression.

Gene name	Protein name	Fold change	p-value
Serpinf1	Pigment epithelium-derived factor	35.82	4.74E-03
Fam118b	Protein FAM118B	13.21	2.45E-02
Gbp4	Guanylate-binding protein 4	10.34	6.90E-03
Ndrg1	Protein NDRG1	6.22	4.74E-03
Syap1	Synapse-associated protein 1	6.02	2.45E-02
Nudt9	ADP-ribose pyrophosphatase, mitochondrial	5.95	1.35E-02
Golt1b	Vesicle transport protein GOT1B	5.27	2.05E-03
Sptlc1	Serine palmitoyltransferase 1	5.18	3.23E-03
Arfgap3	ADP-ribosylation factor GTPase-activating protein 3	5.02	6.90E-03
Thop1	Thimet oligopeptidase	4.93	9.70E-03
Slain2	SLAIN motif-containing protein 2	4.49	6.90E-03
Ethe1	Persulfide dioxygenase ETHE1, mitochondrial	4.14	1.35E-02
Mrps14	28S ribosomal protein S14, mitochondrial	3.95	1.82E-02
Trmt2a	tRNA (uracil-5-)-methyltransferase homolog A	3.37	3.23E-03
Eml2	Echinoderm microtubule-associated protein-like 2	3.19	6.90E-03
Alox5	Polyunsaturated fatty acid 5-lipoxygenase	3.19	4.74E-03
Ftl1	Ferritin light chain 1	3.11	1.82E-02
Ctnnd1	Catenin delta-1	2.52	1.82E-02
Nelfa	Negative elongation factor A	2.45	9.70E-03
Pfkl	ATP-dependent 6-phosphofructokinase, liver type	2.38	9.70E-03
Esyt2	Extended synaptotagmin-2	2.35	6.90E-03
Grhpr	Glyoxylate reductase/hydroxypyruvate reductase	2.34	3.23E-03
Acad8	Isobutyryl-CoA dehydrogenase, mitochondrial	2.26	2.45E-02
Tm9sf3	Transmembrane 9 superfamily member 3	2.18	2.45E-02
Fam162a	Protein FAM162A	2.12	1.82E-02
Agpat4	1-acyl-sn-glycerol-3-phosphate acyltransferase delta	2.11	2.45E-02
Armc10	Armadillo repeat-containing protein 10	2.10	6.90E-03
F13a1	Coagulation factor XIII A chain	2.06	1.82E-02
Ero1a	ERO1-like protein alpha	2.04	9.70E-03
Lrp1	Low-density lipoprotein receptor-related protein 1	2.01	4.31E-04
Casp9	Caspase-9	0.46	1.35E-02
Racgap1	Rac GTPase-activating protein 1	0.38	1.29E-03
Nabp2	SOSS complex subunit B1	0.30	1.82E-02

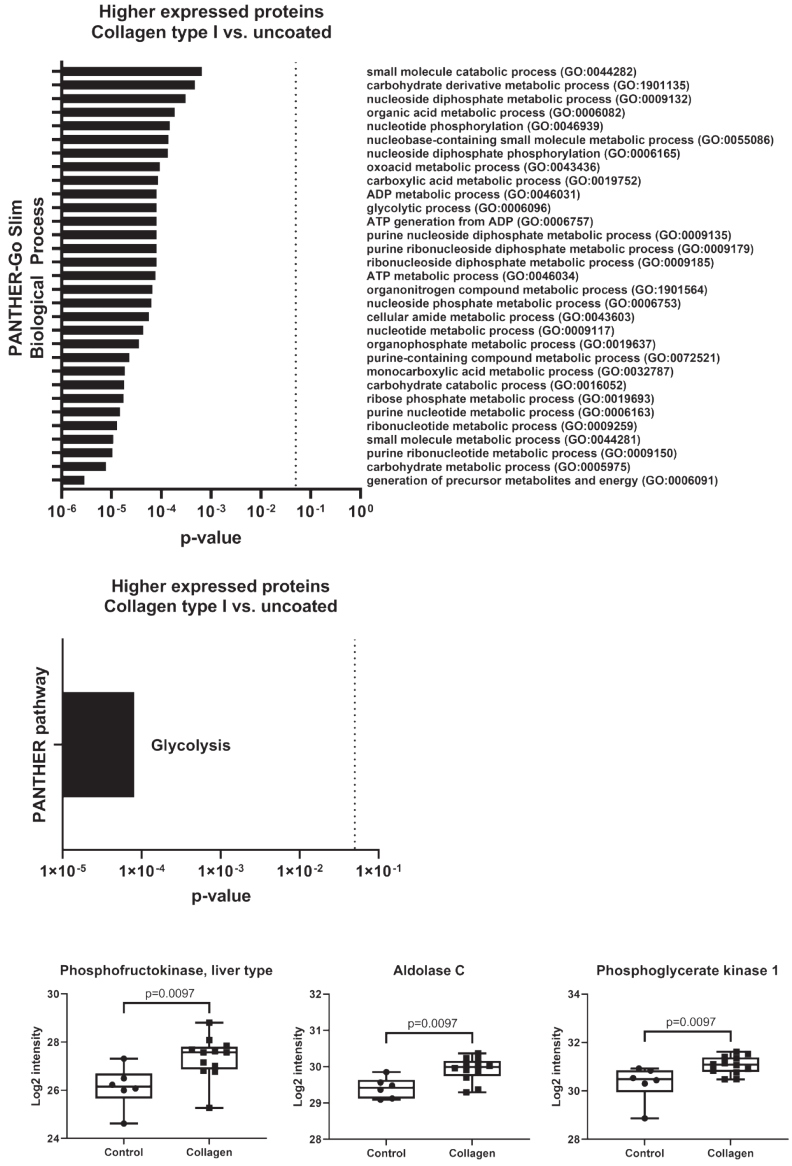

Figure 2: GO enrichment analysis of proteins upregulated by collagen type I. 69 proteins were >1.25-fold upregulated by macrophages cultured on collagen-coated plates (fibrous and globular pooled), compared to uncoated controls. **a.** PANTHER-Go Slim Biological Process analysis. **b.** PANTHER pathway analysis, indicating significant enrichment of the glycolysis pathway. **c.** Three proteins of the glycolysis pathway were significantly upregulated in macrophages grown on collagen (both types pooled, n=6 each) compared to macrophages grown on plastic (control, n=6). Protein intensity expressed as normalized Log2 values and statistically tested with an unpaired Wilcoxon test. p<0.025 was considered significant. Data represented as a box and whiskers plot, where the box extends from the 25th to 75th percentiles and whiskers from min to max values.

Higher expression of hexokinase 2 and phosphoglycerate mutase family member 5 by macrophages cultured on fibrous collagen as compared to globular collagen.

Culturing macrophages on collagen type I clearly affected the expression of proteins. Next, we investigated if the morphology type of collagen would influence protein expression by comparing macrophages grown on fibrous collagen to macrophages cultured on globular collagen. Fibrous collagen led to a more than two-fold higher expression of 23 proteins compared to globular collagen (**Table 2**), with the most pronounced fold-change observed for pigment epithelium-derived factor (Serpinf1). The expression of four proteins was found to be at least two-fold lower in macrophages grown on fibrous collagen. These proteins are pyridoxal kinase (Pdxk), thioredoxin reductase 1, cytoplasmic (Txnrd1), nuclear cap-binding protein subunit 1 (Ncbp1) and translocating chain-associated membrane protein 1 (Tram1). Biological process and pathway analysis of the proteins with a >1.25-fold change different expression (**Supplementary Table 2**) did not yield any significantly enriched pathways.

However, as we found the glycolysis pathway significantly enriched in cells grown on any type of collagen, we specifically investigated important metabolic enzymes in the list of significant proteins (**Supplementary Table 2**) and found hexokinase 2 (Hk2) and phosphoglycerate mutase family member 5 (Pgam5) to be differentially expressed (**Figure 3b**). Therefore, glycolysis may again be one of the biological processes affected by the culture conditions of macrophages (**Figure 3b**). In addition, four proteins in the list are part of the mitochondrial respiratory chain (Cytochrome b-c1, part of the ubiquinol-cytochrome c complex, elongation factor-like GTPase 1, NADH dehydrogenase (ubiquinone), and V-type proton ATPase), possibly pointing at changes in oxidative phosphorylation.

Table 2: Effect of collagen morphology on the protein expression profile of macrophages.

Gene name	Protein name	Fold change F/G	p-value
Serpinf1	Pigment epithelium-derived factor	12.66	3.13E-02
Dctn4	Dynactin subunit 4	9.97	3.13E-02
Rbm42	RNA-binding protein 42	9.86	3.13E-02
Mrps15	28S ribosomal protein S15, mitochondrial	9.52	3.13E-02
Atp7a	Copper-transporting ATPase 1	6.11	3.13E-02
Ppic	Peptidyl-prolyl cis-trans isomerase C	4.97	3.13E-02
Prim2	DNA primase large subunit	3.83	3.13E-02
Trim23	E3 ubiquitin-protein ligase TRIM23	3.64	3.13E-02
Mmp8	Neutrophil collagenase	3.63	3.13E-02
Uba5	Ubiquitin-like modifier-activating enzyme 5	3.40	3.13E-02
Plekha2	Pleckstrin homology domain-containing family A member 2	3.12	3.13E-02
Tmsb4x	Thymosin beta-4	3.09	3.13E-02
Unc45a	Protein unc-45 homolog A	2.61	3.13E-02
Ercc4	DNA repair endonuclease XPF	2.51	3.13E-02
Retreg3	Reticulophagy regulator 3	2.41	3.13E-02
Cybc1	Cytochrome b-245 chaperone 1	2.25	3.13E-02
Yipf4	Protein YIPF4	2.24	3.13E-02
Gdi1	Rab GDP dissociation inhibitor alpha	2.12	3.13E-02
Rdh11	Retinol dehydrogenase 11	2.11	3.13E-02
Rab11b	Ras-related protein Rab-11B	2.10	3.13E-02
Rtn3	Reticulon-3	2.05	3.13E-02
Wtap	Pre-mRNA-splicing regulator WTAP	2.05	3.13E-02
Apoo	MICOS complex subunit Mic26 (Apolipoprotein O)	2.02	3.13E-02
Pdxk	Pyridoxal kinase	0.50	3.13E-02
Txnrd1	Thioredoxin reductase 1, cytoplasmic	0.44	3.13E-02
Ncbp1	Nuclear cap-binding protein subunit 1	0.41	3.13E-02
Tram1	Translocating chain-associated membrane protein 1	0.39	3.13E-02

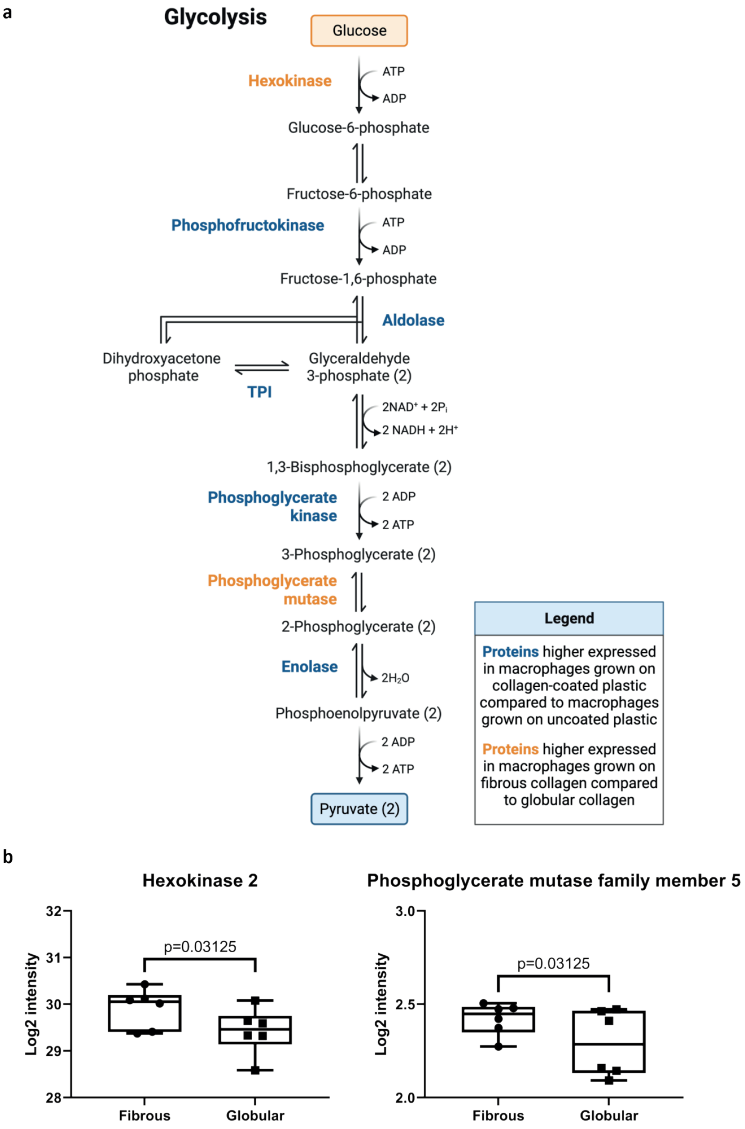

Figure 3: Glycolytic enzymes that were differentially expressed between macrophages cultured on fibrous or globular collagen. a. Glycolysis metabolic pathway. Five proteins of the glycolysis pathway were significantly higher expressed in macrophages grown on collagen-coated plastic (fibrous and globular pooled, n=6 each) compared to macrophages grown on uncoated plastic are indicated in blue. Proteins of the glycolysis pathway that were significantly higher expressed in macrophages grown on fibrous collagen compared to globular collagen are indicated in orange (fold change <0.875 or >1.25). **b.** Two proteins of the glycolysis pathway were significantly higher expressed in macrophages grown on fibrous collagen compared to macrophages grown on globular collagen. Data are expressed as normalized Log2 values and statistically tested with a paired Wilcoxon test and $p<0.05$ was considered significant (n=6). Data represented as a box and whiskers plot, where the box extends from the 25th to 75th percentiles and whiskers from min to max values.

No functional metabolic differences between macrophages cultured on collagen- or uncoated plastic

To investigate whether the higher expression of glycolytic proteins in macrophages cultured on collagen-coated substrates translated into changes in cellular metabolism, extracellular flux analysis was performed to assess glycolytic activity. No significant differences were found in glycolytic function between alveolar macrophages grown on collagen-coated or on uncoated wells (**Figure 4a**). Similarly, no differences in glycolytic function were found between alveolar macrophages cultured on either fibrous or globular collagen (**Figure 4b**). Furthermore, oxygen consumption rates were tracked and here too, no differences were found between macrophages cultured on plastic or macrophages cultured on either type of collagen (**Supplementary Figure 2**).

As we found no differences in glycolytic function, we investigated whether the activity of four of the differentially expressed glycolytic enzymes was affected by culture conditions, i.e. hexokinase, phosphofructokinase, aldolase, and phosphoglycerate kinase. First, we again compared macrophages cultured on any type of collagen versus those cultured on uncoated plastic. We found that all enzyme activities tended to be lower in macrophages cultured on collagen compared to the uncoated control, but only the activity of aldolase was significantly lower (**Figure 5a-d**). We then investigated the effect of the collagen morphology on the activity of glycolytic enzymes and found that macrophages grown on fibrous collagen had significantly higher aldolase activity than macrophages grown on globular collagen (**Figure 5e-h**). Opposite trends between protein expression and protein activity were observed: when protein expression was higher, the activity was lower and vice versa (compare **Figure 2c, 3b, 5a-d, and 5e-h**).

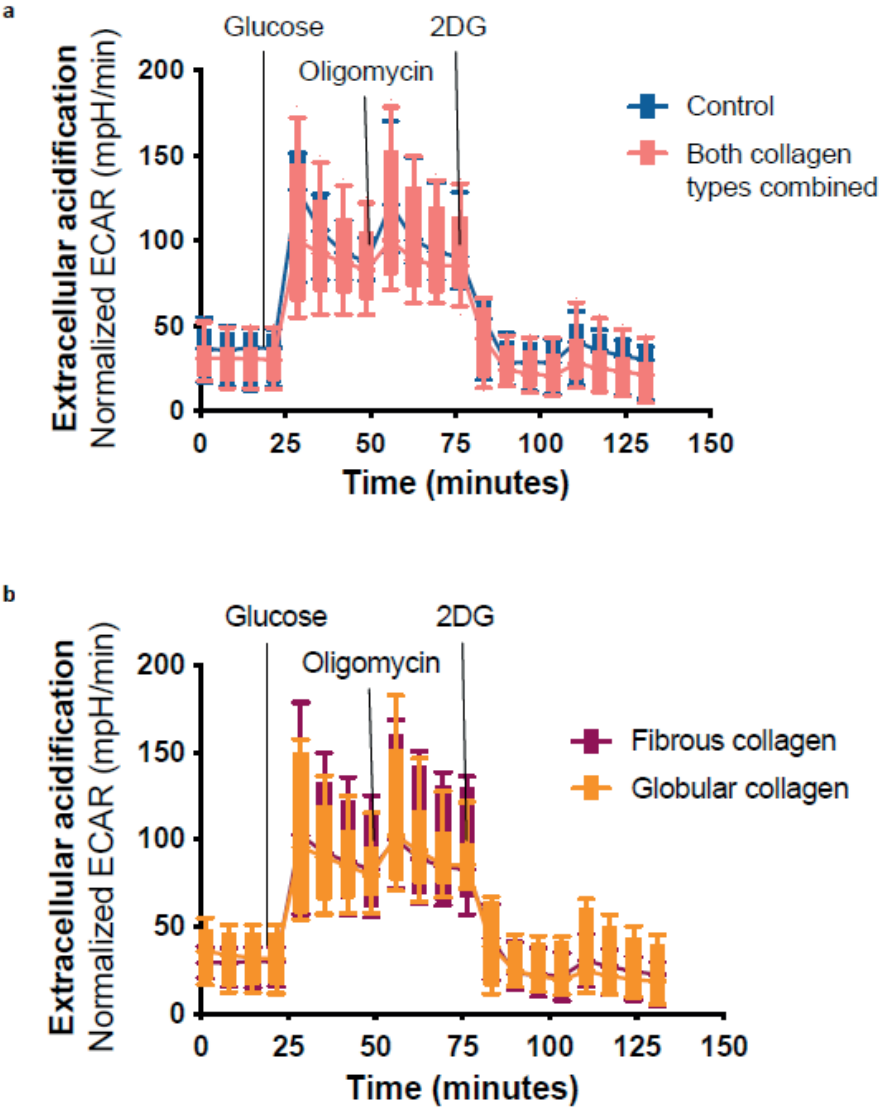

Figure 4: Extracellular acidification rate of alveolar macrophages cultured in collagen-coated or uncoated wells. After 72 hours, extracellular acidification rate (ECAR) was measured by glycolysis stress test using an XFe96 extracellular flux analyzer and rates were normalized to protein concentrations. Macrophages were treated sequentially with glucose, oligomycin (ATP synthase inhibitor), and 2-DG (2-deoxyglucose). **a.** Kinetic ECAR response of macrophages seeded in wells that were either coated with fibrous or globular collagen (data combined) or left uncoated (control). Each data point represents mean ± SD of 6 different experiments. Each single experiment had 6 technical replicates that were averaged. **b.** Kinetic ECAR response of macrophages seeded in wells that were either coated with fibrous or globular collagen. Each data point represents mean ± SD of 6 different experiments. Each single experiment had 6 technical replicates that were averaged. Data represented as a box and whiskers plot, where the box and whiskers extend from the 10th to 90th percentile.

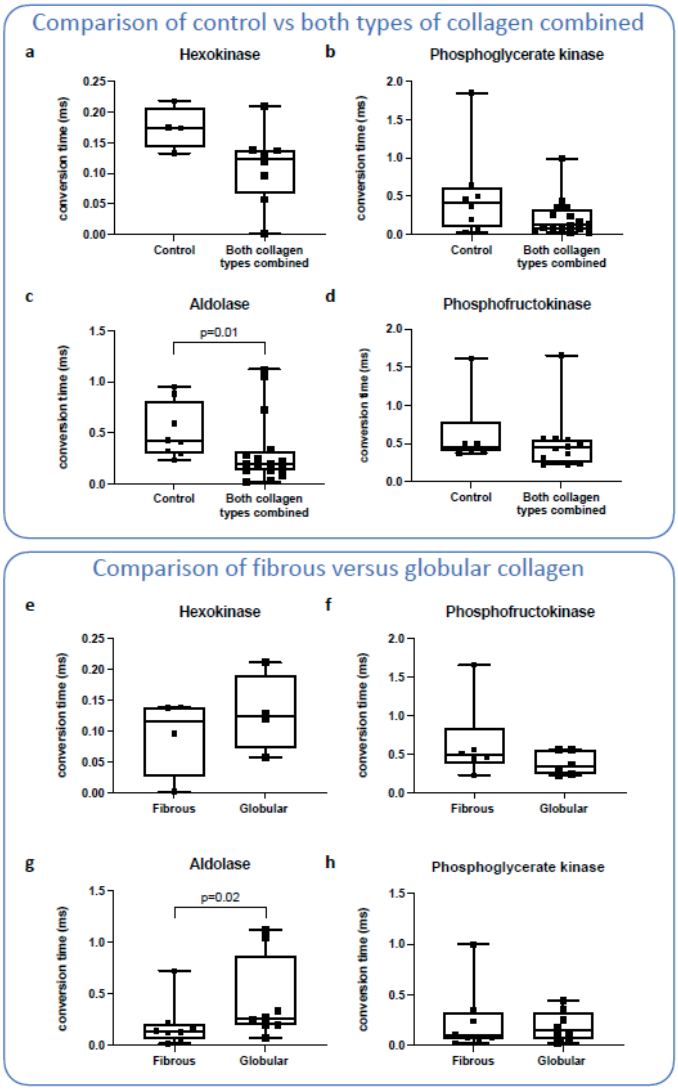

Figure 5: Activity of key glycolytic enzymes in alveolar macrophages in different culture conditions. Macrophages were cultured in wells coated with either fibrous or globular collagen or uncoated. After 72 hours, enzymatic activity of four different glycolytic enzymes was measured in cell lysates. **a-d.** Activity of glycolytic enzymes compared between macrophages cultured in uncoated and collagen type I-coated conditions (fibrous and globular pooled). Only the activity of aldolase was significantly lower in collagen-coated conditions. **e-h.** Activity of glycolytic enzymes compared between macrophages cultured in fibrous collagen-coated and globular collagen-coated conditions. Only the activity of aldolase was significantly higher in globular collagen-coated conditions. Bars represent the mean rate of enzyme activity and each data point represents a different biological replicate (n=4 for hexokinase, n=6 for phosphofructokinase, and n=8 for aldolase and phosphoglycerate kinase). Groups were compared using a Mann-Whitney U test (**a-d**) or Wilcoxon test (**e-h**). $p<0.05$ was considered significant. Data represented as a box and whiskers plot, where the box extends from the 25th to 75th percentiles and whiskers from min to max values.

To investigate if there were any changes to proteins involved in oxidative phosphorylation, we specifically investigated the 33 proteins found in our data involved in the electron transport chain in mitochondria. We found only three proteins higher expressed in macrophages cultured on either globular or fibrous collagen compared to plastic (Cytochrome c oxidase subunit 4, mitochondrial, NADH: Ubiquinone Oxidoreductase Subunit B9, Ubiquinol-Cytochrome C Reductase Core Protein 1) and three lower expressed in macrophages grown on globular collagen compared to fibrous (Cytochrome C Oxidase Subunit 7A2, Superoxide Dismutase 2, Ubiquinol-Cytochrome C Reductase Complex III Subunit VII). Graphs of these six proteins can be found in **Supplementary Figure 3**. The limited number of differentially expressed protein explains why the process of oxidative phosphorylation was not found enriched.

DISCUSSION

In this study, we gained insight into the effects of collagen type I morphologies on the proteomic signature of fetal liver-derived alveolar macrophages. Biological process and pathway enrichment analysis revealed clear effects of collagen on the expression of proteins involved in macrophage metabolism. Macrophages grown on collagen favor the expression of proteins involved in glycolysis, although this did not lead to increased glycolytic capacity, possibly because of a compensatory decrease in activity of those proteins. In addition to changes related to the general presence of collagen, fibrous and globular collagen also showed to have morphology-specific effects on the proteomic profile with prominent induction of Serpinf1 and prominent inhibition of Nabp2 on fibrous compared to globular collagen as the most differentially expressed proteins.

Pathway enrichment analysis revealed that macrophages cultured on collagen expressed higher levels of proteins involved in glycolysis and this was independent of collagen morphology. The expression of ATP-dependent 6-phosphofructokinase, liver type (Pfkl), a rate-limiting enzyme in glycolysis, was more than two-fold higher in macrophages cultured on collagen type I. In macrophages, glycolysis is generally associated with an activated, pro-inflammatory phenotype [13]. However, we previously described higher expression of the mannose receptor CD206 and lower expression of major histocompatibility complex II (MHCII) on macrophages cultured on collagen type I, suggesting a more anti-inflammatory/pro-repair phenotype in these alveolar macrophages [11]. This discrepancy may be explained by the recent finding that alveolar macrophages do not depend on glycolysis to produce pro-inflammatory mediators [14]. Furthermore, glycolysis has been associated with a profibrotic macrophage phenotype in bleomycin-induced pulmonary fibrosis in

mice [15]. In our study, the higher levels of glycolytic enzymes in macrophages grown on collagen did not functionally translate into higher glycolytic activity, based on the extracellular acidification rate analysis. This may have been the result of a compensatory lower activity of those enzymes, as there appeared to be a negative correlation between enzyme expression and activity. However, for proper correlation analysis, both analysis of enzyme concentration and activity would need to be performed on the same sample, which was not the case in our study.

Explanations of why more protein expression did not translate into more enzymatic activity could be found in changes in protein folding, post-translational changes, regulatory changes [16], or allosteric regulation. For instance, phosphofructokinase has been shown to be allosterically regulated by ATP, AMP, fructose 1,6-bisphosphate, fructose 2,6-biphosphate, and citrate [17]. Another possible explanation could be the contributions of different enzyme isoforms. All enzymes of interest have more than one isoform, while the enzymatic activity tests we performed are not isoform-specific. The proteome analysis, however, assessed each specific isoform. Therefore, any difference in activity may have been obscured by contributions of other isoforms. Importantly, our results highlight that using only one analytical approach could lead to biased results when studying metabolic behavior of macrophages. Multiple techniques should be used when possible to gain complementary information [18].

Even though pathway analysis of differentially expressed proteins in macrophages on fibrous versus globular collagen did not highlight any specific metabolic pathways, four of those proteins are part of the mitochondrial respiratory chain. These were cytochrome b-c1, part of the ubiquinol-cytochrome c complex, elongation factor-like GTPase 1, NADH dehydrogenase (ubiquinone), and V-type proton ATPase. The mitochondrial respiratory chain is one of the main energy sources used by the cells and is composed of five different multi-subunit respiratory complexes. Increased oxidative phosphorylation and fatty acid oxidation are usually associated with an alternatively activated, anti-inflammatory phenotype [19]. This is in line with our previous finding demonstrating that Ym1 is increased in macrophages cultured on fibrous collagen [11] and would further explain why we do not see any differences in the glycolytic function.

The most affected protein by collagen and its morphology was the anti-angiogenic glycoprotein pigment epithelium-derived factor (PEDF), encoded by the Serpinf1 gene. PEDF can be secreted by macrophages and is known to bind to collagen type I in a microstructure-dependent manner. Therefore, it is suggested to be involved in collagen fibril assembly [20]. Furthermore, treatment of macrophages with PEDF has been shown to increase macrophage migration [21], which could explain the

higher levels of transmigration in macrophages cultured on fibrous collagen that we found before [11], as they also express higher levels of PEDF. Interestingly, in lung tissue of patients with IPF, more PEDF expression was found than in lung tissue of controls [22]. PEDF is suggested to have a protective effect in the pathogenesis of fibrosis [23] and therefore the higher levels found in fibrosis suggest a compensatory mechanism trying to control fibrosis development. Indeed, two studies have shown that increased expression of PEDF in macrophages attenuated collagen synthesis by fibroblasts in a macrophage-mediated manner [24,25]. This ties in with recent findings of downregulation of PEDF in acute exacerbations of IPF compared to stable disease as these exacerbations predispose to rapid progression of fibrosis [26].

In addition to PEDF, the proteins dynactin subunit 4, RNA-binding protein 42, 28S ribosomal protein S15, and copper-transporting ATPase 1 were also expressed significantly more by macrophages on fibrous collagen than on globular collagen. No relevant data were found connecting dynactin subunit 4, RNA-binding protein 42, or 28S ribosomal protein S15 with macrophage function or lung fibrosis. However, the copper-transporting ATPase 1 (ATP7A) protein is of particular interest, since it has been suggested to play an important role in macrophage wound healing responses. In fact, ATP7A-downregulation inhibited macrophage infiltration in a mouse model for dermal wounding [27]. The higher levels of ATP7A may therefore also be linked to our previous results showing more migration in macrophages cultured on fibrous collagen [11]. Furthermore, ATP7A was shown to be required for copper delivery to members of the lysyl oxidase (LOX) family [28]. These copper-dependent enzymes play an important role in collagen cross-linking and higher activity of these enzymes has been described in patients with IPF [3,29,30]. Higher expression of ATP7A may therefore contribute to remodeling of non-organized fibrous collagen by activating members of the LOX family.

Only four proteins were expressed more than two-fold higher by macrophages cultured on globular collagen than on fibrous collagen. Thioredoxin reductase-1 (Txnrd1) is an important component of the thioredoxin system, in which it reduces and thereby activates thioredoxin by transferring electrons from NADPH. This thioredoxin system has both anti-oxidative as well as anti-inflammatory properties and has been associated with antifibrotic effects in bleomycin-induced pulmonary fibrosis [31,32]. Cotreatment of macrophages with IL4 and recombinant thioredoxin promoted the development of an anti-inflammatory phenotype characterized by higher expression of CD206 [33]. It is therefore conceivable that the higher levels of CD206 we previously found in macrophages cultured on globular collagen [11] are related to the higher levels of Txnrd1. In addition to Txnrd1, three other proteins

were expressed significantly more by macrophages on globular collagen than by macrophages on fibrous collagen. However, the role of these proteins remains to be elucidated as their direct function in macrophages is not yet clear. Of those three, only translocation-associated membrane protein-1 (Tram1) was found to have some connection with fibrosis. This protein was shown to be involved in translocation of proteins through the endoplasmic reticulum and in a study comparing patients with IPF and healthy controls, higher levels of TRAM1 mRNA were found in IPF [34]. The authors hypothesized that TRAM1 is upregulated because IPF is characterized by endoplasmic reticulum stress [34].

Our study had some limitations. The number of proteins that was reproducibly quantified in all conditions was rather limited and only covered 17% (2.870 proteins) of the theoretical mouse proteome database (17.023 proteins). Consequently, GO enrichment analysis did not yield many hits. The absence of a cell cycle synchronization step may have contributed to this issue, but serum starvation is known to interfere with macrophage function and activation [35,36] and was therefore intentionally omitted. As explained before, we tried to limit the variability of macrophage responses to collagen types by using fetal liver-derived macrophages. However, this does make translation to primary alveolar macrophages still an open question. Furthermore, the current study does not provide insight into how monocyte-derived macrophages would respond in comparison to fetal liver-derived alveolar macrophages, which is a critical area of investigation. It is well-documented that in cases of lung injury, monocyte-derived macrophages can replace fetal liver-derived alveolar macrophages in the lungs and that these two types of macrophages differ in their transcriptional and functional profiles [37,38].

In conclusion, this study shows that the presence as well as the morphology of collagen type I have pronounced effects on the proteomic signature of alveolar macrophages. Collagen type I induced expression of proteins associated with macrophage metabolism, specifically glycolysis, while also collagen morphology had specific effects on the macrophage proteome. Although the studied collagen morphologies are not directly translatable to a healthy or fibrotic tissue *in vivo*, it does indicate that changes in collagen morphology can have a major impact on macrophage behavior. Several protein candidates have previously been described to play a role in processes related to fibrosis. Further verification and exploration of collagen type I-induced metabolic changes and morphology-dependent effects on the macrophage proteome will provide better insight into the mechanisms behind macrophage-matrix interactions and possibly yield new targets for the treatment of fibrosis.

AUTHOR CONTRIBUTIONS

GFV, MK, and BNM conceived and designed the study. GFV, SR and AAAO performed the experiments. PvR advised on collagen topography assessments. MK and AB did the proteome analysis. RB and NG advised on proteome analysis. GFV, SR, BNM, MK, AB, AAAO, and AMD analyzed data and all authors interpreted data. GFV and SR wrote the initial draft of the manuscript. All authors critically reviewed the manuscript and approved the final manuscript.

ACKNOWLEDGMENTS

Dr. G. Fejer (Plymouth University) is kindly acknowledged for supplying MPI macrophages.

FUNDING SOURCES

GFV was funded by the Graduate School of Medical Sciences of the University Medical Center Groningen. RB and SR received funding from the European Union's Horizon 2020 research and innovation program under the Marie Skłodowska-Curie grant agreement No 754425 called Prominent. In addition, ERS/EU RESPIRE 3 also funded parts of the study related to the work of MK.

ADDITIONAL INFORMATION

PvR is co-founder, scientific advisor, and shareholder of BiomACS BV, a biomedical-oriented screening company. BNM has received research funding from Boehringer Ingelheim outside the scope of this study. All other authors have no conflicts of interest to declare.

DATA AVAILABILITY STATEMENT

The raw data supporting the conclusion of this article will be made available by the authors upon reasonable request, without undue reservation.

REFERENCES

1. Knuppel, L. *et al.* A Novel Antifibrotic Mechanism of Nintedanib and Pirfenidone. Inhibition of Collagen Fibril Assembly. *Am J Respir Cell Mol Biol* **57**, 77-90, doi:10.1165/rcmb.2016-0217OC (2017).
2. Kristensen, J. H. *et al.* The role of extracellular matrix quality in pulmonary fibrosis. *Respiration* **88**, 487-499, doi:10.1159/000368163 (2014).
3. Tjin, G. *et al.* Lysyl oxidases regulate fibrillar collagen remodelling in idiopathic pulmonary fibrosis. *Dis Model Mech* **10**, 1301-1312, doi:10.1242/dmm.030114 (2017).
4. Wells, R. G. Tissue mechanics and fibrosis. *Biochim Biophys Acta* **1832**, 884-890, doi:10.1016/j.bbadis.2013.02.007 (2013).
5. Booth, A. J. *et al.* Acellular Normal and Fibrotic Human Lung Matrices as a Culture System for In Vitro Investigation. *American Journal of Respiratory and Critical Care Medicine* **186**, 866-876, doi:10.1164/rccm.201204-0754OC (2012).
6. Upagupta, C., Shimbori, C., Alsilmi, R. & Kolb, M. Matrix abnormalities in pulmonary fibrosis. *Eur Respir Rev* **27**, doi:10.1183/16000617.0033-2018 (2018).
7. Manou, D. *et al.* The Complex Interplay Between Extracellular Matrix and Cells in Tissues. *Methods Mol Biol* **1952**, 1-20, doi:10.1007/978-1-4939-9133-4_1 (2019).
8. Wynn, T. A. & Vannella, K. M. Macrophages in Tissue Repair, Regeneration, and Fibrosis. *Immunity* **44**, 450-462, doi:10.1016/j.immuni.2016.02.015 (2016).
9. Zhang, L. *et al.* Macrophages: friend or foe in idiopathic pulmonary fibrosis? *Respir Res* **19**, 170, doi:10.1186/s12931-018-0864-2 (2018).
10. Vasse, G. F. *et al.* Macrophage-stroma interactions in fibrosis: biochemical, biophysical, and cellular perspectives. *J Pathol* **254**, 344-357, doi:10.1002/path.5632 (2021).
11. Vasse, G. F. *et al.* Collagen morphology influences macrophage shape and marker expression in vitro. *Journal of Immunology and Regenerative Medicine* **1**, 13-20, doi:https://doi.org/10.1016/j.regen.2018.01.002 (2018).
12. Fejer, G. *et al.* Nontransformed, GM-CSF-dependent macrophage lines are a unique model to study tissue macrophage functions. *Proc Natl Acad Sci U S A* **110**, E2191-2198, doi:10.1073/pnas.1302877110 (2013).
13. O'Neill, L. A., Kishton, R. J. & Rathmell, J. A guide to immunometabolism for immunologists. *Nat Rev Immunol* **16**, 553-565, doi:10.1038/nri.2016.70 (2016).
14. Woods, P. S. *et al.* Tissue-Resident Alveolar Macrophages Do Not Rely on Glycolysis for LPS-induced Inflammation. *Am J Respir Cell Mol Biol* **62**, 243-255, doi:10.1165/rcmb.2019-0244OC (2020).
15. Xie, N. *et al.* Metabolic characterization and RNA profiling reveal glycolytic dependence of profibrotic phenotype of alveolar macrophages in lung fibrosis. *Am J Physiol Lung Cell Mol Physiol* **313**, L834-L844, doi:10.1152/ajplung.00235.2017 (2017).
16. Drummond, D. A. & Wilke, C. O. The evolutionary consequences of erroneous protein synthesis. *Nat Rev Genet* **10**, 715-724, doi:10.1038/nrg2662 (2009).
17. Kemp, R. G. & Gunasekera, D. Evolution of the allosteric ligand sites of mammalian phosphofructo-1-kinase. *Biochemistry* **41**, 9426-9430, doi:10.1021/bi020110d (2002).

18. Russo, S., Kwiatkowski, M., Govorukhina, N., Bischoff, R. & Melgert, B. N. Meta-Inflammation and Metabolic Reprogramming of Macrophages in Diabetes and Obesity: The Importance of Metabolites. *Front Immunol* **12**, 746151, doi:10.3389/fimmu.2021.746151 (2021).

19. Batista-Gonzalez, A., Vidal, R., Criollo, A. & Carreno, L. J. New Insights on the Role of Lipid Metabolism in the Metabolic Reprogramming of Macrophages. *Front Immunol* **10**, 2993, doi:10.3389/fimmu.2019.02993 (2019).

20. Cauble, M. *et al.* Microstructure dependent binding of pigment epithelium derived factor (PEDF) to type I collagen fibrils. *J Struct Biol* **199**, 132-139, doi:10.1016/j.jsb.2017.06.001 (2017).

21. Martinez-Marin, D. *et al.* PEDF increases the tumoricidal activity of macrophages towards prostate cancer cells in vitro. *PLoS One* **12**, e0174968, doi:10.1371/journal.pone.0174968 (2017).

22. Cosgrove, G. P. *et al.* Pigment epithelium-derived factor in idiopathic pulmonary fibrosis: a role in aberrant angiogenesis. *Am J Respir Crit Care Med* **170**, 242-251, doi:10.1164/rccm.200308-1151OC (2004).

23. Qin, X. *et al.* PEDF is an antifibrosis factor that inhibits the activation of fibroblasts in a bleomycin-induced pulmonary fibrosis rat model. *Respir Res* **23**, 100, doi:10.1186/s12931-022-02027-4 (2022).

24. Moradi-Chaleshtori, M. *et al.* Overexpression of pigment epithelium-derived factor in breast cancer cell-derived exosomes induces M1 polarization in macrophages. *Immunol Lett* **248**, 31-36, doi:10.1016/j.imlet.2022.05.005 (2022).

25. Zhang, Y. *et al.* Secreted PEDF modulates fibroblast collagen synthesis through M1 macrophage polarization under expanded condition. *Biomed Pharmacother* **142**, 111951, doi:10.1016/j.biopha.2021.111951 (2021).

26. Carleo, A. *et al.* Proteomic characterization of idiopathic pulmonary fibrosis patients: stable versus acute exacerbation. *Monaldi Arch Chest Dis* **90**, doi:10.4081/monaldi.2020.1231 (2020).

27. Kim, H. W. *et al.* Human macrophage ATP7A is localized in the trans-Golgi apparatus, controls intracellular copper levels, and mediates macrophage responses to dermal wounds. *Inflammation* **35**, 167-175, doi:10.1007/s10753-011-9302-z (2012).

28. Shanbhag, V. *et al.* ATP7A delivers copper to the lysyl oxidase family of enzymes and promotes tumorigenesis and metastasis. *Proc Natl Acad Sci U S A* **116**, 6836-6841, doi:10.1073/pnas.1817473116 (2019).

29. Aumiller, V. *et al.* Comparative analysis of lysyl oxidase (like) family members in pulmonary fibrosis. *Sci Rep* **7**, 149, doi:10.1038/s41598-017-00270-0 (2017).

30. Chen, L., Li, S. & Li, W. LOX/LOXL in pulmonary fibrosis: potential therapeutic targets. *J Drug Target* **27**, 790-796, doi:10.1080/1061186X.2018.1550649 (2019).

31. Dong, X. *et al.* Inhibitory effects of thalidomide on bleomycin-induced pulmonary fibrosis in rats via regulation of thioredoxin reductase and inflammations. *Am J Transl Res* **9**, 4390-4401 (2017).

32. Hoshino, T. *et al.* Redox-active protein thioredoxin prevents proinflammatory cytokine- or bleomycin-induced lung injury. *Am J Respir Crit Care Med* **168**, 1075-1083, doi:10.1164/rccm.200209-982OC (2003).

33. El Hadri, K. *et al.* Thioredoxin-1 promotes anti-inflammatory macrophages of the M2 phenotype and antagonizes atherosclerosis. *Arteriosclerosis, Thrombosis, and Vascular Biology* **32**, 1445-1452, doi:10.1161/ATVBAHA.112.249334 (2012).

34. Clynick, B. *et al.* Circulating RNA differences between patients with stable and progressive idiopathic pulmonary fibrosis. *Eur Respir J* **56**, doi:10.1183/13993003.02058-2019 (2020).

35. Yang, J. X. *et al.* Synergistic effect of phosphodiesterase 4 inhibitor and serum on migration of endotoxin-stimulated macrophages. *Innate Immun* **24**, 501-512, doi:10.1177/1753425918809155 (2018).

36. Iida, K. T. *et al.* Insulin inhibits apoptosis of macrophage cell line, THP-1 cells, via phosphatidylinositol-3-kinase-dependent pathway. *Arterioscler Thromb Vasc Biol* **22**, 380-386, doi:10.1161/hq0302.105272 (2002).

37. Li, F. *et al.* Monocyte-derived alveolar macrophages autonomously determine severe outcome of respiratory viral infection. *Sci Immunol* **7**, eabj5761, doi:10.1126/sciimmunol.abj5761 (2022).

38. Misharin, A. V. *et al.* Monocyte-derived alveolar macrophages drive lung fibrosis and persist in the lung over the life span. *J Exp Med* **214**, 2387-2404, doi:10.1084/jem.20162152 (2017).

SUPPLEMENTARY MATERIAL

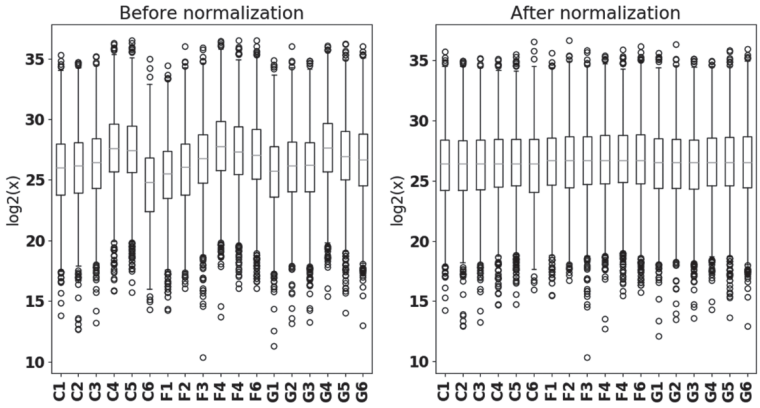

Supplementary Figure 1: Data normalization. Log2 distributions of the proteins for each sample before and after preprocessing. Uncoated (C), fibrous collagen type I (F) and globular collagen type I (G).

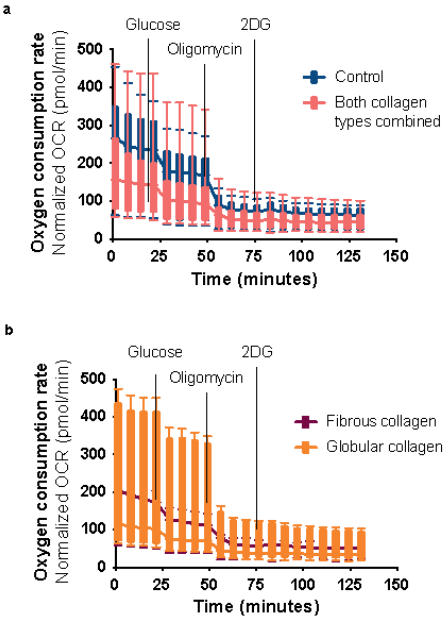

Supplementary Figure 2: Oxygen consumption rate of alveolar macrophages cultured in collagen-coated or uncoated wells. After 72 hours, oxygen consumption rate (OCR) was measured during glycolysis stress test using an XFe96 extracellular flux analyzer and rates were normalized to protein concentrations. Macrophages were treated sequentially with glucose, oligomycin (ATP synthase inhibitor), and 2-DG (2-deoxyglucose). **a.** Kinetic OCR response of macrophages seeded in wells that were either coated with fibrous or globular collagen (data combined) or left uncoated (control). Each data point represents mean ± SD of 6 different experiments. Each single experiment had 6 technical replicates that were averaged. **b.** Kinetic OCR response of macrophages seeded in wells that were either coated with fibrous or globular collagen. Each data point represents mean ± SD of 6 different experiments. Each single experiment had 6 technical replicates that were averaged. Data represented as a box and whiskers plot, where the box and whiskers extend from the 10th to 90th percentile.

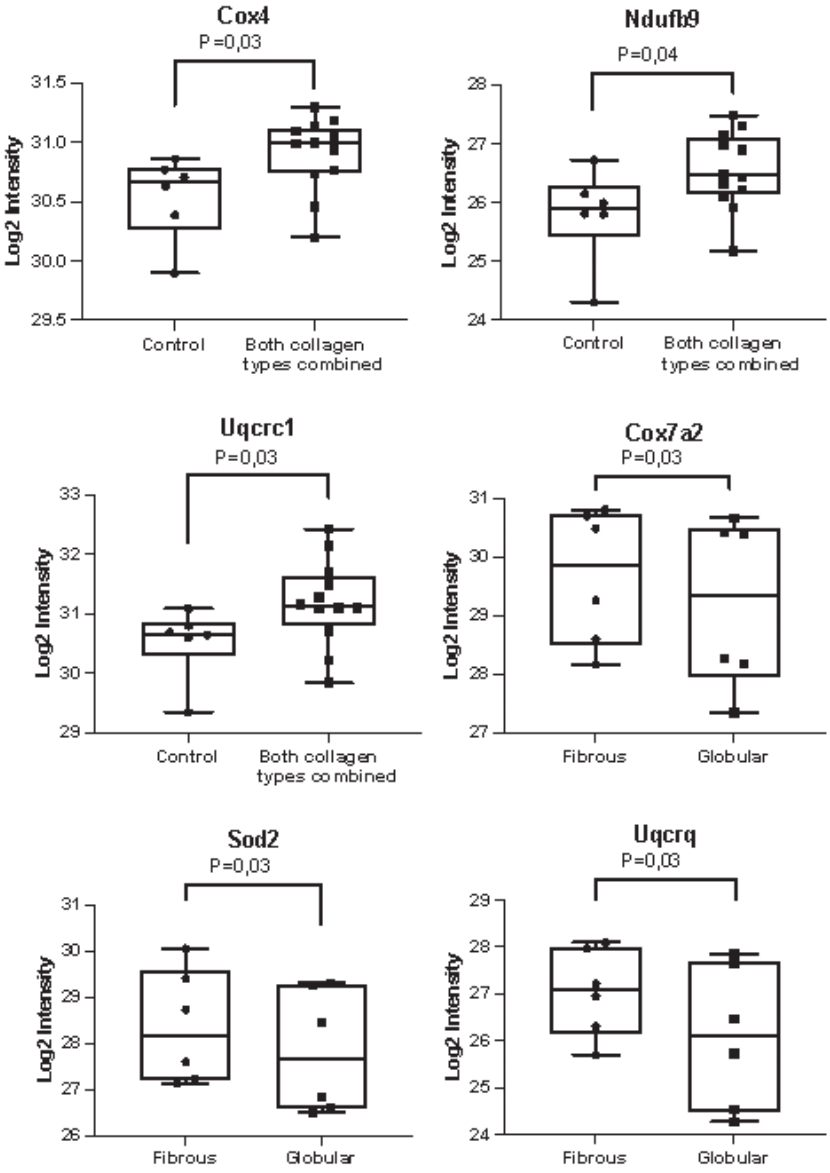

Supplementary Figure 3: Proteins of the electron transport chain that were significantly differentially expressed in macrophages grown on plastics versus either fibrous or globular collagen or significantly differentially expressed in macrophages grown on globular collagen versus either fibrous collagen. Expressed as normalized Log2 values and statistically tested with a Mann Whitney U test (control versus both collagen types combined) or a paired Wilcoxon test (fibrous versus globular collagen) and $p<0.05$ was considered significant (n=6). Data represented as a box and whiskers plot, where the box extends from the 25th to 75th percentiles and whiskers from min to max values. Cox4:Cytochrome c oxidase subunit 4; Ndufb9; NADH: Ubiquinone Oxidoreductase Subunit B9; Uqcrc1: Ubiquinol-Cytochrome C Reductase Core Protein 1; Cox7a1: Cytochrome C Oxidase Subunit 7A2; Sod2: Superoxide Dismutase 2; Uqcrq: Ubiquinol-Cytochrome C Reductase Complex III Subunit VII.

Supplementary Table 1. **Morphology-independent effects of collagen type I on macrophage protein expression.** 77 proteins were differentially expressed by macrophages cultured on collagen type I-coated plastic compared to the uncoated control. Statistically tested with an unpaired Wilcoxon test. p<0.025 was considered significant.

Gene name	Protein name	Fold change	p-value
Serpinf1	Pigment epithelium-derived factor	35.82	4.74E-03
Fam118b	Protein FAM118B	13.21	2.45E-02
Gbp4	Guanylate-binding protein 4	10.34	6.90E-03
Ndrg1	Protein NDRG1	6.22	4.74E-03
Syap1	Synapse-associated protein 1	6.02	2.45E-02
Nudt9	ADP-ribose pyrophosphatase, mitochondrial	5.95	1.35E-02
Golt1b	Vesicle transport protein GOT1B	5.27	2.05E-03
Sptlc1	Serine palmitoyltransferase 1	5.18	3.23E-03
Arfgap3	ADP-ribosylation factor GTPase-activating protein 3	5.02	6.90E-03
Thop1	Thimet oligopeptidase	4.93	9.70E-03
Slain2	SLAIN motif-containing protein 2	4.49	6.90E-03
Ethe1	Persulfide dioxygenase ETHE1, mitochondrial	4.14	1.35E-02
Mrps14	28S ribosomal protein S14, mitochondrial	3.95	1.82E-02
Trmt2a	tRNA (uracil-5-)-methyltransferase homolog A	3.37	3.23E-03
Eml2	Echinoderm microtubule-associated protein-like 2	3.19	6.90E-03
Alox5	Polyunsaturated fatty acid 5-lipoxygenase	3.19	4.74E-03
Ftl1	Ferritin light chain 1	3.11	1.82E-02
Ctnnd1	Catenin delta-1	2.52	1.82E-02
Nelfa	Negative elongation factor A	2.45	9.70E-03
Pfkl	ATP-dependent 6-phosphofructokinase, liver type	2.38	9.70E-03
Esyt2	Extended synaptotagmin-2	2.35	6.90E-03
Grhpr	Glyoxylate reductase/hydroxypyruvate reductase	2.34	3.23E-03
Acad8	Isobutyryl-CoA dehydrogenase, mitochondrial	2.26	2.45E-02
Tm9sf3	Transmembrane 9 superfamily member 3	2.18	2.45E-02
Fam162a	Protein FAM162A	2.12	1.82E-02
Agpat4	1-acyl-sn-glycerol-3-phosphate acyltransferase delta	2.11	2.45E-02
Armc10	Armadillo repeat-containing protein 10	2.10	6.90E-03
F13a1	Coagulation factor XIII A chain	2.06	1.82E-02
Ero1a	ERO1-like protein alpha	2.04	9.70E-03
Lrp1	Prolow-density lipoprotein receptor-related protein 1	2.01	4.31E-04
Nnt	NAD(P) transhydrogenase, mitochondrial	1.90	1.82E-02
Pcbd2	Pterin-4-alpha-carbinolamine dehydratase 2	1.90	9.70E-03
Spcs2	Signal peptidase complex subunit 2	1.89	6.90E-03
Dhrs7	Dehydrogenase/reductase SDR family member 7	1.86	1.82E-02
Afg3l2	AFG3-like protein 2	1.80	2.45E-02
Basp1	Brain acid soluble protein 1	1.77	1.82E-02
Acot9	Acyl-coenzyme A thioesterase 9, mitochondrial	1.76	1.35E-02
Tpm4	Tropomyosin alpha-4 chain	1.75	1.35E-02
Gsn	Gelsolin	1.67	2.45E-02
Pgm1	Phosphoglucomutase-1	1.67	2.45E-02
Bcl10	B-cell lymphoma/leukemia 10	1.65	2.45E-02
Actn4	Alpha-actinin-4	1.64	2.45E-02
Atp5f1e	ATP synthase subunit epsilon, mitochondrial	1.61	9.70E-03

Gene name	Protein name	Fold change	p-value
Plaa	Phospholipase A-2-activating protein	1.60	1.82E-02
Igf2bp2	Insulin-like growth factor 2 mRNA-binding protein 2	1.54	9.70E-03
Tagln2	Transgelin-2	1.53	1.82E-02
Nomo1	Nodal modulator 1	1.53	2.45E-02
Impa2	Inositol monophosphatase 2	1.52	9.70E-03
Hmox2	Heme oxygenase 2	1.52	3.23E-03
Itga5	Integrin alpha-5	1.51	6.90E-03
Aldoc	Fructose-bisphosphate aldolase C	1.50	9.70E-03
Psmd1	26S proteasome non-ATPase regulatory subunit 1	1.49	1.35E-02
Anxa2	Annexin A2	1.48	2.15E-04
Pgk1	Phosphoglycerate kinase 1	1.46	1.35E-02
Erp44	Endoplasmic reticulum resident protein 44	1.44	1.35E-02
Acly	ATP-citrate synthase	1.44	9.70E-03
Map4	Microtubule-associated protein 4	1.40	9.70E-03
Sumf1	Formylglycine-generating enzyme	1.38	2.45E-02
Naa25	N-alpha-acetyltransferase 25, NatB auxiliary subunit	1.37	3.23E-03
Shmt2	Serine hydroxymethyltransferase, mitochondrial	1.36	9.70E-03
Pgd	6-phosphogluconate dehydrogenase, decarboxylating	1.32	2.45E-02
Pin1	Peptidyl-prolyl cis-trans isomerase NIMA-interacting 1	1.31	1.82E-02
Ppp2r1a	Serine/threonine-protein phosphatase 2A 65 kDa regulatory subunit A alpha isoform	1.31	1.82E-02
Vat1	Synaptic vesicle membrane protein VAT-1 homolog	1.30	1.35E-02
Pak2	Serine/threonine-protein kinase PAK 2	1.29	1.82E-02
Itgal	Integrin alpha-L	1.28	6.90E-03
Cyb5r3	NADH-cytochrome b5 reductase 3	1.28	1.82E-02
Lmna	Prelamin-A/C	1.27	1.35E-02
Stx7	Syntaxin-7	1.25	1.82E-02
Hars1	Histidine--tRNA ligase, cytoplasmic	1.22	9.70E-03
Gtf2f1	General transcription factor IIF subunit 1	1.21	1.35E-02
Cndp2	Cytosolic non-specific dipeptidase	1.18	1.35E-02
Rpn1	Dolichyl-diphosphooligosaccharide--protein glycosyltransferase subunit 1	1.12	2.45E-02
Capzb	F-actin-capping protein subunit beta	1.08	1.82E-02
Casp9	Caspase-9	0.46	1.35E-02
Racgap1	Rac GTPase-activating protein 1	0.38	1.29E-03
Nabp2	SOSS complex subunit B1	0.30	1.82E-02

Supplementary table 2. **Collagen morphology-specific upregulation of protein expression.** 142 proteins were differentially expressed by macrophages cultured on fibrous collagen type I-coated tissue culture plastic compared to macrophages in globular collagen-coated conditions. Statistically tested with a paired Wilcoxon test. p<0.05 was considered significant**.**

Gene name	Protein name	Fold change F/G	p-value
Serpinf1	Pigment epithelium-derived factor	12.66	3.13E-02
Dctn4	Dynactin subunit 4	9.97	3.13E-02
Rbm42	RNA-binding protein 42	9.86	3.13E-02
Mrps15	28S ribosomal protein S15, mitochondrial	9.52	3.13E-02
Atp7a	Copper-transporting ATPase 1	6.11	3.13E-02
Ppic	Peptidyl-prolyl cis-trans isomerase C	4.97	3.13E-02
Prim2	DNA primase large subunit	3.83	3.13E-02
Trim23	E3 ubiquitin-protein ligase TRIM23	3.64	3.13E-02
Mmp8	Neutrophil collagenase	3.63	3.13E-02
Uba5	Ubiquitin-like modifier-activating enzyme 5	3.40	3.13E-02
Plekha2	Pleckstrin homology domain-containing family A member 2	3.12	3.13E-02
Tmsb4x	Thymosin beta-4	3.09	3.13E-02
Unc45a	Protein unc-45 homolog A	2.61	3.13E-02
Ercc4	DNA repair endonuclease XPF	2.51	3.13E-02
Retreg3	Reticulophagy regulator 3	2.41	3.13E-02
Cybc1	Cytochrome b-245 chaperone 1	2.25	3.13E-02
Yipf4	Protein YIPF4	2.24	3.13E-02
Gdi1	Rab GDP dissociation inhibitor alpha	2.12	3.13E-02
Rdh11	Retinol dehydrogenase 11	2.11	3.13E-02
Rab11b	Ras-related protein Rab-11B	2.10	3.13E-02
Rtn3	Reticulon-3	2.05	3.13E-02
Wtap	Pre-mRNA-splicing regulator WTAP	2.05	3.13E-02
Apoo	MICOS complex subunit Mic26	2.02	3.13E-02
Pgam5	Serine/threonine-protein phosphatase PGAM5, mitochondrial	2.00	3.13E-02
Gltp	Glycolipid transfer protein	1.97	3.13E-02
Pdhx	Pyruvate dehydrogenase protein X component, mitochondrial	1.92	3.13E-02
Fam177a1	Protein FAM177A1	1.91	3.13E-02
Crebbp	Histone lysine acetyltransferase CREBBP	1.90	3.13E-02
Abcf3	ATP-binding cassette sub-family F member 3	1.90	3.13E-02
Bod1l	Biorientation of chromosomes in cell division protein 1-like 1	1.85	3.13E-02
Efl1	Elongation factor-like GTPase 1	1.77	3.13E-02
Ftl1	Ferritin light chain 1	1.76	3.13E-02
C1qbp	Complement component 1 Q subcomponent-binding protein, mitochondrial	1.76	3.13E-02
Ero1a	ERO1-like protein alpha	1.75	3.13E-02
Tyms	Thymidylate synthase	1.75	3.13E-02
Iqgap2	Ras GTPase-activating-like protein IQGAP2	1.74	3.13E-02
Sdf2l1	Stromal cell-derived factor 2-like protein 1	1.74	3.13E-02
Sel1l	Protein sel-1 homolog 1	1.74	3.13E-02
Sar1b	GTP-binding protein SAR1b	1.72	3.13E-02

Gene name	Protein name	Fold change F/G	p-value
Rhoc	Rho-related GTP-binding protein RhoC	1.71	3.13E-02
Hgh1	Protein HGH1 homolog	1.70	3.13E-02
Itgam	Integrin alpha-M	1.70	3.13E-02
Rps27	40S ribosomal protein S27	1.69	3.13E-02
Aimp1	Aminoacyl tRNA synthase complex-interacting multifunctional protein 1	1.68	3.13E-02
Phf8	Histone lysine demethylase PHF8	1.66	3.13E-02
Acot9	Acyl-coenzyme A thioesterase 9, mitochondrial	1.61	3.13E-02
Ddx6	Probable ATP-dependent RNA helicase DDX6	1.61	3.13E-02
Impa2	Inositol monophosphatase 2	1.60	3.13E-02
Uqcrq	Cytochrome b-c1 complex subunit 8	1.59	3.13E-02
Nup50	Nuclear pore complex protein Nup50	1.57	3.13E-02
Chil3	Chitinase-like protein 3	1.57	3.13E-02
Aup1	Lipid droplet-regulating VLDL assembly factor AUP1	1.56	3.13E-02
Ctsb	Cathepsin B	1.55	3.13E-02
F13a1	Coagulation factor XIII A chain	1.55	3.13E-02
Pcbd2	Pterin-4-alpha-carbinolamine dehydratase 2	1.54	3.13E-02
Ufsp2	Ufm1-specific protease 2	1.53	3.13E-02
Actr1a	Alpha-centractin	1.52	3.13E-02
Ndufv1	NADH dehydrogenase [ubiquinone] flavoprotein 1, mitochondrial	1.51	3.13E-02
Niban2	Protein Niban 2	1.50	3.13E-02
Tpr	Nucleoprotein TPR	1.50	3.13E-02
Ptgs1	Prostaglandin G/H synthase 1	1.50	3.13E-02
Sh3pxd2b	SH3 and PX domain-containing protein 2B	1.48	3.13E-02
Xpnpep1	Xaa-Pro aminopeptidase 1	1.47	3.13E-02
Dnajc2	DnaJ homolog subfamily C member 2	1.45	3.13E-02
Canx	Calnexin	1.44	3.13E-02
Sod2	Superoxide dismutase [Mn], mitochondrial	1.43	3.13E-02
Nudt9	ADP-ribose pyrophosphatase, mitochondrial	1.43	3.13E-02
Srp9	Signal recognition particle 9 kDa protein	1.43	3.13E-02
Cand1	Cullin-associated NEDD8-dissociated protein 1	1.42	3.13E-02
Rab5c	Ras-related protein Rab-5C	1.41	3.13E-02
Elp3	Elongator complex protein 3	1.41	3.13E-02
Anxa6	Annexin A6	1.40	3.13E-02
Npepps	Puromycin-sensitive aminopeptidase	1.40	3.13E-02
Spcs1	Signal peptidase complex subunit 1	1.40	3.13E-02
Lsm7	U6 snRNA-associated Sm-like protein LSm7	1.39	3.13E-02
Ak2	Adenylate kinase 2, mitochondrial	1.38	3.13E-02
Eif3h	Eukaryotic translation initiation factor 3 subunit H	1.38	3.13E-02
Trpv2	Transient receptor potential cation channel subfamily V member 2	1.37	3.13E-02
Hk2	Hexokinase-2	1.37	3.13E-02
Gsn	Gelsolin	1.37	3.13E-02
Tpt1	Translationally-controlled tumor protein	1.35	3.13E-02
Mthfd1	C-1-tetrahydrofolate synthase, cytoplasmic	1.35	3.13E-02

Gene name	Protein name	Fold change F/G	p-value
Itgb5	Integrin beta-5	1.35	3.13E-02
Clta	Clathrin light chain A	1.35	3.13E-02
Tm9sf3	Transmembrane 9 superfamily member 3	1.35	3.13E-02
Fkbp1a	Peptidyl-prolyl cis-trans isomerase FKBP1A	1.35	3.13E-02
Psmd1	26S proteasome non-ATPase regulatory subunit 1	1.33	3.13E-02
Rrp1b	Ribosomal RNA processing protein 1 homolog B	1.33	3.13E-02
Atp2a2	Sarcoplasmic/endoplasmic reticulum calcium ATPase 2	1.32	3.13E-02
Yars1	Tyrosine--tRNA ligase, cytoplasmic	1.31	3.13E-02
Myof	Myoferlin	1.31	3.13E-02
Srsf9	Serine/arginine-rich splicing factor 9	1.31	3.13E-02
Anxa2	Annexin A2	1.30	3.13E-02
Arhgef18	Rho guanine nucleotide exchange factor 18	1.30	3.13E-02
Arpc2	Actin-related protein 2/3 complex subunit 2	1.29	3.13E-02
Arl3	ADP-ribosylation factor-like protein 3	1.29	3.13E-02
Dnajb1	DnaJ homolog subfamily B member 1	1.28	3.13E-02
Ctnnd1	Catenin delta-1	1.28	3.13E-02
Atp6v0a1	V-type proton ATPase 116 kDa subunit a 1	1.28	3.13E-02
Rab14	Ras-related protein Rab-14	1.27	3.13E-02
Hprt1	Hypoxanthine-guanine phosphoribosyltransferase	1.27	3.13E-02
Prdx6	Peroxiredoxin-6	1.25	3.13E-02
Tmx1	Thioredoxin-related transmembrane protein 1	1.24	3.13E-02
Pstpip2	Proline-serine-threonine phosphatase-interacting protein 2	1.23	3.13E-02
Glod4	Glyoxalase domain-containing protein 4	1.23	3.13E-02
Rplp0	60S acidic ribosomal protein P0	1.23	3.13E-02
Ppp6c	Serine/threonine-protein phosphatase 6 catalytic subunit	1.22	3.13E-02
Ywhaq	14-3-3 protein theta	1.21	3.13E-02
Rps26	40S ribosomal protein S26	1.21	3.13E-02
Dync1i2	Cytoplasmic dynein 1 intermediate chain 2	1.21	3.13E-02
Ctps2	CTP synthase 2	1.21	3.13E-02
Casp6	Caspase-6	1.20	3.13E-02
Ik	Protein Red	1.19	3.13E-02
Tmco1	Calcium load-activated calcium channel	1.19	3.13E-02
Drap1	Dr1-associated corepressor	1.18	3.13E-02
Ptges3	Prostaglandin E synthase 3	1.18	3.13E-02
Myo1g	Unconventional myosin-Ig	1.17	3.13E-02
Arl6ip1	ADP-ribosylation factor-like protein 6-interacting protein 1	1.16	3.13E-02
Cox7a2	Cytochrome c oxidase subunit 7A2, mitochondrial	1.16	3.13E-02
Tmx3	Protein disulfide-isomerase TMX3	1.15	3.13E-02
Fabp4	Fatty acid-binding protein, adipocyte	1.15	3.13E-02
Noc2l	Nucleolar complex protein 2 homolog	1.13	3.13E-02
Psmd5	26S proteasome non-ATPase regulatory subunit 5	1.09	3.13E-02
Inpp5f	Phosphatidylinositide phosphatase SAC2	0.84	3.13E-02
Cul2	Cullin-2	0.84	3.13E-02
Rfc4	Replication factor C subunit 4	0.84	3.13E-02

Gene name	Protein name	Fold change F/G	p-value
Psme2	Proteasome activator complex subunit 2	0.84	3.13E-02
Pld4	5'-3' exonuclease PLD4	0.81	3.13E-02
Parp9	Protein mono-ADP-ribosyltransferase PARP9	0.80	3.13E-02
Rpl6	60S ribosomal protein L6	0.79	3.13E-02
Fkbp3	Peptidyl-prolyl cis-trans isomerase FKBP3	0.77	3.13E-02
Hspbp1	Hsp70-binding protein 1	0.76	3.13E-02
Thyn1	Thymocyte nuclear protein 1	0.76	3.13E-02
Trappc12	Trafficking protein particle complex subunit 12	0.57	3.13E-02
Fam3c	Protein FAM3C	0.55	3.13E-02
Uap1	UDP-N-acetylhexosamine pyrophosphorylase	0.51	3.13E-02
Plcb3	1-phosphatidylinositol 4,5-bisphosphate phosphodiesterase beta-3	0.50	3.13E-02
Enpp4	Bis(5'-adenosyl)-triphosphatase enpp4)	0.50	3.13E-02
Pdxk	Pyridoxal kinase	0.50	3.13E-02
Txnrd1	Thioredoxin reductase 1, cytoplasmic	0.44	3.13E-02
Ncbp1	Nuclear cap-binding protein subunit 1	0.41	3.13E-02
Tram1	Translocating chain-associated membrane protein 1	0.39	3.13E-02

5

CHAPTER 5

General Discussion

Metabolism is the process through which the body transforms food and drink into energy by means of chemical reactions. Entire organisms and all living cells require energy, even when in a resting state. Glycolysis was the first metabolic pathway to be described in the 1940s [1]. Newsholme first studied the influence of metabolic fluxes on metabolic pathways [2] and postulated that when product supply and product formation are maintained, a steady-state condition is established with metabolic intermediates being at a constant level. However, in an organism, its organs, and the cells that compose them, steady-state conditions are almost never reached and levels of metabolites change depending on numerous circumstances. In fact, changes in cellular metabolism can contribute to complex pathological events, such as metabolic syndrome, diabetes, and cancer. The same is true the other way around; disease states result in changes in metabolism [3].

MACROPHAGE METABOLISM IS TISSUE-NICHE SPECIFIC.

Macrophages are cells of the innate immune system that are present in all tissues and can rapidly answer to different stimuli. This requires them to adapt to different nutritional resources and change their energy source by going through a process defined as metabolic reprogramming. Macrophage metabolic reprogramming has mostly been associated with the classical and alternative activation states of macrophage polarization [4–7]. However, it is now believed that there is a continuous spectrum of macrophage phenotypes [8]. In this thesis, I show that the traditional view of macrophage metabolic reprogramming is too simplistic. A combination of environmental and pathogenic signals determines macrophage phenotype and metabolism, which in turn shapes the type and magnitude of the response. This aspect has been investigated in the current thesis (**Chapters 3 and 4**).

To gain an overview of the impact of a given tissue niche on macrophage metabolism, I used single cell RNA-seq data from the human protein atlas database (proteinatlas.org) and Ensembl version 103.38 to investigate differences in macrophage metabolic gene expression in different tissues [9]. I filtered for macrophages only and used the Read.count values (representing transcript abundances) multiplied for the nTPM (normalized Transcripts Per Million for each human cell type, used to estimate the gene expression level) and averaged the results if more entries were available for each tissue. After analyzing the data, I created a Gene-Z-Score and corresponding heatmap. The Z score helps determine if a gene's expression level is higher or lower than the mean across all tissues. Interestingly, major differences were found in the expression levels of genes coding for proteins that play important roles in energy metabolism belonging to the TCA cycle, the electron transport chain, and the glycolytic pathway in 20 different tissues (as shown in **Figure 1**). Through

clustering, I identified two groups: cluster 1, consisted of macrophages from the pancreas, lung, kidney, ovary, liver, and testis and derived from peripheral blood mononuclear cells (PBMC) as being more similar than macrophages from the other 13 tissues that were analyzed, belonging to cluster 2. The tissues belonging to cluster 1 are characterized by a high expression of genes involved in the electron transport chain, the TCA cycle, as well as in fatty acid oxidation. Even though we could group the tissues based on similarities, it is clear that the expression of metabolic genes greatly differs among different types of tissue-resident macrophages, even within one cluster. Therefore, their metabolic state appears to be very tissue-specific. Macrophages in cluster 1 all derive from fetal liver monocytes [10] except for PBMC. However, it is difficult to find commonalities for all the tissues belonging to this cluster. The liver and the pancreas have common endocrine and digestive functions. Both the liver and pancreas play a role in the regulation of blood sugar levels. In fact, the pancreas produces insulin and glucagon, which help to regulate blood sugar levels, while the liver stores glucose and converts it to glycogen, which can be released as needed to maintain blood sugar levels. The liver produces bile, which helps to break down fats in the small intestine, while the pancreas produces enzymes that help to break down carbohydrates, proteins, and fats. Other organs that are part of the cluster play a key role in detoxification, are the kidneys, as they help to remove waste products and excess fluid from the body. The lungs also have a detoxifying function as they help remove waste gases such as carbon dioxide from the body.

Moreover, tissues can communicate through circulating proteins, like cytokines and hormones, in order to maintain tissue and organ homeostasis. The levels of these signaling molecules change according to an individual's metabolic status which is altered under pathological conditions, altering therefore also the metabolic status of tissue-resident macrophages [11].

Even though I acknowledge that organs are much more than their tissue-resident macrophages, I hypothesized that macrophages from organs with similar functions might have commonalities in terms of their metabolism, as evidence pointed out that tissue-associated signature transcription factors also regulate metabolism [12,13]. However, although similarities can be found between some of these organs, there is something about the specific tissue niche that is important for macrophage metabolism that we still do not understand.

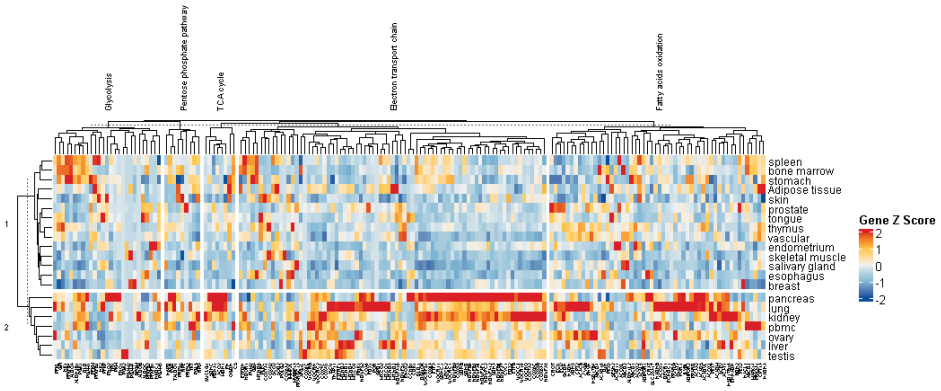

Figure 1: Heatmap of normalized expression of transcripts per million per macrophage of metabolic genes in different tissues. On the x-axis are reported the genes belonging to the different metabolic pathways, which are highlighted on the top part of the figure, on the y-axis the different organs that were investigated are reported. A list of the analyzed genes is available in Supplementary Table 1.

Altogether, our data highlight the necessity to investigate immunometabolism in a tissue-specific framework and emphasize that the mechanisms and consequences of innate memory are influenced by the local microenvironment and disease setting.

MACROPHAGES SHIFT THEIR METABOLISM DEPENDING ON STIMULI AND TISSUE ENVIRONMENT.

The work performed in this thesis has aided in gaining a better understanding of macrophage metabolism in different contexts.

The literature review in **Chapter 2** describes the classical view on macrophage metabolic reprogramming, based on the classification of M1 pro-inflammatory macrophages and M2 anti-inflammatory macrophages. M1 macrophages mainly rely on glycolysis as an energy source and a TCA cycle that is broken at two points, whereas M2 macrophages rely on fatty acid beta-oxidation and mitochondrial oxidative phosphorylation for energy. The overview in **Chapter 2** and the work reported in this thesis show that this is an oversimplification. For example, adipose tissue macrophages polarize to a metabolically activated phenotype in the context of Diabetes Mellitus type 2 without obvious proinflammatory stimuli (**Chapter 2**), while alveolar-like macrophages respond to proinflammatory stimuli without relying on glycolysis as an energy source but mainly using mitochondrial respiration (**Chapter 3**), changing their metabolic sources based on the tissue environment, namely different types of collagen (**Chapter 4**).

Adipose tissue macrophages, which are often described as metabolically activated macrophages, are characterized by lipid uptake leading to foam cell formation in the setting of metabolic dysfunction (**Chapter 2**). Elevated lipids and glucose concentrations in the adipose tissue lead to changes in metabolism due to an increased energy demand accompanied by increased glycolytic activity, increased lactate production, increased oxidative phosphorylation, and activation of lysosomal pathways to catabolize the free fatty acids when compared to adipose tissue macrophages in lean individuals. Some of these metabolic changes are comparable to those in macrophages when activated by inflammatory stimuli such as LPS, including the use of glycolysis as the primary energy source, but the majority of these metabolic changes are specific to metabolically activated macrophages.

In the lungs, there are three populations of macrophages: tissue-resident alveolar macrophages, monocyte-derived alveolar macrophages, and interstitial macrophages. Tissue-resident alveolar macrophages are the most abundant macrophages in the lungs residing in the airspaces of the lung alveoli. They play an essential role in defending the lung against foreign particles and pathogens and are involved in the regulation of lung inflammation. Monocyte-derived alveolar macrophages are derived from circulating monocytes and are recruited to the lungs in response to inflammation or injury. Interstitial macrophages are found in the lung connective tissue and are responsible for detecting and engulfing any foreign substances that enter the lung interstitium, and for interacting with the adaptive arm of the immune system [14].

In **Chapters 3 and 4** tissue-resident alveolar-like macrophages were used as a model to show how macrophages shift their metabolism in response to stimuli or to different tissue environments. These cells, defined also as Max Plank Institute (MPI) cells, are self-renewing and non-transformed cells originating from fetal liver monocytes of C57BL/6J mice. MPI cells were used as a model of alveolar macrophages, as they functionally and phenotypically closely resemble tissue-resident alveolar macrophages [15].

In **Chapter 3** we investigated how murine alveolar-like macrophages change their metabolism after lipopolysaccharide (LPS)-induced activation in the presence or absence of two different lysine deacetylase inhibitors. We first studied whether these cells undergo classic metabolic reprogramming when treated with LPS as an inflammatory stimulus. Surprisingly, we found that these alveolar-like macrophages did not activate the glycolytic pathway, but rather undergo changes at the level of the TCA cycle, since the metabolites malate, succinate, and α-ketoglutarate were higher compared to control. This finding is in line with a break in the TCA cycle at two points, namely after succinate and citrate/isocitrate leading to the accumulation

of these metabolites, as reported previously [4]. In our system, succinate and malate concentrations increased and this has been reported to happen in pro-inflammatory macrophages due to the inactivation of the enzyme succinate dehydrogenase (SDH). SDH is a component of the electron transport chain that normally converts succinate to fumarate. This reduction in SDH activity leads to the accumulation of succinate and malate, which are used in several ways to support immune responses [16]. Succinate is a key signaling molecule that activates the transcription factor HIF-1α, which in turn promotes the expression of pro-inflammatory genes encoding for interleukin-1β (IL-1β) and tumor necrosis factor-α (TNF-α) [17]. Increased levels of α-ketoglutarate in pro-inflammatory macrophages due to glutamine anaplerosis, when glutamine is converted via α-ketoglutarate into succinate through glutaminolysis or through an upregulated γ-aminobutyric acid (GABA) shunt. α-Ketoglutarate is a key metabolite that feeds into several biosynthetic pathways, including amino acids and nucleotides synthesis, as well as ATP production. In pro-inflammatory macrophages, the higher α-ketoglutarate levels may support the production of cytokines and other immune effector molecules [18]. However, for the other TCA breakpoint, we did not find any evidence in our system, as we did not observe an accumulation of citrate and/ or an increased glycolytic function, associated with the ``classically activated`` metabolic reprogramming [19]. This is in line with recently published data showing that tissue-resident alveolar macrophages do not rely on glycolysis to respond to LPS as a pro-inflammatory stimulus [20,21].

Since stimulation of alveolar-like macrophages with LPS resulted in higher production of the pro-inflammatory cytokine TNF-α, which was inhibited by cotreatment with two different lysine deacetylase inhibitors, we wanted to investigate the role of metabolic changes in the anti-inflammatory response of these cells. Treatment with the inhibitors also resulted in higher levels of the anti-inflammatory cytokine IL-10. This finding is in agreement with earlier results showing that these inhibitors have an anti-inflammatory effect in smoke-exposed mice and in LPS-exposed lung slices [22,23] (further discussed in paragraph “KDACi’s anti-inflammatory effect”).

The lysine deacetylase inhibitor (KDACi) RGFP966 had a significant effect on mitochondrial respiration by increasing the spare respiratory capacity as well as the level of maximal respiration compared to treatment with LPS alone. This deacetylase inhibitor, which had a stronger anti-inflammatory effect at the cytokine level among the KDACis used on LPS-treated macrophages, induced macrophage repolarization towards an anti-inflammatory phenotype. This phenomenon is thought to be accompanied by metabolic reprogramming, when macrophages rely more on oxidative phosphorylation, as demonstrated by the higher mitochondrial

respiration. This is consistent with the current literature on immunometabolism indicating that alveolar macrophages rely on oxidative phosphorylation for cytokine production [21,24] and more generally with what has been shown to occur in macrophages having an anti-inflammatory phenotype [25].

However, no changes were observed when the cells were pre-treated with MS275, which may be because this KDACi has a weaker anti-inflammatory effect. In fact, when cells were treated with this compound, only differences at the level of gene expression were observed. It is possible that differences were observed at the gene expression level but not in metabolism because the measurements were taken at a specific time point, and transcription and translation still had to occur before the effects of changes in gene expression are fully expressed in metabolism. In fact, after a gene is transcribed, the resulting mRNA molecule must be processed and transported to the cytoplasm, where it is translated into a protein. The rate of protein synthesis is influenced by several factors, including amino acids availability, translation efficiency, and mRNA molecule stability. Therefore, if differences in gene expression are observed but not in metabolism, it may be because the effects of changes in gene expression have not yet been fully translated into changes in the levels of metabolic enzymes or metabolites. In addition to the time required for transcription and translation, other regulatory mechanisms can influence the correlation between gene expression and metabolism. For example, post-transcriptional and post-translational modifications can affect the stability and activity of metabolic enzymes, even if their gene expression levels remain unchanged.

After investigating how alveolar-like macrophages shift their metabolism in response to different pro- and anti-inflammatory stimuli, we investigated how the metabolic pathways would change depending on the morphological and mechanical characteristics of the tissue.

In **Chapter 4** alveolar-like macrophages were seeded on plastic, plastic coated with fibrous collagen, or plastic coated with globular collagen. Fibrous collagen is obtained at a neutral pH, while an acidic pH results in globular collagen. From a previous study, it was already known that culturing macrophages on either type of collagen coating led to a higher expression of surface markers associated with M2-like polarization (CD206) compared to control macrophages seeded on an uncoated surface [26], and this expression was higher in macrophages seeded on globular collagen compared to fibrous. In macrophages seeded on fibrous collagen, instead, higher levels of the surface marker YM1, a marker of anti-inflammatory, pro-repair, macrophages, were demonstrated compared to macrophages seeded on globular collagen. Accompanying these differences in marker expression changes

in the shape, and transmigration of these cells were shown, but no mechanistic conclusions could be drawn on why these changes occurred and that is why I proceeded to further investigate this system by applying differential proteomics and metabolic analysis. The proteome data highlighted differences in the expression of proteins involved in the glycolytic pathway across all culture conditions. Following this finding, it was decided to investigate whether the glycolytic function was altered by measuring the enzymatic activity of the altered glycolytic enzymes and by performing extracellular flux analysis. Interestingly, no differences were observed in glycolytic function, but it was observed that there were opposite trends between protein expression and protein activity (when protein expression was higher, the activity was lower, and vice versa) which explains why no functional differences were observed.

Altogether, our results highlight not only the necessity to investigate immunometabolism in a tissue-specific framework but also that multiple experimental approaches are necessary to understand how macrophages respond under specific conditions.

CHARACTERIZATION OF TISSUE-RESIDENT MACROPHAGES

Macrophages are highly versatile immune cells that can exhibit diverse characteristics and functions depending on their microenvironment. It is important to characterize macrophages to understand how they respond under different circumstances, especially during inflammatory responses. As was exemplified in **Chapter 2** macrophage characterization involves various techniques, each providing different insights into their behavior. However, no single technique can provide a complete picture of macrophage responses, which is why I think that it is necessary to use a combination of techniques to gain a more complete understanding of their behavior.

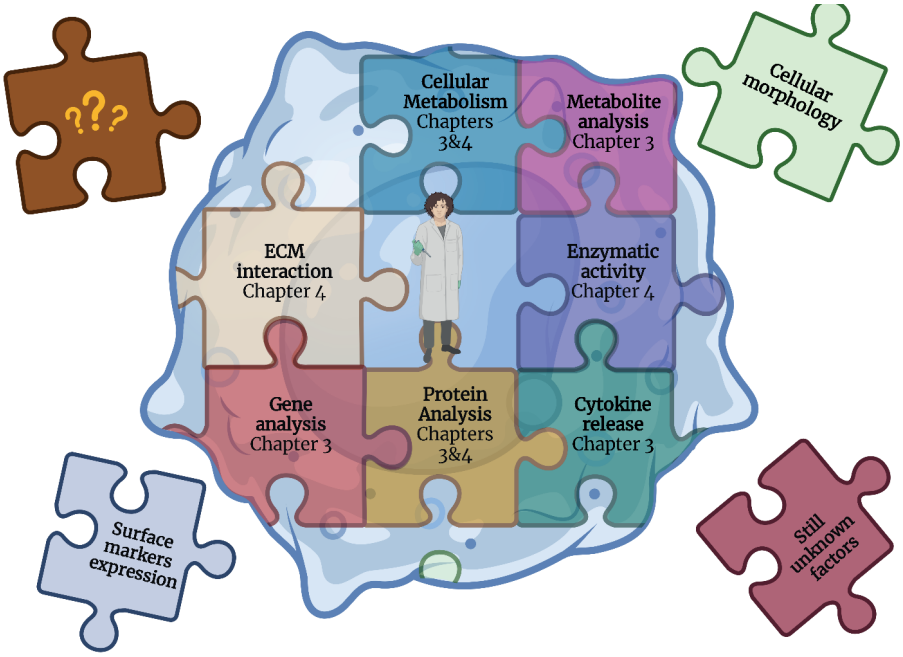

Figure 2: Graphical overview of macrophage characteristics investigated in the experimental chapters.

As illustrated in **Figure 2**, in this thesis, macrophages have been characterized by studying:

Cytokine Release: Macrophages release signaling molecules called cytokines in response to infections or inflammatory stimuli. Measuring the types and amounts of cytokines produced can provide information about the pro- or anti-inflammatory state of the macrophage. This helps to understand their functional role during an immune response. In **Chapter 3**, we investigated the cellular excretion of three important cytokines involved in alveolar macrophage function: IL-10, IL-6, and TNF-α. These cytokines play distinct roles in modulating macrophage activities, and their balance is crucial for determining the outcome of immune responses. IL-10 is primarily known as an anti-inflammatory cytokine; when released, it acts as a negative feedback mechanism to reduce excessive immune responses and inflammation. IL-10 suppresses the production of pro-inflammatory cytokines such as TNF-α, IL-1, and IL-6 [27]. This helps prevent an exaggerated immune response that can lead to tissue damage and chronic inflammation. IL-10 also promotes tissue repair and the resolution of inflammation [28]. On the other hand, TNF-α is a potent

pro-inflammatory cytokine that plays a central role in initiating and amplifying inflammatory responses by inducing the production of other pro-inflammatory mediators [28]. For instance, TNF-α activates endothelial cells and, through the production of chemokines by macrophages, other immune cells, such as neutrophils are recruited to the site of infection or inflammation. TNF-α can also enhance the phagocytic capacity of macrophages and their ability to eliminate intracellular pathogens [29]. IL-6 is a pleiotropic cytokine that has pro-inflammatory functions when it signals in trans via soluble IL-6 receptors binding to gp130 [30]. IL-6 can be induced by other cytokines, including TNF-α, and controls the development of chronic inflammatory diseases [31].

Protein Analysis: Techniques such as western blotting, immunoprecipitation, and mass spectrometry can be used to study changes in protein expression and post-translational modifications within macrophages. This helps to understand changes in signaling pathways and the production of specific proteins involved in the immune response. In **Chapters 3 and 4** I investigated the intracellular proteome of tissue-resident alveolar-like macrophages with the goal of gaining insights into the molecular mechanisms leading macrophages behavior and their roles in immune responses, in combination with KDACi treatment. I have made use of both targeted and untargeted approaches. Untargeted proteomics involves analyzing all detectable proteins in a sample. I started by employing this approach as it provides a more comprehensive view of the proteome and it provided a direction into which to further focus our research. In targeted proteomics, on the other hand, I selected specific proteins of interest for analysis. This approach is useful as I wanted to focus on a particular subset of proteins relevant to our study, the proteins involved in macrophage metabolism. Using a targeted approach also offers an increased detection sensitivity and improved protein quantification over an untargeted approach.

Gene analysis: Gene expression profiling, also known as transcriptomics, is a technique that simultaneously assesses the mRNA expression levels for thousands of genes. There are several approaches to studying mRNA: techniques such as microarrays that can offer a snapshot of the transcriptome compared to a control condition, and RNA sequencing (RNA-Seq) and reverse transcription-quantitative polymerase chain reaction (RT-qPCR) can quantify the expression levels of (particular) genes. The identification of genes whose expression is increased or downregulated during macrophage activation can provide insight into the pathways and processes involved in macrophage activation. In **Chapter 3**, in order to validate the effects of KDAC inhibition, we performed reverse transcription-quantitative

polymerase chain reaction (RT-qPCR) to investigate the expression of genes linked to a macrophage anti-inflammatory phenotype.

Cellular Metabolism: Investigating macrophage metabolism is crucial for understanding their functional state. Methods like Seahorse XF analysis or ^{13}C-glucose tracing can assess parameters like mitochondrial respiration, glycolysis, and fatty acid oxidation. These measurements help in deciphering the bioenergetic changes occurring in activated macrophages. In **Chapter 4** the extracellular flux analysis was used to investigate how the metabolism of alveolar-like macrophages changed when they were seeded on different surfaces and in **Chapter 3** to explore how it might change when treated with an inflammatory stimulus (LPS) combined with anti-inflammatory agents (KDACis). This technique allows to measure oxygen concentration (Oxygen Consumption Rate (OCR)) and pH (Extra Cellular Acidification Rate (ECAR)) in the media of live cells in real-time, therefore indirectly measuring energy metabolism.

Enzymatic Activity: Studying enzymatic activity can reveal how these enzymes are regulated during macrophage activation and their contribution to metabolic processes like glycolysis, oxidative burst, and lipid metabolism. In **Chapter 4** the activity of glycolytic enzymes was measured in alveolar-like macrophages that were either seeded on plastic or on collagen-coated plastic.

Metabolite Analysis: Metabolomics allows researchers to analyze the metabolic profile of macrophages. Changes in metabolites like glucose consumption, lactate production, or lipid metabolism can indicate how macrophages are responding to inflammation. Metabolite analysis provides insights into their energy requirements and metabolic adaptations during activation. In **Chapter 3** gas chromatography–mass spectrometry (GC-MS) and high-performance liquid chromatography (HPLC) with fluorescence detection were used to measure metabolites in the context of alveolar-like macrophages stimulated with LPS and treated with KDAC inhibitors. Major TCA cycle metabolites and the TCA cycle substrate amino acids were quantified.

Other techniques that we have not applied in our manuscripts but that are of relevance and described in **Chapter 2** include measuring surface markers or antigens that can be detected by techniques such as flow cytometry or immunohistochemistry, the visualization of cellular morphology using microscopy techniques, or methods using functional assays such as phagocytosis assays, oxidative burst assays, and chemotaxis assays.

Although each of these techniques provides valuable information about macrophages, none can provide a comprehensive view on their own. Indeed, macrophage responses are highly dynamic and multifaceted. Using a combination of techniques would allow researchers to gain a more complete and nuanced understanding macrophage behavior under different conditions. By integrating data from many different assays, researchers can get a more accurate picture of macrophage activation, enabling the development of targeted therapies for inflammatory diseases and infections.

KDACI'S ANTI-INFLAMMATORY EFFECT

In **Chapter 3** we have applied the above-mentioned approaches and knowledge to understand how lysine deacetylase inhibitors (KDACi) impact alveolar-like macrophages in the context of inflammation and metabolism.

Our study confirmed the anti-inflammatory effects of MS275 (KDAC1,2, and 3 inhibitor) and RGFP966 (KDAC3 inhibitor) in combination with LPS exposure, previously described by Leus *et al.* [22,23]. In fact, we observed decreased TNF-α excretion in cells stimulated with LPS and treated with the inhibitors, and RGFP966 in particular, compared to cells that were only LPS-stimulated. Similar findings were found for IL-6. We hypothesized that the inhibition of lysine deacetylation, a post-translational modification, could affect, among other things, the stability and activity of metabolic enzymes, therefore inducing changes in macrophage metabolism. Unexpectedly, we observed minimal changes in macrophage metabolism despite reduced inflammation upon KDACi treatment. This suggests that alveolar-like macrophages might not rely heavily on metabolic reprogramming in response to inflammation, contrary to other macrophage types.

Our proteomics analysis revealed that KDACi, especially KDAC3 inhibition, reduces inflammation by potentially enhancing protein ubiquitination. This modulation of ubiquitination could be a key driver of the anti-inflammatory effects of KDACi. Additionally, we noted that specific proteins, like INCA1 (Inhibitor Of CDK, Cyclin A1 Interacting Protein 1), JAM-A (junctional adhesion molecule A), and MMP12 (macrophage metalloelastase 12), were differentially expressed in response to KDACi treatment, suggesting their roles in macrophage behavior. Our study provides insights into the complex interplay between KDACi, inflammation, and metabolism in alveolar-like macrophages.

In summary, KDACi, particularly KDAC3 inhibition, dampens inflammation in alveolar-like macrophages, possibly through enhancing ubiquitination, without drastically altering their metabolism. This highlights the potential of targeting

protein ubiquitination for treating chronic inflammatory diseases like COPD, which are often unresponsive to traditional therapies.

CONCLUSION AND NEW PERSPECTIVES

Based on the results described in this thesis, I believe that studying macrophage metabolic plasticity from multiple different angles is a promising direction that should be implemented for developing more effective therapies for chronic diseases and inflammatory disorders like COPD. In particular, new developments such as single-cell metabolomics and transcriptomics can help study metabolic plasticity at the single-cell level. This approach can reveal heterogeneity within macrophage populations and provide insights into how different macrophage subsets contribute to disease progression. It may also help identify novel metabolic pathways that are dysregulated in specific disease contexts. In summary, I believe that future research should consist of integrated multi-omics approaches, in which metabolomics, proteomics, transcriptomics, and epigenomics data are combined to produce comprehensive molecular profiles of macrophages in different disease states. Integrating these data may help identify key regulators of macrophage plasticity and potential therapeutic targets. In the future, it may be of interest to develop and test drugs that target specific metabolic pathways in macrophages and investigate the therapeutic potential of modulating macrophage metabolism to reduce inflammation.

By pursuing these lines of research, the field can gain a deeper understanding of macrophage metabolic plasticity in the context of chronic diseases. This knowledge could pave the way for the development of more targeted and effective treatments, thereby improving the prognosis and quality of life for patients with these conditions.

REFERENCES

1 Meyerhof O, Junowicz-Kocholaty R. The equilibria of isomerase and aldolase, and the problem of the phosphorylation of glyceraldehyde phosphate. Journal of Biological Chemistry. 1943 Jul;149(1):71–92.

2 Crabtree B, Newsholme EA. Sensitivity of a Near-Equilibrium Reaction in a Metabolic Pathway to Changes in Substrate Concentration. Eur J Biochem. 1978 Aug;89(1):19–22.

3 Ain N, Gull H. Metabolic Changes and Their Characterization. 'Essentials of Cancer Genomic, Computational Approaches and Precision Medicine. Singapore: Springer Singapore; 2020; pp 35–70.

4 Palsson-McDermott EM, O'Neill LAJ. The Warburg effect then and now: From cancer to inflammatory diseases. BioEssays. 2013 Nov;35(11):965–73.

5 Ryan DG, O'neill LAJ. Krebs Cycle Reborn in Macrophage Immunometabolism. Annual Review of Immunology . 2020;38:289–313.

6 Williams NC, O'Neill LAJ. A role for the krebs cycle intermediate citrate in metabolic reprogramming in innate immunity and inflammation. Front Immunol. 2018 Feb;9(FEB):1.

7 O'Neill LAJ, Kishton RJ, Rathmell J. A guide to immunometabolism for immunologists. Nat Rev Immunol. 2016 Aug;16(9):553–65.

8 Murray PJ, Allen JE, Biswas SK, Fisher EA, Gilroy DW, Goerdt S, et al. Macrophage Activation and Polarization: Nomenclature and Experimental Guidelines. Immunity. 2014 Jul;41(1):14–20.

9 Karlsson M, Zhang C, Méar L, Zhong W, Digre A, Katona B, et al. A single–cell type transcriptomics map of human tissues. Sci Adv. 2021 Jul;7(31). DOI: 10.1126/sciadv.abh2169

10 Gautier EL, Yvan-Charvet L. Understanding macrophage diversity at the ontogenic and transcriptomic levels. Immunol Rev. 2014 Nov;262(1):85–95.

11 Wang F, So KF, Xiao J, Wang H. Organ-organ communication: The liver's perspective. Theranostics. 2021;11(7):3317.

12 T'Jonck W, Guilliams M, Bonnardel J. Niche signals and transcription factors involved in tissue-resident macrophage development. Cell Immunol. 2018 Aug;330:43–53.

13 Okabe Y, Medzhitov R. Tissue-Specific Signals Control Reversible Program of Localization and Functional Polarization of Macrophages. Cell. 2014 May;157(4):832–44.

14 Hou F, Xiao K, Tang L, Xie L. Diversity of Macrophages in Lung Homeostasis and Diseases. Front Immunol. 2021 Sep;12:3930.

15 Fejer G, Wegner MD, Gyory I, Cohen I, Engelhard P, Voronov E, et al. Nontransformed, GM-CSF-dependent macrophage lines are a unique model to study tissue macrophage functions. Proceedings of the National Academy of Sciences. 2013 Jun;110(24):E2191–8.

16 O'Neill LAJ, Pearce EJ. Immunometabolism governs dendritic cell and macrophage function. J Exp Med. 2016 Jan;213(1):15–23.

17 Tannahill GM, Curtis AM, Adamik J, Palsson-McDermott EM, McGettrick AF, Goel G, et al. Succinate is an inflammatory signal that induces IL-1β through HIF-1α. Nature. 2013 Apr;496(7444):238–42.

18 Liu S, Yang J, Wu Z. The Regulatory Role of α-Ketoglutarate Metabolism in Macrophages. Mediators Inflamm. 2021 Mar;2021:1–7.

19 O'Neill LAJ, Kishton RJ, Rathmell J. A guide to immunometabolism for immunologists. Nat Rev Immunol. 2016 Sep;16(9):553–65.

20 Lottes RG, Newton DA, Spyropoulos DD, Baatz JE. Alveolar type II cells maintain bioenergetic homeostasis in hypoxia through metabolic and molecular adaptation. Am J Physiol Lung Cell Mol Physiol. 2014 May;306(10):L947.

21 Khaing P, Summer R. Maxed out on glycolysis: Alveolar macrophages rely on oxidative phosphorylation for cytokine production. Am J Respir Cell Mol Biol. 2020;62(2):139–40.

22 Leus NGJ, Van Der Wouden PE, Van Den Bosch T, Hooghiemstra WTR, Ourailidou ME, Kistemaker LEM, et al. HDAC 3-selective inhibitor RGFP966 demonstrates anti-inflammatory properties in RAW 264.7 macrophages and mouse precision-cut lung slices by attenuating NF-κB p65 transcriptional activity. Biochem Pharmacol. 2016 May;108:58–74.

23 Leus NGJ, Van Den Bosch T, Van Der Wouden PE, Krist K, Ourailidou ME, Eleftheriadis N, et al. HDAC1-3 inhibitor MS-275 enhances IL10 expression in RAW264.7 macrophages and reduces cigarette smoke-induced airway inflammation in mice. Sci Rep. 2017 Mar;7(1):1–18.

24 Andrews JT, Voth DE, Huang SCC, Huang L. Breathe In, Breathe Out: Metabolic Regulation of Lung Macrophages in Host Defense Against Bacterial Infection. Front Cell Infect Microbiol. 2022 Jul;12. DOI: 10.3389/FCIMB.2022.934460

25 Viola A, Munari F, Sánchez-Rodríguez R, Scolaro T, Castegna A. The metabolic signature of macrophage responses. Front Immunol. 2019 Jul;10(JULY):1462.

26 Vasse GF, Kühn PT, Zhou Q, Bhusari SA, Reker-Smit C, Melgert BN, et al. Collagen morphology influences macrophage shape and marker expression in vitro. J Immunol Regen Med. 2018 Mar;1:13–20.

27 Ip WKE, Hoshi N, Shouval DS, Snapper S, Medzhitov R. Anti-inflammatory effect of IL-10 mediated by metabolic reprogramming of macrophages. Science (1979). 2017 May;356(6337):513–9.

28 Boorsma CE, Draijer C, Melgert BN. Macrophage Heterogeneity in Respiratory Diseases. Mediators Inflamm. 2013 Feb;2013:1–19.

29 Parameswaran N, Patial S. Tumor Necrosis Factor-α Signaling in Macrophages. Crit Rev Eukaryot Gene Expr. 2010;20(2):87–103.

30 Arango Duque G, Descoteaux A. Macrophage Cytokines: Involvement in Immunity and Infectious Diseases. Front Immunol. 2014 Oct;5. DOI: 10.3389/fimmu.2014.00491

31 Baran P, Hansen S, Waetzig GH, Akbarzadeh M, Lamertz L, Huber HJ, et al. The balance of interleukin (IL)-6, IL-6·soluble IL-6 receptor (sIL-6R), and IL-6·sIL-6R·sgp130 complexes allows simultaneous classic and trans-signaling. Journal of Biological Chemistry. 2018 May;293(18):6762–75.

SUPPLEMENTARY MATERIAL

Pathway	Genes
Glycolysis	ALDH3B1; ALDOA; ALDOB; ALDOC; BPGM; DLD; ENO1; ENO2; GPI; HK1; HK2; HKDC1; PFKFB1; PFKFB2; PFKFB3; PFKFB4; PFKL; PFKM; PFKP; PGAM1; PGAM2; PGAM4; PGAM5; PGK1; PGK2; PKM; TPI1
TCA cycle	MDH1; ACO2; CS; FH; OGDH; PDHA1; SDHC; SUCLG1
Electron transport chain	AFG1L; CCNB1; CDK1; COA6; COX4I1; COX4I2; COX5A; COX5B; COX6A1; COX6A2; COX6C; COX7A1; COX7A2; COX7C; COX8A; COX8C; CYC1; DGUOK; DLD; ENOX2; ETFRF1; ETFA; ETFB; ETFDH; FDX1; FDX2; GBA; GPD1; IMMP2L; ISCU; MTCH2; MT-CO1; MT-CO2; MT-CO3; MT-ND1; MT-ND2; MT-ND3; MT-ND4; MT-ND5; MT-ND6; MYBBP1A; NDUFAF1; NDUFS1; NDUFS2; NDUFA10; NDUFA12; NDUFA5; NDUFA7; NDUFA8; NDUFB3; NDUFB6; NDUFB8; NDUFB9; NDUFC2; NDOR1; PINK1; PLEC; POLG2; POR; PPARGC1A; PUM2; SCO2; SDHA; SDHB; SDHC; SDHD; SOD2; THAP11; UQCC3; UQCR10; UQCR11; UQCRB; UQCRC1; UQCRC2; UQCRFS1; UQCRH; UQCRQ
Fatty acids oxidation	ABCD1; ABCD2; ABCD3; ABCD4; ACAA2; ACACB; ACAD10; ACAD11; ACADM; ACADS; ACADVL; ACAT1; ACAT2; ACOX1; ACOX2; ACOX3; ACOXL; ACSL5; ADH5; ADIPOR1; ADIPOR2; ALDH1L2; AUH; BDH2; CPT1A; CPT2; CRAT; CROT; CYGB; DECR1; ECHDC1; ECI1; ECI2; EHHADH; GCDH; HACL1; HADH; HADHA; HADHB; HSD17B10; HSD17B4; ILVBL; MAPK14; PEX2; PEX5; PEX7; PHYH; POR; PPARD; PPARG; PRKAA1; SCP2; SESN2; SLC25A17
Pentose phosphate pathway	H6PD; PGD; PGLS; PRPS1; PRPS2; RPE; RPIA; TALDO1; TKT

Supplementary Table 1: List of genes and corresponding metabolic pathways analyzed to create Figure 1 obtained from the KEGG (Kyoto Encyclopedia of Genes and Genomes) database.

A

Appendix

English summary
Nederlandse Samenvatting
Italian summary (Riassunto in Italiano)
Acknowledgements
Curriculum Vitae

ENGLISH SUMMARY

Chronic obstructive pulmonary disease (COPD) and diabetes are widespread chronic diseases worldwide. COPD, characterized by persistent airflow limitation, significantly impacts lung function, causing respiratory symptoms and contributing to comorbidities like cardiovascular disease, affecting patients' quality of life. Diabetes, encompassing type 1 and type 2 variations, results in high blood sugar levels due to insulin imbalance, leading to various complications such as retinopathy and nephropathy.

Both COPD and diabetes are characterized by chronic inflammation, marked, among many features, by the presence of pro-inflammatory cytokines affecting all tissues. Macrophages, cells of the immune system, play a pivotal role in chronic inflammation and in the intricate relationship between immune and metabolic processes in tissue. Chronic inflammation influences changes in energy metabolism also through lysine acetylation in proteins, altering gene expression and impacting cellular energy processes like glycolysis and fatty acid oxidation. This connection highlights the interplay between immune responses and metabolic pathways in these chronic conditions, emphasizing the significance of understanding their complex interactions for developing targeted therapies.

This thesis aimed to deepen our understanding of macrophages within chronic inflammation, focusing on their diverse phenotypes and metabolic nuances across various tissue niches.

In **Chapter 2** the focus is on the involvement of macrophages in obesity and type 2 diabetes mellitus. It describes distinct phenotypes associated with these conditions and sheds light on variations in cellular metabolite levels, revealing how microenvironments influence macrophage behavior. This chapter also illustrated the most common ways to characterize macrophages, with particular attention paid to their metabolism.

Subsequently, the investigation delved into the effects of KDAC inhibitors (KDACis) on primary murine alveolar-like macrophages activated by lipopolysaccharide (LPS), described in **Chapter 3**. While minimal metabolic changes were observed between conditions, the study revealed that when macrophages were treated with KDACis, a reduction in inflammatory mediators and an enhancement in proteins related to ubiquitination was observed, potentially offering new therapeutic avenues for COPD.

In **Chapter 4** we explored how collagen morphology influences macrophage behavior and metabolism. We uncovered changes in glycolysis-related protein

expression but no significant alterations in enzyme activity in this metabolic pathway, again highlighting the intricate interplay between macrophages and their microenvironment, critical in tissue repair to fibrosis in the lungs.

Overall, this thesis summarized the core findings of the field, emphasizing the diverse metabolic adaptations of macrophages in conditions like obesity, type 2 diabetes mellitus, and lung disorders. It showcased the capacity of macrophages to adapt their metabolism based on distinct tissue environments, significantly influencing their behavior.

Furthermore, this thesis showcased the potential of KDACis in reducing inflammation, offering promising avenues for treating chronic inflammatory diseases like COPD. This thesis stressed the importance of employing various techniques to characterize macrophage behavior under diverse conditions comprehensively.

For future directions, this thesis suggests using single-cell metabolomics, proteomics and transcriptomics to unravel macrophage population heterogeneity and identify novel metabolic pathways crucial in disease states. It also advocates for an integrated multi-omics approach, combining various omics techniques for comprehensive macrophage profiling, potentially revealing crucial regulators and therapeutic targets.

In conclusion, this thesis established a foundational understanding of macrophage behavior within chronic diseases. It hinted at tailored treatments targeting macrophage metabolism to alleviate chronic inflammation, potentially improving patient prognosis significantly.

NEDERLANDSE SAMENVATTING

Chronische obstructieve longziekte (COPD) en diabetes zijn wijdverspreide chronische ziekten. COPD, gekenmerkt door een aanhoudende obstructie van de luchtwegen, heeft aanzienlijke invloed op de longfunctie, veroorzaakt ademhalingsproblemen en draagt bij aan comorbiditeiten zoals hart- en vaatziekten. Diabetes, zowel type 1 als type 2 varianten, leidt tot hoge bloedsuikerspiegels door een gebrekkige insulineproductie of een gebrekkige respons op insuline, met als gevolg verschillende complicaties zoals retinopathie en nefropathie.

Zowel COPD als diabetes worden gekenmerkt door chronische ontsteking. Zowel COPD als diabetes worden gekenmerkt door chronische ontsteking met aanwezigheid van pro-inflammatoire cytokines die alle weefsels aantasten. Macrofagen, cellen van het immuunsysteem, spelen een cruciale rol in zowel chronische ontstekingen als in de complexe relatie tussen immuun- en metabole processen in weefsels. Chronische ontstekingen kunnen veranderingen veroorzaken in zowel genexpressie als verscheidene metabole processen, zoals glycolyse en vetzuuroxidatie. De wisselwerking tussen immuunreacties en metabole processen, onder deze chronische ziekten, onderstreept het belang van het begrijpen van deze complexe interacties voor de ontwikkeling van gerichte therapieën.

Het doel van dit proefschrift was het uitdiepen van de kennis omtrent de rol van macrofagen binnen chronische ontsteking, met de nadruk op hun diverse fenotypen en metabole nuances in verschillende situaties.

In **Hoofdstuk 2** ligt de focus op de betrokkenheid van macrofagen bij obesitas en type 2 diabetes mellitus. Het beschrijft verscheidene macrofaag fenotypen geassocieerd met deze aandoeningen en werpt licht op variaties in niveaus van cellulaire metabolieten, waarbij wordt onthuld hoe macrofagen beïnvloedt worden voor de micro-omgeving. Dit hoofdstuk illustreert ook de meest voorkomende manieren om macrofagen te karakteriseren, met speciale aandacht voor hun metabolisme.

Vervolgens gaat het onderzoek in op de effecten van lysine deacetylase-remmers (KDACis) op muis primaire alveolaire macrofagen geactiveerd door lipopolysaccharide (LPS), zoals beschreven in **Hoofdstuk 3**. Hoewel er tussen de verschillende omstandigheden slechts minimale metabolische veranderingen worden waargenomen, toont de studie aan dat wanneer macrofagen worden behandeld met KDACis, er een vermindering van ontstekingsmediatoren en een toename van eiwitten gerelateerd aan ubiquitinatie wordt waargenomen. Deze vindingen bieden nieuwe aanknopingspunten voor de ontwikkeling van therapeutische ingangen voor COPD.

In **Hoofdstuk 4** onderzoeken we hoe de morfologie van collageen het gedrag en metabolisme van macrofagen beïnvloedt. We ontdekken veranderingen in de eiwitexpressie gerelateerd aan glycolyse. Er waren echter geen significante veranderingen in enzymactiviteit in dit metabole pad. Dit benadrukt opnieuw de ingewikkelde interactie tussen macrofagen en hun micro omgeving, die cruciaal is voor weefselherstel, maar ook betrokken is bij de ontwikkeling van fibrose in de longen.

Over het algemeen vat dit proefschrift de kernbevindingen van het vakgebied samen en benadrukt het de diverse metabole veranderingen van macrofagen in aandoeningen zoals obesitas, type 2 diabetes mellitus en longaandoeningen. Het toont de capaciteit van macrofagen om hun metabolisme aan te passen op basis van verschillende situaties die ze tegenkomen in weefsels.

Bovendien toont deze proefschrift de potentie van KDACis voor het verminderen van ontsteking, wat veelbelovende mogelijkheden biedt voor de behandeling van chronische inflammatoire ziekten zoals COPD. Daarnaast benadrukt dit proefschrift het belang van het inzetten van verschillende technieken voor de uitgebreide karakterisatie van macrofagen onder diverse omstandigheden.

Voor toekomstig onderzoek beveelt dit proefschrift het gebruik van single-cell metabolomics, proteomics en transcriptomics aan. Dit is belangrijk om de heterogeniteit van macrofaagpopulaties te ontrafelen en nieuwe cruciale metabole routes te identificeren binnen ziektebeelden. Verder pleit het proefschrift ook voor een geïntegreerde multi-omics aanpak, waarbij verschillende omics-technieken worden gecombineerd ter identificatie van macrofaagprofielen, en mogelijke vervolgstappen in het vinden van cruciale regulatoren en therapeutische doelen.

Tot slot laat dit proefschrift een fundamenteel begrip van het gedrag van macrofagen binnen chronische ziekten zien en wijst het op de potentie van op maat gemaakte behandelingen, met name gericht op het metabolisme van macrofagen en de verlichting van chronische ontstekingen en de potentie hiervan om de prognose van patiënten aanzienlijk te verbeteren.

ITALIAN SUMMARY (RIASSUNTO IN ITALIANO)

La malattia polmonare ostruttiva cronica (detta anche broncopneumopatia cronica ostruttiva (BPCO)), le malattie cardiovascolari e il diabete sono patologie croniche diffuse in tutto il mondo. La BPCO, caratterizzata da una limitazione persistente del flusso d'aria, influisce significativamente sulla funzione polmonare e sulla qualità della vita, mentre il diabete, che comprende le varianti di Tipo 1 e Tipo 2, comporta livelli elevati di zucchero nel sangue a causa di un disequilibrio dell'insulina, portando a varie complicazioni.

Sia la BPCO che il diabete sono caratterizzati da infiammazione cronica, contraddistinta, tra le molte caratteristiche, dalla presenza di citochine pro-infiammatorie che influenzano tutti i tessuti. Nella BPCO, l'esposizione a lungo termine a irritanti attiva un'infiammazione cronica, causando sintomi respiratori e contribuendo a comorbilità come le malattie cardiovascolari. Allo stesso modo, nel diabete, l'infiammazione si verifica nei tessuti coinvolti nella regolazione dell'energia, portando a resistenza all'insulina e complicazioni come la retinopatia e la nefropatia.

I macrofagi, cellule del sistema immunitario, giocano un ruolo fondamentale nell'intricata relazione tra processi immunitari e metabolici. L'infiammazione cronica influisce sui cambiamenti nel metabolismo energetico attraverso l'acetilazione della lisina nelle proteine, alterando l'espressione genica e influenzando processi energetici cellulari come la glicolisi e l'ossidazione degli acidi grassi. Questa connessione evidenzia l'interazione tra le risposte immunitarie e le vie metaboliche in queste patologie croniche, sottolineando l'importanza della comprensione delle loro interazioni per lo sviluppo di terapie mirate.

Questa tesi aveva lo scopo di approfondire la nostra comprensione dei macrofagi nell'ambito dell'infiammazione cronica, concentrandosi sui loro diversi fenotipi e le loro sfumature metaboliche in vari contesti tessutali.

Nel **Capitolo 2**, l'attenzione è focalizzata sul coinvolgimento dei macrofagi nell'obesità e nel diabete di Tipo 2 (T2DM). Si sono scoperti fenotipi distinti associati a queste patologie e si è fatta luce sulle variazioni dei livelli dei metaboliti cellulari, rivelando come i microambienti influenzino i comportamenti dei macrofagi. Questo capitolo ha anche illustrato i modi più comuni per caratterizzare i macrofagi, con particolare attenzione al loro metabolismo.

Successivamente, questa tesi ha investigato gli effetti degli inibitori delle lisine deacetilasi (KDACis) sui macrofagi alveolari murini primari attivati dal lipopolisaccaride (LPS), descritto nel **Capitolo 3**. Sebbene siano stati osservati

minimi cambiamenti metabolici tra le condizioni, lo studio ha rivelato che quando i macrofagi sono stati trattati con i KDACis, si è osservata una riduzione dei mediatori infiammatori e un potenziamento delle proteine correlate all'ubiquitinazione, offrendo potenzialmente nuove strade terapeutiche per la BPCO.

Nel **Capitolo 4** abbiamo esplorato come la morfologia del collagene influenzi il comportamento e il metabolismo dei macrofagi. Abbiamo scoperto cambiamenti nell'espressione proteica correlata alla glicolisi, ma nessuna alterazione significativa nell'attività degli enzimi coinvolti in questa via metabolica, evidenziando ancora una volta l'interazione intricata tra macrofagi e il loro microambiente, fondamentale nella riparazione dei tessuti e nella fibrosi polmonare.

Nel complesso, questa tesi ha riassunto le scoperte fondamentali nel campo, evidenziando le diverse adattazioni metaboliche dei macrofagi in condizioni come l'obesità, il T2DM e i disturbi polmonari. Ha dimostrato la capacità dei macrofagi di adattare il loro metabolismo in base ai diversi ambienti tessutali, influenzando significativamente il loro comportamento.

Inoltre, lo studio ha mostrato il potenziale dei KDACis nel ridurre l'infiammazione, offrendo vie promettenti per il trattamento di patologie infiammatorie croniche come la BPCO. Questo studio, e la tesi nel suo complesso, hanno sottolineato l'importanza di impiegare varie tecniche per caratterizzare in modo esaustivo il comportamento dei macrofagi in condizioni diverse.

Per il futuro, questa tesi suggerisce di utilizzare tecniche metabolomiche e trascrittomiche a livello delle singole cellule per svelare l'eterogeneità delle popolazioni di macrofagi e identificare nuovi percorsi metabolici cruciali nelle malattie. Si propone anche un approccio multi-omico integrato, combinando varie tecniche omiche per un profilo completo dei macrofagi, rivelando potenziali regolatori cruciali e bersagli terapeutici.

In conclusione, questa tesi ha fornito una comprensione fondamentale dei comportamenti dei macrofagi nelle malattie croniche e ha suggerito trattamenti mirati che puntano al metabolismo dei macrofagi per alleviare l'infiammazione cronica, migliorando potenzialmente significativamente la prognosi dei pazienti.

ACKNOWLEDGEMENTS

Wow, what a journey! I can't believe I'm at the point of wrapping up my thesis. Huge shoutout to everyone who made this wild ride possible; your support means the world to me! It's been a rollercoaster of research, late nights, and way too much coffee. But I wouldn't be here without the incredible people who had my back. Time to give credit where credit's due!

First and foremost, I would like to express my gratitude to my promoters, **Rainer Bischoff** and **Barbro Melgert**. Thank you for giving me the opportunity to join your departments and develop my PhD projects.

Dear **Rainer**, thank you for introducing me to the world of chromatography and mass spectrometry. I will forever be amazed by your deep knowledge of the most disparate topics. Thanks for helping me develop my critical and analytical thought. My favorite memory will always be dancing together at your retirement party. I wish you more happy days like that.

Dear **Barbro**, thank you for unexpectedly welcoming me into your group. I came to Groningen with a love for biology and immunology, but thanks to you, I discovered my passion for macrophages. Traveling to Iceland and then enjoying the Blue Lagoon together with Rosa was an unforgettable experience. I wish you success in all your future endeavors, involving macrophages and beyond.

Thanks to **Marcel Kwaitkowski** and **Natalia Govorukhina** for your help, especially at the beginning of my Ph.D.

I would like to thank the members of my assessment committee: **Prof. M. Schmidt**, **Prof. G. Hopfgartner**, and **Prof. F.J. Dekker**, for taking the time to review my thesis. I look forward to discussing the findings described in my thesis with you during my defense.

Big thanks to my awesome co-authors for their fantastic teamwork and collaborative spirit in crafting our manuscripts.. Many thanks in particular to our dedicated laboratory technicians for their invaluable support and expertise throughout my research endeavors!

Thanks to the **Analytical Biochemistry group**: thank you for witnessing my growth in the lab, and sharing not only the chemistry know-how but also memorable moments like Christmas dinners and lab outings. Special thanks to **Jos** for his enduring patience, **Hjalmar** for being an amazing co-supervisor, and **Karin** for the pleasure of collaboration: from our shared love for chocolate to a joint publication! Wishing you great success and exciting adventures worldwide.

Alienke, your companionship at the start of my PhD journey was truly invaluable. Thanks for sharing your knowledge and being a wonderful friend; I'm delighted you're back in Groningen, and let's catch up more often! **Alex**, your support for the "Tuesday salads" was fantastic. May the future bring you and Monique much happiness. **Janine**, facing challenges together and planning lab outings have been a joy. Best of luck in all your future endeavors! **Ali**, your unwavering positivity is inspiring. Wishing you and your family the very best. **Baubek**, your dynamism is impressive. I'm confident you'll achieve all your goals. Thanks for keeping the "old guard" in touch. **Ola**, your kindness and cheerful personality have brightened many lab days; thank you. **Bas**, it was a pleasure being colleagues, and I'm glad we still cross paths in Assen.

To the incredible members of the **Molecular Pharmacology group**, I'm deeply grateful for your company, constant support, and collaborative spirit over the years. Being part of this group transformed my PhD journey, and I'll forever appreciate your warm welcome. **Martina**, our "editor-in-chief," thank you for embracing me into the MF family and making me part of an amazing team. Your thoughtful gestures, from card notes to flowers, meant a lot. **Amalia**, your kindness and interest in my project were truly appreciated; collaborating with you was a pleasure. **Reinoud**, not only do I admire your work, but the karaoke nights were a blast, thanks for joining! **Marina**, your help inside and outside the hood made a difference. Sharing an office with you was a pleasure, and your welcoming smile brightened my days. **Rocio**, your creativity shines in everything you do; I'm thrilled that we got to spend time together during your first visit in Groningen and that now we have more occasions to meet! **Luke**, thank you for the fun times at the department, gossiping with you has no contenders! **AnaLau**, I am really happy that you joined the department and we could spend some time together, our shared birthday is a memory I'll cherish. **Tinting**, thank you for always greeting me with a hug and a smile, and thank you for introducing me to hot pot, I am now obsessed.

To my lovely office mates, Dan, Rosa, Shanshan, Alejandro, Nad'ka, thank you for welcoming me in the office and making it the best working space, I dearly miss our potluck lunches. **Dan**, I am so happy that I got to share my daily life with you, you are not only a very dedicated scientist but also a very kind and smart friend. I miss our chats and I wish you all the best. **Rosa**, it was a pleasure to share the office with you, but even more to share the experience of traveling to Iceland and looking not only for whales but also northern lights, and succeeding both times! I wish you all the best in Canada. **Shanshan**, thank you for all your help and kindness, you were missed when you left the group.

To all the other PhD students in the department, **Melody**, **Yang**, **Hong**, **Luis**, **Leshan**, and **Shilei**, I wish best of luck and to enjoy your PhD.

Even if not part of the group anymore I would like to thank **Marina TL** and **Angelica**, for their lab help and, more importantly, for the enjoyable chats over wine, salsa dances, and sewing evenings. I would like to express my gratitute also to **Asmaa**, thank you for not only teaching me how to use the Seahorse but for the enjoyable chats while doing so.

I want to express my gratitude to my fellow **PROMINENT** PhDs, **Frederik**, **Anna**, **Sok Cin**, **Faizan**, **Sara**, **Vicente**, **Noura**, **Zaid**, **Vika**, **Idil**, **Sonia**, **Karla**, **Angelina**, **Martina**, and **Sajad**, for sharing this incredible journey with me. Facing challenges, exchanging tips, and sharing countless laughs with 15 fellow arrivals in Groningen created a unique bond. Wishing each of you a bright and joyful future. **Angelina**, our shared moments from PROMINENT events to parties and chats on the fourth floor have been wonderful. Your dedication, talents, and big heart make you an incredible woman. **Zaid**, thank you for being a fantastic office mate, always up for a chat and a laugh. Wishing you and your family happiness. Special thanks to **Sieta** for guiding us every step of the way with a kind smile and encouraging word.

To my new **ICON** colleagues, your encouragement and support during this last year have meant a lot. A special shoutout to **Riejanne**, **Wikke**, **Anienke**, and **Alfredo**.

Thanks to the "**Mice ladies**", **Martina**, **Vika**, **Esther**, **Lysbeth**, **Karla**, and **Sonia**, for the ladies' weekends, brunches, and anything involving food! Your laughter and deep conversations, along with making me part of your growing families, have been a true joy. **Martins**, we have shared so much over the years that I am not sure where to start, I guess just by saying thank you for your friendship, thank you for being the organizer of the group, and including me in many of your hobbies (I hope we will get back to pottery at some point!), thank you for sharing your culinary talents, and thank you for the continues life advices. I look forward to see what the future will bring. **Karlita**, I admire your dedication to everything that you do in life, I wish I had a tenth of your energy! Thank you for the good chats, for trusting me with your furry babies, and for welcoming us all in your house from day one. I am sure you will achieve great things.

To the friends that made my days in Groningen better, **Tiago**, **Luis**, **Sio**, **Prajit**, **Kim**, **Ligia**, **Takuya**, **Kim**, and **Erika**, thank you for the constant support, the fun nights and countless brunches. To my Mexican crew, our trip has created a bond that I hope will not break, I cherish you all deeply. **Carli**, your energy is an unending ball

of fun, always ready for the next adventure. Here's to more adventures; swimming with sharks was just the beginning! Deep down, I know you're a cuddle bear, and I look forward to seeing more of that warmth. **Semmy**, you're a hidden gem. Discovering your brilliance, fun spirit, and kindness during our trip was a delight. Thanks for always bringing good vibes with you. **Tegan**, my fellow potterhead and dance lover, it's a joy to call you a friend. Thanks for including me in your plans; every time is a blast. Here's to more occasions for shared fun and laughter!

Nad'ka, I don't think I know another person that lives life as intensely as you do. Thank you for infusing enthusiasm into everything you do and always giving your all. Thank you for welcoming me into your family and your home. Thank you for sharing a bed with me, no matter the country we are in. You have a big heart and you wear it on your sleeve, don't let anyone change that. I wish you the best for your future, both in your personal life and professional, I am sure whatever goal you will decide to pursue, you will achieve. Thank you for your friendship.

Josesito bebe, your soul is truly remarkable: you are fun, loving, smart, and affectionate (when you want, just like a cat, thank you for showing me that side too). Thanks for introducing me to the world of plants (though my addiction might argue otherwise!), thank you for pushing me in our CrossFit classes, thank you for making me braver and convincing me to swim with sharks. Thank you for supporting me through every high and low life as thrown us in these years, thank you for being my friend and family, I love you. I miss you, and remember, wherever I am, there's always a home for you, complete with a plate of cecina!

To my wonderful **paranymphs**, Sonia and Alejandro, thank you for being my rocks and safe space throughout my PhD.

Sonia, you probably find this very cheesy, but I am going to write it anyway (xD). Thank you for being my friend from day one, thank you for sharing this path with me and making it a fun drive all the way through. I couldn't imagine being here without you, I love you, and I look forward to what the future will bring us.

Alejandro, Ale THE BEST, you probably do not realize the role that you played in my journey, we started our friendship as a CrossFit team and you are now my second family. You are the most talented person that I know, whatever you touch becomes gold, and it must be because of your golden heart. Every moment spent with you makes me happy, it doesn't matter if we are discussing R functions, anime episodes, or love life. Thank you for teaching me that YOLO and sharing part of that life with me, let's keep enjoying life together for as long as possible.

Johnathan, thank you for your support these last months, I hope many more will come. Mi stima bo.

Vorrei ringraziare la mia famiglia per il continuo supporto durante questi anni lontano. Essere così lontani non è sempre facile, eppure siamo riusciti a mantenere un rapporto stupendo, vi voglio tanto bene. **Mami** e **Papi**, grazie per aver accettato il fatto che trasferirmi fosse la scelta migliore per me ed avermi sostenuta in tutto e per tutto. Grazie per avermi aiutata con i mille traslochi, per essere venuti a trovarmi ogni volta che potevate, per avermi fatto sentire vicina, anche se lontana. Grazie per avermi tirata su quando ero giù di morale, aver celebrato le mie vittorie come se fossero le vostre (perché lo sono), e non aver mai smesso di credere in me. **Zii** e **Camilla**, grazie per essermi venuti a prendere all'aeroporto ogni volta che tornavo, grazie per i messaggi (e i video!) nei momenti di bisogno, grazie per "i pacchi da giù", grazie per aver imparato ad imprecare in Olandese. Grazie per avermi dedicato del tempo ogni volta che potevate, siete impareggiabili. Un grazie speciale a Zia Chiara per essere venuta ad aiutarmi, e ad aiutare mamma, in un momento difficile, essere insieme ha reso tutto più facile.

Lastly, as Snoop Dogg said "I want to thank me for believing in me, I want to thank me for doing all this hard work I wanna thank me for never quitting. I wanna thank you for always being a giver. I wanna thank you for trying to do more right than wrong. I wanna thank me for being me at all times."

CURRICULUM VITAE

Sara Russo, the author of this thesis, was born in Pisa, Italy, on the 7th of August, 1992. Following her high school graduation in 2011, she began her bachelor's degree in Biotechnology at the Faculty of Mathematics, Physics, and Natural Sciences in Pisa. She successfully completed her Bachelor's degree in 2015, and subsequently pursued a Master's degree in Medical Biotechnology at the University of Bologna (Bologna, Italy). During her Master's program, Sara Russo dedicated one year to her internship at the Department of Experimental, Diagnostic, and Specialty Medicine (DIMES) at the University of Bologna. Her research focused on studying the role of Aurora kinases A and MDM2 in the stability of the tumor-suppressor SETD2, exploring pathogenetic and therapeutic implications in the advanced forms of Systemic Mastocytosis. She graduated with honors in 2018.

In September 2018, Sara moved to the Netherlands to undertake a Ph.D. position at the University of Groningen, within the Departments of Analytical Biochemistry and Molecular Pharmacology as part of the Marie Skłodowska-Curie joint program. Under the supervision of Rainer Bishoff and Barbro Melgert, her doctoral research aimed to unravel some the molecular mechanisms underlying chronic inflammation. Her work also explored new drug therapies in the context of Diabetes Type II, Idiopathic Pulmonary Fibrosis, and Chronic Obstructive Pulmonary Disease, with a specific focus on macrophages and their metabolism. The research presented in this thesis was conducted during her Ph.D. Besides her research, Sara presented her work at both national and international conferences and took on the role of supervising master's and bachelor's students.